



LUND UNIVERSITY

WUI-NITY 4

An Industry-Ready WUI Fire Evacuation Model

Ronchi, Enrico; Wahlqvist, Jonathan; Rohaert, Tuur; Kuligowski, Erica; Wu, Junfeng; Zhou, Xiangmin; Singh, Dharendra; Rein, Guillermo; Mitchell, Harry; Kalogeropoulos, Nikolaos; Gwynne, Steve; Xie, Hui; Thompson, Peter; Kinatader, Max; Berthiaume, Maxine; Bénichou, Nouredine; Kimball, Amanda

2024

Document Version:

Publisher's PDF, also known as Version of record

[Link to publication](#)

Citation for published version (APA):

Ronchi, E., Wahlqvist, J., Rohaert, T., Kuligowski, E., Wu, J., Zhou, X., Singh, D., Rein, G., Mitchell, H., Kalogeropoulos, N., Gwynne, S., Xie, H., Thompson, P., Kinatader, M., Berthiaume, M., Bénichou, N., & Kimball, A. (2024). *WUI-NITY 4: An Industry-Ready WUI Fire Evacuation Model*. Fire Protection Research Foundation.

Total number of authors:

17

General rights

Unless other specific re-use rights are stated the following general rights apply:

Copyright and moral rights for the publications made accessible in the public portal are retained by the authors and/or other copyright owners and it is a condition of accessing publications that users recognise and abide by the legal requirements associated with these rights.

- Users may download and print one copy of any publication from the public portal for the purpose of private study or research.
- You may not further distribute the material or use it for any profit-making activity or commercial gain
- You may freely distribute the URL identifying the publication in the public portal

Read more about Creative commons licenses: <https://creativecommons.org/licenses/>

Take down policy

If you believe that this document breaches copyright please contact us providing details, and we will remove access to the work immediately and investigate your claim.

LUND UNIVERSITY

PO Box 117
221 00 Lund
+46 46-222 00 00



RESEARCH FOUNDATION

RESEARCH FOR THE NFPA MISSION

WUI-NITY 4: An Industry-Ready WUI Fire Evacuation Model

Final Report by:

Enrico Ronchi, Jonathan Wahlqvist, Arthur Rohaert
Lund University, Sweden

Erica Kuligowski Junfeng Wu and Xiangmin Zhou
Royal Melbourne Institute of Technology, Australia

Dhirendra Singh
Data61/CSIRO, Australia

Guillermo Rein, Harry Mitchell and Nikolaos Kalogeropoulos
Imperial College London, UK

Steve Gwynne, Hui Xie, Peter Thompson
Movement Strategies, UK

Max Kinateder, Maxine Berthiaume and Nouredine Bénichou
National Research Council, Canada

Amanda Kimball
Fire Protection Research Foundation, USA

October 2024

© 2024 Fire Protection Research Foundation
1 Batterymarch Park, Quincy, MA 02169 | Web: www.nfpa.org/foundation | Email: foundation@nfpa.org

Foreword

The Fire Protection Research Foundation expresses gratitude to the report authors: Enrico Ronchi, Jonathan Wahlqvist, Arthur Rohaert, Erica Kuligowski, Junfeng Wu, Xiangmin Zhou, Dharendra Singh, Guillermo Rein, Harry Mitchell, Nikolaos Kalogeropoulos, Steve Gwynne, Hui Xie, Peter Thompson, Max Kinateder, Maxine Berthiaume, Nouredine Bénichou, and Amanda Kimball.

The authors also wish to acknowledge the technical panel of the project for their support and guidance throughout the work conducted. The authors would also like to thank all the participants of the project workshop. Special thanks are expressed to the National Institute of Standards and Technology (NIST) for providing the project funding.

The content, opinions and conclusions contained in this report are solely those of the authors and do not necessarily represent the views of the Fire Protection Research Foundation, NFPA, Technical Panel or Sponsors. The Foundation makes no guaranty or warranty as to the accuracy or completeness of any information published herein.

This report was prepared by the Fire Protection Research Foundation, Lund University, Movement Strategies, Imperial College London and National Research Council of Canada using Federal funds under award 60NANB22D179 from the National Institute of Standards and Technology ("NIST"), U.S. Department of Commerce. The statements, findings, conclusions, and recommendations are those of the author(s) and do not necessarily reflect the views of NIST or the U.S. Department of Commerce.

About the Fire Protection Research Foundation

The [Fire Protection Research Foundation](#) plans, manages, and communicates research on a broad range of fire safety issues in collaboration with scientists and laboratories around the world. The Foundation is an affiliate of NFPA.



About the National Fire Protection Association (NFPA)

Founded in 1896, NFPA is a global, nonprofit organization devoted to eliminating death, injury, property and economic loss due to fire, electrical and related hazards. The association delivers information and knowledge through more than 300 consensus codes and standards, research, training, education, outreach and advocacy; and by partnering with others who share an interest in furthering the NFPA mission.

[All NFPA codes and standards can be viewed online for free.](#)

NFPA's [membership](#) totals more than 65,000 individuals around the world.



Keywords: wildfire, wildland-urban interface, WUI, evacuation, fire models, pedestrian models, traffic models, WUI modelling, vulnerability mapping

Report number: FPRF-2024-08

Project Manager: Amanda Kimball

Project Technical Panel

Paolo Intini, University of Salento, Italy

Michael Kinsey, Ashton Fire, UK

Ruggiero Lovreglio, Massey University, New Zealand

Kasper Pannell, GHD, USA

Dana Duong, National Research Council, Canada

Natalia Cooper, National Research Council, Canada

Ashley Nixon, National Research Council, Canada

Hamed Mozaffari Maaref, National Research Council, Canada

Project Sponsor

National Institute of Standards and Technology (NIST)

Abstract

In recent years, WUI fire evacuation models have started to be developed. Several now exist, although they are primarily research tools unable to be applied in practice or commercially available tools with limited functionality. For this step – moving from research to practice – such models need to build their credibility through data for their development, testing and application. The WUI-NITY tool has been developed over several previously NIST-funded projects. This project aims at providing a set of useful methods for the development and validation of wildfire evacuation models. This includes social media data mining techniques for the investigation of evacuation behavior and the use of virtual reality technology to explore driving behavior during wildfire scenarios. Those two methods are exemplified through a set of data collection and analysis efforts for which results are made freely available to any interested party. This report also presents the latest enhancements of the WUI-NITY tool and its associated trigger buffer tool K-Peril. This includes the implementation of a microscopic traffic model (SUMO) and the definition of stochastic trigger boundaries. Finally, this report presents information useful for a model user to configure a WUI-NITY simulation through a dedicated user guide. All these activities contribute to the development of a tool that can be used for free by any interested party to investigate wildfire evacuation behavior.

Table of contents

Acronyms.....	12
Symbols.....	13
1. Introduction	14
1.1. Project aim.....	15
1.2. Report structure	15
2. Social media data for understanding evacuation behaviors.....	17
2.1. Scope and objectives	17
2.2. Problem statement	17
2.3. Literature review on social media data mining for the analysis of human behavior in wildfires	19
2.3.1. Data collection.....	19
2.3.2. Data cleaning.....	19
2.3.3. Data categorization.....	21
2.4. Methodology design in social media data mining for human behavior analysis in wildfires	21
2.4.1. Data collection.....	22
2.4.2. Large Language Model (LLM) based data filtering	23
2.4.3. Active learning-based data cleaning refinement	24
2.4.4. Data categorization and summarization	30
2.5. Datasets	31
2.6. Prototype	31
2.6.1. Architecture	32
2.6.2. Graphical User Interface overview	32
2.6.3. Demonstration scenarios	33
2.7. Testing.....	40
2.7.1. Testing on data cleaning algorithms	41
2.7.2. Comparing data cleaning accuracy to human experts.....	43
2.7.3. Accuracy evaluation of data categorization	44
2.8. Findings, limitations and future work	47
2.9. Conclusions	49
3. Virtual reality experiments	50
3.1. Using Virtual Reality to study driving behavior.....	51
3.1.1. Head-mounted displays (HMD).....	51
3.1.2. Validity of driving simulators	53
3.2. Driving behavior in reduced visibility conditions	54
3.2.1. Light extinction	54

3.2.2.	Smoke.....	56
3.2.3.	Headway.....	57
3.3.	Overview of current VR studies.....	58
3.4.	Pilot VR study on visibility.....	58
3.4.1.	Objectives.....	59
3.4.2.	Methods.....	59
3.4.3.	Results and discussion.....	65
3.5.	Main VR driving study in Canada	70
3.5.1.	Methods.....	70
3.5.2.	Results	75
3.5.3.	Discussion	92
3.6.	Main VR driving study in Sweden.....	94
3.6.1.	Methods.....	94
3.6.2.	Results and discussion.....	105
3.6.3.	Conclusion.....	115
3.7.	Summary.....	115
4.	WUI-NITY enhancements: integration of the microscopic traffic model SUMO.....	117
5.	Enhancing the k-PERIL model into a probabilistic trigger buffer model.....	121
5.1 –	Standardization of inputs/outputs for use in WUI-NITY	121
5.2 –	Development and refinement.....	122
5.3 –	Integration and implementation into WUI-NITY.....	124
6.	User guide and demonstration documentation.....	125
Appendix 1:	WUI-NITY user guide	126
A1.	Introduction – why you might use this model	133
About this guide.....		135
Download and install WUI-NITY		136
System requirements for WUI-NITY		136
A2.	Data preparation and user inputs.....	137
Map preparation.....		137
Population Definition.....		140
Fire and smoke simulation.....		142
Landscape file (.lcp)		143
Topographic data (elevation, slope, aspect layers)		145
Canopy cover layer		150
Fuel map layer.....		152

Combine the raster layers to generate a landscape file	152
Fuel models file (.fuel)	160
Initial fuel moisture file (.fmc)	160
Weather file (.wtr).....	161
Wind file (.wnd).....	162
Ignition points file (.ign).....	163
Graphical fire input file (.gfi)	164
Traffic network and routing	165
Road network and route collection	165
Transportation options	165
Evacuation settings	168
Evacuation group file (.eg)	168
Response Curve file (.rsp)	169
Evacuation goal file (.ed).....	169
Other evacuation settings.....	170
Summary	172
A3. Guided workflow interface	174
The workflow design paradigm	174
WUI-NITY Graphical User Interface	175
The workflow GUI.....	176
WUI-NITY Project File (.wui)	177
The workflow menu.....	177
Prepare population, map and traffic network data	177
Configure Location and Size of Region.....	178
Population Data.....	178
Evacuation goal(s)	180
Evacuation group(s) and response(s)	181
Evacuation settings	183
Routing data	184
Traffic	185
Landscape data.....	186
Fire Characteristics	186
Running simulations	187
The Output Window	189
Simulation outputs	190
A4. Demonstration case	192
Data preparation.....	192
The process of applying WUI-NITY to build the simulation case.....	193

Prepare population, map and traffic network data.....	193
Configure location and size of the region.....	194
Configure population data	195
Configure evacuation goals	197
Configure response curves and evacuation groups.....	199
Configure evacuation settings.....	202
Configure routing data	203
Configure traffic settings	204
Prepare landscape file, fuel models file and other supporting files.....	204
Specify fire characteristics files and edit fire model settings	205
Execute Simulations	205
Simulation settings and outputs	206
Evacuation objective and assumptions	206
Configure evacuation and traffic settings	206
Simulation outputs	207
A5. Summary	211
User guide references	213
Report references	215

Acronyms

AI	Artificial Intelligence
ANOVA	Analysis of Variance
Blair	Behavior Labelling AI for Research
CalTrans	California Department of Transportation
CSV	Comma Separated Values
ChatGPT	Chat Generative Pre-trained Transformer
ETC	Estimated Time of Completion
GUI	Graphical User Interface
HMD	Head Mounted Display
ITI	Inter Trial Interval
Llama	Large Language Model Meta AI
LLM	Large language Model
NRC	National Research Council Canada
PD	Pixel Density
PeMS	Performance Measurement System
PERIL (k-PERIL)	Population Evacuation tRIgger aLgorithm)
RGB	Red Green Blue
SSQ	Simulator Sickness Questionnaire
SUMO	Simulation of Urban Mobility
V&V	Verification and Validation
VE	Virtual Environment
VR	Virtual Reality
VRSQ	Virtual Reality Sickness Questionnaire
WUI	Wildland-Urban Interface
WUIASET	Wildland-Urban Interface Available Safe Egress Time
WUIRSET	Wildland-Urban Interface Required Safe Egress Time

Symbols

α	Significance level [-]
C	Constant for relating visibility to smoke density [-]
c	Concentration of the absorbing species [mol/m ³]
D	Distance [m]
Dis	Distance of the traffic sign to the participant [m]
ε	Molar extinction coefficient [m ³ /mol/m]
f	Fraction of the true color values [-]
h	Distance headway [m]
K	Extinction coefficient (or fog density/smoke density) [m ⁻¹]
I_0	Intensity of light ray before passing through a medium [-]
I	Intensity of light ray after passing the distance D through smoke [-]
p	Uncertainty
q_0	Sum of confidence weights
v	Speed [m/s]
V	Visibility [m]
w_i	Confidence weights

1. Introduction

Previous projects funded by the National Institute of Standards and Technology produced an integrated software platform called WUI-NITY (Ronchi et al. 2020; Wahlqvist et al. 2021) that enables the simulation of WUI evacuation scenarios linking three domains: fire spread, pedestrian decisions and movement, and traffic movement. Thus far, macroscopic sub-models have been embedded and the system has been made available for any interested parties. The platform enables input from a range of external sources (e.g., FARSITE (Finney 1998), OpenStreetMap¹, population distribution data sources such as the Gridded Population of the World², and others) and is able to generate outputs on many systems (e.g., different types of operative systems). WUI-NITY is also associated with the k-PERIL system (Mitchell 2019; Mitchell et al. 2023), a sub-model that generates trigger buffer estimates supporting emergency management.

In previous WUI-NITY projects, the model usability and accuracy was improved by the development of a Graphic User Interface (GUI), and through the development of a suite of verification and validation (V&V) tests for this and other wildfire evacuation models (Ronchi et al. 2021). In addition, work has included the collection of data to facilitate further validation and model development. We identified freely available state-level traffic data that are collected on an ongoing basis to track traffic speeds, flows, densities and other characteristics on major highways. The Performance Measurement System (PeMS) database, created and maintained by the California Department of Transportation (CalTrans³), was used in this effort. We first developed a methodology for data extraction of relevant traffic movement data, which we then used to extract traffic movement data from a set of case studies which were published in open access for any interested parties (Rohaert et al. 2023c, a).

In the current WUI-NITY4 project, we explored the use of innovative data collection techniques to improve our understanding of wildfire evacuation behavior. This includes the development of a methodology for social media data mining related to wildfire evacuation behavior, based on the concept of active learning (Carr et al. 2015), see Section 2. Virtual reality (VR) and driving simulators were used in parallel to study traffic evacuation movement variables specific to wildfire scenarios (e.g., interaction with embers/smoke in relation to traffic density (See section 3). Further work has also been performed to improve the WUI-NITY tool, including the integration of a microscopic traffic model (see Section 4). In addition, the concept of stochastic trigger boundaries (Kalogeropoulos et al. 2023) was introduced within the K-Peril tool, which works in parallel with our tool WUI-NITY by making use of its outputs related to the WUIRSET (Wildland-urban interface required safe egress time). This tool is meant to help decision makers such as emergency managers in identifying suitable time for evacuation orders (see Section 5).

An important part of any software development work is to ensure ease of use. For this reason, this work has also been focusing on improving the usability of the WUI-NITY tool by providing a detailed step-by-step user guide which could facilitate the use of the graphic user interface of the tool (see Appendix 1 and Section 6). This enables the use of the model for a wide range of possible application scenarios.

¹ <https://www.openstreetmap.org/>

² <https://sedac.ciesin.columbia.edu/data/collection/gpw-v4>

³ <https://dot.ca.gov/programs/traffic-operations/mpr/pems-source>

1.1. Project aim

This project aims to address a consistent challenge in our field which impedes the practical use of wildfire evacuation tools: the overwhelming lack of data on wildfire evacuation. Data in this context includes human behavior and movement during both the pre-travel time (i.e., evacuation rates and departure times) and the travel time period (i.e., routing, destinations, and movement under different conditions, including traffic congestion or presence of smoke). In this project, our team focused on methods to collect and analyze evacuation data using two different approaches. These approaches capture evacuation behavior at the individual level (via VR technology) and at the broader, aggregate level via social media (big) data mining. This project aids users of wildfire evacuation models to enable simulation of emergent behavior, rather than pre-determining behavioral responses via scripted inputs. These data also assist in the ability to further develop and validate wildfire evacuation models like WUI-NITY or others for various types of fire and evacuation scenarios. Along with data collection, a set of efforts aimed at enhancements to the WUI-NITY tool and its associated trigger buffer tool K-Peril have also been performed. This has been performed in parallel with work aimed at facilitating the WUI-NITY use.

1.2. Report structure

This report is structured as follows. Section 1 includes an introduction covering the previous work conducted within the research efforts associated with the development and validation of WUI-NITY tool for wildfire evacuation modelling. This includes a general overview of the work conducted in the current project and the overall aim of the project, along with the description of the structure of this report.

Section 2 focuses on the presentation of a new method developed for social media data mining related to wildfire evacuation behavior and presents a prototype for its application called *Blair*. This work critically explored the use of social media data mining to study evacuation behavior and movement patterns in wildfire events. The key behavior and movement patterns considered in the exemplary application of the tool are route and destination choices during evacuation. First, a literature review was performed to identify the capabilities and limitations of existing social media data mining techniques in relation to the study of evacuation. The review explored the sources of social media data, the types of data that can be collected via these platforms, and the methods that exist for data extraction, filtering, and analysis when using these data to study wildfire evacuation. This work was followed by the development of a methodology to perform this type of work. This has been implemented into the *Blair* prototype and presented through the exemplary analysis of datasets related to three cases studies (the 2018 Kincade Fire, the 2019 Getty Fire and the 2019 Tick Fire).

Section 3 presents the work conducted to investigate the use of VR for the study of evacuation behavior during wildfire events. This work included reviewing the current methods adopted for the representation of smoke and reduced visibility conditions during an evacuation in VR in relation to driving behavior. A pilot VR study was then conducted to investigate the perception of reduced visibility in VR, followed by two main VR data collection efforts conducted in Canada (at NRC) and Sweden (at Lund University). The VR experiments focused on a set of virtual driving scenarios in reduced visibility conditions in which traffic density was manipulated. This allowed us to improve our understanding of the relationship between traffic density and reduced visibility conditions through the study of distance headway and provide data that can inform wildfire

evacuation model development and validation. In addition, this work provides insights into the strengths and limitations of VR as a research tool that should be considered in future work.

Section 4 provides an overview of the key enhancements performed in the WUI-NITY tool. The main improvement is the implementation of a microscopic traffic modelling mode through the integration of the open-source traffic model SUMO (Simulation of Urban Mobility) (Behrisch et al. 2011).

Section 5 presents an overview of the research efforts performed to make the k-PERIL tool able to represent stochastic trigger boundaries. The tool relies on a set of estimations of the wildland-urban interface required safe egress time (WUIRSET) which can be obtained through tools like WUI-NITY and then produces a set of probabilistic trigger buffers, which then helps to inform emergency management decisions such as the issuing of evacuation orders.

Section 6 provides a brief description of the work conducted to improve the usability of the WUI-NITY tool through the development of a user guide highlighting the workflow necessary to get a simulation to run. This section provides a general overview on the work conducted while the actual user guide is presented as an appendix of this report (see Appendix 1).

2. Social media data for understanding evacuation behaviors

Due to the popularity of social media platforms, social media-based human behavior analysis provides a promising prospect for planning, educating, and making decisions about wildfire evacuations. Therefore, this part of the work focused on the use of social media data in the context of wildfire and WUI fire evacuation behavior.

2.1. Scope and objectives

The main scope of this part of the work was the use of social media data mining approaches to understand human behavior during wildfire evacuation. The data examined includes resident behavior and movement during two crucial phases:

- **Pre-travel time periods:** During this phase, individual evacuation decisions and their motivations are investigated. Understanding these early choices is vital for effective preparedness.
- **Travel time periods:** Here, residents' evacuation route choices are investigated. This was performed along with the study of transportation mode. These insights can inform evacuation logistics and resource allocation.

To extract and analyze this data, a new data mining problem was defined, called “social media data mining for bushfire human behavior analysis”. As a result, a novel method for solving this problem was developed. The uniqueness of this method lies in its utilization of active learning techniques—hence the name active bushfire human behavior analysis. By actively engaging with the data, meaningful patterns and characteristics of human behavior can be identified. Additionally, a prototype named *Blair* (a short name for **B**ehavior **L**abelling **AI** for **R**esearch on social media data about wildfire evacuation) was implemented. *Blair* serves as a powerful tool for capturing rich-context data from social media platforms.

Accordingly, the tasks described in this section have two specific objectives: (1) to conduct a literature review to find a feasible method for social media data mining related to human behavior in wildfires, and (2) to develop a prototype to demonstrate that this method can extract social media data for human behavior analysis, which allow a better understanding of evacuation behavior during wildfires.

2.2. Problem statement

The input for our work is social media data related to wildfire events. Social media platforms include online services such as X (formerly known as Twitter), Facebook, Instagram, YouTube, TikTok, Reddit, and microblogs. These platforms facilitate communication and interaction by allowing users to create and share content in posts. Posts on social media can contain text, images, videos, sound, links, or a combination of these. Users utilize posts to share information with their followers and the broader social media audience. Social posts are usually uncertain, since these messages are generated by worldwide social users without supervision and usually include ambiguous texts such as word variations, abbreviations or synonyms (Zhou and Chen 2022). Thus, analyzing social media data is challenging. Despite these limitations, social media data remains valuable for analyzing human behavior.

Recent advancements in data mining and machine learning techniques, such as (Houston et al. 2015; Zhang et al. 2019; Kumar and Ukkusuri 2020; Martín et al. 2020; Morshed et al. 2021; Li

et al. 2021) have effectively reduced the cost of data processing and analysis. In one of these studies (Kumar and Ukkusuri 2020), geotag tracking sequences were used to classify X (Twitter) users into three categories during a hurricane evacuation: those outside the evacuation zone, evacuees, and non-evacuees. The datasets available for *Blair* testing were associated with wildfires with power outages that disable geotagging in most parts of the evacuation zone. Consequently, the normally rare geotags in social media posts became even rarer in the posts relevant to wildfire evacuations. For this reason, the text content of social media posts was *Blair*'s main source of information, in line with approaches by (Houston et al. 2015; Zhang et al. 2019; Martín et al. 2020; Morshed et al. 2021; Li et al. 2021). The analysis of texts was feasible, as wildfire evacuees can send social media posts once they are out of no-signal areas in the evacuation zone. Analyzing the textual content of these posts provides valuable first-hand descriptions of evacuation experiences on social media, complementing second-hand reports.

The output of the data mining approach in use are the results of analysis. This includes the evacuation decisions, the types of evacuation destinations of evacuees, their locations during evacuation, and the corresponding posts for more context details.

- The *evacuation decisions* are indications that a resident or visitor in the affected area evacuated (or not). In instances where the person or group of people may have stayed in place, they could have done so to protect their property (i.e., defend in place) or shelter in place. In addition, this output also provides some indication of the factors that affected the decision to evacuate (if mentioned in the post).
- The *types of destinations* are the categories of places the evacuees stay when evacuated from home, including hotel/motel/rental, friend/relative's home, evacuee's second home/recreational vehicles/campsite, designated emergency shelter, etc.
- The *locations* are the names of places such as cities, suburbs, or towns.

These aspects of the results are designed to meet the task aim in enhancing evacuation planning, especially considering the four-step transportation model often used to model wildfire evacuation (see (Intini et al. 2019b; Kuligowski 2020) for more details on the four-step model). Outputs on people's evacuation decisions enhance evacuation planning by helping us understand if people decided to leave an area or not and under what circumstances this may be the case (Pel et al. 2012; Murray-Tuite and Wolshon 2013; McLennan et al. 2019). This part of the output supports the first step (i.e., trip generation) of the four-step transportation model. The destination types and locations enhance evacuation planning by assisting us to understand where people will evacuate to (Murray-Tuite and Mahmassani 2004; Lindell and Prater 2007; Cuéllar et al. 2009). This part of the output is related to the second step (i.e., trip distribution) of the four-step transportation model.

The goals of our social media data mining are to effectively and efficiently perform the following tasks that map the input to the output:

- (1) Find social media posts relevant to first-hand information about wildfire evacuation behavior.
- (2) Categorize and summarize these relevant posts to support the human behavior analysis.

The first task finds the relevant posts containing information on the relevant evacuation behavior (referred to as outputs, earlier). Most posts are irrelevant. Irrelevant posts must be excluded from the output. Otherwise, they will degrade the quality of the output and waste time in the second task. The second task involves information extraction from the relevant posts. The information

must be extracted to obtain the relevant output, particularly on evacuation decisions (and factors that influenced these decisions), the types of evacuation destinations of evacuees, and their locations during evacuation.

2.3. Literature review on social media data mining for the analysis of human behavior in wildfires

A literature review was undertaken as an initial step. The full review has been submitted for publication (Wu et al. 2024) and this section is a shortened version of the full review. It is shortened to focus on the following purposes:

1. Describing the essential steps in social media data analysis.
2. Finding the existing techniques for each essential step.
3. Discussing whether existing techniques are feasible.

Many future applications are far beyond the scope of this literature review, such as:

- Evacuation model calibration and validation;
- Emergency communication;
- Personalized evacuation training; and
- Resource allocation for evacuation preparedness.

The essential steps of *Blair* include data collection, data cleaning, and data categorization. These steps are supposed to be executed in the mentioned order. In other words, these steps work best when they are organized in a pipeline that runs them one by one. In each of these steps, existing approaches are discussed to justify the choices made to overcome the challenges encountered.

2.3.1. Data collection

The data collection approach described in (Bruns and Liang 2012) progressively enlarges the set of collected data by iteratively appending more hashtags and keywords for the search of data on a social media platform. It is a general approach for collecting social media data related to a hazard event. However, a simpler approach was adopted here. One hashtag was used to retrieve data for a wildfire event in the past. It was decided to not apply the method of (Bruns and Liang 2012) due to issues with data availability (e.g., high cost of accessing the data). Fortunately, the collected data were still useful because wildfire-related social media data tend to be hashtag-friendly. Here are the reasons why a single hashtag can be used:

1. In some regions in the US, Canada and Australia, wildfires occur frequently. When they happen, they require urgent community engagement. As a result, hashtags are commonly used for faster responses on social media.
2. Multiple wildfire events often occur simultaneously, necessitating event-specific hashtags such as “#KincadeFire” and “#TickFire”.

2.3.2. Data cleaning

Data cleaning involves two steps. The first step is removing punctuation and hyphens, correcting spellings, etc., so that the artificial intelligence algorithm has less noise to deal with. This part is standard for most approaches, so it does not require reviewing specific techniques. The second step is labelling. In *Blair*, this labelling is about identifying whether the data are relevant to social media users’ evacuations. Machine learning is the usual way for data labelling, as a machine learning model maps input data to labels. However, to label data automatically using a machine

learning model, we need to train the model with some labelled data first. A large amount of labelled data are generally needed to train an accurate machine learning model. The labelling of the training data is usually burdensome because it takes too much time and human effort to label sufficient data for the model training.

To remedy the high cost of data labelling, weak supervision (Dai et al. 2021; Shetab Boushehri et al. 2022), transfer learning (Farahani et al. 2020), and active learning (Carr et al. 2015) are all feasible solutions.

Weak supervision aims to ease the annotation bottleneck by using existing labels as a general guide for clustering data into sets with a high probability of containing the required labels. In *Blair*, weak supervision could have involved using partially labelled data (i.e., incomplete supervision (Dai et al. 2021)) or heuristic rules (i.e., inexact supervision (Shetab Boushehri et al. 2022)) to automatically annotate relevant human behavior patterns during evacuations. However, the quality of the partially labelled data and/or heuristic rules determines the accuracy of the weakly-supervised data labelling. In this case, it is indeed challenging to label partial data or develop heuristic rules with sufficiently high quality.

Transfer learning reduces the negative impact of limited data by transferring knowledge from a source domain to a target domain. For the *Blair* data mining approach, transfer learning could have involved using pre-trained models (e.g., from related hazard scenarios) to initialize an evacuation behavior identification model and then fine-tuning it with a subset of data from the targeted wildfire-prone area. However, obtaining a pre-trained model would require significant efforts, as it is too difficult to ensure the quality of data labels when labelling human behavior in a huge dataset of related hazard scenarios. Furthermore, it is quite difficult to balance the accuracy and the cost of fine-tuning. If the subset of data from the targeted wildfire-prone area is too small, it often leads to inaccurate fine-tuning. If the subset is too large, the cost of labelling the subset is too high.

Active learning, a type of machine learning, enables the model to select the most informative data samples for labelling, rather than relying on a random or predefined subset (Carr et al. 2015). In other words, the principle of active learning is that, when it comes to training machine learning models using labelled data, the quality of the labelled data is more important than the quantity. Active learning can significantly reduce the user’s burden in data labelling while ensuring the accuracy of the model trained using the labels, thus lowering the associated cost and time. When coupled with a large language model, active learning became the easiest way for social media data mining in *Blair*. Large language models, such as Chat-GPT, Llama, and Google Gemini Pro, are artificial intelligence systems capable of understanding and generating human-like text. The ease in using active learning is the reason it was adopted.

Features need to be selected for the machine learning approach used in data labelling. In the context of machine learning, a feature refers to an individual, measurable property or characteristic of a phenomenon. These features play a key role in effective algorithms for tasks such as pattern recognition, classification, and regression. For hazard-related social media analysis, existing works utilize content features (Döhling and Leser 2011; Abel et al. 2012; Cameron et al. 2012; Olteanu et al. 2014; Cobo et al. 2015; Hodas et al. 2015; Imran et al. 2016; Abirami et al. 2019; Chowdhury

et al. 2020), spatial features (Abel et al. 2012; Hernandez-Suarez et al. 2019), temporal features (Balech et al. 2021), and social network features (Abel et al. 2012; Bruns and Liang 2012; Opdyke and Javernick-Will 2014; Cobo et al. 2015). Content features are those about the content of the posts. Spatial features relate to geotags (i.e. identify the location of the social media posts). Temporal features are the time series statistics of the posts, such as number of posts per day with a hashtag or a keyword. Social network features are those about how well connected a user of the social media platform is to other users, such as the number of followers and the number of friends on the platform. Our survey paper (Wu et al. 2024) contains a detailed literature review of these features.

2.3.3. Data categorization

To obtain the output of *Blair*, human behavior with respect to evacuation decisions, destination types, and locations need to be automatically categorized. Existing work on behavioral categorization in (Şahin et al. 2019) trained a text classifier to categorize behavior. However, their method has shortcomings in relation to *Blair*’s needs. First, *Blair* needs data categorization rather than classification. Classification requires to know the labels before seeing the data, while the categorization label is not always known before seeing the data. For example, the fact that a “looter” is a factor affecting evacuation decisions in any particular fire is not known until a social media post from an evacuee is found complaining about looting and identifying it as a reason to stay. Even considering a set of hypotheses of a categorization label, the method described in (Şahin et al. 2019) would still yield inaccurate results. That is because there is not enough data to train classifiers with sufficient accuracy. Typically, only 1-2% of the input data is relevant, and less than half of the relevant data includes evacuation decisions (and/or their factors), destination types, and locations. Consequently, training data are not sufficient. Thus, the categorization technique in (Şahin et al. 2019) is unsuitable for the task conducted in this work.

2.4. Methodology design in social media data mining for human behavior analysis in wildfires

The first effort in the development of a methodology for social media data mining was to obtain first-hand information related to personal experiences only, rather than news or others’ stories posted by social media users. Therefore, the results obtained from the social media posts were restricted to those posted by the author about their own, personal evacuation-related stories, behaviors, and/or decisions.

An active learning-based human behavior analysis framework for wildfires has been designed. Figure 1 shows the workflow of the framework. This workflow has four steps:

- In **data collection**, we collect data from social media.
- In **LLM-based data filtering**, we use a Large Language Model (LLM) to remove most of the irrelevant posts, thus obtaining the initial results of data cleaning.
- In **active learning-based data cleaning refinement**, the accuracy of the data cleaning results is improved using active learning.
- In **data categorization and summarization**, the clean data are categorized and summarized according to the output requirement of *Blair*.

These four steps are tagged with subsection numbers in Figure 1. The third step, i.e., active learning-based data cleaning optimization, is the most complicated step. Thus, it is expanded hierarchically into more details in Figure 1.

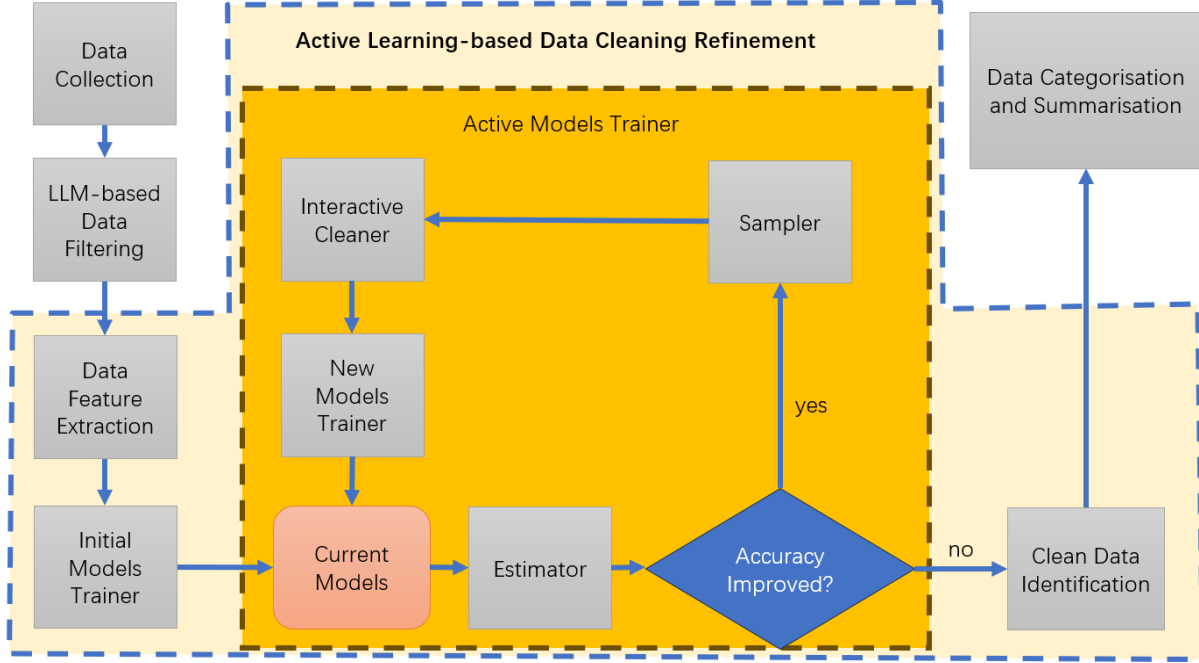


Figure 1. Workflow of active learning-based human behavior analysis framework for wildfires.

2.4.1. Data collection

The input data of our method is collected using only one hashtag for each dataset. This is for the same reason for using only one hashtag, as earlier explained. For example, we used “#KincadeFire” to collect a dataset from the 2019 Kincade fire in California, and used “#TickFire” to collect a dataset from the 2019 Tick Fire also in California. The input social media data is required to be stored in a table that includes the following columns: text, post id, user id, time, and geo-tag. The column containing the text is used in data cleaning and data categorization. All columns are used in data summarization.

Tweets were collected daily using the “search_tweets” function from the “rtweet” R package, which interfaces with Twitter’s Representational State Transfer (REST) and streaming Application Programming Interface (API). Each day, the function retrieved up to 18,000 recent tweets for each given hashtag. These tweets were then stored in separate CSV files—one file per hashtag—where the file name included the collection date. Before passing the CSV files to the Blair program, the daily tweet collections were merged into one large CSV file per hashtag, removing any duplicates, as some recent tweets could have reappeared the following day.

To store social media data, a table with essential columns was created: text, post ID, user ID, time, and geo-tag. The text column served the purposes of data cleaning and categorization, while all columns contributed to data summarization. Since the merged tweet collections already contained these columns (and more), the relevant ones were extracted from each hashtag’s large CSV file and saved them in smaller CSV files.

The daily collection, merging, and column extractions were automated using scripts: an R script for daily collection and two Python scripts for other tasks. Prior Twitter being rebranded as X, data

collection was free. However, X now charges for tweet collection, i.e., the free option is not available anymore.

2.4.2. Large Language Model (LLM) based data filtering

An important step in the approach in use is the definition of the type of features to be analyzed. As previously mentioned, spatial features like geotags are unsuitable for wildfire evacuation data due to their scarcity. Datasets available from wildfires in which power outages occur may contain a very small number of posts with geo-tags, thus geotags are not suitable features. Temporal features are unnecessary when using a single hashtag for data collection, as wildfire data are easy to find through hashtags. Social network features are prominent among first responders and news agents but not common among evacuees. Among the content features, hashtags, keywords (Döhling and Leser 2011; Abel et al. 2012; Chowdhury et al. 2020), topic features (Imran et al. 2016; Abirami et al. 2019), text statistics features (Olteanu et al. 2014; Hodas et al. 2015), and bags of words (Abel et al. 2012; Cobo et al. 2015) were considered. However, hashtags, keywords, text statistics, and bags of words do not effectively distinguish relevant posts related to the first-hand information about evacuation behavior. Therefore, only topic features are available options. Example topic features are described in (Imran et al. 2016; Abirami et al. 2019), which are based on clustering or other techniques.

The first data cleaning step in *Blair* adopts a large language model (LLM) to find social media posts relevant to the post author’s evacuation decisions and behaviors, so it is called LLM-based data filtering (Davis and Veloso 2016). A large language model is a neural network model (i.e., a type of machine learning model) with a large amount of model parameters (Chang et al. 2024), known for its ability to achieve general-purpose language generation and perform various natural language processing tasks (Chowdhary and Chowdhary 2020). These tasks include but are not limited to classification, summarization, translation, and question answering. Well-known large language models include ChatGPT 3.5 (175 billion parameters), ChatGPT 4 (1.5 trillion parameters), Google Gemini Pro (60 billion parameters), and Llama 2 (70 billion parameters) (Minaee et al. 2024). These models are designed to understand and generate text like a human, based on the vast amount of data used to train them. In *Blair*, Google Gemini Pro was adopted using an unofficial C# Software Development Kit (SDK) based on Google Generative AI Representational State Transfer (REST) and streaming Application Programming Interface (API). The SDK is called “Google_GenerativeAI”. This choice was based on cost (Gemini Pro is free) and the ease of programming.

LLM-based data filtering filters each post in the input dataset by asking the large language model a question:

“Does the post explicitly mention the author’s evacuation in the first person?”

If the answer is yes, the post will be forwarded to the next step. Otherwise, the post will be regarded as irrelevant and removed.

LLM-based data filtering may need another data cleaning step to remedy its inaccuracy. If the large language model data filtering was comparable to a human expert, it would be sufficient to complete the data cleaning step. Unfortunately, while LLM-based data cleaning does identify most

of the relevant posts, it also takes some irrelevant posts as relevant due to an error called hallucination. Every large language model has exhibited hallucination thus far (McKenna et al. 2023). In the world of LLM, hallucination refers to the tendency of the models to produce text that appears to be correct but is actually false or not based on the input provided (Ji et al. 2023). In this context, hallucination refers to the faulty reasoning of LLM that mistakes irrelevant posts as relevant.

2.4.3. Active learning-based data cleaning refinement

Using LLM-based data filtering, the initial data cleaning results were obtained. This reduced the amount of data to process and increased the efficiency of this step significantly. The efficiency here means the wall clock time to run this step. Active learning is used in this step to refine the data cleaning results, i.e., to remove those irrelevant posts LLM considers as relevant. The refinement mitigates the hallucination of LLM, thus improving accuracy. This subsection first explains what the active learning does, then describes the workflow of this step. Note that although this step is based on active learning, it is not just active learning. Active learning is used in a sub-step. Other sub-steps are as important as the active learning sub-step.

Active learning aims at removing irrelevant posts from the results from LLM-based data cleaning. As mentioned earlier, the hallucination of the LLM must be mitigated to increase the accuracy of data cleaning.

The hallucination-mitigation technique adopted in active learning-based data cleaning is called *chain of verification* (Dhuliawala et al. 2023). The chain of verification is based on the idea of iterative verification. The key to the chain of verification is to plan multiple verification questions to fact-check the answer to an initial question. In *Blair*, this active learning-based data cleaning algorithm asks the large language model some verification questions to fact-check the answer to this initial question. In this chain of verification, the algorithm needs to learn from human experts on how to select verification questions dynamically. This is where active learning is required. Comparing two example posts makes it possible to understand this dynamic process.

The following is the first example post:

“Hey @XXXX [REDACTED] some of us #KincadeFire evacuees are trying to get rentals in #XXXX [REDACTED], but we are getting charged major fees, can you help?”

To check whether this post is relevant to the post author’s evacuation, the active learning-based method first checks the author’s location, which is outside the evacuation zone. When the post author is outside the evacuation zone, the post is often easier to associate with the status of evacuation. The next step is to check the status of evacuation. In this example, since the author mentions they are trying to find a rental place to stay, it is assumed they are under evacuation. Thus, this post is relevant to the post author’s evacuation.

Considering a second example post:

“I’m in XXXX [REDACTED], my power just went out. Anyone else out here after evacuating too? Did your power go out? @XXXX [REDACTED] #KincadeFire”

To check whether this post is relevant to the post author’s evacuation, the active learning-based method first checks the author’s location, which is in an evacuation zone, as the author of the post mentioned this place “after evacuating”. When the post author is in an evacuation zone, it is often more difficult to determine the status of evacuation. In this example, the LLM is confused with the status of evacuation. It judges that the status is under evacuation, which is true for the place but false for the author of the post. Thus, instead of checking the status of evacuation, the LLM can check whether the author of the post wants to evacuate. The author of the post tried to find anyone else who did not leave the place after evacuating. Thus, the LLM is unsure about whether the author wants to evacuate or not. Based on this, this post is possibly irrelevant to the post author’s evacuation. This kind of dynamic selection of verification questions is what the active learning needs to learn.

The workflow of the active learning-based data cleaning is a four-step algorithm that learns the chain of verification (Dhuliawala et al. 2023) for improving data cleaning accuracy. This includes:

- **Data feature extraction** collects the answers to the verification questions and stores them in a table. The table serves as the input data features of the active learning.
- **Initial models trainer** trains multiple initial models for the chain of verification using at most 100 initial labelled samples.
- **Active models trainer** applies an active learning technique to improve the models for the chain of verification in multiple rounds. In each round, it requires the user to label at most 50 samples.
- **Clean data identification** removes irrelevant posts from the results of LLM-based active learning, using the final models obtained from the last round of active models trainer.

The four steps in this algorithm are performed in this exact order and are detailed here.

(1) Data feature extraction

Blair adopts batch-processing in the chain of verification to improve communication efficiency. As discussed earlier, the verification questions in the chain are normally asked according to the answers to previous questions. However, *Blair* requires the Internet to access the service of the LLM remotely, via a software as a service application programming interface. Dynamically determining which verification question to follow up previous questions causes a serious communication bottleneck due to many fine-grained Internet communications between *Blair* and the LLM. Fine-grained communications are the process of sending and receiving small messages for the communications (see Figure 2). Each message causes a delay on the communication channel, as the senders and receivers need to get ready before transferring the message. Thus, these many fine-grained Internet communications cause many delays. To remove the communication bottleneck, *Blair* asks the large language model all of these verification questions in batches (see Figure 2). Batch communication forms a small number of coarse-grained communications, which requires sending and receiving only a small number of large messages. The coarse-grained communications exchange approximately the same amount of data as the fine-grained communications, but they cause only a small number of delays in message transferring. As a result, they are much faster than the fine-grained communications in a broad-band internet connection.

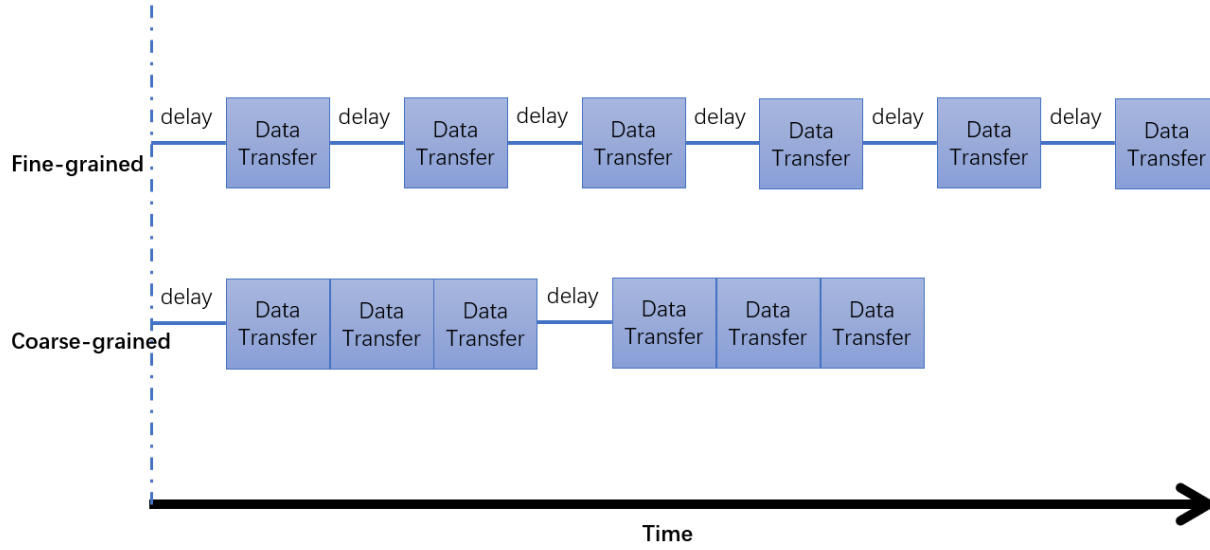


Figure 2. Schematic representation of fine-grained vs coarse-grained communication approaches in the chain of verification.

The batch-processing does not change the dynamic nature of the chain of verification. With the answers to the verification questions in batches, the dynamic selection of verification questions in the chain of verification is realized in steps (2) and (3) with decision trees. In (2), it is explained that a decision tree is a machine learning model for classification that determines the classification result by a dynamic chain of feature values, so applying a decision tree is equivalent to asking verification questions in a chain dynamically.

The answers to the verification questions are stored in a data feature table for each dataset. Machine learning models, including decision trees, require their input data to be organized as a table of features. Features represent the attributes or characteristics of the data that the machine learning model uses for prediction or classification. They are represented as the columns of the table, one column per feature. In *Blair*, each feature corresponds to a verification question designed to extract additional information from any social media post for the chain of verification. The rows of the table contain individual instances or samples of the dataset, with each instance described by the feature values in the columns. In our method, each feature value is either “yes”, “no” or “unsure”. The feature value is an answer to the verification question of the feature.

Verification questions are designed to balance accuracy and efficiency. *Blair* uses 20 verification questions that need to be answered by the large language model. These questions can be categorized into five groups: location-based questions, status-based questions, emotion-based questions, destination-based questions, and information type-based questions. These questions are detailed below:

- (i) **Location-based questions**, i.e., the questions about the author’s location with respect to the evacuation zone:
 - a. Was the author outside the evacuation zone?
 - b. Was the author near the evacuation zone?
 - c. Was the author in the evacuation zone?
- (ii) **Status-based questions**, i.e., the questions about the status of the evacuation:
 - a. Did the author decide to stay at a dangerous place that needed to be evacuated?

- b. Did the author refuse to evacuate?
 - c. Did the author want to evacuate but could not?
 - d. Had the author not yet decided to evacuate?
 - e. Was the author preparing to evacuate?
 - f. Was the author under evacuation?
 - g. Was the author returning home while their home was being evacuated?
 - h. Was the author returning home because their evacuation had been lifted?
 - i. Had the author already returned home after being evacuated?
- (iii) **Emotion-based questions**, i.e., the questions about the emotion of the evacuee:
 - a. Did the author hope not to be evacuated?
 - b. Did the author hope their evacuation would be lifted?
- (iv) **Destination-based questions**, i.e., the questions about evacuation destinations:
 - a. Was the author trying to find a place to stay as they were evacuated from home?
 - b. Did the author find a place to stay as they were evacuated from home?
 - c. Did the author offer their place for an evacuee to stay?
- (v) **Information type-based questions**, i.e., the questions about the type of information:
 - a. Does the post describe the author’s personal experience?
 - b. Is the post reported as news?
 - c. Does the post refer to a reported news story?

Although these questions cannot guarantee 100% accuracy in the chain of verification, they provide a balance between accuracy and efficiency. More verification questions can lead to better accuracy but worse efficiency, since the LLM needs to answer each verification question for each row of the data feature table.

(2) Initial models trainer

This step includes training the initial models of the chain of verification. As mentioned before, the chain of verification is an effective technique to mitigate the hallucination of the LLM. A model of the chain of verification is typically a decision tree. A decision tree is a non-parametric supervised learning algorithm used for both classification and regression tasks. A decision tree consists of decision nodes (or nodes for short) in a hierarchical tree structure. A node evaluates a feature to split the data. There are three types of nodes in a decision tree: 1) A root node is the starting point of the decision tree without an incoming branch. 2) Internal nodes are the nodes with both an incoming branch and some outgoing branches. 3) Leaf nodes are the end points without outgoing branches. They represent possible outcomes.

The chain of verification selects verification questions according to the answers to previous questions in the chain dynamically. A decision tree fulfils this dynamic question selection:

- (i) The feature of each node in the decision tree corresponds to a verification question. In other words, each node in the decision tree corresponds to a verification question.
- (ii) The node checks the answer to its verification question to determine which child node or verification question is next in the chain, which makes the dynamic question selection.

For the training, the algorithm asks the *Blair* user to label at most 100 initial samples about the relevance of each sample. These labels are the data cleaning labels, not the feature values in the

data feature table. In the machine learning problem of this sub-step, the data feature table is the input, while the data labels provided by the user form the output. These initial samples are chosen to maximize the difference in their feature values. The labels can only be “T” for true or “F” for false, regarding whether the posts are relevant to post author evacuations. To guarantee being unbiased in the chain of verification, this algorithm trains multiple initial models, and each model is trained on a different subset of these initial samples.

(3) Active models trainer

This trainer aims at progressively improving the accuracy of the models with a minimum number of additional samples to label. It is where the active learning is performed, thus there is an “active” mention in its name. Its workflow is a loop that contains six sub-steps that will be overviewed here briefly and explained in detail later:

- **Current models:** Pointing the current models to the latest models in the procedure.
- **Estimator:** Estimating the improvement of accuracy of the models on the sampled data and the uncertainty of models on each of the unsampled data.
- **Stopping criteria:** Deciding whether to exit or to continue the loop.
- **Sampler:** Selecting the most uncertain unlabeled data as samples.
- **Interactive cleaner:** Asking the user of the tool to label the samples.
- **New models trainer:** Train new models using the labelled samples from previous rounds plus this round.

A loop means the next sub-step of the last sub-step is the first sub-step, and the next sub-step of any other sub-step is the next one in this list. The loop has an entry point at the first sub-step (i.e., current models), as well as an exit point at the third sub-step (i.e., stopping criteria).

The sub-steps of this trainer are detailed here:

(3.1) Current models: For the first round, the current models will be pointed to the initial models. For each of the later rounds, the current models will be pointed to the new models trained in the previous round. Note that the current models are only pointing to the latest models, not replacing the old models with the latest models. Old and new models are both required because of the estimation of improvement in accuracy. All labelled samples until this round are involved in the accuracy estimate later. Thus, the accuracy cannot be estimated before this round, forbidding replacing the old models with the latest models.

(3.2) Estimator: There are two estimations to make, one is the improvement of accuracy, the other is the uncertainty of each of the unsampled data in the data feature table. The estimation of the improvement accuracy is calculated by comparing the accuracy of the current models and the accuracy of the previous models on all the labelled samples. The estimation of the uncertainty of an unlabeled data is calculated using the following Equation 1.

$$uncertainty(p) = \sum_{s=0}^2 q_s \log \frac{1}{q_s}, \quad [\text{Equation 1}]$$

where q_0 is the sum of confidence weights, w_i ; each of them measures the confidence of the i -th model based on votes “no” to the relevance. If the i -th model does not vote “no”, its confidence of

the vote is not added into q_0 . Similarly, q_1 is the sum of w_i that vote “unsure”, while q_2 is the sum of w_i that vote “yes”. Equation 1 is based on classic information entropy.

(3.3) Stopping criteria: The decision is made based on accuracy improvement. If the accuracy is improved in current models, the workflow is directed to (3.4) so that the loop can proceed to the next round. Otherwise, the workflow is directed to (4), i.e., the loop is stopped, and the current models become the final models.

(3.4) Sampler: The top m ($m = 50$) most uncertain data are found by sorting unlabeled data in descending order by their uncertainty values. The uncertainty values are calculated in Estimator (i.e., (3.2)). These top k uncertain data are the samples of the current round that require the user to label. We choose $m = 50$ because the human expert who performs experiments on our method feels tired if the number of samples in each round exceeds 50. The number of samples in each round cannot be too small either, otherwise the active learning will need to go through many rounds, reducing *Blair* efficiency.

(3.5) Interactive cleaner: *Blair* asks the user to label the samples obtained from the sampler (i.e., (3.4)). For each sample, the user needs to judge whether the post of the sample is relevant to the post author’s evacuation. If the post is relevant, the user puts a “T” in the label. Otherwise, the user puts an “F”. When the user replies, *Blair* checks whether all the samples are labelled. If not, *Blair* reminds the user to label all the samples. This repeats until the user finishes the labels of the samples. This “repeat” is an inner loop inside 3.5, not the loop of (3.1) to (3.6).

(3.6) New models trainer: With the new labelled samples added to the training data, the training data of the models become larger. *Blair* trains new models on the enlarged training data. *Blair* makes sure each model is trained on a different subset of the training data, so that these models together can be unbiased in the chain of verification. Note that the new models do not replace the old models directly, because both the new and the old models are used in computing the accuracy improvement in the estimator (i.e., (3.2)). Finishing this sub-step will lead the loop to (3.1) again.

(4) Clean data identification

This step identifies clean data in two parts. The first part is the labelled samples. The second part is the unlabeled data in the data feature table. These two parts are detailed as follows:

- The clean data of the first part are the sample posts labelled as relevant to the post authors’ evacuations. Since the labels are provided by the human user of our tool, these labels are usually reliable. With this confidence, the algorithm puts a “T” (meaning true) in the output label column of each post from the first part.
- The clean data from the second part are the data that are predicted as relevant by the final models of the active learning. Without confidence, this algorithm puts a “?” (meaning unsure) in the output label column of each post from this part. The human user of our tool can review the posts with “?” labels and reject some of them by changing the output label to “F”. They do not need to change “?” labels to “T” for accepting the other data because our method accepts them by default. This not only alleviates the burden of the user, but also records which part the data come from clearly. The data coming from the first part are those with “T”, while the data coming from the second part are those with “?” or “F”.

Normally the number of identified data in the second part is much smaller than the number of rows in the data feature table, which is even smaller than the amount of data in the whole dataset. So, the number of the data in the second part is usually small.

2.4.4. Data categorization and summarization

This step contains two sub-steps:

- Data categorization is performed according to aspects including evacuation decisions, destination types, and evacuation locations.
- The data are summarized according to these categories as well as user IDs, time, and geo-tags.

The sub-steps are explained here.

Data categorization: In data categorization, *Blair* instructs the LLM to extract evacuation decisions, destination types and locations from the posts in the cleaned data. More specifically, *Blair* asks the large language model to answer some questions about these aspects in a machine-readable format, and then extracts the following useful parts from the answers using regular expression matching. The parts to be extracted include:

- The evacuation decisions and their influential factors, e.g., power outage, smoke, wind, looters, and traffic congestion.
- The destination types, i.e., the types of places to stay during evacuation, including hotels, motels, rentals, relative or friend's home, designated emergency shelters, etc.
- The locations, i.e., the places with names that are mentioned in the posts.

Although the LLM needs to answer the questions in the specified format, it often fails to follow the instructions. In many cases, it answers the questions in similar formats. For this reason, regular expression matching is implemented. Regular expression matching, often referred to as regex, allows searching for specific patterns within strings. These patterns can include metacharacters, quantifiers, and other syntax to represent sets, ranges, or specific characters. The extracted parts of the answers serve as the categorization labels.

Blair instructs the LLM to perform these tasks for each post. Some posts contain some of these aspects, while others do not. Therefore, *Blair* allows the LLM to recognize the absence of these aspects. To mitigate hallucinations of the LLM in data categorization, *Blair* instructs the model to extract labels multiple times for these aspects. Only those extracted aspect labels that appear more than half of the time are considered true aspect labels.

Data summarization: The statistics of the categorized data are calculated to produce the data summarization. The statistics are the following numbers:

- Social media users that post about their evacuation;
- Relevant posts that have geotags;
- A given number of dates that have the top numbers of relevant posts;
- Relevant posts of each aspect label.

Here, whether a post is relevant to a label in a categorized aspect depends on whether the label is extracted from the post during data categorization. There are often many labels in an aspect. For example, in the aspect of the factors influencing the evacuation decisions, there can be air quality,

smoke, police shooting, looters, power outage, and many more other factors. For each label, the number of its relevant posts is calculated. Thus, there are often many numbers reported in the summary. Fortunately, they are all straightforward statistics that can be obtained by counting numbers.

2.5. Datasets

To exemplify the use of *Blair*, three datasets were used. It does not imply that *Blair* can only operate on these datasets. In fact, our method is versatile and can be applied to other datasets as well. The aim here is to assist readers in forming concrete concepts about what the use of *Blair* for this type of datasets entails.

The three datasets include the posts from Twitter (now referred to as X) about the Kincade Fire, the Getty Fire, and the Tick Fire, respectively. This section briefly describes each fire event and the Twitter datasets for each.

1. The Kincade Fire was a devastating wildfire that struck Sonoma County, California in the United States. It ignited northeast of Geyserville in The Geysers on October 23, 2019, and continued to spread until it was fully contained on November 6, 2019. This fire consumed about 315 km² (121 mi²) of land and over 186,000 residents were ordered to evacuate (Rohaert et al. 2023c).
2. The Getty Fire⁴, which occurred in Brentwood (Los Angeles, California) was a wildfire that was first reported on October 28, 2019, and containment efforts continued until November 5, 2019. The fire forced thousands of people to flee, destroyed 10 homes, and damaged 15 residences.
3. The Tick Fire⁵, which also occurred in Los Angeles County, California, burned approximately 19 km² (7.3 mi²) of land. It ignited on October 24, 2019, and rapidly expanded, posing a significant threat to over 10,000 structures. The fire forced the mass evacuation of 40,000 people from the Santa Clarita Valley and remained a challenge for firefighters due to gusty winds and high temperatures.

Each dataset of the posts is stored in a spreadsheet that represents a table with five columns: Tweet ID, user ID, Tweet posting time, geotag (if any), and the text of the Tweet, where a tweet is a Twitter post. Each row in the table corresponds to a tweet, except for the first row which serves as the table header. The Kincade Fire dataset contains 11,934 tweets, the Getty Fire dataset contains 7,609 tweets, and the Tick Fire dataset contains 4,066 tweets. The tweets in these datasets were collected by the National Research Council Canada using the Twitter API when those wildfires occurred. They were collected using the following: hashtags #KincadeFire, #GettyFire, and #TickFire, respectively.

2.6. Prototype

The *Blair* prototype for social media data mining was developed to understand human behavior during wildfires. The name, *Blair*, is short for **B**ehavior **L**abelling **A**I for **R**esearch on social media

⁴ <https://www.lafd.org/news/getty-fire>

⁵ <https://www.fire.ca.gov/incidents/2019/10/24/tick-fire>

data about wildfire evacuation. The proposed active learning method was implemented in *Blair*. *Blair* needs Dot Net (.NET) Desktop 6 runtime to run⁶.

2.6.1. Architecture

The architecture of *Blair* is shown in Figure 3.

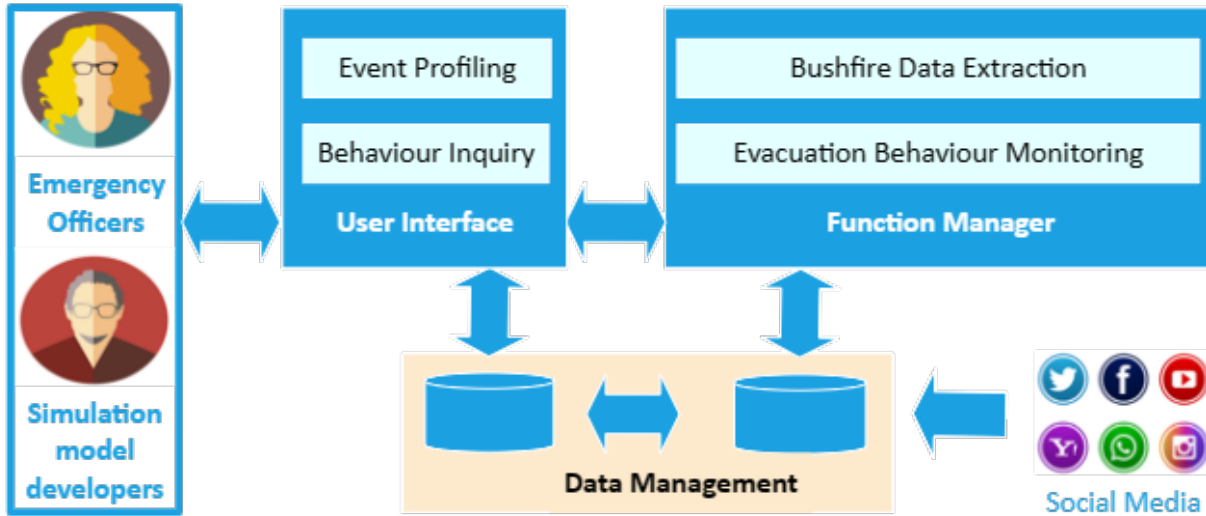


Figure 3. Architecture of *Blair* (prototype for **Behavior Labelling AI** for **Research on social media data** about wildfire evacuation).

Blair is designed to extract and mine social media data to study how people evacuate and move during wildfire events. Its design includes:

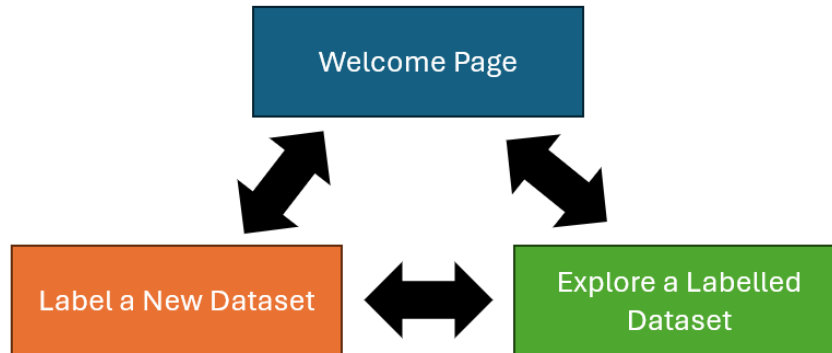
- Wildfire data extraction: It finds and categorizes data related to wildfires based on various factors, such as evacuation decisions, destination types, and locations.
- Evacuation behavior monitoring: It provides statistics on evacuation behaviors from the extracted data for monitoring purposes. However, the monitoring is performed on the collected datasets rather than monitoring social platforms in real-time.
- Graphical user interface (GUI): It supports these functions:
 - Event profiling: It summarizes basic information for each dataset.
 - Behavior inquiry: It allows users to search for behaviors by various combination of conditions, such as conditions on date range, location, evacuation decision, and destination type.
- Data management: The input data of each dataset are stored in a CSV file. The CSV file contains a table that includes these columns: text, post id, user id, time and geotag. The output data of each dataset are stored in an XLSX file. The output data contain the post id and text of each relevant post as well as its categorization labels.

2.6.2. Graphical User Interface overview

The Graphical User Interface (GUI) of *Blair* is outlined in Figure 4. The GUI has three pages, as detailed below. The user of *Blair* can navigate to the other two pages from each page.

⁶ If the user of *Blair* does not have Dot Net installed, it can be found at <https://dotnet.microsoft.com/en-us/download/dotnet/6.0>.

- **Welcome page:** When a user initiates *Blair*, it presents a welcome page. The welcome page introduces what *Blair* does. It also asks the user to set an API key of Google Gemini Pro (the large language model used in the prototype).
- **Data labelling:** The data labelling for data extraction is provided on the “label a new dataset” page. The labelling is driven by active learning, so the user only needs to label a small amount of data. The large amount of data in the rest of the dataset are labelled automatically by *Blair*.
- **Data exploration:** The last page of *Blair* supports exploring the data by presenting a summary of human behavior in the data and offering an interactive query on any such behavior.



• Figure 4. Navigation among three pages in the GUI of *Blair*.

2.6.3. Demonstration scenarios

The use of the GUI of *Blair* is here shown using the 2019 Tick Fire dataset as an example. The examples can be used to guide users into the analysis of any dataset.

Phase 1: Start *Blair*

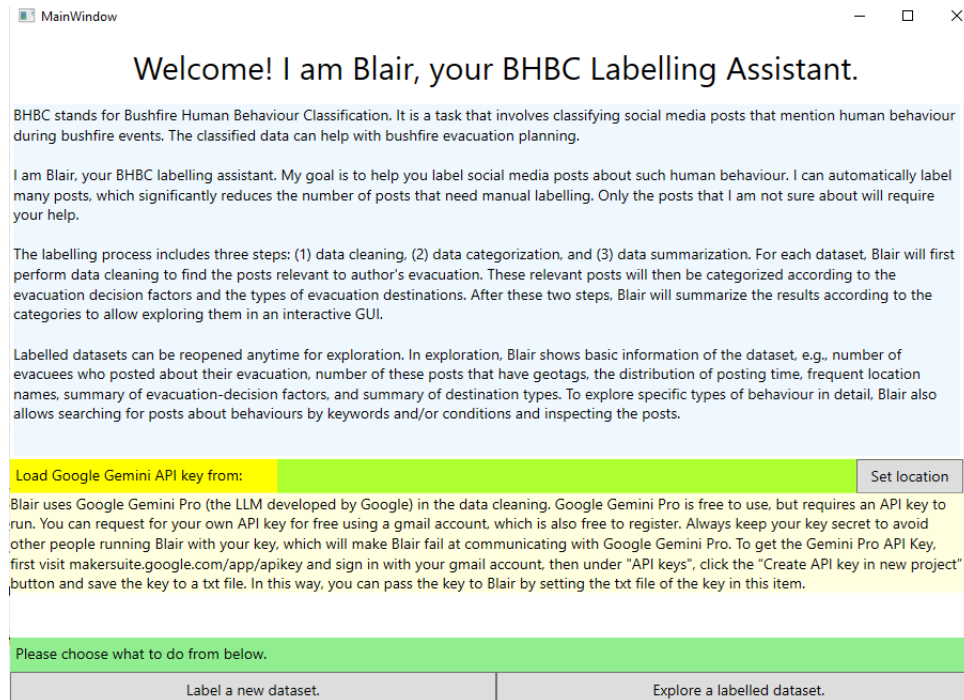


Figure 5 Screenshot of the welcome page of *Blair*.

When the user starts *Blair*, a welcome page will appear (see Figure 5). The welcome page introduces *Blair* to the user, then asks the user to provide a Google Gemini API Key from a text file. The light-yellow part of the interface explains how to get a free API key for this. At the bottom of the welcome page, there are two buttons leading to the other two pages respectively.

Phase 2: Label a new dataset

Figure 6. Screenshot of the initial “Label a new dataset” page.

The workflow in this scenario, demonstrated in Figures 6 to 11, is the same as the workflow in Figure 1. It has four steps, where the operations of each step will be detailed after the overview of these steps:

- (i) **Set input data** (Figures 6 and 7): The user sets input data on the GUI page. The collection of the input data must follow the earlier explained methodology before setting the data.
- (ii) **Start LLM-based data cleaning** (Figure 8): The algorithm performs the data cleaning when prompted by the user clicking a button.
- (iii) **Optimize data cleaning based on active learning** (Figures 9 and 10): The operations are consistent with the loop in subsection 4.3.3. Blair works with the user interactively to optimize the data cleaning results for several rounds.
- (iv) **Get data-cleaning output** (Figure 11): The operations for the identification of final data-cleaning results are performed. After clicking a button to obtain the output results, the user needs to review a small number of results marked with “?”.

The operations of these steps are detailed as follows:

Set input data: As the user enters the “Label a New Dataset” page, they will see the GUI as shown in Figure 6.

First-time users might not know about what is input data and what is output data. They are probably unfamiliar with other elements on this page as well. The “?” buttons are prepared for them. Clicking a “?” button will show the help tip for the corresponding part. Figure 7 shows what the page will become if we click some of the “?” buttons. Please note that each help tip can be hidden using the same “?” button that reveals it.

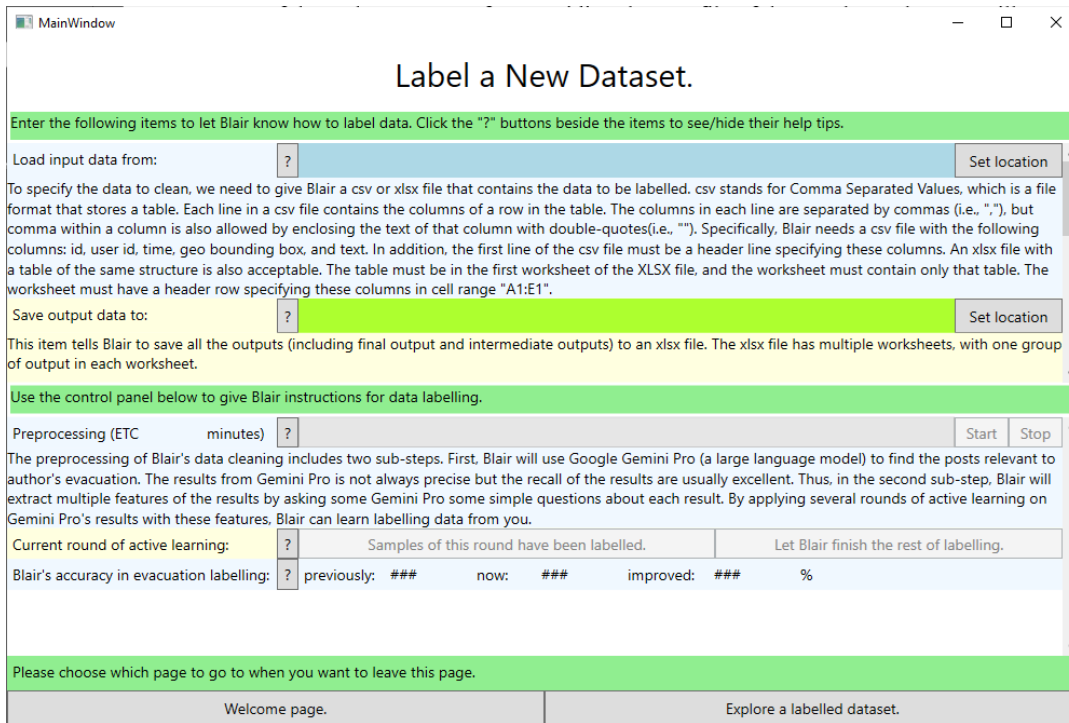


Figure 7. The “Label a New Dataset” page with some of the help tips shown.

Start data cleaning: Once the user sets the input and output files for labelling and clicks the “start” button in the control panel, *Blair* will preprocess the input data and obtain the first-round sample of active learning, as shown in Figure 8. The computational time for preprocessing will depend on the size of input dataset. For example, the Kincade Fire dataset that was used in this project contained 11934 posts. The use of a windows-machine with Intel Core i7-9750H CPU @2.6GHz and 32GB memory resulted in six hours for preprocessing during our tests. The preprocessing time is (approximately) linearly proportional to the number of posts in the dataset. The progress bar of preprocessing tells us how much work Blair has finished in this preprocessing task. The ETC (*Estimated Time of Completion*) in minutes on the left of the progress bar provides an estimate on how much time it needs to finish the rest of preprocessing. The “Stop” button on the right side can stop the preprocessing temporarily if, for example, the user wants to close the computer for a while.

Figure 8. The “label a new dataset” page with the preprocessing task started.

Optimize data cleaning based on active learning: After the preprocessing is finished, the user will find the “Start” and “stop” buttons disabled and the two active learning buttons below the preprocessing progress bar enabled. As shown in Figure 9, disabled buttons are greyed while enabled buttons are presented in their normal color. The two active learning buttons, i.e., “Samples of this round have been labelled” and “Let Blair finish the rest of labelling”, are for different purposes. The “Samples of this round have been labelled” button is used to tell Blair that user has labelled the samples of the current round in a worksheet named “Round x samples” in the output file, where x is the index or number of the current round shown on the control panel of this page. Figure 10 shows the “Round 0 samples” worksheet of the output file in Microsoft Excel. Column C are the labels the user manually puts into the worksheet. The Blair user needs to determine the labels according to the texts in Column B. The texts in column B are the texts of the sampled posts. Round 0 will normally have 100 samples while each of the later rounds has no more than 50 samples. After saving the labels of these samples, the user can click the button “Samples of this round have been labelled”. Blair will start the next round of active learning and give the user a new round of samples to label, so that it can learn from the user how to label the rest of the data. As shown in Figure 11, the change in the accuracy is shown in the control panel to determine when to end the active learning. If the percentage of improvement is too small (e.g., less than 1%) or negative, the user can click “Let Blair finish the rest of labelling” to get a final output. Figure 11 shows that the improvement of accuracy is “-1.1” in round 4 of active learning, so the user can click “Let Blair finish the rest of labelling” in this round. Note that there is no need to label round 4 samples before clicking that.

ID	text	relevance
118752396	@ProFREWjr Yes from the #Tickfire. There's a new fire in the Sepulveda Basin but it's not big enough F	
118778983	Yes at the #TickFire https://t.co/LZCAnXTf9e F	
118758054	Never been evacuated for a fire before. First time for everything I guess 🙄 #TickFire 🙄 T	
118750566	Currently about to evacuate and my eyes and throat is BURNING from the air and ash falling omg #tic T	
118758053	Some of my family is being evacuated due to the #TickFire. I'll be off here for the most part until I an F	
118867880	@GavinNewsom How does one get help? Where can we go?? Is there a website, phone number, off F	
118773734	In what is starting to feel like an annual event, friends, family members, and extended family mem T	
118757970	My cousin's house before he evacuated. That was about 5 hours ago so his house is probably gone. # F	
118773230	This was what my house looked like at 2:15am this morning when we had to evacuate. We didn't get T	
118811552	After being evacuated from my home due to wild fires I checked into the @Residencelnn in El Segur T	
118748902	🚒URGENT FIRE ALERT 🚒 #TickFire is approaching #TheGentleBarn quickly and we're under MANDA T	
118749782	#TickFire Sigh. And my hose has a hole in it. ./ I need to run out and get a new one right now. The dai F	
118797250	Evacuation lifted. Get to go home tomorrow!! Wondering how close the fire got to us and what we'll T	
118789205	Day two of evacuation 😊 #TickFire T	
118792307	I'm still under evacuation. I haven't been home since I left for work Thursday morning. #TickFire T	
118748955	This is the #tickfire from my front yard. Looks (frighteningly) closer than it is... https://t.co/BGsaztqD F	
118759595	So we had to evacuate. My daughter said it feels like we're in a dream. #tickfire #SantaClarita T	
118759615	I got evacuated 😊 #TickFire T	
118750164	#tickfire this is from my front porch. 🙏 prayers for all those effected https://t.co/KUbausz81 F	
118768603	I've been awake all night waiting for police to tell me it's time to leave. The smoke is horrible. My dc F	
118781662	@CaltransDist7 @santaclarita @PalmdaleCity @cityoflanaster @CHP_Newhall #GranadaHills to #Lai F	
118798821	Heres some more vids of the fire by my house still praying and hoping out house is okay 🙏 thanks (F	
118761023	@CPVenturaBeach. Checked in, grabbed a margarita at the bar, & made it JUS T	
118781423	The context on the fire related ones is the #TickFire is way too close to my house and I got evacuate T	

Figure 9. Labelled round 0 samples in the output file.

Label a New Dataset.

Enter the following items to let Blair know how to label data. Click the "?" buttons beside the items to see/hide their help tips.

Load input data from: D:\Data\Blairs\tickfire.csv [Set location]

Save output data to: D:\Data\Blairs\tickfireoutput.xlsx [Set location]

Use the control panel below to give Blair instructions for data labelling.

Preprocessing (ETC minutes)	?	[Start] [Stop]
Current round of active learning:	4	[?] Samples of this round have been labelled. [?] Let Blair finish the rest of labelling.
Blair's accuracy in evacuation labelling:	?	previously: 0.77 now: 0.76 improved: -1.1 %

Please choose which page to go to when you want to leave this page.

Welcome page. [] Explore a labelled dataset. []

Figure 10. A screenshot showing that the accuracy improvement is too small in this round (less than 1%). Therefore, the user can click the button: "Let Blair finish the rest of labelling".

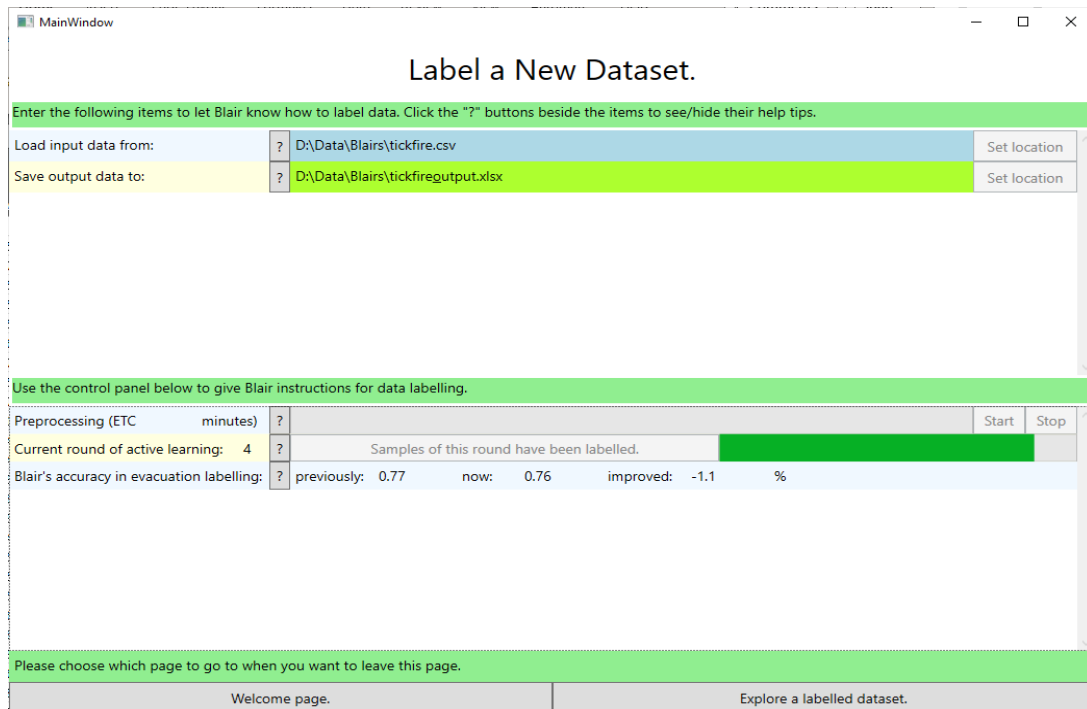


Figure 11. A progress bar appears on the “Let Blair finish the rest of labelling” button to tell you the progress of final output generation.

Get data-cleaning output: Clicking the “Let *Blair* finish the rest of labelling” button allows the user to obtain the output. After clicking the button, Blair will take about 20 minutes to generate the final output. A progress bar on that button will show the progress of output generation, as shown in Figure 11. The user needs to review the results in the “Final output” worksheet of the output file and replace some of the “?” labels with “F”.

Phase 3: Explore a labelled dataset

On the “Explore a Labelled Dataset” page of *Blair*’s GUI, the user can explore a dataset labelled using the “Label a New Dataset” page. The exploration has two steps: data summarization and interactive query of bushfire evacuation behavior.

Data summarization: Opening the output data file on the “Explore a Labelled Dataset” page, the user will be provided with a summary of the labelled data as shown in Figure 12. Note that in Figure 12, there is highlighted text reminding the user to review the final output and review some posts in the final output, change the “?” labels to “F” to reject them as irrelevant posts, for better data exploration. The user only needs to review a small number of posts, as normally there are only a small number of those with “?” in “About author’s evacuation” column in the spreadsheet of the final output, so it will not take too much of the user’s time. In this way, *Blair* obtains user-confirmed results for quality exploration of the dataset.

Interactive inquiry: Switching to the tab “Interactive Inquiry of Evacuation Behavior” on the same page allows the user to query the posts with specified conditions. Figure 13 shows, as an

example, that there are five matched posts for a query with time condition (find posts between “24/10/2019 – 26/10/2019”) and location condition (find posts mentioning “canyon country”).

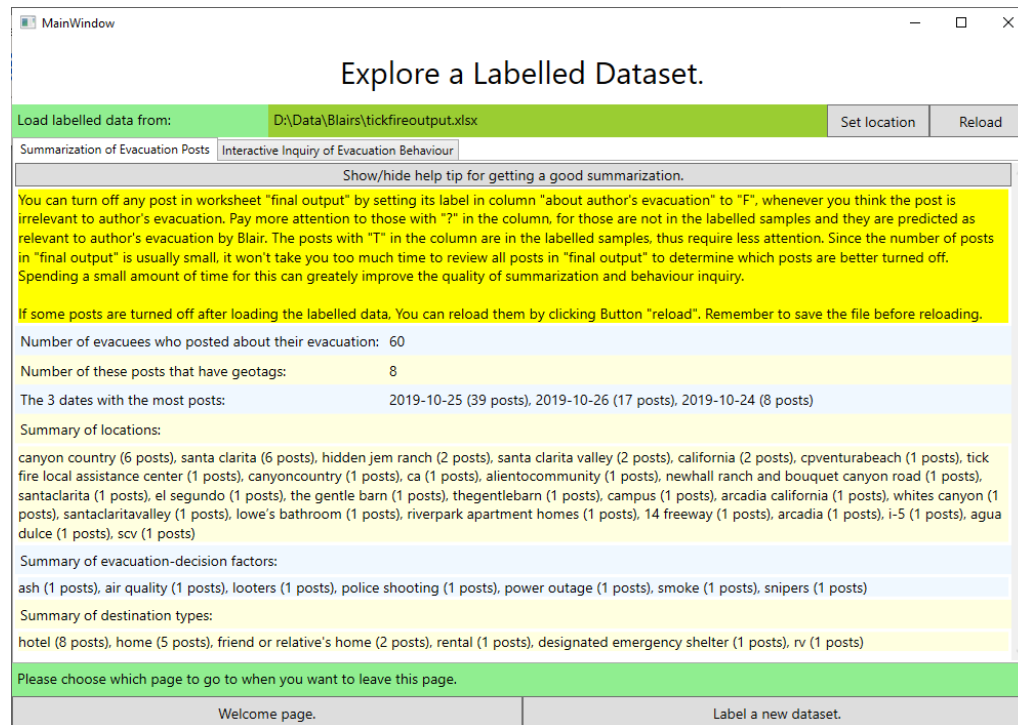


Figure 12. Summarization of the labelled dataset on page “explore a labelled dataset”.

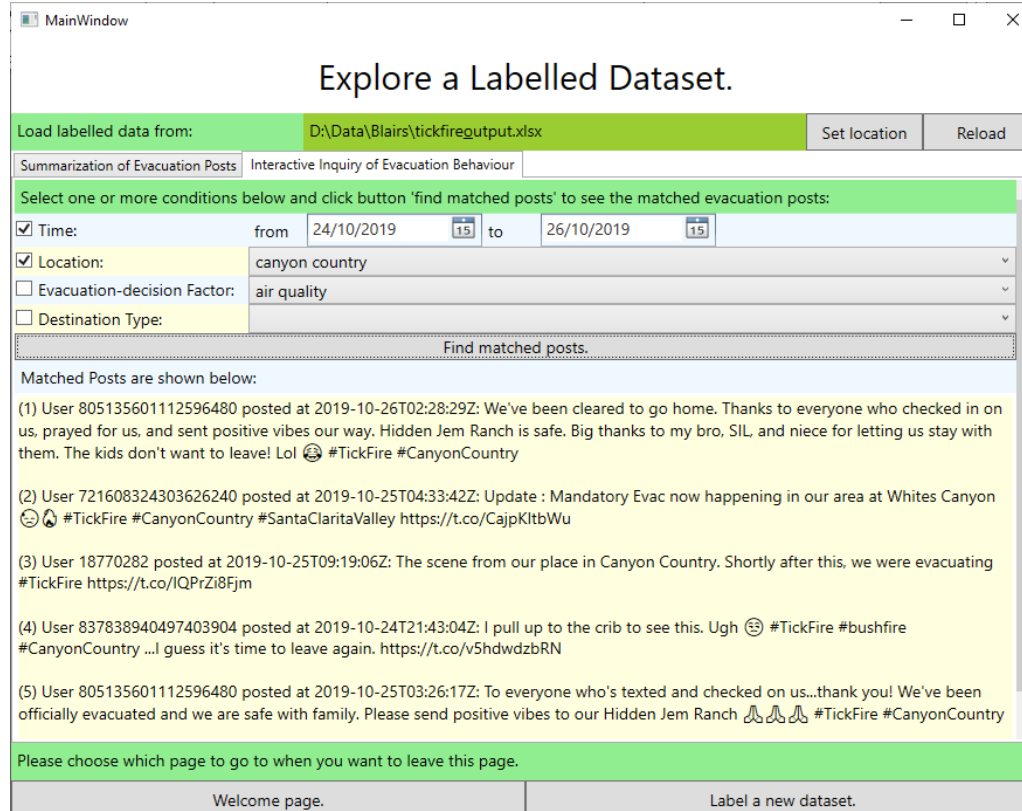


Figure 13. Five posts are matched for a query with time and location conditions.

2.7. Testing

We have conducted two groups of tests for the accuracy evaluation of data cleaning results, and another group of tests to evaluate the accuracy of data categorization.

- **A/B tests (also known as split testing)** are first conducted on the data-cleaning algorithms. This included comparing four versions of the data cleaning algorithms for each dataset with respect to whether each post is relevant to the post author’s evacuation. One of these algorithms is the final adopted algorithm of *Blair*. The adopted algorithm provides the user-confirmed results of *Blair* (i.e., those shown on *Blair*’s data exploration page, see earlier section of this report for details).
- The second group of tests are the **effectiveness and efficiency tests** for data cleaning. For this purpose, data cleaning results are compared between those with *Blair* and those without *Blair*. *Blair* results are those produced by the tool and confirmed by the user. The results without *Blair* are from the manual labels of two human experts in the Kincade Fire dataset. Manual labels are referred to as the labels manually assigned by human experts without using *Blair*.
- The last group of tests are the **validation tests**. The tests are performed using ground truth of the categorization labels in the final output. The ground truth is provided by a human expert.

In these experiments, we use recall, precision, and F1 score to compare the results.

- **Recall** measures how well a model identifies true positives out of all actual positive instances. It answers the question: “Of all the actual positive cases, how many did the model correctly predict?” So it is the ratio between relevant retrieved instances and all relevant instances.

$$Recall = \frac{Relevant\ retrieved\ instances}{All\ relevant\ instances}$$

- **Precision** assesses how well a model predicts true positives among all predicted positive instances. It answers the question: “Of all the predicted positive cases, how many are actually positive?” So it is the ratio between relevant retrieved instances and all retrieved instances.

$$Precision = \frac{Relevant\ retrieved\ instances}{All\ retrieved\ instances}.$$

- The **F1 score** combines both precision and recall into a single metric, providing a balanced evaluation of the model. It is the harmonic mean of precision and recall.

$$F1 = \frac{2}{\frac{1}{Recall} + \frac{1}{Precision}}.$$

For each of the metrics above, the higher the metric value the better. Precision and recall are two metrics for trade-off. It is usually not possible to obtain high scores for both at the same time. In many other research projects (e.g., (Miao and Zhu 2022)), methods draw upon a precision-recall curve, and let the users of their methods select a good balance between these two metrics. This is

not feasible for *Blair*. There is no parameter to control the trade-off efficiently because the data labelling process is very time consuming. To remedy this issue, the most balanced setting is currently adopted as default so that this task is released from the user.

2.7.1. Testing on data cleaning algorithms

During the development of our *Blair* prototype, four different algorithms of final output generation were tested, giving the following four set of results:

1. Results from *Blair*'s labels confirmed by user review, referred to hereafter as "confirmed results". These results are adopted in the final version of our prototype. So, the algorithm giving these results is the final adopted algorithm in *Blair*.
2. Results from *Blair*'s labels confirmed by the condition of the text containing the following keywords: "evac", "reloc", "leave" and "left", referred to hereafter by "keyword confirmed results". In other words, if *Blair*'s label is "T" or "?" and the text of the post contains any of those keywords, a post is in this set of results. Keyword confirmed results are not adopted in our final prototype.
3. Results from *Blair*'s unconfirmed labels, referred to as "unconfirmed results". These are the final output results before the user reviews them and turns off the irrelevant results by replacing "?" or "T" with "F" in the label column. Unconfirmed results are not adopted in the final *Blair* prototype.
4. Keyword filtering results without *Blair*, or "keyword filtering results" for short, are where the keywords are the same as #2, i.e., if a post contains any of those keywords, it is in this set. Keyword filtering results are not adopted in the *Blair* final prototype.

In this set of four tests, results for each dataset are compared with respect to whether each post is relevant to the post author's evacuation (i.e., the data cleaning results) as introduced before the output part of the problem definition. Confirmed results are the most reliable set of data cleaning results because they are confirmed by the *Blair* user (i.e., a human expert may be more reliable than an algorithm when the data to analyze is in a small number (Kumar and Sharma 2022)), so the confirmed results are considered as ground truth for the comparisons in Figures 14 to 17. These figures show the accuracy of these four sets of results in three metrics: recall, precision, and F1 score. Figures 14 to 17 shows their accuracies for the Kincade Fire dataset, the Getty Fire dataset and the Tick Fire dataset respectively.

Blair adopts confirmed results on its data exploration page, which are the best compared with the other three sets of results, i.e., it has the highest recall, precision, and F1 score at the same time. In particular, the confirmed results are 669%, 614%, and 614% better than keyword filtering results in the F1 score of the Kincade Fire dataset, Getty Fire dataset, and Tick Fire dataset respectively. This is why *Blair* adopts these confirmed results for data exploration.

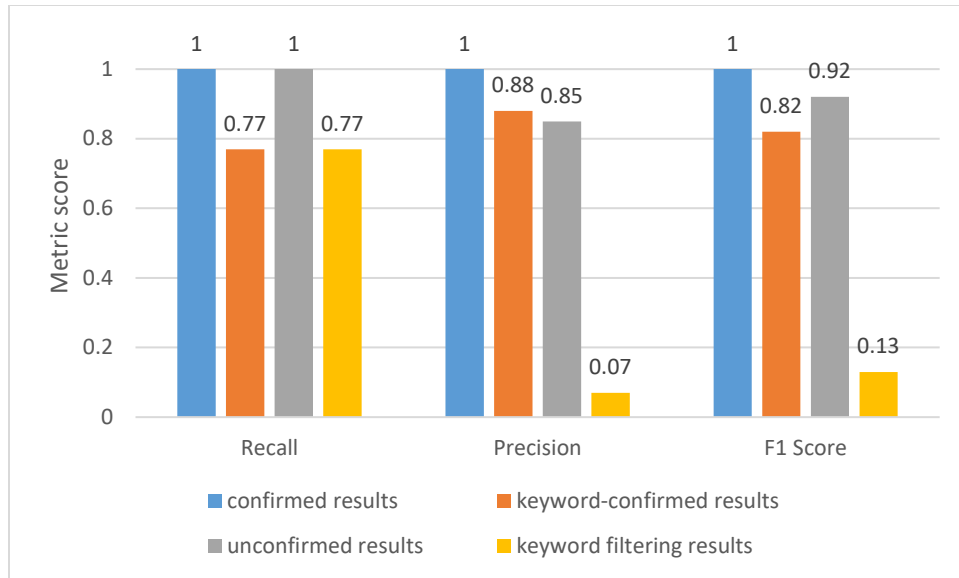


Figure 14. Data cleaning accuracy evaluation without manual labels in the Kincade Fire dataset.

For the F1-score in the Kincade Fire dataset shown in Figure 15, confirmed results are 21% better than keyword confirmed results, 8% better than unconfirmed results, and 669% better than keyword filtering results.

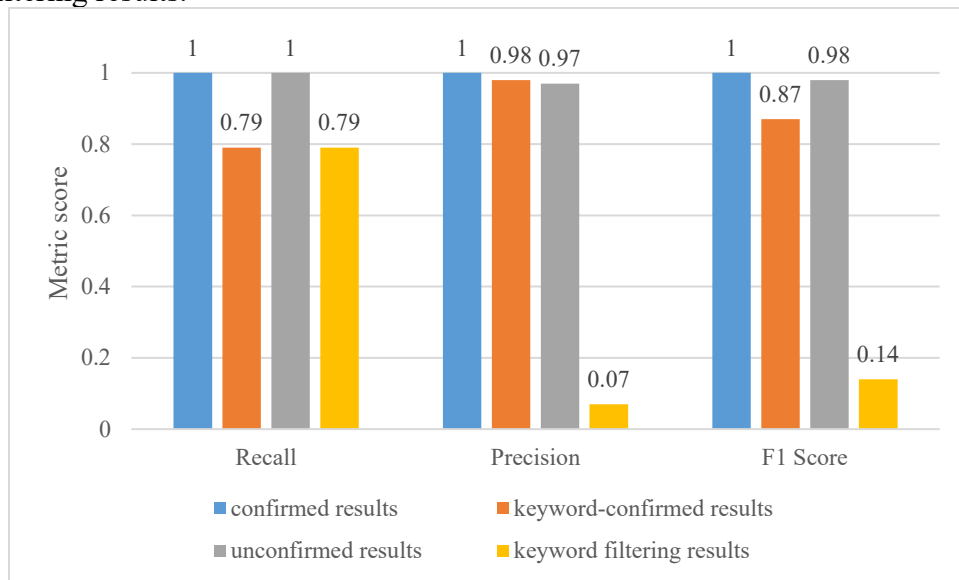


Figure 15 Data cleaning accuracy evaluation without manual labels in the Getty Fire dataset.

For the F1-score in the Getty Fire dataset shown in Figure 15, confirmed results are 14% better than keyword confirmed results, 1% better than unconfirmed results, and 614% better than keyword filtering results.

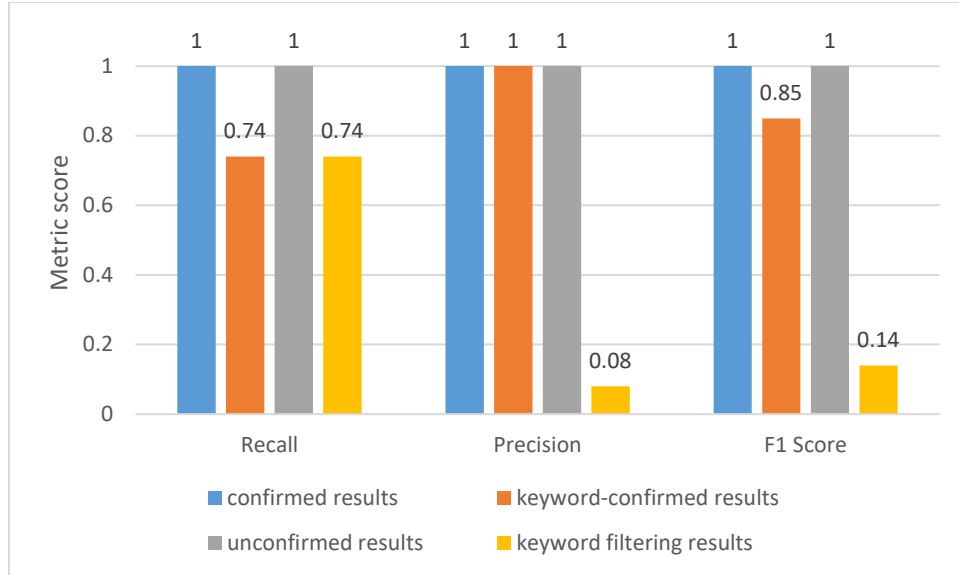


Figure 16 Data Cleaning Accuracy Evaluation without manual labels in Tick Fire dataset.

For the F1-score in the Tick Fire dataset shown in Figure 16, confirmed results are 17% better than keyword confirmed results, as good as unconfirmed results, and 614% better than keyword filtering results.

2.7.2. Comparing data cleaning accuracy to human experts

In this set of tests, the confirmed results from *Blair* were compared with the results from manual labelling with respect to whether each post is relevant to the post author's evacuation. The manual labels are obtained without using *Blair*. To acquire manual labels, the entire dataset is labelled by human experts. For this task, two human experts in the research team manually labelled the Kincade Fire dataset. Together, they found 91 posts where the posts' authors discussed aspects of their *own* evacuation process during the respective fire event. *Blair* found 220 relevant posts that were confirmed by user review in only one day, which is 241% as many of the manual labelled results and 14 times faster. Among these 220 posts, there were 28 manually labelled results that were not included in *Blair*'s confirmed results. However, *Blair* was able to uncover 157 additional relevant posts (i.e., confirmed results) that the manual labelling process missed. Assuming that the ground truth is a combination of the manually labelled results and *Blair*'s confirmed results, *Blair*'s results have a significantly higher recall (0.88 vs 0.36) and F1-score (0.94 vs 0.53) while the precision is guaranteed to be 1 as in both cases, the relevant posts are confirmed by human experts (see Figure 17).

Some examples of the manually labelled results that were not identified as relevant in *Blair*'s results are listed below:

- (1) "Made it to [REDACTED], lets hope the fire doesnt follow me...that wind is no joke but really the scariest thing is the lack of smoke..you cant see it or smell it even near the evacuated areas cuz the wind is blowing it away so the fire can really sneak up on u #Kincadefire"
- (2) @XXXX [REDACTED] @XXXX [[REDACTED]] We wanted to stay in SF as evacuees from #KincadeFire. Couldn't go to SF (where lodging was offered) - because our possessions were in car. Pretty sad state of affairs with car break-ins so common. :-(

- (3) All centers full in [REDACTED]. [REDACTED] center itself evacuating. We can't get out of our driveway because it's a solid traffic jam (and this is a side street). It seems they need more evacuation centers if they put this many people on mandatory evacuation. #kincadefire
- (4) Still evacuated. Down in [REDACTED]. Second day out. No power. Charging phones from cars. ❤️ to all. Be safe. #kincadefire
- (5) "Temperatures have increased dramatically #KincadeFire (my #[REDACTED] family evacuated last night, staying with my 92/89 year old parents with no power in #[REDACTED])"

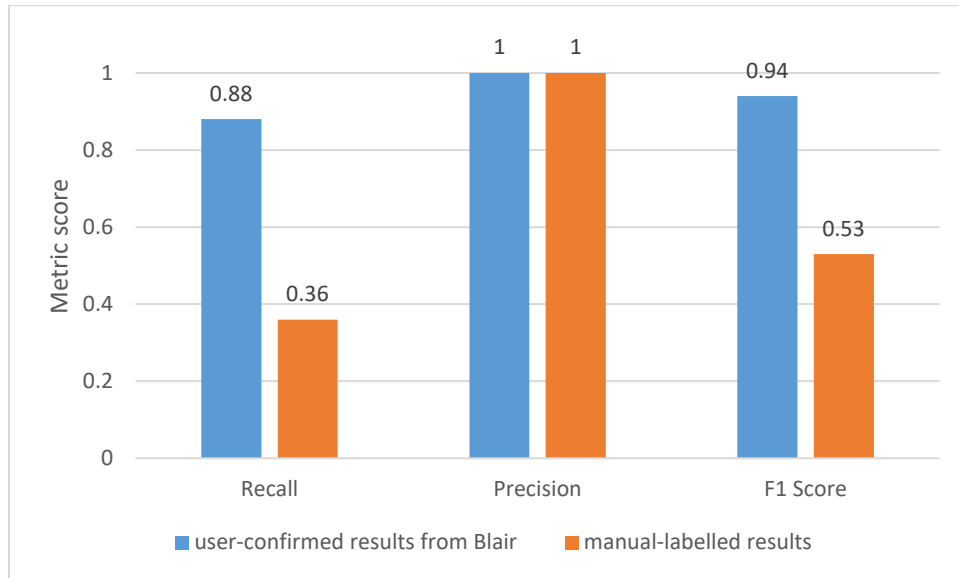


Figure 17. Data cleaning accuracy evaluation with manual labels in Kincade Fire dataset.

Some examples of *Blair*'s evacuation-related results that were not identified during the manual labelling process are listed here:

- (1) Evacuation, round 2. This time at night with more family in tow. #kincadefire
- (2) Normal lifestyle tweets will resume next week, but wanted to let everyone know about the professional + friendly staff @ XXXX [REDACTED] in San Francisco who kindly gave me a special rate when I had to evacuate because of the #KincadeFire. Lovely boutique hotel #[REDACTED] #[REDACTED]
- (3) We just got back to our home safe and sound after being evacuated. @XXXX [REDACTED] and @ XXXX [REDACTED] are, along with all the first responders involved, truly amazing. Thank you! #kincadefire
- (4) This is how we roll. So thankful to our friends letting us stay at their home while we wait out the #kincadefire #evactuationlife
- (5) We are immensely grateful to the team of @XXXX [REDACTED] and many local districts who strategically managed this unbelievable response #KincadeFire fire buffer right at our doorsteps. We are safe home now taking it all in and checking in on #wellbeing #resilience with neighbors.

2.7.3. Accuracy evaluation of data categorization

In this group of tests, the accuracy of data categorization for each dataset was evaluated by comparing the data categorization labels from *Blair* with the data categorization labels from a

human expert in our research team, who is also the developer of the *Blair* prototype. The evaluation results are shown in Figures 18 to 20.

Figure 18 shows the accuracies of data categorizations in the Kincade Fire dataset using three metrics: recall, precision and F1 score. Since there are three aspects of data categorization: locations, evacuation decisions, and destinations, Figure 18 shows three bars in each metric. It was found that the recall, precision, and F1 score of locations are the highest among the three, those of destination types are the second highest, and those of factors are the lowest. This is due to different levels of difficulty in labelling the categories in these aspects. Locations are the easiest to label since they are explicitly mentioned in the posts with mostly fixed words. Destination types are the second easiest to label since they are often explicitly mentioned in the posts with words varying from post to post. Evacuation-affecting factors (i.e., the factors affecting evacuation decisions) are rarely explicitly mentioned in the post. Instead, the factors must be discovered with some reasoning, thus they are the most difficult to label among these three aspects.

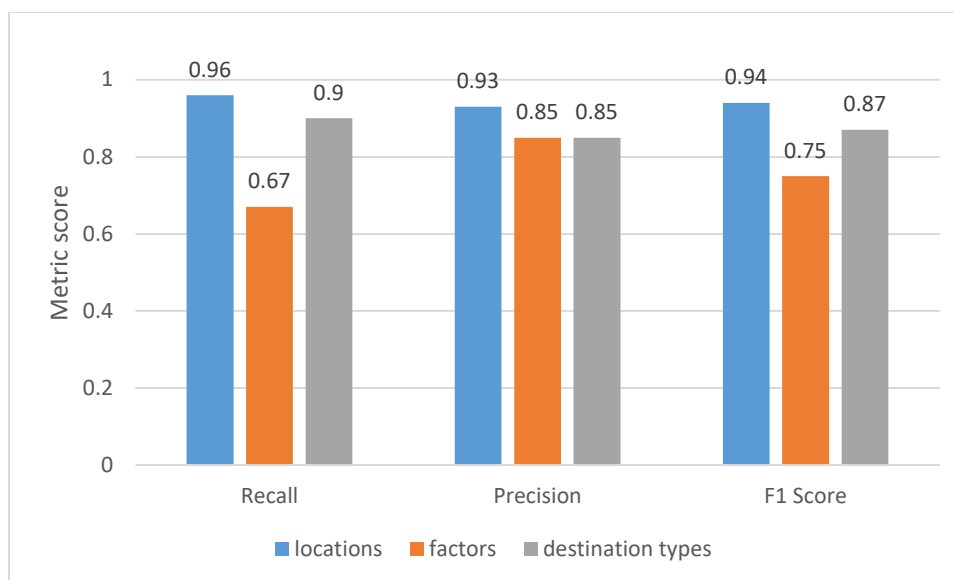


Figure 18. Data categorization accuracy in the Kincade Fire dataset.

Figure 19 shows the accuracy of data categorization in the Getty Fire dataset. The accuracy is still the highest in location, the second highest in destination type, and the lowest in factors that influence evacuation decisions. However, the precision of the factor labelling in this dataset is much lower than it is in the Kincade Fire dataset. This is probably due to the fact that the Getty Fire occurred in Los Angeles (a larger city) while the Kincade Fire occurred in Sonoma County (a more suburban county/region). The quantity of factors affecting evacuation decisions in a fire in proximity to a city are often more than the factors far away from the city because there are more people and more facilities in a city.

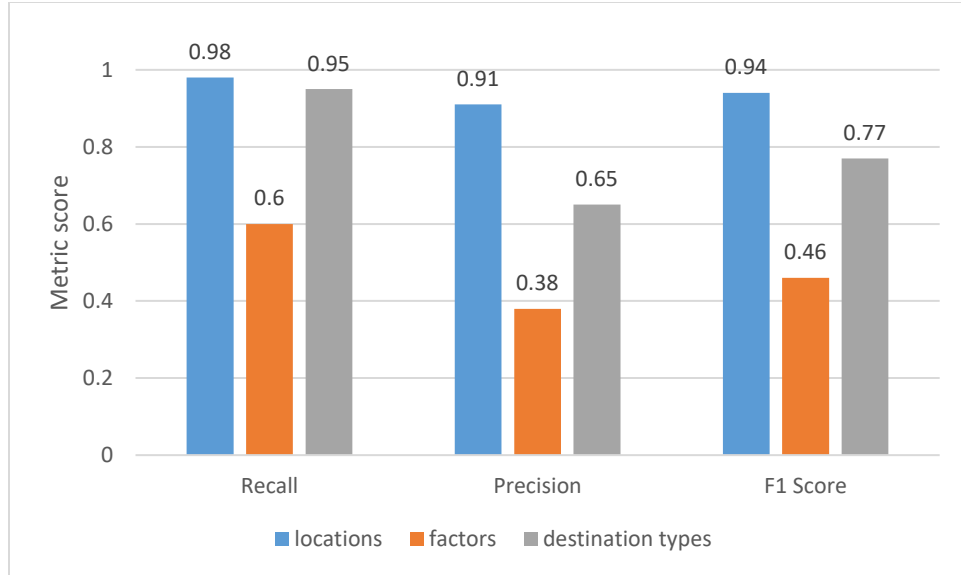


Figure 19. Data categorization accuracy in the Getty Fire dataset.

Figure 20 shows the accuracy of data categorization in the Tick Fire dataset. The accuracy in this dataset is similar to the accuracy in the Getty Fire dataset. Since the Tick Fire occurred near Los Angeles and the Getty Fire occurred in Los Angeles, their similarity is understandable. The destination type labelling is more accurate in this dataset than those in the other two datasets. This speculation is possibly linked to the differences in type available for evacuation (e.g., the Tick Fire spread very fast and thus, many posts were probably written in haste with straightforward information about destination types).

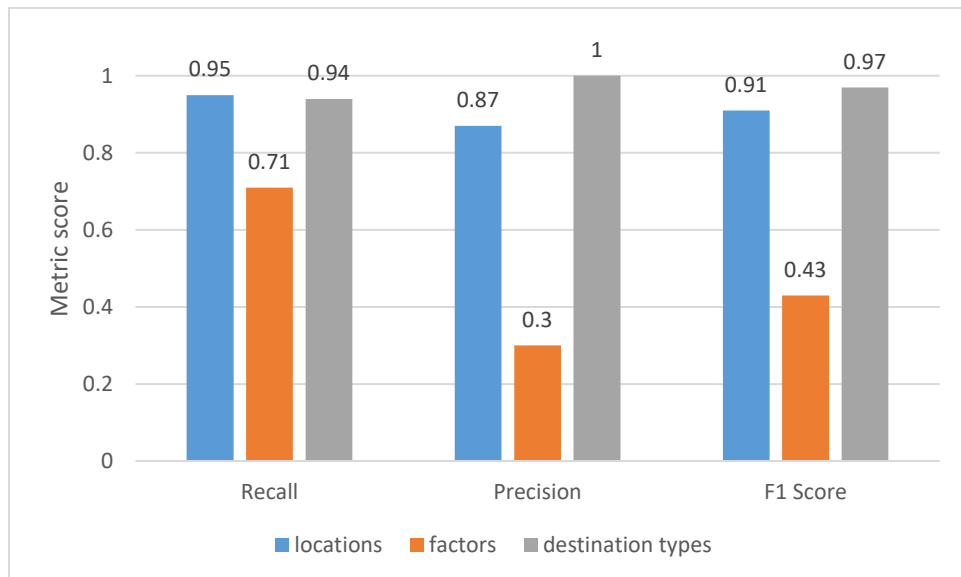


Figure 20 Data categorization accuracy in Tick Fire dataset.

2.8. Findings, limitations and future work

A methodology and a tool for social media data mining of wildfire evacuation behavior, called *Blair* were developed in this part of the work. *Blair* is able to provide some important insights about human behavior during wildfire evacuation scenarios. A list of key findings is presented here along with *Blair* limitations and suggested future work.

Considering the limitations, the review revealed that by analyzing the GPS coordinates (so called “geotags”) of tweets from evacuees, researchers can gain insights into evacuation and return times. Unfortunately, this approach (Kumar and Ukkusuri 2020) was not applicable to our task given the small number of posts with geotags. This is not uncommon as wildfires may be associated with power outages. A text analysis was instead conducted. This implies that there may be a mismatch between the content of the text and the exact location where the post was written.

Data protection issues should also be considered when using social media data mining methods. For instance, the LLM used could be installed on a local server to protect data. The large language model adopted in *Blair* is the Google Gemini Pro on Google’s server, thus meaning that we currently rely on Google’s privacy principles in regards to data protection.

Besides the generic challenges to social media data mining (i.e., uncertainty and ambiguity), there are more challenges unique to the wildfire application field. As described earlier, *Blair* analyses wildfire evacuation behavior considering first-hand information. The analysis is conducted on the fine-grained details contained in only a very small fraction of the social media posts, i.e., relevant to wildfire evacuation behavior. The fine-grained level of detail is much higher than in many other social media data mining methods for disaster/hazard analysis. For example, (Houston et al. 2015; Zhang et al. 2019; Martín et al. 2020) identified social media posts relevant to disaster/hazard events but not specifically on evacuation behavior. For comparison, the datasets of Twitter (X) posts adopted in the case studies about three California wildfires, 100% of the posts were relevant to the hazard (i.e., a wildfire) but only 1-2% of the posts were relevant to evacuation behavior. The number of tweets (i.e., Twitter posts) relevant to an individual’s own, personal evacuation journey is smaller than the number that was expected. For example, the Kincade Fire dataset contained 11,934 posts, with an expectation of over 1,000 posts being relevant to our application field. Nevertheless, less than 220 posts were eventually found relevant. This corresponds to 1.8% of the dataset. Similarly, only 146 relevant posts (1.9%) are found in the Getty Fire dataset that contains 7609 posts, and only 75 (1.8%) are found in the Tick Fire dataset (4066 posts). However, the tweets identified as relevant did present first-hand information in a rich context. This implies that social media data mining can identify some distinct and important evacuation behaviors that can be used by researchers and/or practitioners interested in better understanding evacuation-related trends in previous fire events.

Retrieving social media posts about a specific wildfire is relatively simpler than retrieving posts about other types of hazards. It is speculated here that this is because wildfires occur frequently in some regions, and when they happen, they require urgent community engagement. As a result, hashtags are commonly used for faster responses on social media. In addition, multiple wildfire events often occur simultaneously, necessitating event-specific hashtags.

The use of a LLM for social media data mining was found to be very useful. For example, in the Kincade Fire dataset with 11,934 posts, using a LLM (Google Gemini Pro), *Blair* found 220 relevant posts in one day, while two human experts of our group found only 91 relevant posts over a two-week period. To be fair, the human experts have other priorities in their work and daily lives and it is estimated they committed approximately 50-60 hours in total for this task. However, this is exactly the point of using automated AIs. Humans cannot focus on a task 24 hours a day while AI tools can. The resulted improvement in efficiency and accuracy is encouraging.

The literature review also helped identify a range of open challenges: 1) Social media data can be noisy and contain irrelevant or misleading information (including fake news). Distinguishing between reliable information and misinformation is a critical challenge; 2) Social media data may not be representative of the entire population, potentially leading to biased insights. Addressing these biases and ensuring the inclusivity of the analysis is important; 3) Determining the exact location of users during evacuations is crucial. Geolocation data can be inaccurate or missing, making it difficult to identify users in affected areas; 4) Interpreting social media posts requires understanding of the context, as statements may not always be straightforward. Also, determining the urgency and severity of evacuation-related posts can be difficult; 5) During wildfire emergencies, people may use non-standard language, abbreviations, or domain-specific terms. Developing accurate language models and lexicons for hazard-related content can be difficult; 6) People share information through various media formats, such as text, images, sounds and videos. Integrating and analyzing these diverse data sources to gain a more comprehensive understanding of behaviors is a challenge.

In *Blair*, while not all existing challenges of social media data mining are fully addressed, a rather refined level of categorization is possible. The categorization requires an understanding of the post contents and allows categorizing data according to evacuation decisions, destination types and locations. Previous work (Li et al. 2021) categorized behavior into two categories (pre-evacuation and on-evacuation) or categorized social media posts according to direct and indirect witnesses of the evacuation behavior (Morshed et al. 2021). Therefore, *Blair* is deemed to bring a positive contribution in the research efforts related to social media data mining for evacuation scenarios.

A known issue of social media data mining is that the boundaries between relevant and irrelevant posts are often unclear. The judgement of the relevance might even vary among different human experts. To address this issue, other research efforts (Li et al. 2021) may involve many manual steps to perform the data analysis. *Blair* is based on the premise that reducing the manual steps is preferable in achieving high performance in terms of both effectiveness and efficiency.

Another important aspect to consider is the situation in which the questions used in active learning trigger more false positives, i.e., situations in which the entropy of the decision tree becomes greater and information gain becomes lower. This means that future research could explore ways to optimize the number of iterations in active learning by systematically testing and designing the set of questions asked by the LLM.

In the future, additional research is needed to further advance and improve the prototype. For instance, inspired by the evaluation results obtained, features for both LLM-filtered data and keyword-filtered data can be extracted. Currently, the extracted features for LLM-filtered data

have already been used in *Blair*, but the extracted features for keyword-filtered data have not. Using both approaches can improve the accuracy of results. In addition, automatic keyword selection for the keyword filtering step is also worthy of exploration. In our testing, only four keywords, i.e., “evac”, “reloc”, “leave”, and “left”, were used. Future research can consider extracting other keywords semantically related to “evac”.

The data exploration step of *Blair* can be further improved. For example, evacuation routes can be shown on a map; there are other evacuation-related decisions that are not currently captured in the prototype, that can be added in the next version, including mode and route choice. Additionally, several tweets identified the exact city or geographical direction of travel in which the evacuee travelled to reach their destination. This is not currently tracked in the prototype, and *Blair* could therefore be expanded to capture this important information. Geotag monitoring can also be added for datasets with abundant geotags. Comparison of data summaries between different wildfire events can be performed as well.

2.9. Conclusions

In this chapter, the domain of social media data mining to understand human behavior during wildfire evacuations was investigated. A new data-mining approach was proposed using a combination of techniques including large language model and active learning. The *Blair* prototype was introduced as well. Through extensive testing, *Blair* has proven its capabilities: it can accurately and efficiently discover a high number of relevant posts when compared with manual labelling by human experts. *Blair* achieves this goal by using a large language model (i.e., Google Gemini Pro, which is free to use) and the technique of active learning. The former grants our method improved text comprehension abilities, while the latter streamlines efficiency by minimizing the need for extensive data labelling.

3. Virtual reality experiments

This section of the report describes the Virtual Reality (VR) driving behavior studies conducted at NRC and Lund University. The studies investigated how changing visibility conditions due to wildfire smoke might affect individual driving behavior – in particular headway, i.e., the distance between the driving vehicle and the one ahead of it on the same lane. The section begins with an overall introduction and review of relevant prior work, including how smoke and visibility are related, driving behavior under low visibility conditions, and the validity of VR driving simulators.

During wildfire evacuation, smoke from wildfires can travel miles ahead of the fire front (Goodrick et al. 2013), potentially obscuring evacuees' visibility on the roads. This puts populations near the WUI at substantial risk during a wildfire evacuation. In cases of rapid fire spread, communities may be forced to evacuate quickly and under dangerous conditions, such as heavy ember showers or reduced visibility due to smoke (e.g., during the Camp Fire in California in 2018 (Wong et al. 2020)). In addition, authorities may wish to guide evacuees towards specific evacuation routes (e.g., using signage or information passed on to route guidance systems to balance demand on the routes available). Data on how these factors influence driving behavior, and as a consequence, evacuation outcomes in wildfires, are unfortunately quite scarce. This scarcity is likely due to ethical, logistical, and methodological limitations in data collection when using many traditional methods, such as field observations.

Previous studies have examined how to model traffic during an evacuation from a natural hazard using different methods, including geographical information systems data and social network data, e.g., (Lindell and Prater 2007; Pel et al. 2010; Sadri et al. 2017; Tamakloe et al. 2021; Kim et al. 2021; Wu et al. 2024; Cova et al. 2024). These data can provide valuable insights on traffic behavior, such as traffic densities or speeds. However, to the best of our knowledge, these data are not tied to information on environmental conditions that can influence individual and aggregate driving behavior. For instance, precise data on visibility at the road level have rarely been reported.

This gap is relevant given that visibility conditions can significantly deteriorate during wildfires, potentially affecting the speeds that evacuees can maintain. Given that reliable data on ground level visibility and driving behavior (e.g., on macroscopic traffic patterns) are difficult to find, controlled empirical studies in simulated environments might provide an opportunity to close this gap. Driving simulators, for example in Virtual Reality (VR) allow for the testing of behavioral hypotheses by comparing relative differences in results under safe and controlled conditions and thus offers a complementary tool to existing data collection approaches. VR allows high-fidelity simulation of a given scenario in a way that is safe, sufficiently ecologically valid and also cost-efficient (Kinatader et al. 2014; Arias et al. 2021).

In order to provide useful data for macroscopic traffic simulations, two quantities are relevant: driving *speed* and traffic *density* (or headway) (Rohaert et al. 2023c, a). A first attempt to study individual driving behavior in VR during wildfire evacuation scenarios was performed at Lund University, which found that individual drivers decreased their speed in reduced visibility conditions (see Figure 21) (Wetterberg et al. 2021a). It is currently unclear though how traffic density is affected by reduced visibility.



Figure 21. Screenshot from a driving behavior task in VR performed at Lund University during wildfire evacuation in the presence of smoke (K is equal to 0.5 m^{-1} in this example). Figure taken from (Wetterberg et al. 2021a).

To address this gap, this work explored the use of VR experiments for controlled empirical studies on wildfire evacuations, particularly in the WUI. This will allow for research on evacuee behavior under the conditions outlined above for a broad range of contexts and conditions that may occur during a wildfire evacuation. Specifically, VR technology was used to study traffic evacuation movement variables which are currently impossible to systematically investigate from existing macroscopic databases (e.g., interaction between driving parameters and embers/smoke). However, it should be noted that like any other empirical method this approach has limitations, such as narrower field-of-view, vergence-accommodation conflict, distance compression, etc. (see details below and in the limitations section of the studies). The goal of the work presented is to use this approach to complement other modes of data collection given the implausibility of performing traditional experiments involving driving behavior in reduced visibility conditions exploring key unknowns.

3.1. Using Virtual Reality to study driving behavior

VR is an established research instrument to study human behavior in general. There are a range of VR methods based on different equipment that vary in how stimuli are presented to participants and what participants can do while being immersed in a simulation (Slater and Sanchez-Vives 2016; Cipresso et al. 2018). For example, Head Mounted Displays (HMD) – VR headsets that are worn like ski goggles, Cave Automatic Virtual Environment (CAVE) systems, or multiscreen driving simulators are common methods and can vary significantly in sophistication. The work discussed here focusses on HMDs and their application to driving simulation. For a broader discussion of VR as a research method the reader is guided to (Suh and Prophet 2018; Cipresso et al. 2018; Liberatore and Wagner 2021; Khanal et al. 2022).

3.1.1. Head-mounted displays (HMD)

When using VR to study driving behavior, some limitations need to be taken into consideration, such as the head-mounted display's (HMD) resolution and field-of-view. Binocular HMDs typically have two lenses, presenting a separate and slightly different image to each eye. This generates a sense of depth perception through stereoscopy. Most current generation HMDs have an angular resolution ranging from approximately 10 to 15 pixels per degree (Blissing and Bruzelius 2018). However, a visual acuity of 20/20 corresponds to an angular resolution of 60

pixels per degree (Xiong et al. 2021). The HMD's resolution can impact an object's appearance in a virtual environment. For example, text might look blurrier in VR than in the real world. In the context of driving studies, participants might have more difficulty reading traffic signs, such as speed limit signs, especially from a distance.

In addition, the horizontal field-of-view is narrower in VR than in the real world. Specifically, the horizontal field-of-view of most current generation HMDs ranges from 90 to 100 degrees (Blissing and Bruzelius 2018) whereas a healthy individual's horizontal field-of-view (including both eyes) is approximately 200 degrees in the real world (Arthur 2000; Blissing and Bruzelius 2018). In other words, individuals have a wider view of the environment without needing to move their head in the real world compared to VR. This could make driving tasks involving peripheral vision more challenging in VR. Large head movements while driving in VR can also induce cybersickness in users.

Another issue that can arise in VR is the vergence-accommodation conflict (see Figure 22 for an illustration of this effect). When looking at an object, both eyes receive a slightly different image. To create a single image of the object, the brain uses vergence (the eyes fixate on the object) and accommodation (the lens of the eyes change shape to create a clear, focused image). In the real world, the distance where the two eyes converge on the object and the distance where the object appears in focus are the same. However, in VR, there is a mismatch between the distance of vergence and the distance of accommodation. For instance, the eyes might converge on an object that appears far away in the virtual environment (vergence), but the distance to focus on the object is shorter as the display is close to the user's eyes (accommodation). This sensory conflict can lead to blurred vision, eyestrain, and headaches in users (Blissing and Bruzelius 2018).

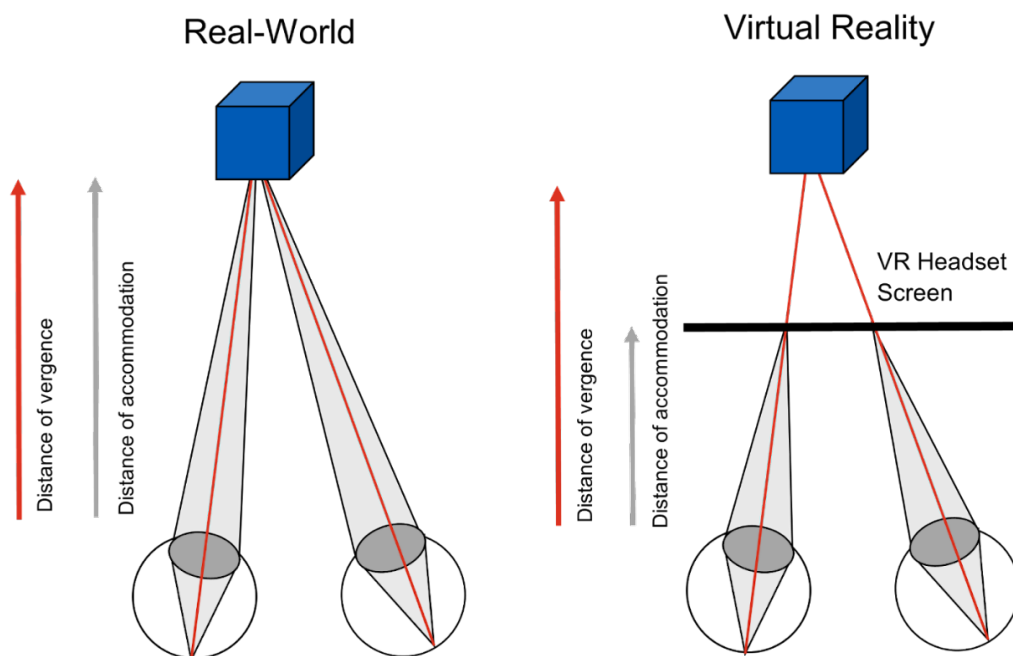


Figure 22. Illustration of the vergence-accommodation conflict (based on Figure 1 in (Zhan et al. 2020), 2020 and Figure 2.5 in (Peillard 2020)).

When studying headway and visibility in VR, it is important to take VR's limitations into consideration as they can have an impact on users' perception. For example, previous studies have shown that users tend to underestimate distances in VR (Creem-Regehr et al. 2005; Renner et al. 2013; Paes et al. 2017; Buck et al. 2021), which could potentially affect the distance that they keep with the vehicle in front of them when driving in VR. Rendering smoke in VR to reproduce poor visibility conditions from the real world can also be challenging. For instance, it is difficult to reproduce physically accurate light backscattering effects when rendering smoke in VR (Wahlqvist and Rubini 2023a).

Despite these limitations, VR has been used to study human behavior in poor visibility conditions in a range of contexts. For example, VR is used in helicopter flight simulators to reproduce brownout and whiteout phenomena which significantly reduce visibility, e.g. due to dust or snow (Gerlach 2011; Priot and Albery 2012; Meima 2021). A degraded visual environment is dangerous for pilots as it can lead to spatial disorientation and the loss of situational awareness, which can cause accidents (Priot and Albery 2012; Meima 2021). Previous studies have examined the effectiveness of visual display systems to support pilots under different visibility conditions, e.g., cognitive workload (Innes et al. 2021) or using augmented reality (Meima 2021). While this research does not directly relate to wildfires, it is important to take reduced visibility into consideration as it can impact human behavior during a wildfire evacuation (e.g., vehicle speed when driving through smoke).

3.1.2. *Validity of driving simulators*

Driving simulators are used in a wide range of applications, such as training (Allen et al. 2010), impact of distractions on driving, autonomous systems development, road design (Bruck et al. 2021), etc. Driving simulators typically use monitors, projector screens, or a VR headset to display the driving scenario. Some driving simulators also have a motion base and/or a real-world vehicle or cab to increase the simulator's realism (Philips et al. 2015).

Two important concepts when evaluating driving simulators are fidelity (relating to research tools and variables) and validity (relating to research outcomes) (Wynne et al. 2019). In a report by the U.S. Department of Transportation, Philips and Morton (2015) defined physical fidelity as “the degree to which the simulator replicates the physical properties of the driving situation” (p. 4) and behavioral fidelity as “the simulator's ability to replicate driver behavior observed in the real world” (p. 4). Wynne et al. (2019) define validity as how accurately a driving simulator represents or reproduces driving in the real world. They divide validity into *absolute validity* (i.e., when the results obtained from the driving simulator exactly match those obtained in the real world) and *relative validity* (i.e., when the results obtained from the driving simulator show similar patterns or effects as the real world).

Previous studies have shown similar driving behavior in driving simulators as in the real world. For example, a study (Zhang et al. 2020) compared driving behavior in the real world versus in a five-monitor driving simulator. They found that spot speed (i.e., vehicle speed measured in a specific location), car-following distance (distance headway in meters), time headway (in seconds), and reaction delay time were similar in a driving simulator to the real world. However, they also noted that participants seemed to drive more aggressively in the driving simulator than

in the real world. Other studies have also reported that participants can engage in riskier or more aggressive driving in a simulator than in the real world, such as driving at higher speeds (Törnros 1998) and accepting lower critical gaps when passing other vehicles (Llorca and Farah 2016). This may be due to participants' awareness that the scenario is artificial and perceived higher safety (e.g., no physical consequences if they collide with virtual objects), or due to the hardware and software used to immerse participants (e.g., type of display device, number of monitor screens used, realism of the driving scenario).

Classic driving simulators make use of one or more monitor screens. A few driving studies were conducted using an HMD to immerse users in driving scenarios in VR. VR offers many benefits compared to classic driving simulators, such as binocular depth cues, presence and high immersion (Blissing and Bruzelius 2018). However, VR also has some limitations (as previously mentioned), including lower resolution and field-of-view, optical artifacts, latency, accommodation-vergence conflict, higher risk of cybersickness, and being unable to view one's own body without implementing additional tracking (Blissing and Bruzelius 2018). In one study (Goedicke et al. 2018) conducted a study using qualitative methods (i.e., interviews) to evaluate a proof-of-concept VR driving simulator used in the context of autonomous driving. During the study, participants were immersed in a driving scenario via a VR headset while physically seated in a car in the real world, which was physically driven by a second driver. Participants reported appreciating the sensory experience, but they also suggested that technical improvements be made to the simulator (e.g., improving the quality of the graphics). Another study (Hartfiel and Stark 2021) compared gaze behavior in two VR driving simulators (static, motion base enabled; and dynamic, motion base disabled) versus in the real world. The results indicated no significant differences in gaze behavior between the two simulator conditions and the real-world condition. A third study (Taheri et al. 2017) used a VR headset to immerse participants in a clear weather driving scenario and found that participants' driving performance gradually improved as they became more familiar with the driving simulator (e.g., maintaining a consistent speed). In summary, the results from these studies suggest that driving in VR can produce similar patterns as driving in the real world (relative validity). However, VR's limitations should be considered when designing the driving simulator and the driving scenario.

3.2. Driving behavior in reduced visibility conditions

3.2.1. *Light extinction*

Extinction or attenuation, often denoted as A (or OD), is a dimensionless measure of the attenuation of light as it passes through a medium. It quantifies how much a medium reduces the intensity of light that passes through it, as given by the Beer-Lambert Law (Equation 2) [10].

$$\frac{I_0}{I} = e^{-KD} = e^{-\epsilon cD} \quad [\text{Equation 2}]$$

Where I_0 is the initial intensity of light before passing through the medium (in this context, the smoke) and I is the intensity of light that remains after being attenuated over the distance D . The molar extinction coefficient ϵ [$\text{m}^3/\text{mol}/\text{m}$] and the concentration of the absorbing species c [mol/m^3] are often combined into the extinction coefficient K . The extinction coefficient, later referred to as fog density or smoke density in this report, relates as more or less inversely proportional to visibility, quantified as a distance.

Two indicators that relate to visibility need to be differentiated: visibility itself (i.e., how far one can see) and the extinction coefficient K (i.e., a measure of how a substance or medium attenuates or scatters light as it passes through). Visibility, as a distance, refers to how far a person can see or the distance at which objects become visible (Fridolf et al. 2019). It is often measured in meters or kilometers and indicates the clarity of vision in a given environment. In the case of wildfires, visibility is crucial for evacuees who need to navigate through smoke to reach safety. Higher values of the extinction coefficient K indicate a greater reduction in transmitted light, making the smoke opaquer and hindering visibility: more smoke particles scatter and absorb light, significantly diminishing the amount of light reaching the observer's eyes.

In the field of *human behavior in fires*, the visibility of emergency signs has been well studied (Akizuki 2024). Jin proposed a simple model which relates the visibility, expressed as a distance, to the smoke density as in the formula in Equation 3 (Jin 2008).

$$V = C/K \quad \text{[Equation 3]}$$

Where V is the visibility [m], K is the extinction coefficient or smoke density [1/m] and C is a constant value [-]. The validity of this model is however limited, among other reasons because the value of C is not universal. Some examples of factors that influence the value are listed below (Ronchi and Nilsson 2018):

- Environmental factors: the number, color, intensity and position of lights, the size of the object being observed, as well as its contrast and difference in color in comparison to the background.
- Factors related to the smoke: the values also depend on the chemical composition of the smoke, the color of the smoke, and the tendency of the smoke to irritate the eyes.
- Factors related to the signs: the lighting on the signs, the contrast with the surroundings, the size and the colors of the signs.
- Factors related to the observer: visual acuity. This refers to the sharpness and clarity of an individual's vision, specifically their ability to discern fine details and perceive objects at a specific distance, typically measured using an eye chart at a standard viewing distance.

The **extinction coefficient**, often denoted as K , is a measure of how a substance or medium attenuates or scatters light as it passes through (Mulholland 1995). The higher the extinction coefficient, the greater the attenuation and/or scattering of light. The relationship between extinction coefficient and visibility can be described by the following general principles:

1. **High extinction coefficient:** A higher extinction coefficient indicates increased attenuation and scattering of light. In the context of visibility, this often means reduced visibility. The light travelling through the atmosphere interacts more with particles and substances, leading to hazier conditions.
2. **Low extinction coefficient:** Conversely, a lower extinction coefficient suggests that light is less attenuated or scattered. In this case, visibility tends to be better, as there is less interference with the transmission of light through the medium.

3.2.2. *Smoke*

One important variable to consider during a wildfire evacuation are the environmental conditions, such as smoke, fog/haze, ember showers, and fire, which can reduce visibility and impact driving during the evacuation. One study (Mueller and Trick 2012) examined the impact of reduced visibility due to fog on driving speed (and other variables, such as collisions) in novice and experienced drivers using a six-monitor driving simulator. The results showed that both groups drove slower in simulated fog compared to clear visibility. However, the results suggested that the experienced drivers drove faster in clear visibility and slower in simulated fog than the novice drivers. This suggests that driving experience can have an impact on driving behavior in reduced visibility. However, it is unclear whether this effect would also be observed when driving in wildfire smoke.

Few studies have examined the impact of reduced visibility due to smoke on driving behavior during an evacuation. A study was conducted in VR (Wetterberg et al. 2021a) examining the effect of different levels of smoke by employing an exponential fog and adjusting the extinction coefficient K (No smoke/fog, Low: $K = 0.05 \text{ m}^{-1}$, Medium: $K = 0.10 \text{ m}^{-1}$, High: $K = 0.15 \text{ m}^{-1}$, and Very high: $K = 0.20 \text{ m}^{-1}$) on driving behavior in VR. They found that participants' driving speed decreased as visibility worsened, which is in line with studies performed on walking behavior in smoke (Ronchi and Nilsson 2018; Fridolf et al. 2019). Another study (Intini et al. 2022) made use of the data collected in VR (Wetterberg et al. 2021a) to calibrate two macroscopic traffic models taking into account the relationship between reduced visibility and driving speed. However, the impact of other environmental conditions (e.g., daytime versus nighttime, ember showers) on driving behavior during a wildfire evacuation remains unknown.

Most studies that examined the effect of smoke on human behavior in fire evacuations have focused on pedestrian movement in building and tunnel fire evacuations. For example, one study (Fujii et al. 2021) examined the impact of lit emergency exit signs (present or absent), smoke density (four levels), and lighting (illumination or non-illumination) on walking speed in a corridor-like experimental space. The results showed that participants tended to walk faster in higher visibility conditions when the corridor was illuminated, and the lit emergency exit sign was present. Other studies have examined the impact of smoke on walking speed during tunnel fire evacuations. For example, several tunnel experiments (Fridolf et al. 2013, 2015; Ronchi et al. 2018) (e.g. in road and rail tunnels) examined the effect of smoke density on walking speed. The results indicated that participants tended to walk slower in reduced visibility conditions.

However, wildfires differ from building and tunnel fires in several ways. For example, a tunnel or building fire tends to occur in an enclosed space whereas a wildfire tends to ignite in an open space (e.g., a forest). As such, the flammable material present also differs between wildfires (e.g., vegetation) and tunnel or building fires (e.g., furniture, vehicles). In addition, during a wildfire evacuation, most individuals will typically evacuate the area in a vehicle as the fire can spread quickly and over a large area whereas during a building evacuation or tunnel fire evacuation, individuals will evacuate on foot. Given these differences and the gaps in research on driving behavior in wildfire evacuations, it would be important to further explore how reduced visibility and other environmental conditions influence driving behavior during wildfire evacuations.

3.2.3. *Headway*

Another important variable to consider during a wildfire evacuation is headway. Headway has been defined in different ways in the literature, but, in general, refers to the “following distance or time between a leading and a following vehicle in traffic” (Biswas et al. 2021). At the same driving speed, a longer headway translates into a lower traffic flow, and will lead to longer evacuation times. A shorter headway can lead to accidents since drivers might not have enough time to brake if the vehicle in front of them slows down or stops suddenly. This can be dangerous in emergency situations, such as during wildfire evacuations, as accidents could lead to heavier traffic congestion and road closures and increase the amount of time required to evacuate the area (Rohaert et al. 2023c). Modern cars also include advanced driver assistance systems (ADAS), which may impact the choice of headways (Bianchi Piccinini et al. 2014). It remains unknown whether ADAS affects the choice of headways during wildfire evacuations.

Previous studies have examined headway during driving in naturalistic settings (i.e., in the physical environment) and in driving simulators in normal weather conditions. For instance, one study (Zhu et al. 2016) investigated headway under various environmental conditions in a naturalistic setting. The results suggest that individuals tend to drive slower and maintain a larger headway at nighttime compared to daytime. However, it remains unclear whether this also applies to driving at nighttime during a wildfire. In one study (Risto and Martens 2014) the choice of headway in real-world driving and in a driving simulator was investigated. The authors found that self-chosen headway in the real world and in the driving simulator were similar. In another study (Risto and Martens 2013) the difference between time headway and distance headway instructions was explored using a driving simulator. The results indicated a difference between time headway and distance headway instructions in terms of relative estimation errors (the relative difference between instructed and chosen headway, i.e., overestimation or underestimation) but not in terms of absolute estimation errors (the absolute difference between instructed and chosen headway). The results from these two studies suggest that driving simulators are a valid tool to make relative comparisons of driving behavior between experimental conditions. However, in both studies, participants drove in normal weather conditions – it is still unknown how environmental conditions related to wildfires, such as smoke, impact headway.

A few studies explored time and distance headway in reduced visibility due to fog using driving simulators. One study (Gao et al. 2020) investigated time and distance headway in clear and hazy conditions. Participants were immersed in both weather conditions using a driving simulator with a cylindrical projection system. The results indicated that participants maintained a smaller time and distance headway in the clear weather condition than in the hazy weather condition. In another study (Broughton et al. 2007), the authors examined time and distance headway in simulated fog using a driving simulator with four projection screens. Participants were immersed in one of three visibility conditions (clear, moderate simulated fog, or dense simulated fog) and drove behind a lead vehicle in two trials. During each trial, the lead vehicle drove at a different speed (approximately 50 km/h or 80 km/h). Interestingly, the results suggested that participants in the simulated fog conditions could be separated into two groups: (1) participants that stayed within the visible range of the lead vehicle (“non-laggers”) and (2) participants that lagged beyond the visible range of the lead vehicle (“laggers”). In other words, one group of participants drove faster and maintained a smaller time and distance headway to maintain visual contact with the lead vehicle whereas the other group of participants drove slower and maintained a larger time and

distance headway in the simulated fog conditions. A third study (Kang et al. 2008) investigated the impact of five simulated fog densities (0, 0.05, 0.10, 0.15, and 0.20 m⁻¹) on distance headway. In the study, participants were immersed in a desktop driving simulator and followed a lead vehicle that drove at three different speeds (40, 60, and 80 km/h). Participants completed a total of 30 trials. The results suggested that participants maintained a larger distance headway when the lead vehicle drove at a faster speed than when it drove at a slower speed. In addition, it seemed that distance headway decreased in the highest density fog condition compared to the lower density fog conditions. Another study (Saffarian et al. 2012) investigated why individuals maintain short headways in fog. Specifically, the authors examined the impact of headway on the feeling of risk and lateral control in simulated clear and foggy conditions using a driving simulator. Interestingly, the authors found that overall, in a clear automated condition where participants only needed to steer the vehicle (the throttle and braking were automatically controlled), the feeling of risk and steering activity were higher when participants lost visual contact with the lead vehicle compared to when the lead vehicle was visible. The authors suggested that the lead vehicle served as a guide in lateral control.

3.3. Overview of current VR studies

To the authors' knowledge, no studies have yet examined headway specifically during emergency evacuations, particularly during wildfire evacuations, which present unique environmental hazards, such as smoke, fog/haze, ember showers, and fire. This makes studying driving behavior in a naturalistic setting challenging and dangerous. In addition, most studies seemed to have examined headway using driving simulators with monitors or projection screens. It is unclear whether similar effects would be observed if a VR (i.e., with a head-mounted display) driving simulator was used.

For the WUI-NITY 4 project, a pilot VR study on visibility (as a distance) and two larger VR driving studies were conducted. One of the larger studies was conducted at the NRC in Canada, and the second one was conducted at Lund University in Sweden. The pilot study investigated the impact of different environmental conditions on visibility using VR. For additional details on the pilot study, see section Pilot VR study on visibility. The larger driving studies presented in this report examined time and distance headway under various environmental conditions using VR.

The subsequent sections are divided as follows: (1) description of the pilot study on visibility, (2) description of the main driving study conducted in Canada, (3) description of the main driving study conducted in Sweden, (4) general discussion of the results from all the studies, and (5) overall conclusion.

3.4. Pilot VR study on visibility

During the summer of 2023, a pilot study was conducted with 20 participants at the NRC to assess the impact of varying levels of smoke and fog on visibility as a distance in VR. Note that visibility was measured in meters. The results from the pilot study helped to inform the design and interpret the results of the main driving studies. In this section, the objectives, methods, and results of the pilot study are presented.

3.4.1. Objectives

In the study conducted by Wetterberg et al. (Wetterberg et al. 2021a), researchers used VR simulations to investigate how different levels of visibility influence evacuees' driving behavior during wildfire evacuations. By manipulating the extinction coefficient in the VR simulations, they could observe how reduced visibility due to smoke affects driving speed, headway choices, and other driving behavior variables.

When analyzing the results of the pilot study, it can be useful to relate the light extinction of the smoke in the virtual environment to the visibility as a distance (whilst keeping in mind the above-mentioned limitations on the validity of Jin's visibility model, see Visibility section).

This pilot study aimed to understand how smoke affects visibility (i.e., how far one can see) in the virtual environment and how these factors impact participants' driving decisions and safety. By gaining insights into these relationships, researchers can contribute to improving evacuation strategies and enhancing safety measures for communities in wildfire-prone areas. Specific objectives of the pilot study included:

1. Examining how varying extinction coefficients in a virtual environment affects the visibility.
2. Examining the visibility difference in the different scenarios of the larger driving studies, which include two different lighting conditions (day/night), two different atmospheric conditions (white fog/orange smoke), regardless of the level of smoke.

The research team put forward the following hypotheses:

1. In VR simulations, the visibility will be limited due to the finite resolution of the head-mounted display (1440 x 1600 pixels per eye in our set-up). Therefore, objects at further distances might be difficult to observe, even in low optical densities (good visibility conditions). The inversely proportional relationship between the smoke density and the visibility might be cut in these cases (combinations of high distance and low smoke density).
2. The visibility will be worse at night, due to the lower level of light.

Moreover, the differences in visibility in the two different atmospheric conditions (white fog/orange smoke) will be explored as well.

3.4.2. Methods

A convenience sample of 20 participants was recruited from the NRC via recruitment posters on the NRC campus and word-of-mouth to complete the study in VR. The inclusion and exclusion criteria were as follows.

Inclusion criteria:

- Participants must be at least 18 years of age.
- Participants must have normal or corrected-to-normal vision.

Exclusion criteria:

- History of cardiovascular or vestibular conditions or respiratory diseases.
- History of epilepsy, severe motion sickness while traveling, eye disease, or recurrent migraines.
- Symptoms of COVID-19 or having been exposed to COVID-19 within the last 14 days on the day of data collection.

Three independent variables were manipulated:

- The atmospheric conditions (two values: fog vs. smoke);
- The light conditions (two values: daytime vs. nighttime); and
- The smoke and fog density (five values for the extinction coefficients, based on (Wetterberg et al. 2021a)). Every participant took part in all twenty trials. The trials were completely randomized.

The dependent variable was the performance of a signal detection task. Participants were asked to read the speed limit displayed on traffic signs that were placed at varying distances. The distance at which they can no longer do so clearly was considered the measure of visibility.

The study used a variation of a bisection task (or staircase method in psychophysics) in which stimuli were presented in increasing or decreasing distance depending on the participants' response to the stimulus. For example, if a participant was able to correctly read a sign at a given distance, the next sign would be presented further away. In turn, in cases where a participant was not able to read the sign, the next stimulus would be presented a little closer. This method is efficient because it does not present stimuli that are well above or below threshold (i.e., trivially easy or impossible to detect).

Participants did not complete any measures prior to the VR experiment.

During the VR experiment, visibility was assessed by asking participants to read speed limit signs (i.e., a participant's ability to read the speed limit signs). Participants' responses were manually recorded (for additional details, see the VR setup and stimuli section).

Following the VR experiment, participants completed the Snellen visual acuity test (their right and left eyes were tested separately). The standard testing distance was adjusted to 10 feet (3.05 m). Participants then filled out an online questionnaire via LimeSurvey. The questionnaire inquired about participants' age, their gender, visual impairments (e.g., glaucoma), and visual acuity (scores obtained from the Snellen visual acuity test; one score for the right eye and a second score for the left eye).

Participants were immersed in the virtual environment via a Vive Pro Eye VR headset (screen: dual OLED 3.5" diagonal, resolution: 1440 x 1600 pixels per eye, refresh rate: 90 Hz, FOV: 110 degrees). The virtual environment did not have sound. Two SteamVR Base Stations 2.0 from Vive tracked participants' position in VR. An HP computer ran the virtual environment (Windows 10, Intel® Xeon® Silver 4114 processor, CPU @ 2.20 GHz 2.19 GHz (2 processors), 96.0 GB RAM) with an NVIDIA graphics card (NVIDIA® GeForce RTX 2080). Participants were seated in a car seat mock-up, which included a Toyota Corolla car seat and a Thrustmaster 300RS steering wheel and acceleration and brake floor pedals (see Figure 23). However, participants did not use the steering wheel or the floor pedals during the pilot study as the experiment did not involve driving. Participants filled out the online questionnaire on a second computer in the laboratory.

The VR trials were developed using Unity version 2020.3.141f. The color of the smoke and fog were determined by visually inspecting photos of real-world wildfire smoke and fog and reproducing the colors as closely as possible in Unity (see Figure 24 and Table 1).

The smoke and fog were implemented through a script using Unity's fog settings:

- Fog color: set the color of the fog using RGB values. For each condition, the RGB values were based on image internet searches. The RGB values are in Table 1.
- Fog mode: set the fog mode to "Exponential".
- Fog density: set the fog density values (e.g., 0.20). This value corresponds to the extinction coefficient of the smoke or fog.



Figure 23. Photo of a researcher wearing the VR equipment.

Table 1. Overview of rendering settings and image sources (photographs) and associated example renderings.

		Day	Night
Zero density (no fog, no smoke)	Directional light intensity	8	0.25
	Zero density (no smoke, no fog)	Day skybox Sun color 255, 214, 190 Ambient light 191, 191, 191 Equator ambient 153, 133, 130 Ground 51, 45, 43 Fog density 0.003 Fog color 0, 0, 0	Night skybox Sun color 181, 205, 255 Ambient light 10, 10, 10 Equator ambient 59, 59, 59 Ground 105, 89, 89 Fog density 0.003 Fog color 0, 0, 0
Fog	Directional light intensity	8	1
	Color (*)	200, 200, 220	45, 55, 65
Smoke	Directional light intensity	8	1
	Color (*)	240, 180, 110	90, 30, 5

(*) Colour: Tint color of empty panoramic skybox, tint fog color, color environmental light (single color), and directional light color.

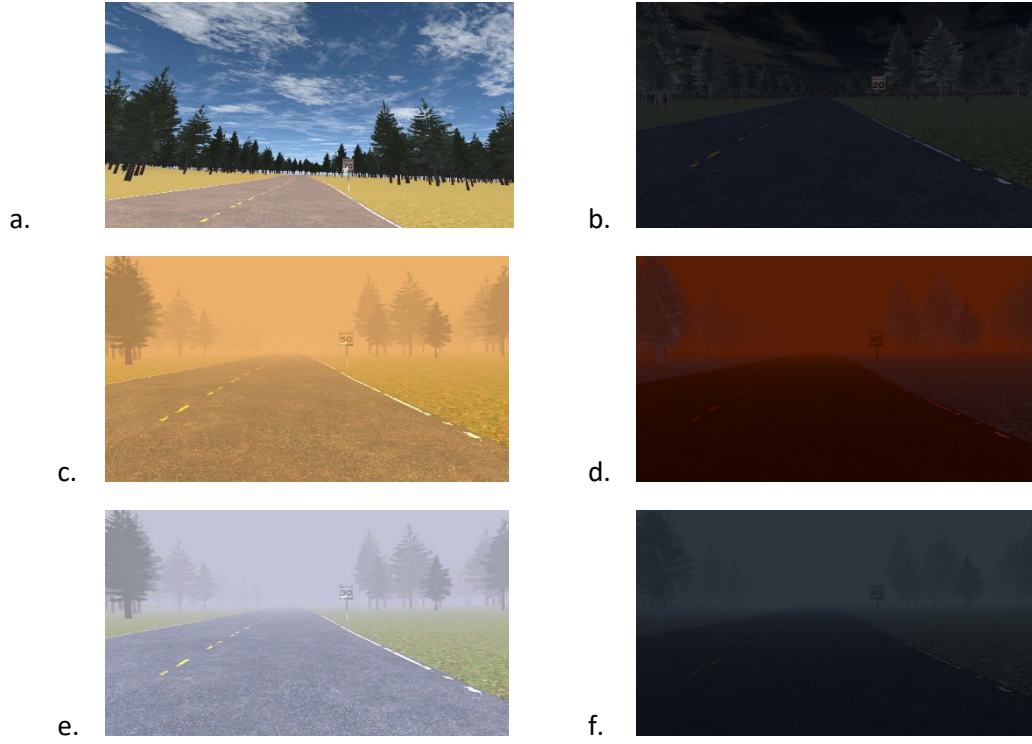


Figure 24. Illustration of the virtual environment. a) day – clear sky scenario; b) night – clear sky scenario; c) day – smoke scenario with Unity fog; d) night – smoke scenario with unity fog; e) day – fog scenario with Unity fog; f) night – fog scenario with Unity fog.

Implementing realistic fog or smoke light physics in real-time visualizations in Unity is challenging due to the computational costs involved in simulating complex light interactions, such as multiple scattering and volumetric effects (Wahlqvist and Rubini 2023a). Achieving accurate visuals for scattering, absorption, and emission of light within a dynamic, three-dimensional fog or smoke environment demands sophisticated calculations that may exceed the real-time processing capabilities of current hardware. Therefore, the fog and smoke were rendered using the built-in fog function, which is applied post-process.

Unity’s fog function applies an interpolation between the “true color values” after the process, and the color of the smoke. The fraction of the true color values that is left f , decreases according to the natural logarithm (see Equation 4).

$$f = e^{-KD} \quad [\text{Equation 4}]$$

Where the fog density K in the unity function and the distance D to the distance from the depth buffer. Here, the same symbol K is used as in Equation 2, as the fog density in Unity blend the true colour with a fog colour similarly to real light attenuation (the Beer-Lambert law).

The built-in fog function processes rapidly and therefore is commonly used in video games to add the perception of depth and improve performance by avoiding rendering objects at far distances.

It is also commonly used by researchers (Wetterberg et al. 2021a; Davis et al. 2023). Nevertheless, some limitations of the post-process function should be mentioned:

- The fog/smoke is distributed uniformly over the entire field of view. Real fog and smoke might vary in thickness over space.
- The fog/smoke is static. Aerodynamic effects by wind and obstacles are not included.
- There are no interactions with light. The “true color” of the object behind the fog is calculated assuming the same directional light from the sun and environmental light. Light is not absorbed and scattered as it would be by real fog and smoke.

The experiment has a full factorial design. This means that the participants completed 36 trials (two light conditions * two atmospheric conditions * nine smoke densities) in VR. Each trial took less than one minute. The trials were completely randomized. The structure of the trials (see Figure 25) can be summarized as follows:

- Start experiment: create output file, load environment.
- Inter trial interval (ITI): time interval between 2 trials.
- Initialize trial: load the variables needed for the current trial.
- Trial: one trial; in which a given condition is shown; begins with the scene being shown to participants; ends after participants provide a response (i.e., either a number or states that they cannot read the sign).
- End trial: fade out, remove completed condition from trial list.
- Quit experiment: save output file.

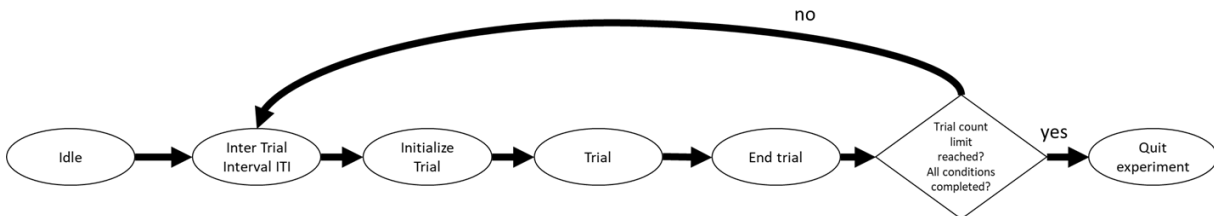


Figure 25. Flowchart of trial structure in Unity.

During the trials, the participant sat in the driver’s seat of the mock-up car seat (see Figure 23; note that the participant was stationary and did not drive) and read out loud the speed limit on the traffic signs along the road.

The position of the traffic sign was changed in accordance with the bisection method (or staircase method in psychophysics) (see Figure 26) so that the distance of the traffic sign to the participant (*Dis*) can be obtained with a certain accuracy (so that the interval $[Min, Max]$ is no longer wider than the tolerance *Tol*). An example of this method is shown in Figure 27. In the default version of the bisection method, the distance (*Dis* in Figure 26) is at the middle of the interval $[Min, Max]$. Here, the values are modified to make it more likely the participant can read the sign. Therefore, it will take more iteration to reach the same accuracy, but the participant will be able to read the sign more often and experience less frustration.

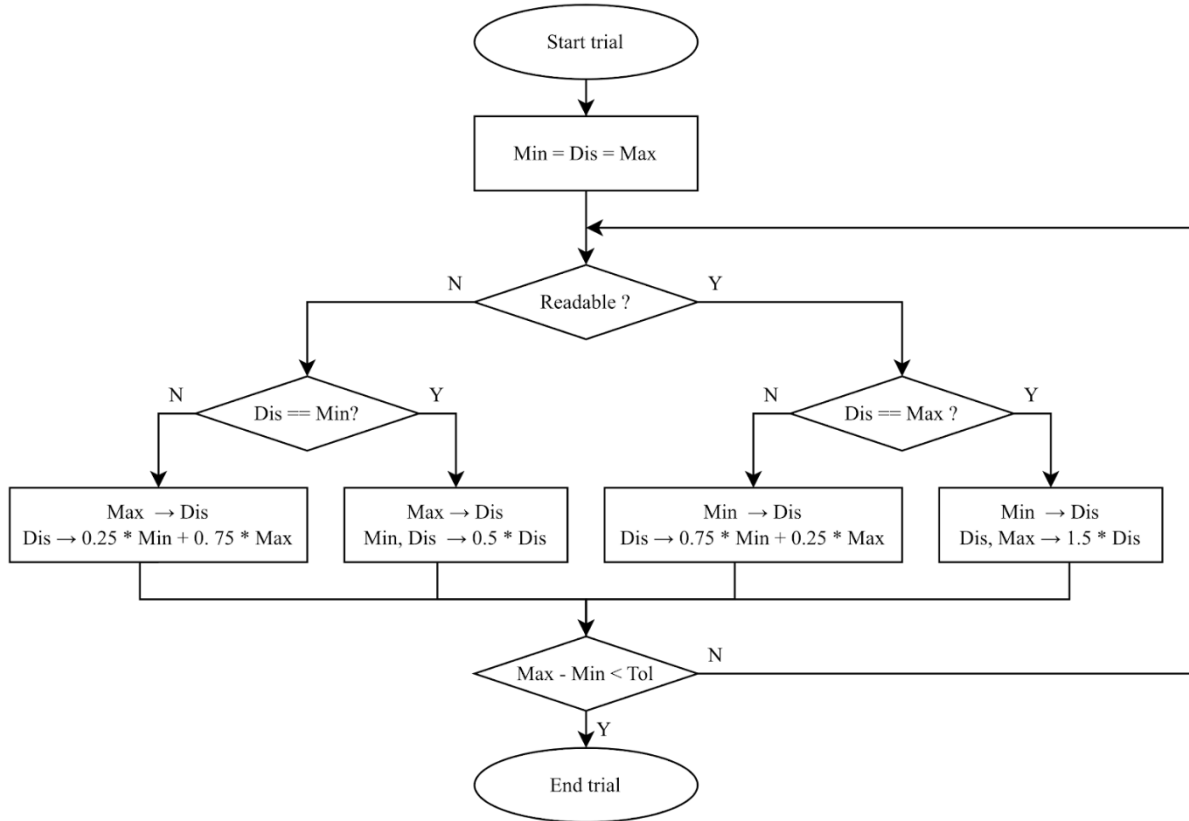


Figure 26. Flowchart of the bisection method applied to obtain the visibility during one trial.

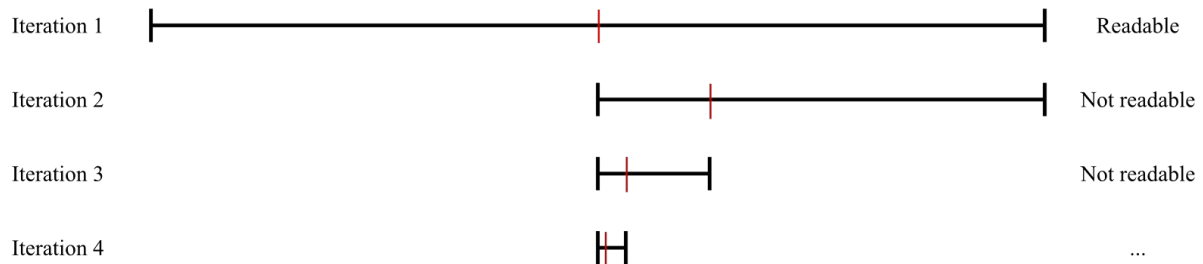


Figure 27. Schematic example of how the bisection method halves the interval in which the tested position (red) lies.

In each trial, the bisection method was applied until a tolerance of 0.10 m was achieved. Every participant participated in all nine trials, the order of which was randomized. Each trial had a different level of smoke ($K = 0.003, 0.05, 0.10, 0.15, 0.20, 0.40, 0.60, 0.80, \text{ and } 1.00 \text{ m}^{-1}$).

When participants arrived for the in-person appointment, the researcher greeted them and briefly explained the study's session procedure (see Figure 28 for a flowchart of the data collection process). Prior to the VR experiment, participants read and signed the informed consent form. The researcher answered the participants' questions.

The researcher then explained the VR equipment and participants' task in VR. Once the participant confirmed being ready to start, the researcher asked them to take a seat in the car seat and put on

the VR headset. During each trial, participants were presented with a speed limit sign placed at varying distances on the side of the road. The speed limit on the sign varied between 10 and 90 (presented in a random order), in increments of 10. The researcher asked participants to read the speed limit on the sign out loud. The researcher manually recorded whether their response was correct (Y) or incorrect (N) in Unity. Once the application was stopped, Unity generated an output file containing the recorded responses. It should be noted that if participants were unable to read the speed limit on the sign, this was considered incorrect.

Once all the trials were completed, participants completed the Snellen visual acuity test. They then filled out the online questionnaire. Finally, the researcher verbally debriefed participants to tell them more about the objectives of the study and answered any questions the participants had.



Figure 28. Illustration of the data collection process for the study.

3.4.3. Results and discussion

In total, twenty people participated in the pilot study. Nine of them identified their gender as female and ten as male (one participant did not fill out the questionnaire). The age of the participants ranged between 20 and 60 years (average: 36 years, standard deviation: 12 years). Three participants reported being farsighted, twelve reported being nearsighted, and four reported not having any visual impairment.

All participants participated in all trials. The results are shown in Figure 29, which shows the visibility as a function of the extinction coefficient for the four combinations of the light conditions (day and night) and the atmospheric conditions (fog and smoke).

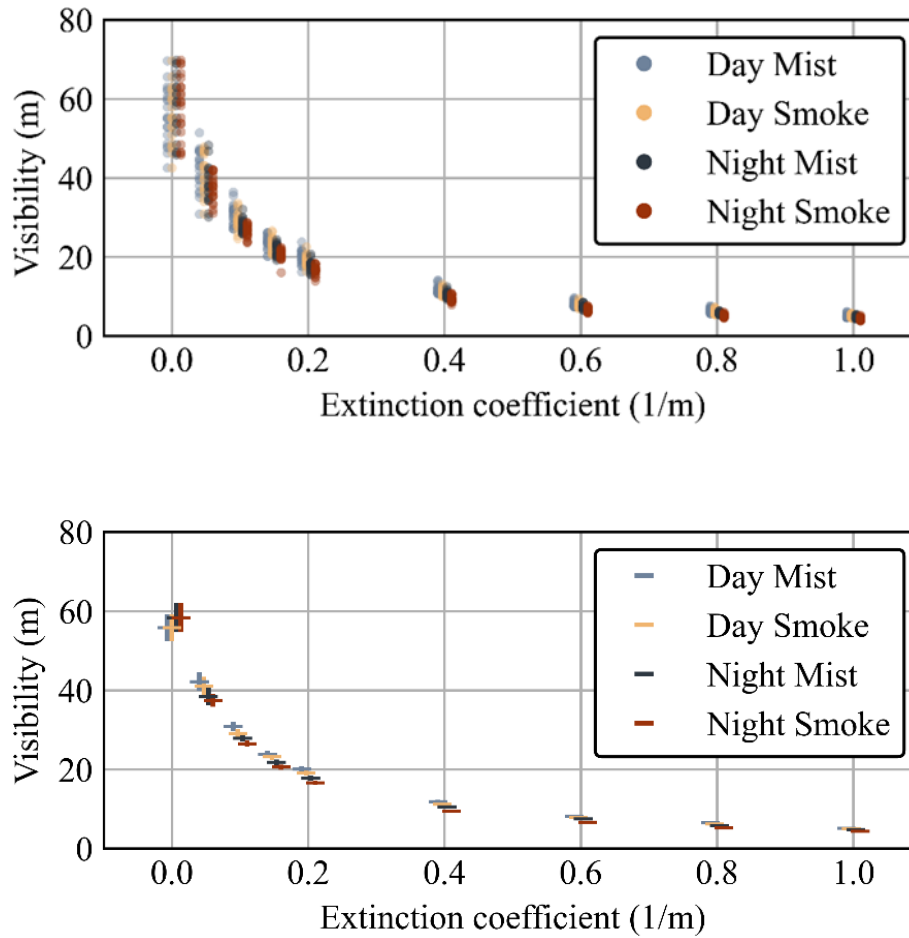


Figure 29. The visibility as a function of the extinction coefficient for the four combinations of the light conditions (day and night) and the atmospheric conditions (fog and smoke). The upper figure presents all data points. The lower figure presents the averages. The vertical line on the markers covers the 95% confidence interval, calculated using a two-tailed student t-test. Note that the confidence interval is small, due to the high confidence.

Two conclusions can be drawn from inspecting the data visually: (1) the smoke density strongly influences the visibility of the speed signs, (2) although the visibility seems to be slightly better for the daytime scenario and the fog scenario, in comparison to the nighttime scenario and the smoke scenario, the practical relevance (effect size) is small and might be statistically insignificant. These observations are further confirmed by the results of a mixed linear model analysis.

The mixed linear model was used to assess the effects of light conditions (day and night), atmospheric conditions (fog and smoke), and extinction coefficient on visibility, while accounting for repeated measures by participants (720 observations across 20 participants). The model was fitted using the Restricted Maximum Likelihood (REML) method as implemented in the Python package *Statsmodels* (Seabold and Perktold 2010). Only the effect of the extinction coefficient was statistically significant ($p < 0.05$): the model indicates a strong negative relationship between extinction and visibility.

Table 2. The results of the mixed linear model analysis. Significance is confirmed for the extinction coefficient.

Variable	Condition	Coefficient	Standard error	z	p value	Confidence interval	
Intercept		37.567	0.774	48.556	0.000	36.051	39.084
Light	Night	-1.391	0.756	-1.839	0.066	-2.873	0.091
Atmosphere	Smoke	-0.744	0.756	-0.984	0.325	-2.227	0.738
Extinction		-40.256	1.122	-35.884	0.000	-42.455	-38.057
Participant Variability		0.000	0.148				

Figure 30 shows the visibility as a function of the extinction coefficient, averaged over all participants and scenarios.

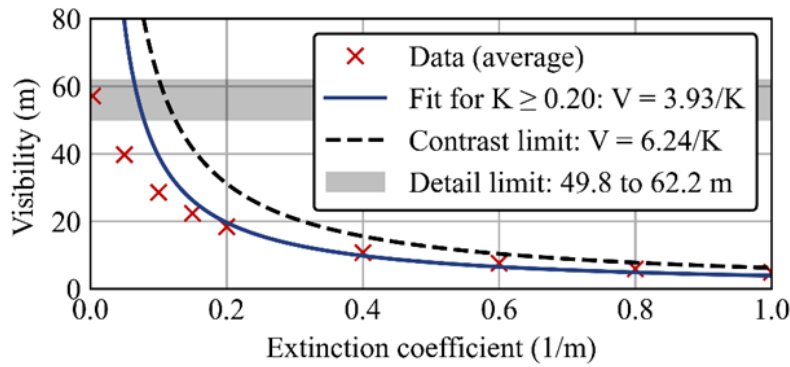


Figure 30. The visibility as a function of the extinction coefficient. Besides the data (red), a calibrated fit of Jin's relationship is shown, as well as the limitations to the visibility due to the lack of contrast and detail.

Two main visual effects can be attributed to the visibility: the loss of contrast and the lack of detail. Both effects are discussed below.

The loss of contrast in the virtual environment, particularly due to the presence of smoke, poses a limitation to the visibility of the speed limit on the traffic sign in the study. As the smoke thickness increases, the contrast between the traffic sign and its background decreases (See Equation 5).

$$f_{lim} = e^{-KV_{lim}} \rightarrow V_{lim} = -\ln(f_{lim}K) = -\frac{\ln\left(\frac{0.5}{256}\right)}{K} = \frac{6.24}{K} \quad [\text{Equation 5}]$$

The absolute maximum visibility (V_{lim}) is determined by the definite steps between color values (256 RGB values in this case). Contrast values f that are smaller than $0.5/256$ will be rounded to the same pixel value, and the hardware will not present absolute white and absolute black with the same pixel value in the virtual environment.

This limit is also presented in Figure 30. For high smoke levels, the data approximates this limit, indicating that this effect might define the visibility. For low smoke levels, the visibility is limited by another effect: the loss of detail.

The loss of detail in the virtual environment is another factor that limits visibility in the study. When the smoke levels are lower and the participants can read the speed limit from a further distance, the speed signs cover fewer pixels on the HMD. An absolute maximum distance can be theorized, assuming a minimum resolution, required to identify the speed limit. Figure 31 shows that four pixels in the vertical direction are not enough to read the speed limit, while five pixels are.

Resolution (pixels)	0	1	2	3	4	5	6	7	8	9
3	0	1	2	3	4	5	6	7	8	9
4	0	1	2	3	4	5	6	7	8	9
5	0	1	2	3	4	5	6	7	8	9
6	0	1	2	3	4	5	6	7	8	9

Figure 31. The speed limits, displayed with different resolutions. The limit of which numbers can be identified is assumed to lie in between 4 and 5 pixels (in the vertical direction).

The relationship between the maximum visibility V , the required resolution RR , the size (height H) of the traffic sign and the pixel density PD of the HMD (expressed as pixels per degree) can be described by Equation 6.

$$V_{lim} = \frac{H}{2 \tan\left(\frac{\alpha_{lim}}{2}\right)} = \frac{H}{2 \tan\left(\frac{RR}{2PD}\right)} \quad [\text{Equation 6}]$$

Figure 32 illustrates the geometry graphically.

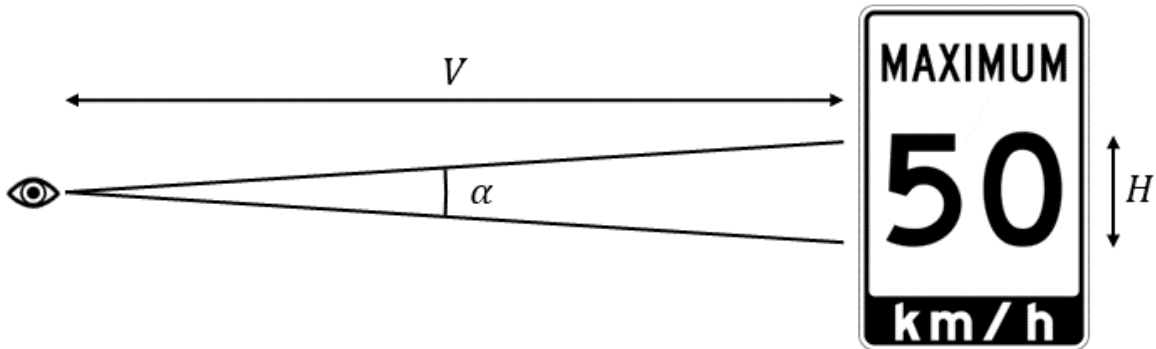


Figure 32. Sketch of the geometrical relationship between the height of the speed limit, the required visual angle and the visibility.

The height H of the speed limit equals 325 mm. The required resolution lies between 4 and 5 pixels (see Figure 31). The Vive HTC Pro Eye has an average pixel density of 13.36 pixels per degree. With a required resolution between 4 and 5 pixels, this means that the maximum visibility lies between 49.8 and 62.2m. Note that the retinal resolution of the human eye is about 60 pixels per degree, and that the average person would therefore be able to read this sign from 223 to 279 m in real life.

The visibility limit due to the loss of detail is also presented in Figure 32. Note that the upper limit of the interval corresponds well with the average visibility the participants experienced with the lowest smoke level ($K = 0.003/\text{m}$). The reason why the data lies closer to the upper limit is most likely because the precise pixel density is higher in the center of the screen, and because the participants' view in the virtual environment is dynamic (participants can move their head around to pan the traffic sign over the pixels in different ways to obtain more information).

Some researchers have attempted to relate visibility as a distance to the extinction coefficient. One commonly used model was derived by Jin (Jin 1978). Employing the same principle of a contrast threshold as above (see Equation 3) was obtained.

The constant C in Equation 3 was then calibrated from experiments and found to be between 2 and 4 for reflecting emergency signs and between 5 and 10 for light emitting emergency signs. It should be noted that the validity of Equation 7 and the calibrated constant have been disputed (Jin and Yamada 1985; Collins et al. 1992; Elhokayem 2022). As the simplified model does not take into account the contrast of the signs, the scattering properties of the smoke, the properties of the light sources or the relative positions of the observer, signs and lights. Moreover, as the visibility of emergency signs has been studied for building fires, the model has been calibrated for lower visibilities and higher smoke densities.

Figure 30 also presents Jin's model, fitted to the data from this study. Note that the data has only be fitted to smoke levels $K \geq 0.20$, as the asymptotic nature of the mathematical equation leads to poor fits for K -values close to 0. After calibration, the constant C equals 3.94, similar to the reflecting emergency signs in Jin's study.

It is crucial to acknowledge that the findings from the pilot study serve as a foundation for the main driving studies. The visibility derived from this study serves to understand car following behavior, as the idea of headway only makes sense when participants are able to distinguish the car ahead of them. Some limitations need to be addressed:

- It is important to note that the translation from controlled pilot conditions to dynamic driving scenarios introduces additional complexities that may affect the generalizability of the results. Moreover, visibility is defined as the readability of traffic signs.
- The visibility that was obtained from the pilot study is measured as the readability of the speed limit, as participants could easily report what they saw. The visibility of the leading car in the main studies does not translate directly to the readability of a traffic sign.
- As shown in the results and discussion section, the visibility in VR is mainly limited by the pixel density of the HMD (which is more than four times lower than the retinal resolution of the human eye) and the 8-bit RGB color space (256 intensity levels for each of the three

color channels). This means that the visibility of the traffic signs would be better in real life for the average participant.

3.5. Main VR driving study in Canada

During the fall of 2023, a larger VR driving study involving 51 participants (39 complete datasets) was conducted at the NRC. The cohort of participants differed from the cohort of the pilot study, although it is possible a few participants partook in both studies. The purpose of the VR driving study in Canada was to collect objective (output files from a driving scenario) and self-report data (responses to questionnaires and open-ended feedback) from participants that will inform future work. Specifically, the study aimed to better understand the effect of time of day, environmental conditions, and varying density levels of smoke or fog on driving behavior.

In addition, following a first pilot study conducted in 2022 to assess the usability of the driving simulator, the research team made some improvements to the virtual environment (VE), specifically to its interface and frame rate. For additional details on this pilot study, see the full report for the WUI-NITY 3 project (Ronchi et al. 2023). A secondary objective of the main driving study was to assess the usability of the driving simulator following these improvements.

Following a literature review, the research team put forward the following hypotheses:

1. Participants will drive faster during daytime than during nighttime.
2. Participants will drive faster in conditions with a low density of smoke or fog than in conditions with a high density of smoke or fog (based on (Wetterberg et al. 2021a)).
3. Participants will maintain a larger headway during nighttime than during daytime (based on (Zhu et al. 2016)).
4. Participants will maintain a larger headway in conditions with a high density of smoke or fog than in conditions with a low density of smoke or fog (based on (Rohaert et al. 2023c)).

3.5.1. Methods

Both the pilot study and the main driving study were approved by the NRC's Research Ethics Board (NRC-REB) under protocol #2023-63. All participants signed an informed consent form prior to taking part in the studies.

A convenience sample of participants was recruited from the NRC via internal bulletins and word-of-mouth to complete the driving scenario in VR. Interested individuals were provided with detailed information about the study and could schedule a session to take part in the study if they met the study's inclusion criteria (see below). Individuals were excluded if they met any of the exclusion criteria (led to one exclusion). Following a power analysis using G*Power, the research team aimed to recruit participants until they reached up to 40 complete data sets. The following parameters were used for the power analysis:

- Test family: F tests;
- Statistical test: ANOVA: Repeated measures, within-between interaction;
- Type of power analysis: A priori: Compute required sample size – given α , power, and effect size;
- Effect size: 0.20⁷;

⁷ As we did not have prior knowledge of the effect size, we assumed a medium effect size.

- α err prob: 0.05;
- Power ($1-\beta$ err prob): 0.95;
- Number of groups: 2;
- Number of measurements: 10^8 ;
- Correlation among repeated measures: 0.5;
- Nonsphericity correction ϵ : 1.

Inclusion criteria:

- At least 18 years old;
- Normal or corrected to normal vision;
- Driver's license.

Exclusion criteria:

- History of cardiovascular or vestibular conditions or respiratory diseases;
- History of epilepsy, severe motion sickness while traveling, eye disease, or recurrent migraines;
- Symptoms of COVID-19 or having been exposed to COVID-19 within the last 14 days on the day of data collection.

Following the pilot VR study on visibility (see section Pilot VR study on visibility for details), a larger data collection was conducted in Canada. Three independent variables were manipulated:

- Time of day (daytime vs. nighttime);
- Smoke (wildfire) vs. fog (no fire); and
- Five levels of smoke and fog obtained by adjusting the extinction coefficient K (based on the results from the pilot study: no smoke, low smoke, medium smoke, high smoke, and very high smoke).

All participants were randomly assigned to either the smoke (daytime and nighttime) **or** the fog (daytime and nighttime) experimental condition (the time of day was presented in a randomly assigned order). Participants first completed a practice trial to familiarize themselves with the equipment (1 trial) followed by the assigned experimental condition (10 trials). The research team decided to have participants complete only the smoke or the fog condition after completing pilot testing as individuals reported feeling cybersickness after driving for an extended period in the driving simulator.

Participants' experience (e.g., usability, presence) and their driving behavior (headway, speed) were examined as dependent variables.

Participants completed all the questionnaires via an online survey tool, LimeSurvey. Participants filled out the pre-experiment questionnaires prior to the immersions in VR and the post-experiment questionnaires following the immersions in VR.

⁸ We aimed to limit the amount of time spent in VR due to the length of each trial and participant's cybersickness.

Background questionnaire

The background questionnaire inquired about participants' age, gender, driver's license, driving experience, VR and gaming experience, previous experience with evacuating from a wildfire, etc. Participants completed the demographic questionnaire prior to the VR immersion.

Driving behavior

During the VR immersion, participants' driving behavior (timestamps, position and rotation, speed, headway) was automatically recorded via output files generated by Unity.

Driving scenario

This questionnaire inquired about the driving scenario using a Likert-type scale from -3 to 3 (e.g., "How aggressive of a driver would you consider yourself?", "How afraid were you of getting in an accident during the simulation?"). The questionnaire also contained an open-ended question: "How much was your speed choice affected by the wildfire smoke (or fog) and by knowing you were performing an evacuation (or by knowing that a fog warning was issued)?" The questions were based on (Wetterberg et al. 2021a).

Usability

This questionnaire contained items about the driving simulator's usability (e.g., "I thought the VR driving simulator was easy to use"), which were rated on a Likert scale from 1 (*strongly disagree*) to 5 (*strongly agree*). The items were based on the System Usability Scale (Brooke and others 1996).

Presence

A single item on presence assessed the extent to which participants felt like they were actually "there" in the virtual environment: "On a scale from 0 (*not at all*) to 10 (*totally*), to which extent do you feel present in the virtual environment, as if you were really there?" The question was based on (Bouchard et al. 2008).

Cybersickness

The Virtual Reality Sickness Questionnaire (VRSQ) (a short version of the Simulator Sickness Questionnaire [SSQ], (Kim et al. 2018)) was used to assess cybersickness. It is rated on a scale of 0 (*none*) to 3 (*severe*).

Feedback survey

A short questionnaire contained open-ended questions to obtain qualitative feedback about participants' experience (e.g., "How satisfied were you overall with your VR experience? Why?", "Are there any specific components about the VR driving simulation that you liked and/or did not like? Please explain why you liked or did not like them.").

Participants were immersed in the driving scenario using the same VR equipment as the pilot study on visibility (see section Pilot VR study on visibility for details), except that the Vive Pro Eye's built-in headphones delivered audio during the driving scenario. Participants were seated in the car seat mock-up and used the Thrustmaster 300RS steering wheel and acceleration and brake floor pedals to navigate in the driving scenario (see Figure 23). The same computers were used to run the driving scenario and to fill out the online questionnaires.

The VR driving scenarios were developed using Unity version 2020.3.141f. The same procedure as the pilot study was used to implement the fog and smoke colors and density values in Unity (see Figure 24).

Participants were immersed in a driving simulator via the VR headset and completed a total of 11 trials (one practice trial and 10 experimental trials, see Experimental conditions section for full list of experimental conditions). The order of the trials was randomly assigned.

In all trials, participants were the driver (no passenger) and viewed the scenario from a first-person perspective (see Figure 33 for an illustration). Depending on the experimental condition that the participant was completing, the scenario took place during daytime or nighttime, contained visual effects related to smoke or fog, and displayed varying levels of smoke. The scenario did not contain any other visual effects (e.g., no ember showers).

The practice trial took place during the daytime in a clear sky scenario (i.e., no visual effects related to wildfires or fog in the scenario) on the same highway as the experimental conditions. The highway was a two-lane road (one lane in each direction). Each lane was approximately 3 m in width. There were no other vehicles in the trials (i.e., the scenarios only contained the lead vehicle and the vehicle driven by participants). The highway was mostly straight and was flat to minimize cybersickness in participants (during piloting, larger curves led to more severe cybersickness). The speed limit was 70 km/h. The road did not have any intersections, stop signs, or traffic lights. There were trees on either side of the road to simulate driving through a forest. The practice trial's purpose was to familiarize participants with the VR equipment and navigating in the VE. Participants were asked to follow the vehicle in front of them (i.e., the lead vehicle, which is controlled by AI) without passing or overtaking it, but no other specific actions to follow or instructions were presented. When the trial began, the lead vehicle was approximately 15 meters in front of them. Once they reached the end of the road, the trial ended, and the application stopped automatically.

Participants' task in the baseline and experimental trials was identical to the practice trial. Participants drove on the same highway as they did during the practice. Once a trial was ended, participants were teleported back to the starting position to begin the next trial. The time of day and environmental conditions (i.e., smoke vs. fog and level of visibility) varied depending on the experimental condition. The Unity application recorded and generated an output with participants' position and rotation, speed, and distance between the vehicle they were driving and the lead vehicle. Once participants completed all trials, the application stopped automatically, and participants were asked to fill out the online questionnaires (see Figure 34 for an illustration of the trial structure in Unity).

Both the practice and baseline take place in the day – clear sky scenario. Also, note that there were no streetlamps in the night scenarios.

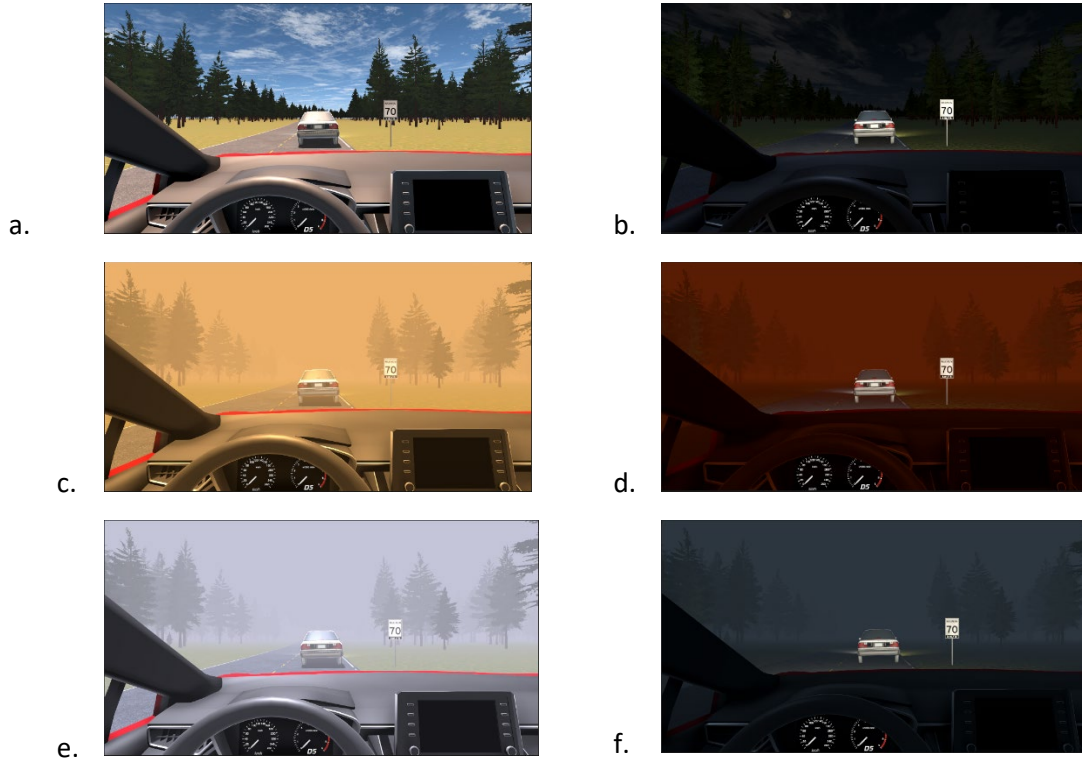


Figure 33. Illustration of participant's view in each condition. a) day – clear sky scenario; b) night – clear sky scenario; c) day – smoke scenario with Unity fog; d) night – smoke scenario with Unity fog; e) day – fog scenario with Unity fog; f) night – fog scenario with Unity fog.

The trial structure in Unity is presented in Figure 12.

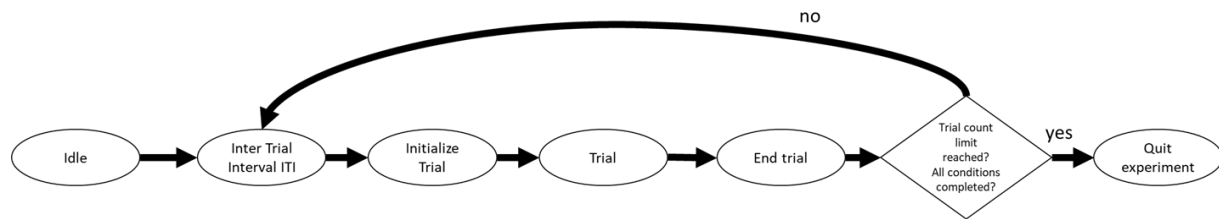


Figure 34. Flowchart of trial structure in Unity.

1. Start experiment; create output file; load environment.
2. ITI: The time interval between two trials; usually the screen is black then.
3. Initialize trial: Load the variables needed for the current trial (e.g., experiment condition, teleport player to start position); begin data recording; ends with fade in.
4. Trial: One instance of the experiment task; starts with the participant being in the start position and ends if a number of end conditions are met (e.g., reaching an end zone, time out).
5. End trial: Fade out; increase trial count by 1; stop data recording; remove completed condition from trial list.
6. Quit experiment: Save output file.

When participants arrived for the in-person appointment, a researcher greeted them and briefly explained the study's session procedure (see Figure 35 for an illustration of the data collection process). Participants were then given time to read and sign the informed consent form. The researcher answered any questions posed by participants. Participants then filled out the pre-experiment online questionnaires (background questionnaire and VRSQ).

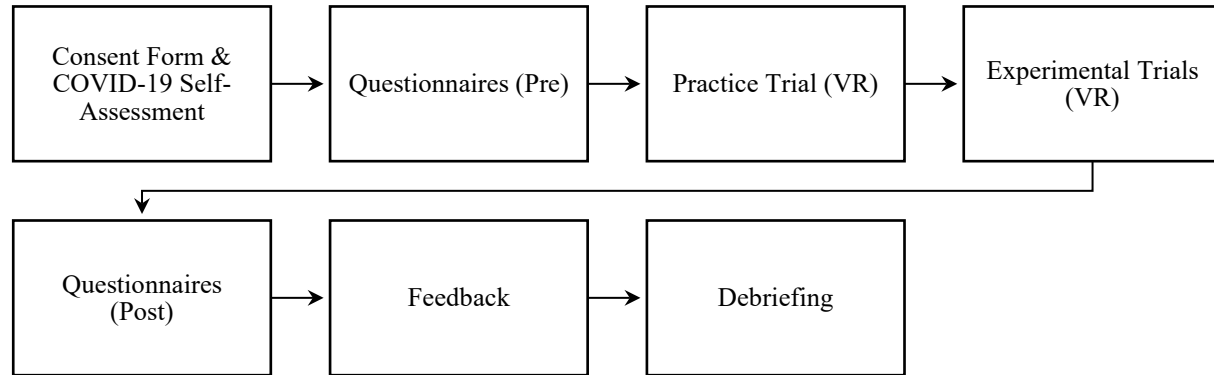


Figure 35. Illustration of the data collection process for the study.

Once participants finished filling out the questionnaires, the researcher explained the equipment and participants' task in VR (see Figure 36 for an illustration of the process). They also explained that participants might experience cybersickness and asked them to inform them if they did. The researcher then asked participants if they had any questions or concerns and reiterated that participants could choose to stop the study at any time for any reason. If not, they asked participants to sit in the car seat and wear the VR headset. Participants completed the practice trial followed by block 1 (smoke or fog) and block 2 (fog or smoke), with a break outside of VR between blocks.

Once all the blocks were completed, participants filled out the post-experiment questionnaires (driving scenario, usability, presence, VRSQ, and feedback survey). The researcher then verbally debriefed participants to tell them more about the objectives of the study and answer any questions they had.



Figure 36. Illustration of the process for the VR immersions for the study

3.5.2. Results

Parametric and non-parametric tests were conducted to analyze the questionnaire data. The normality assumption for parametric tests was not met and the data contained some outliers. However, when performing the non-parametric Wilcoxon Signed-Rank Test, ties in the data were obtained, which if removed could bias the data. Given that similar results were obtained for parametric and non-parametric tests and the robustness of parametric tests, only the results from the parametric tests are presented below. Open-ended feedback collected from participants was analyzed by identifying patterns in participants' comments.

Fifty-one participants took part in the study (smoke condition = 27; fog condition = 24). However, eleven participants were unable to complete the VR experiment due to cybersickness ($n = 9$), driving off the pavement and being unable to get back on the road ($n = 1$) and technical issues ($n = 1$). Most participants who withdrew from the study due to cybersickness withdrew during the practice trial or the first block of the VR experiment. One participant experienced severe cybersickness. In addition, the data of one participant was excluded due to distracted driving. The analysis of the driving data (driving speed and distance and time headway) included trials of 44 participants ($n = 44$). However, five participants did not finish all ten trials, leading to a total of 423 trials. The inferential analysis of the self-report data included participants with a partial or a complete dataset ($n = 44$), as long as they filled out both the pre- and post-scenario questionnaires. The descriptive analysis of the self-report data included all available datasets (pre-scenario: $n = 51$; post-scenario: $n = 44$). Note that only participants who completed most of the VR experiment filled out the post-scenario questionnaires as the questions could only be answered if participants completed the driving scenario.

During the VR experiment, Unity logged timestamps, the trial number, the trial name, the position, speed and distance headway of the vehicle driven by the participant.

Participants had the assignment to follow the car in front of them. Through the first fifty seconds of the experiment, the speed of the leading car increased linearly from 10.8 km/h (3 m/s) to 64.8 km/h (18 m/s), meaning that the constant acceleration equaled 0.3 m/s^2 . The leading car then maintained a constant speed (64.8 km/h) for 20 seconds before the experiment ended. The speed of the participants and the leading car are illustrated in Figure 37. Figure 38 presents two trials for which the participant did not follow the leading vehicle.

Not all participants followed the leading vehicle. It is assumed that the participants were only following the car in front of them when they drove the same speed and were still able to see the car. Therefore, two criteria were used to determine if a participant was following during the last twenty seconds of the trial:

- 1) **Speed criterion:** $17 \text{ m/s} < \text{avg}(v) < 19 \text{ m/s}$

The average speed of the participant lies between 61.2 m/s and 68.4 m/s. This means that the difference in average speed is less than 1 m/s and that the distance headway therefore does not increase or decrease with more than 20 m during the 20-second interval.

- 2) **Visibility criterion:** $\min(h) < 6.24/K + 4.5 \text{ m}$

The minimum gap (distance headway h minus the vehicle length of 4.5 m) is smaller than the distance at which all contrast is lost, and all pixels look the same. Here, the minimum headway is chosen, rather than the average headway. This is because some participants choose to keep the leading car on “the edge of their visible field”, decreasing speed when the car is visible, and increasing speed when the car becomes invisible.

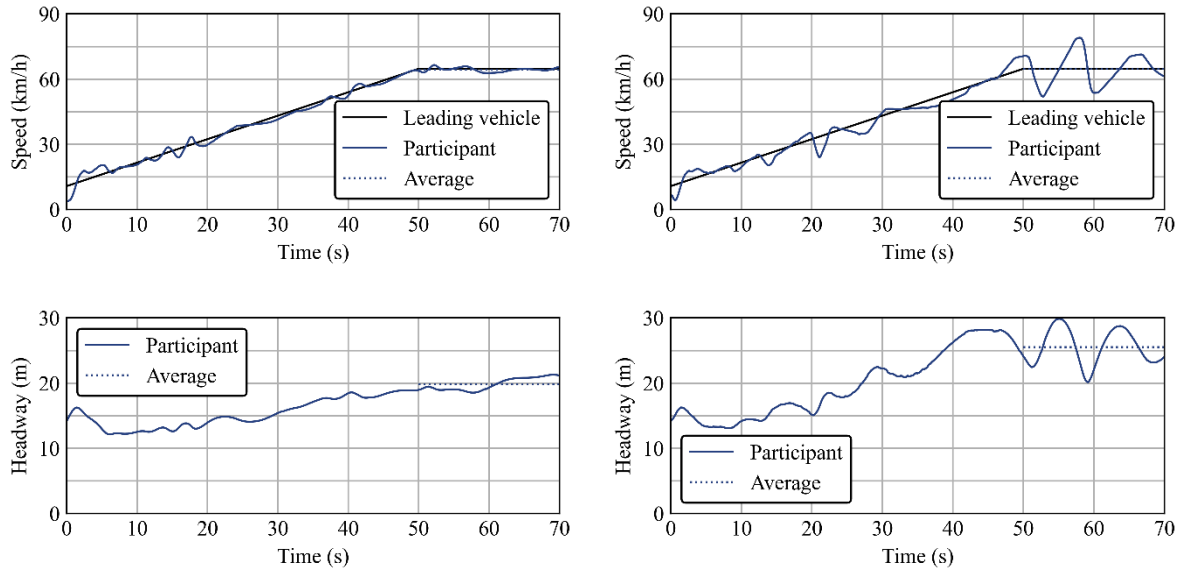


Figure 37. Speed (top) and headway (bottom) of the participants in relation to trial time for two trials during which the participant followed the leading car. Participant P04 (left) maintained a more constant speed than Participant P13 (right).

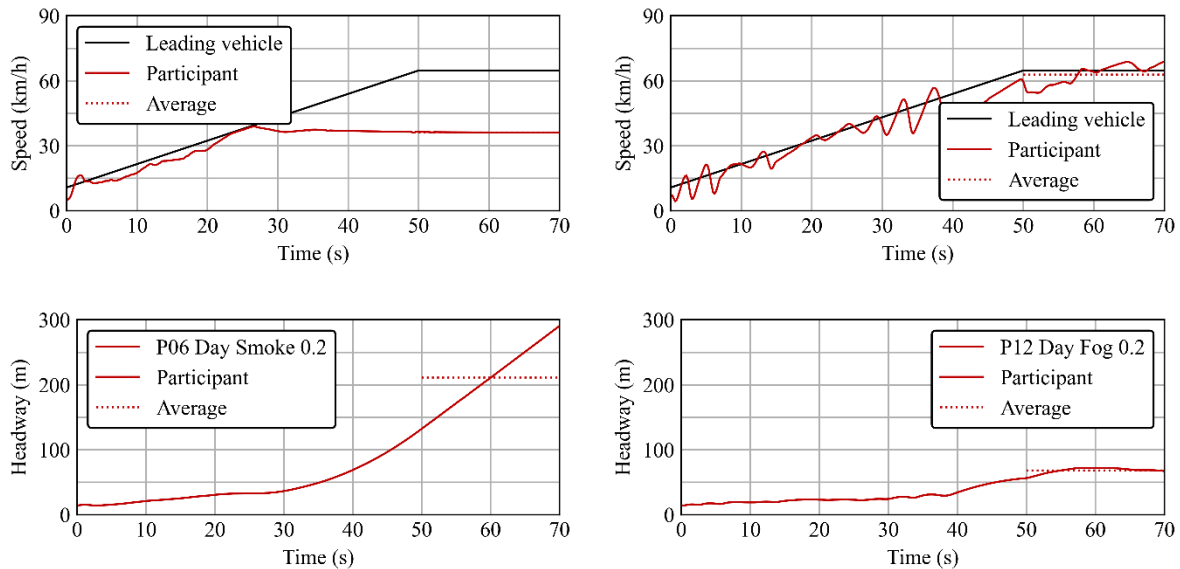


Figure 38. The speed (top) and headway (bottom) of the participants for two trials during which the participant followed the leading car. Note that participant P06 (left) decided to drive 36 km/h and therefore, the headway continued to grow. Participant P12 (right) reached a speed close to 64.8 km/h but was too far behind the leading car to see it.

Figure 39 shows the distributions of minimum headway and speed. The overlap between both criteria is presented in Table 3. In total, 423 trials are considered. For 356 (75%) of these completed trials, both criteria were met or not met. For the remaining 105 (25%) of the trials, one criterion was met and the other was not.

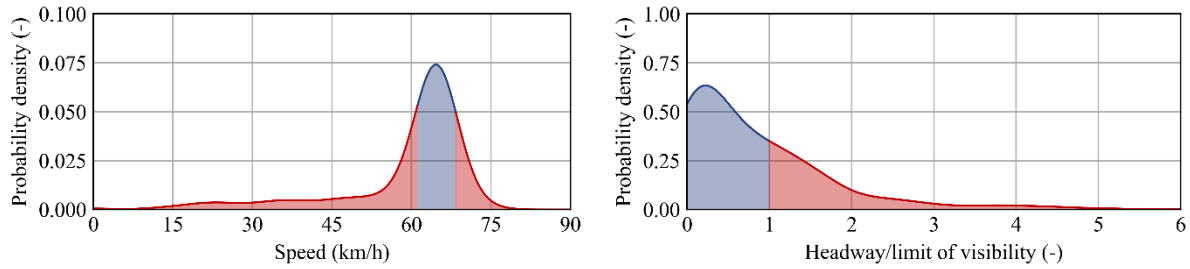


Figure 39. Left: probability of average speed. The blue area represents participants that drove approximately the same speed as the leading vehicle and the red area represents participant that are not following the leading vehicle. Right: probability of the minimum headway during the last twenty seconds of all trials. The headway has been scaled by the limit of visibility ($6.24/K$): for values greater than one, the leading car is not distinguishable from the fog or smoke and the participant is considered to no longer follow the leading vehicle.

Table 3. Confusion matrix showing number of trials in which headway and speed criteria were (not) met.

		Speed Criterion	
		Met	Not Met
Visibility criterion	Met	240 (57%)	49 (12%)
	Not met	56 (13%)	78 (18%)

Figure 40 presents the proportion of trials in which the “following” criterion was met for the experimental conditions. Between the “Day” and “Night” scenarios, there was no visible difference. The following percentage appears to be 10 % higher for the “Fog” trials compared to the “Smoke trials”. The following behavior also varied substantially with the visibility in the trial. 90% of the participants followed in the trials without smoke or fog ($K = 0.003 \text{ m}^{-1}$), while only 26% of the participants followed when smoke or fog was thin ($K = 0.05 \text{ m}^{-1}$). Interestingly, and somewhat unexpectedly, for thicker smokes, the percentage of following participants increased again. A possible explanation could be that in thin smoke, participants felt more comfortable driving alone, while in thicker smoke, they preferred to stay close to the leading car and use it as a reference to know where the road was located.

The last graph in Figure 40 shows that participants were more likely to follow during the last five trials they completed. This indicates that the participants might not have followed the leading vehicle in the beginning as they struggled with handling the vehicle simulator. Another reason might be that they decided to drive more carefully at the start as they had not yet learned the course of the trial (more specifically, the repeated road geometry and the speed profile of the leader). Due to the randomized trial order for each participant, this learning effect should not lead to biases when looking at the effect of light, atmosphere or extinction coefficient. This observation aligns with findings from Intini et al. (Intini et al. 2019a), which suggest that increased route familiarity can lead to faster driving and more confident behavior.

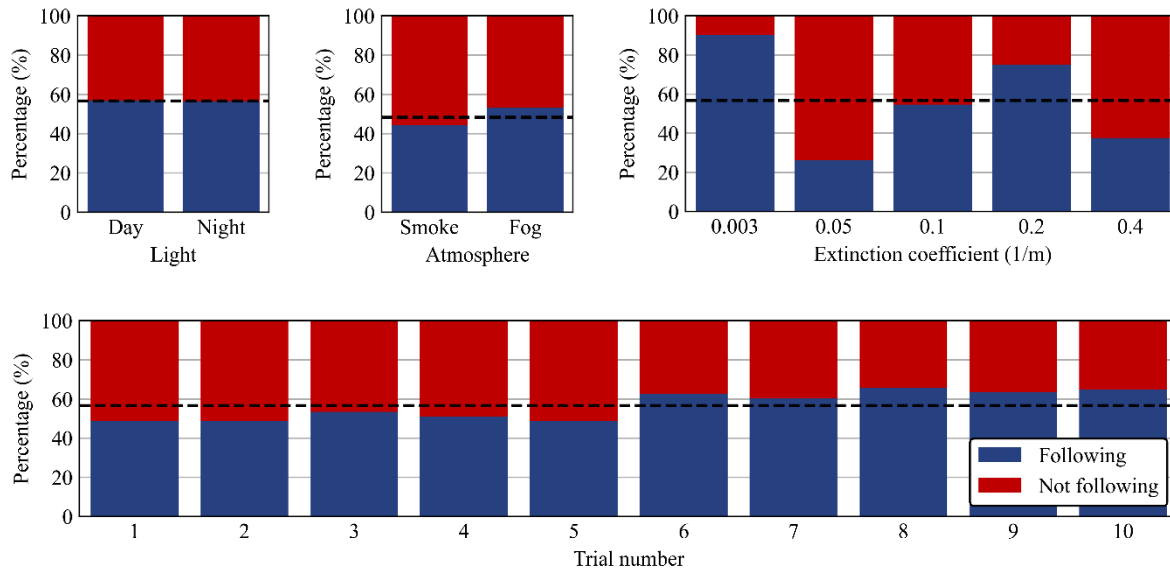


Figure 40. Following ratio (percentage of trials in which participants follow the leading car) across experimental conditions. The black dotted line presents the average following ratio across all trials (57%). For the second plot, the headways with an extinction factor equal to 0.003 are omitted (because the “no fog” is identical to the “no smoke” trial).

To assess the statistical significance of the differences in participants' following behavior, three two-tailed chi-squared tests were conducted. A Bonferroni correction was applied to the significance threshold to correct for multiple testing ($\alpha_{cor} = \alpha/3 = 0.05/3$). Table 4 summarizes the statistics and p values. The tests revealed no significant difference between "day" and "night" scenarios or between "fog" and "smoke" conditions, but a highly significant effect of the extinction coefficient.

Table 4. Chi-squared statistics and probability values

	Degrees of Freedom	Chi-squared Value	Probability of the hypothesis (p value)
Light conditions	1	0.00	1.000
Atmospheric conditions*	1	2.55	0.110
Extinction factor	4	95.07	1.100 e-19

* Note that for the atmospheric conditions, the scenario without fog/smoke ($K = 0.003$) is not included in the test. Therefore, only 339 trials are considered. For the light conditions and the extinction coefficient, all 423 trials are considered.

Figure 41 presents the headway for different categories. Descriptively, the headway does not seem to differ between the day and night scenarios. It also seems to be similar for the fire and the fog scenario, although probability distribution is wider for the fog scenario, indicating that participants' headways varied more.

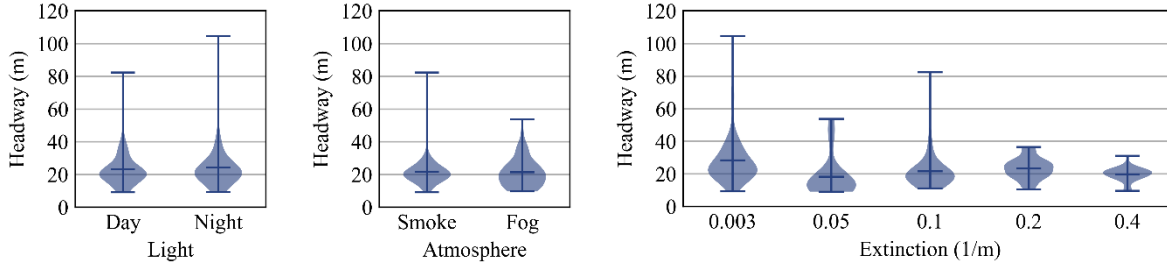


Figure 41. Violin plots of the distance headway for different categories. The bars indicate the extrema and the mean value. For the middle plot, the headways with an extinction factor equal to 0.003 are omitted (because the “no fog” is identical to the “no smoke” trial).

The extinction coefficient seems to have a strong effect on the headway: The average distance headway increases with decreasing visibility. A possible explanation would be that the participants keep a large distance because their risk perception increases with decreasing visibility. However, for the scenario with no smoke/fog ($K = 0.003/\text{m}$), the headway is greatest. Note that in this scenario, most people followed (see Figure 40). Participants who kept large headways may not follow in the scenarios with decreased visibility, leading to a bias in the data. Further, individual variability within each visibility condition was notable, with some participants keeping minimal headway regardless of visibility.

The effect of the light conditions (day and night), atmospheric conditions (fog and smoke), and the extinction factor on the distance headway is quantified using a mixed-effects model. In this analysis, 240 observations across 42 participants were included, with an average of 5.7 observations per participant. Here, the extinction coefficient was considered a categorical variable, as the effect of the extinction on the headway does not appear to be monotone. The model was fitted using the Restricted Maximum Likelihood (REML) method as implemented in the Python package *Statsmodels* (Seabold and Perktold 2010). The model successfully converged, indicating reliable results. The results of the MEM analysis, as presented in Table 5, reveal that only the extinction coefficient significantly influences the headway, with reduced visibility (from little too much smoke) leading to decreased headway distances. This suggests that participants adjust their behavior based on visibility.

Table 5. Mixed-Effects Model Analysis of Distance Headway (significant p values in bold).

Variable	Condition	Coefficient	Standard error	z	p value	Confidence interval	
Intercept		27.97	2.213	12.637	0.000	23.632	32.307
Light	Night	0.88	1.156	0.761	0.447	-1.385	3.144
Atmosphere	Fog	0.82	2.922	0.281	0.779	-4.907	6.548
Extinction	0.05 m^{-1}	-5.333	2.299	-2.32	0.020	-9.838	-0.827
Extinction	0.10 m^{-1}	-5.141	1.711	-3.005	0.003	-8.494	-1.788
Extinction	0.20 m^{-1}	-3.575	1.544	-2.315	0.021	-6.601	-0.548
Extinction	0.40 m^{-1}	-4.386	1.971	-2.225	0.026	-8.249	-0.523
Participant Variability		71.667	2.996				

Participants filled out questionnaires in LimeSurvey before and after the VR experiment. The results from descriptive and inferential analyses are presented below. See Table 6 for descriptive statistics of the questionnaire data. Note that one outlier for the VRSQ (cybersickness measure) was identified by visually inspecting the data; the outlier is included in the descriptive statistics for the VRSQ in Table 6.

Table 6. Descriptive Statistics from Self-Report Questionnaires (Pre: $n = 51$; Post: $n = 44$).

Questionnaire	Mean	SD	Min	Max
Driving Scenario – Post				
Aggressiveness	-0.30	1.71	-3	3
Fear of accident	-0.11	1.54	-3	2
Urgency	0.57	1.52	-3	3
Perceived risk	1.39	1.53	-3	3
Risk of harm	0.89	1.70	-2	3
Vehicle handling	-0.39	1.43	-2	2
Mockup realism	1.25	1.30	-2	3
Visual realism	0.25	1.71	-3	3
Usability – Post				
Ease of use	4.52	0.85	1	5
Comfort	4.16	1.06	1	5
Functionalities	4.02	1.09	1	5
Presence – Post	6.48	1.80	2	10
VRSQ – Pre				
Oculomotor	6.21	10.39	0	50
Disorientation	2.22	9.49	0	66.67
Total	4.22	8.90	0	58.33
VRSQ – Post				
Oculomotor	11.93	11.70	0	50
Disorientation	5.91	8.89	0	40
Total	8.92	9.26	0	45

Note. Means, standard deviations (SD), minimum values (Min), and maximum values (Max) are rounded up to two decimal places.

A descriptive analysis of the background data of all 51 participants (see Table 7) showed that most participants had their driver's license for over 10 years, drove on a daily basis, owned a car, and gained most of their driving experience in Canada. Most participants had some experience with playing video games, but few had experience using VR. Four participants had previous experience with wildfires (evacuation or fire suppression). Participants were between the ages of 24 and 66 ($M = 40.41$, $SD = 9.79$).

Table 7. Frequency of Responses from the Demographics Questionnaire (n = 51).

Item	Responses	Frequency	Percentage
Gender	Woman	26	50.98%
	Man	25	49.02%
License ownership	Between 7 and 8 years	1	1.96%
	Between 8 and 9 years	1	1.96%
	Between 9 and 10 years	2	3.92%
	More than 10 years	47	92.16%
Driving experience (frequency)	Daily	42	82.35%
	Weekly	8	15.69%
	Seasonal	1	1.96%
Driving experience (distance)	< 50 km/week	8	15.69%
	50-100 km/week	13	25.49%
	100-150 km/week	8	15.69%
	150-200 km/week	6	11.76%
	200-250 km/week	5	9.80%
	250-300 km/week	4	7.84%
	> 300 km/week	7	13.73%
Country where most driving experience gained	In Canada	50	98.04%
	Outside Canada	1	1.96%
Car ownership	Own a car	48	94.12%
	Do not own a car	3	5.88%
Experience with transmission	Automatic transmission	29	56.86%
	Equally familiar with both types	18	35.29%
	Manual transmission	4	7.84%
Experience with VR	Never used it	24	47.06%
	Tried using it a few times	24	47.06%
	Used to use but not anymore	2	3.92%
	Use less than every month	1	1.96%
Experience with video gaming	Never played	6	11.76%
	Tried playing a few times	7	13.73%
	Used to play but not anymore	17	33.33%
	Play less than every month	5	9.80%
		5	9.80%
	Play every month	8	15.69%
	Play every week	3	5.88%
	Play daily		
Experience with wildfire evacuation	No	47	92.16%
	Yes	4	7.84%

Note. Percentages are rounded up to two decimal places; some percentages might not add up exactly to 100%.

Nine participants withdrew from the study due to cybersickness (17.65% of the sample). Eight out of nine (88.89%) of the participants who withdrew were women. All participants who withdrew were above the age of 30 ($M = 48.67$, $SD = 9.51$) and had little or no previous experience using VR. The mean age of participants who completed the study was 38.78 ($SD = 8.83$). The results of a Mann-Whitney U test showed that there was a significant difference in mean age between the participants who completed the study versus those who withdrew ($U = 76.5$, $p = 0.007$). However, there was no significant difference between the two groups in terms of previous experience using VR ($U = 231$, $p = 0.192$). Mann-Whitney U tests were conducted instead of independent samples t-tests as the two groups were of unequal size. To examine whether the two groups differed in terms of gender, Fisher's Exact Test was performed (instead of a Chi-Square Test of Independence) as some cells had expected frequencies below 5. The results of Fisher's Exact Test were also not significant ($p = 0.099$).

Participants' ratings from the Driving Scenario questionnaire ranged from -3 to 3. A descriptive analysis showed that mean participant ratings were neutral or slightly positive. The item "Perceived risk" had the highest mean rating ($M = 1.39$, $SD = 1.53$). The item "Vehicle handling" had the lowest mean rating ($M = -0.39$, $SD = 1.43$).

Independent samples t-tests (see Table 8) indicated that the difference in mean ratings for the items "Perceived risk" and "Risk of harm" between conditions was significant. However, none of the other mean item ratings were significantly different between conditions. Note that the results above were significant even after applying the Holm-Bonferroni correction: $\alpha/(N\text{-rank}+1)$, or $.05/(8\text{-rank}+1)$ as eight independent samples t-tests were performed for the Driving Scenario questionnaire. See Figures 42-43 for individual and mean ratings from the Driving Scenario Questionnaire.

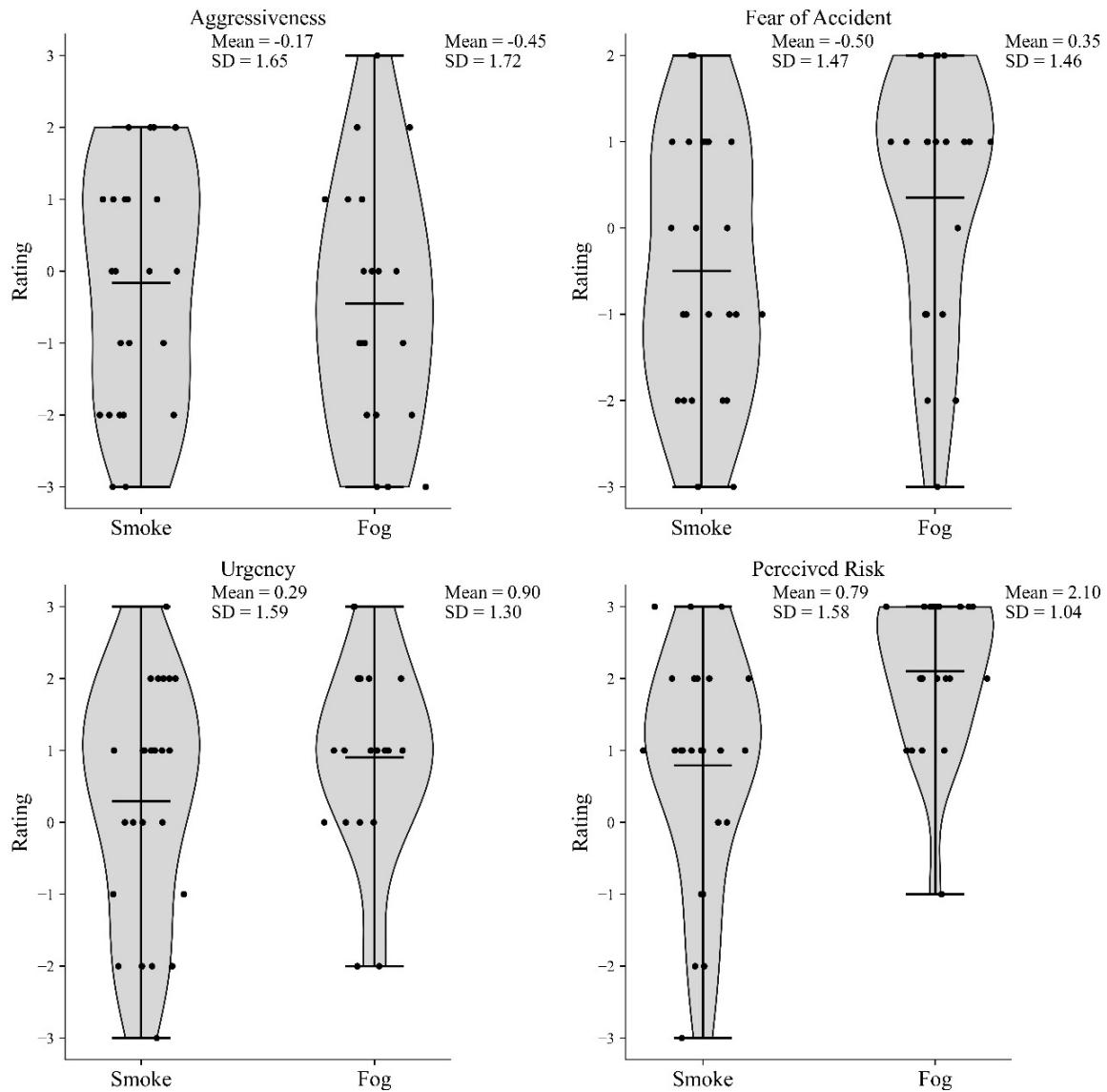


Figure 42. Individual and mean ratings from the driving scenario questionnaire (aggressiveness, fear of accident, urgency, perceived risk) by condition ($n = 44$). The markers represent individual data points; the line inside the violins represents the mean.

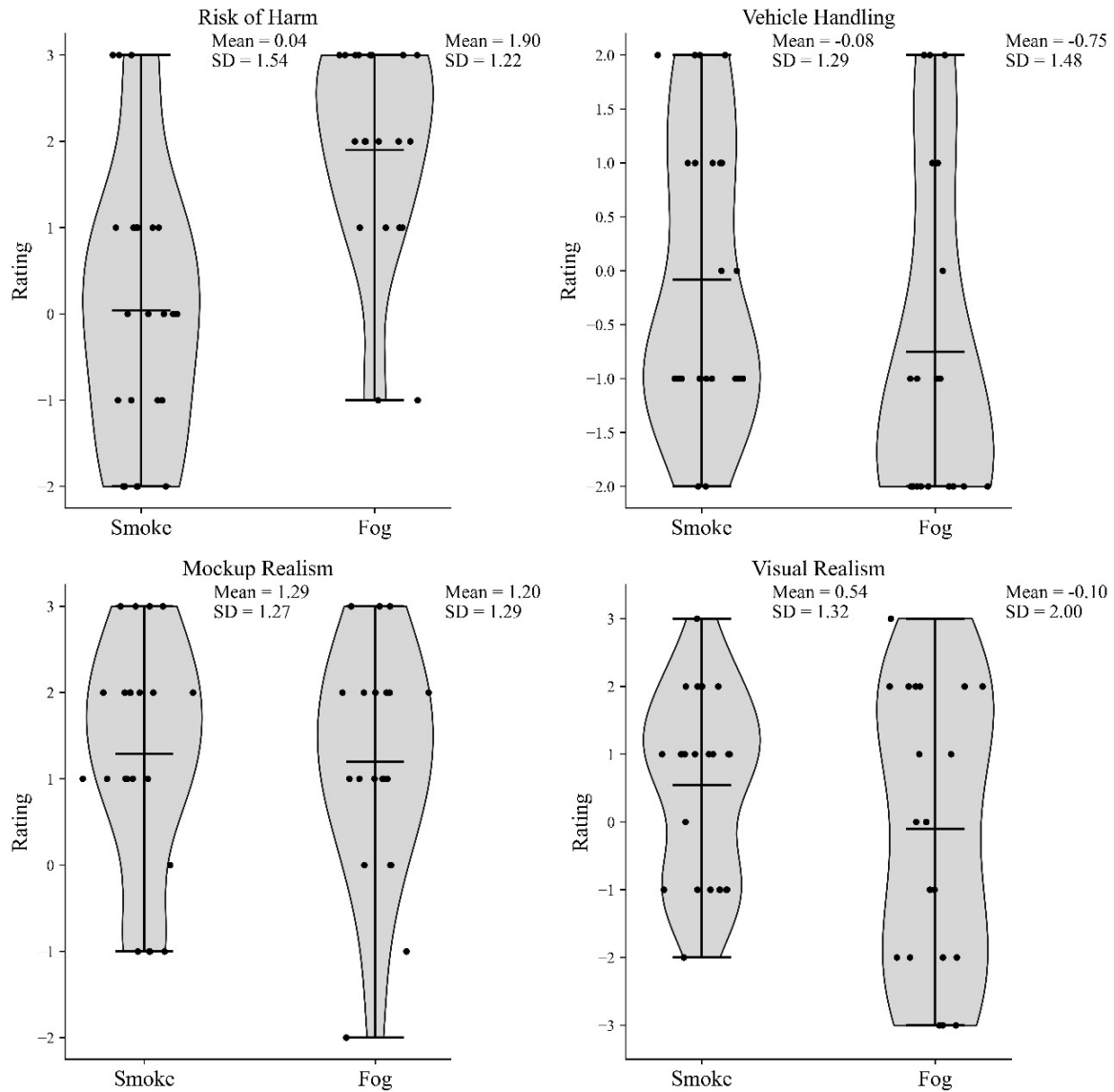


Figure 43. Individual and mean ratings from the driving scenario questionnaire (risk of harm, vehicle handling, mockup realism, visual realism) by condition ($n = 44$). The markers represent individual data points; the line inside the violins represents the mean.

Table 8. Results from independent samples *t*-Tests between smoke and fog conditions ($n = 44$, except VRSQ: $n = 43$).

Questionnaire	<i>df</i>	<i>t</i>	<i>p</i>	<i>d</i>
VRSQ – Pre				
Oculomotor	41	0.20	0.841	0.06
Disorientation	41	-1.46	0.152	-0.41
Total	41	-0.19	0.854	-0.05
VRSQ – Post				
Oculomotor	41	0.79	0.433	0.24
Disorientation	41	-0.68	0.501	-0.21
Total	41	0.21	0.834	0.06
Driving Scenario – Post				
Aggressiveness	42	0.54	0.589	0.16
Fear of accident	42	-1.87	0.068	-0.57
Urgency	42	-1.34	0.188	-0.41
Perceived risk	42	-3.10	0.003**	-0.94
Risk of harm	42	-4.27	0.0001***	-1.29
Vehicle handling	42	1.56	0.126	0.47
Mockup realism	42	0.23	0.818	0.07
Visual realism	42	1.25	0.220	0.38
Usability – Post				
Ease of use	42	-1.27	0.210	-0.39
Comfort	42	-0.81	0.425	-0.24
Functionalities	42	0.40	0.691	0.12
Presence – Post	42	-0.41	0.684	-0.12

Note. Statistics are rounded up to two decimal places; *p* values are rounded up to three decimal places.

** = $p \leq 0.01$; *** = $p \leq 0.001$.

Participants' ratings from the Usability Questionnaire ranged from 1 (*Strongly disagree*) to 5 (*Strongly agree*). A descriptive analysis indicated that mean participant ratings were positive. The item "Ease of use" had the highest mean rating ($M = 4.52$, $SD = 0.85$). The item "Functionalities" had the lowest mean rating ($M = 4.02$, $SD = 1.09$). Independent samples *t*-tests (see Table 8) showed that the difference in mean usability ratings for each item ("Ease of use", "Comfort", and "Functionalities") between the smoke and fog conditions was not significant. See Figure 44 for individual and mean ratings from the Usability Questionnaire by condition.

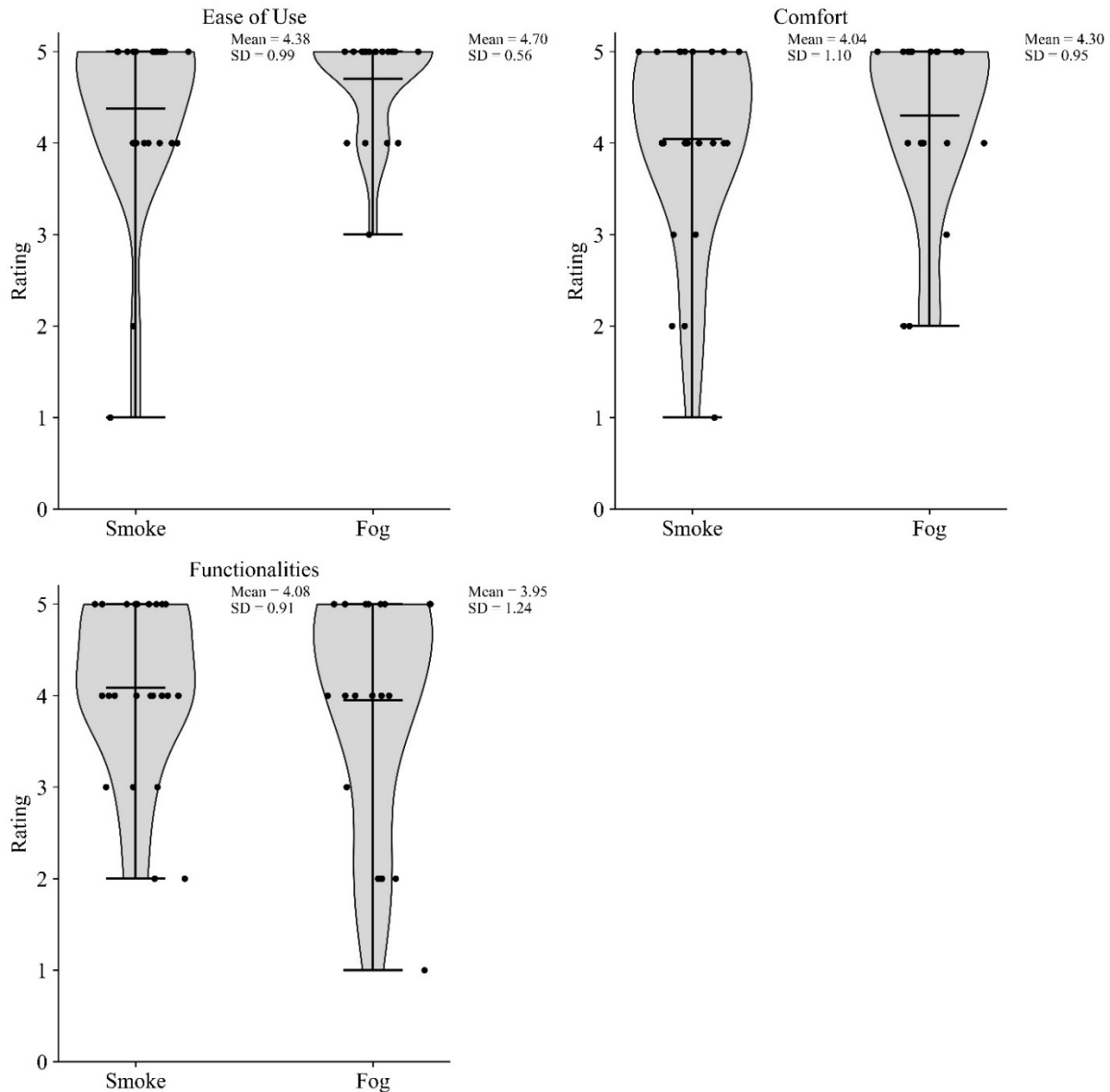


Figure 44. Individual and Mean Ratings from the Usability Questionnaire by Condition ($n = 44$). The markers represent individual data points; the line inside the violins represents the mean.

Participants' ratings from the single-item presence measure ranged from 2 to 10 (0 being the lowest possible score and 10 the highest for this measure). A descriptive analysis showed that mean participant ratings were positive. An independent samples t-test (see Table 8) showed that the difference in mean presence ratings between the smoke and the fog conditions was not significant. See Figure 45 for individual and mean ratings from the single-item presence measure.

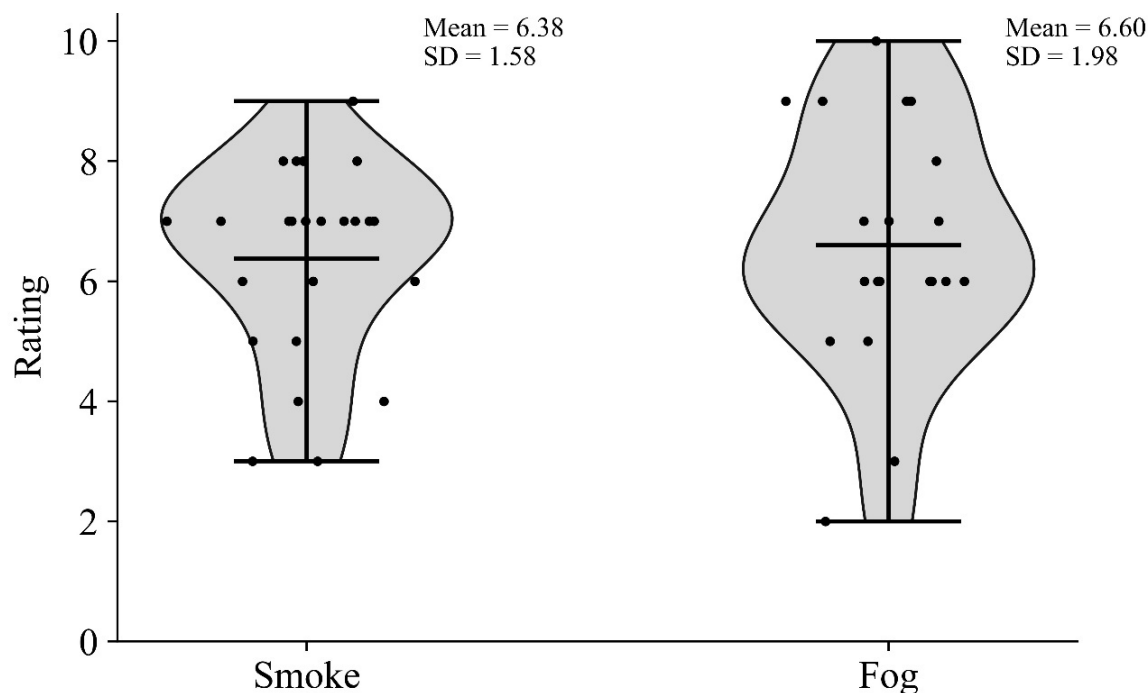


Figure 45. Individual and Mean Ratings from the Presence Item by Condition ($n = 44$). The markers represent individual data points; the line inside the violins represents the mean.

The results from the descriptive analysis suggest that cybersickness increased over time. One outlier was identified by visually inspecting the data (see the orange markers in Figure 46). When the outlier was included in the computation of mean scores, mean VRSQ Oculomotor scores increased from 6.21 (pre) to 11.93 (post). Mean VRSQ Disorientation scores increased from 2.22 (pre) to 5.91 (post). Mean VRSQ Total scores increased from 4.22 (pre) to 8.92 (post). When the outlier was excluded from the computation of mean scores, mean VRSQ Oculomotor scores increased from 5.33 (pre) to 11.05 (post). Mean VRSQ Disorientation scores increased from 0.93 (pre) to 5.12 (post). VRSQ Total scores increased from 3.13 (pre) to 8.08 (post).

Independent samples t-tests (see Table 8) showed that the difference in mean cybersickness scores (Oculomotor, Disorientation, and Total scores) between the smoke and the fog conditions was not significant pre-scenario or post-scenario. Note that the outlier was not included in the independent t-tests.

These results should be interpreted with caution as participants who withdrew from the study during the practice trial ($n = 9$) did not complete the post-scenario questionnaires. Many of the participants who withdrew reported experiencing motion sickness or nausea. As such, the mean VRSQ scores might be higher than those reported here.

See Figure 46 for individual and mean scores from the VRSQ by condition. Note that the line plots in the figure only include complete datasets (i.e., participants filled out the VRSQ pre- and post-scenario).

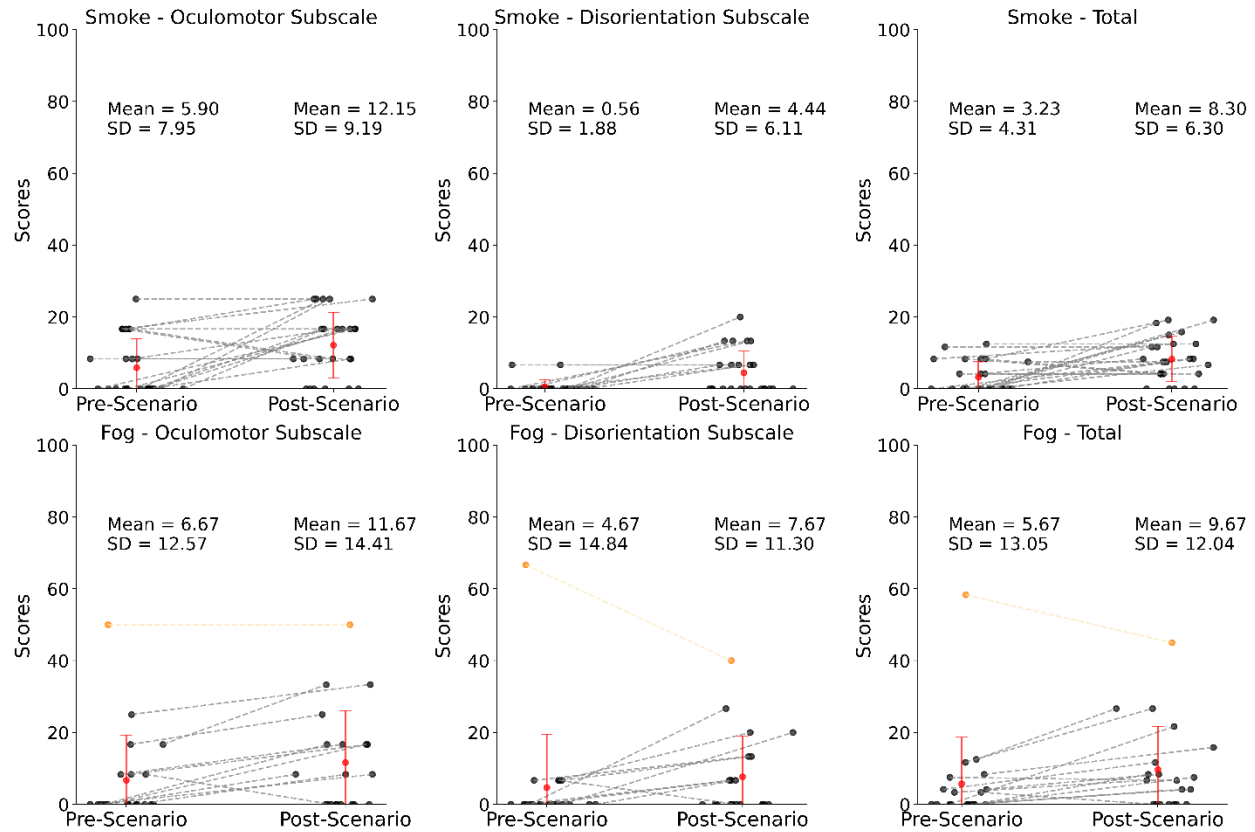


Figure 46. Individual and Mean Scores from the Virtual Reality Sickness Questionnaire by Condition ($n = 44$). The black markers represent individual data points; the orange markers represent an outlier; the red markers represent the mean. The plots only include complete datasets.

Paired samples t-tests (see Table 9) showed that the difference between mean pre- and post-scenario cybersickness scores (Oculomotor, Disorientation, and Total scores) was significant for both the smoke condition and the fog condition. The results were significant even after applying the Holm-Bonferroni correction: $\alpha/(N\text{-rank}+1)$, or $.05/(6\text{-rank}+1)$ as six paired samples t-tests were performed. Note that the outlier, identified by visually inspecting the data (see the orange markers in Figure 46), was not included in the paired-samples t-tests.

Table 9. Results from paired samples *t*-tests between pre- and post-scenario VRSQ Scores (smoke: *n* = 44; fog: *n* = 43).

Condition	Questionnaire	<i>df</i>	<i>t</i>	<i>p</i>	<i>d</i>
Smoke	VRSQ – Pre-Post				
	Oculomotor	23	-3.19	0.004**	-0.65
	Disorientation	23	-3.08	0.005**	-0.63
	Total	23	-3.55	0.002**	-0.72
Fog	VRSQ – Pre-Post				
	Oculomotor	18	-3.31	0.004**	-0.76
	Disorientation	18	-2.48	0.023*	-0.57
	Total	18	-3.32	0.004**	-0.76

Note. Statistics are rounded up to two decimal places; *p* values are rounded up to three decimal places.

* = $p \leq 0.05$; ** = $p \leq 0.01$.

The feedback survey contained five open-ended questions:

1. How much was your speed choice affected by the wildfire smoke and by knowing you were performing an evacuation? How much was your speed choice affected by the fog and by knowing that a fog warning had been issued?
2. How satisfied were you overall with your VR experience? Why?
3. Are there any specific components about the VR driving simulation that you liked and/or did not like? Please explain why you liked or did not like them.
4. What improvements do you think could be made to the VR driving simulation to become closer to real world driving?
5. What other comments do you have about your experience?

In terms of variables that affected speed choice, many participants noted that visibility affected the speed at which they were comfortable driving. For example, one participant reported: “*My speed choice was very affected by the amount of fog and visibility.*” Another participant commented that their driving speed in VR was similar to the real world: “*I felt I was driving much slower with poor conditions. I think my speed was reflective of how I would actually drive in the given conditions.*” However, participants reported other reasons for their speed choice. For example, several participants indicated being aware that the driving scenario was artificial and driving faster than they would in similar conditions in the real world. One participant mentioned: “*I knew that this was a simulation, therefore no true accident would occur. Therefore, my speed may have been more rapid than a real-life scenario.*” Other comments were related to task completion or compliance, perceived risk, and accident prevention. For example, one participant stated: “*My speed choice was mainly dictated by the task at-hand of following the vehicle in front of me given the circumstances. I understood it to be that the urgency of the situation did not warrant concern for the speed choice but rather a great focus on safe exit from the dangerous environment, hence the accelerations and decelerations based on the behavior of the lead vehicle.*” Another participant noted: “*My speed choice was very [a]ffected by the warning, and even more so by the actual visualization of the fog. Speed choice was decided in each scenario to prevent both accident, and off-roading.*” Many participants also commented that they tried to remain close to the lead vehicle. For example: “*My goal was mainly to follow the car in front of me, so I was trying to keep their*

speed. However, when the car would disappear, I think my speed went up because I was trying to get back to it. I would then follow the lines instead of the car.” Another participant commented: *“needed to stay close to other car in order to see where I was going in fog.”* Another participant mentioned: *“More fog = more speed/closer distance behind other vehicle.”*

Participants seemed to experience higher overall satisfaction when the VR experience was in line with their expectations. For example, one participant mentioned: *“Very satisf[ied], probably because of my expectations, i.e., I volunteered to experience a piece of study different from my own area of research, which was at the same time quite representative of my life outside of work (driving).”* Another participant indicated being more dissatisfied with the VR experience: *“It was ok. I was expecting more adverse driving conditions and more challenge (ex. quick decision making, roadblocks or obstacles)”*. While participants reported finding some components of driving in VR similar to the real world, many noticed differences between the driving simulator and real-world vehicles. For example, one participant found the driving simulator’s deceleration abrupt, which contributed to cybersickness: *“It was pretty good. My only feedback is that when you released the accelerator the sim car felt like it was slowing down quite abruptly and this made me feel nauseous. The sim in general was good. That’s about how I would feel in a forest with fog. In real life I would be able to pace the car better.”* Some participants reported finding the VR headset uncomfortable. For example: *“I liked the VR experience but it felt more like a video game. The headset was a bit uncomfortable because I was w[e]aring glasses.”*

Positive feedback included finding the VR driving scenario realistic, fun/enjoyable, safe, easy to use, and immersive. Participants appreciated the simplicity of the driving task, the physical driving simulator/mock-up, and the rendering of the smoke/fog (e.g., felt like they were actually driving in smoke/fog) and of day/night. For example, one participant noted: *“I found the fog to be realistic to an actual driving experience, I liked that the VR allowed me to realistically experience driving, such that I could even sit up further to better view the lines on the road.”*

Negative feedback included finding the VR driving scenario unrealistic/artificial and suggesting improvements to visual graphics, audio, and vehicle/floor pedal responsiveness. For example: *“I disliked the car’s handling because it felt like it didn’t roll, that is, continue[d] cruising when taking my foot off the gas. Often when following a vehicle closely, like in a fog situation, I would be shifting my foot from gas to brake rapidly, adjusting my speed, but it felt like as soon as I took my foot off the gas, the car was braking. I also disliked that the course was so straight and boring, I expected more turns or obstacles.”*

Participants suggested increasing scenario complexity by including additional components, such as obstacles, burning trees, and traffic. For example, one participant suggested adding *“Bur[n]ing trees either in the distance or on the side of the road. A lot more vehicles lined up trying to get out. Emergency vehicles along the road lights flashing. I think this is the reality for many people experiencing an emergency evacuation.”* Another participant suggested including *“More curves to the road, stop signs, car in front braking here and there, incoming traffic from other side of the road or from other streets, for the night version it would be nice to have lamp posts to show the effect of street lights mixed with the fog, maybe small animals to dodge on the side of the street. The reason I suggest these obstacles is that we get used to the simulation after one try so having the same road again without any obstacles does not reflect realistic driving.”* A third participant suggested making changes to the audio and including haptic feedback: *“The audio and accelerator*

can use a few changes. Also, in the even[t] of a nearby fire, the noise can be very loud (high winds). This could be something to add as well. Sometimes with high winds and heat, the car can also move (vibrate). This could add another effect to mimic real world driving.” One participant also suggested providing a longer familiarization period with the driving simulator: *“A bit more time to get used to "the car" - If a car acceleration/deceleration feels wonky, I want to drive a lot more carefully until I get used to it.”*

Several participants did not include any additional comments in the feedback survey. However, one participant indicated that they gained a better understanding of what it would be like to drive in a wildfire: *“I appreciate the experience as I would not otherwise know what driving in a wildfire would be like”*. Another participant also made suggestions to increase the sense of urgency: *“I totally missed the sense of urgency, risks or danger that the scenarios were supposed to convey. I was way too focused on keeping the vehicle between the lines and not going too fast (a concern I certainly would have in a real situation). One way to improve this may be incorporating sound (e.g. a soundtrack simulating emergency sounds or the radio calling for evacuations, etc.”*

3.5.3. Discussion

The following hypotheses were put forward: (1) participants will drive faster during daytime than during nighttime, (2) participants will drive faster in conditions with a low density of smoke or fog than in conditions with a high density of smoke or fog, (3) participants will maintain a larger headway during nighttime than during daytime, and (4) participants will maintain a larger headway in conditions with a high density of smoke or fog than in conditions with a low density of smoke or fog.

The results from the speed and the headway data suggest that some participants drove faster and maintained a smaller headway to try to maintain visual contact with the lead vehicle whereas others drove slower and maintained a larger headway and lost visual contact with the lead vehicle in conditions with higher smoke or fog. Broughton et al. (Broughton et al. 2007) observed a similar effect where participants either stayed within the visible range of the lead vehicle (“non-laggers”) or lagged beyond the visible range of the lead vehicle (“laggers”) when driving through simulated fog conditions in a driving simulator. The results from the current study also seem to support (Saffarian et al. 2012) who suggested that the lead vehicle might act as a guide. Many participants from the current study reported that they tried to remain close to the lead vehicle. One participant mentioned that they followed the lead vehicle closely to see where to drive in the fog. Patterns in individual driving speed suggest that some participants tried to “catch up” to the lead vehicle once they lost sight of them.

In the feedback survey, many participants reported that they were afraid of colliding with the lead vehicle (fear of accident) or of driving off the pavement. In contrast, other participants indicated that they were aware that this was a simulation and that no accident in the physical environment would occur. This suggests that participants who perceived the VR driving scenario as artificial/low risk focused more on task completion (e.g., following the lead vehicle) while participants who perceived the scenario as realistic/high risk focused more on scenario conditions (e.g., driving slower in poor visibility conditions). In other words, participants’ perception of the scenario and feeling of risk might have contributed to their driving behavior (e.g., higher speed, smaller headway or lower speed, larger headway). This result is similar to Saffarian et al. (Saffarian

et al. 2012) who found that overall, participants' feeling of risk and steering activity were higher when they lost visual contact with the lead vehicle compared to when the lead vehicle was visible.

It is possible that participants' level of presence also played a role in how "real" they found the VR driving scenario. If participants felt like they "were there" and that the events in the driving scenario were actually occurring, their driving may have been more similar to the real world. In contrast, if participants felt like they were in a laboratory and that the events were not actually occurring, their driving may have been different from the real world. The results from the single-item presence measure indicated that overall, participants' level of presence in the virtual environment was good. In the feedback survey, several participants mentioned feeling immersed in the virtual environment or that they found the driving scenario immersive and realistic. However, other participants reported finding the driving scenario unrealistic or noticing artifacts that "broke" their feeling of being in the virtual environment, such as lags.

Interestingly, the results from the driving scenario questionnaire showed that mean participant ratings for perceived risk and risk of harm were higher for the fog condition than for the smoke condition. This might be due to the wording of task instructions being slightly different for each condition. Specifically, participants in the smoke condition were told that the local public authority had ordered a mandatory wildfire evacuation whereas those in the fog condition were told that the local public authority had issued a fog warning. These instructions might have contributed to varying levels of perceived risk and risk of harm in participants depending on their assigned condition. In addition, only four out of 51 participants had previous experience with a wildfire whereas most participants likely had previous experience with fog. Perhaps, participants rated perceived risk and risk of harm higher for fog as they could relate to driving in fog in the real world or the fog scenario was more in line with their expectations. For instance, many participants in the smoke condition expected certain elements that were not in the virtual environment, such as burning trees, obstacles, and emergency response vehicles.

The results from the usability items suggest that overall, participants found the driving simulator easy to use and comfortable and that it had the functionalities that they expected it to have. In the feedback survey, participants reported finding components of the VR driving scenario similar to the real world, such as the visual appearance of fog. However, participants also noticed differences between the driving simulator and real-world vehicles (e.g., pedal responsiveness). A few participants reported that their driving behavior in VR was different from their driving behavior in the real world. For instance, participants noted that they would drive slower in poor visibility conditions in the real world. Participants also indicated that they would not drive as closely to the vehicle in front of them in poor visibility conditions in the real world. Participants suggested making improvements to the driving scenario to increase realism. Specific suggestions focused on improving or including additional visual components (burning trees, obstacles, traffic), audio components (wind, warnings on the radio, more realistic engine sound), and haptic components (vibrations).

Another limitation of the current study was the responsiveness of the floor pedals. Many participants commented on the floor pedal responsiveness being worse than in a real-world vehicle. Specifically, participants reported that the virtual vehicle accelerated too slowly when pressing on the gas pedal and decelerated too quickly when releasing it. This could have an impact on driving

speed and headway as it was more difficult to control the vehicle's speed. The pedal responsiveness will be fine-tuned in future work. Participants also suggested having a longer familiarization period with the driving simulator and the VR equipment. This would also help participants familiarize themselves with the vehicle handling and vehicle physics.

The results from the VRSQ showed that cybersickness scores were significantly higher post-scenario than pre-scenario, which is in line with (Venkatakrishnan et al. 2019) who found that SSQ scores were significantly higher following an immersion in a VR driving scenario than before the immersion. Approximately 18% of participants (nine out of 51) withdrew from the current study due to cybersickness. Of those who withdrew, 88.89% (eight out of 9) were over 40 years old and 88.89% were women. Participants noted that being unable to keep a constant speed and perceiving visual motion without corresponding physical motion induced motion sickness. Previous driving simulator studies have found that women (Almallah et al. 2021) and older adults were more susceptible to simulator or motion sickness (Brooks et al. 2010; Matas et al. 2015; Palacios-Alonso et al. 2022). Most of the participants who withdrew from the current study did not complete the post-scenario questionnaire, which included the VRSQ. This might have biased the cybersickness results, and it is a limitation of the study. The research team tried to balance obtaining data to meet the study objectives and making design choices to try to minimize cybersickness. For example, participants completed one of the two scenarios (i.e., smoke or fog). While completing both scenarios would have increased statistical power, it would also have increased the risk of cybersickness. Minimizing user discomfort and cybersickness is important for a positive VR experience. Further improvements should be made to the pedal responsiveness and vehicle physics. Participants withdrawing from the study due to cybersickness also suggests that VR is not for everyone.

3.6. Main VR driving study in Sweden

During the spring of 2024, a second large study was performed, this time at Lund University in Sweden. The study involved 37 participants (usable data were eventually obtained from 30 of them).

Objectives: The purpose of the VR wildfire evacuation study in Sweden was to collect data from the participants (both data about the times and positions in the virtual environment, as well as the responses to questionnaires and open-ended feedback). This study aimed to inform future work on wildfire evacuation behavior. Specifically, the study aimed to better understand the effect of smoke (i.e. reduced visibility conditions) on the car following behavior. This car-following behavior is explicitly modelled in microscopic traffic simulations and can be used to deduct a speed density relationship used for macroscopic traffic simulations.

The research team proposed the following hypotheses: When smoke is dense, and visibility is poor:

- Participants who are alone on the road will drive slower (Wetterberg et al. 2021a).
- Participants who follow a car ahead of them will keep a greater distance headway from that car (Intini et al. 2022).

3.6.1. Methods

In this section, the methods employed to design the experiment are discussed.

Ethical aspects: The VR experiment was conducted in accordance with the Swedish Act (2003:460) concerning the ethical review of research involving humans. The study was approved by the Swedish Ethical Review Authority (dossier number 2023-04122-01). All participants signed an informed consent form prior to taking part in the studies. The study has been pre-registered on *AsPredicted.org* (#162906), an online platform that allows researchers to pre-register their hypotheses, methods, and analysis plans before conducting their studies to enhance transparency and reduce biases in scientific research.

Participants: A convenience sample of participants was recruited. The experiment was advertised on accindi.se, an online platform where individuals can sign up to participate in scientific studies and market research surveys, earning compensation for their involvement. Additionally, informational posters were distributed on the university campus, and word-of-mouth advertising further promoted the study. As pre-registered, the sample size was limited to no more than 80 participants and participation was to occur until the end of June 2024.

Participation was only allowed if the interested individuals met all the requirements below:

- Must be 18+ years old
- Have normal or corrected-to-normal vision.
- Have a driver's license.
- Can communicate in English.
- Are not using a hearing aid that is incompatible with over-the-ear headphones.
- Do not suffer from epilepsy.
- Do not suffer from severe motion sickness or car sickness.
- Do not suffer from migraines.
- Do not suffer from stress or anxiety-related disorders.
- Have not had a concussion before.

Eventually, by the end of June 2024, 37 volunteers took part in the experiment. Participants were asked to complete pre-experiment and post-experiment questionnaires to capture demographic information, baseline measures, and feedback on their experience, including any symptoms of cyber sickness. All collected data was anonymized to protect participants' privacy.

Participants were continuously monitored for signs of discomfort or cybersickness during the VR sessions, and they were explicitly offered the option to withdraw from the study at any time without providing a reason. At the beginning of the experiment, after signing the informed consent form, participants received a voucher worth 100 SEK (\approx \$9.60 US).

Hardware solution: The VR setup included the HTC Vive Pro 2 headset. The In-Plane Switching Liquid Crystal Display screens with a combined resolution of 5K (2448×2448 pixels per eye) offered a field of view of 120° (horizontally) and could operate at a refresh rate of 120 Hz.

The desktop computer powering the VR system was equipped with an Intel Core i7-10700F CPU, operating at a base frequency of 2.90 GHz, with the capability to boost up to 4.8 GHz. This processor featured 8 cores and 16 logical processors and operated with a thermal design power of 65 watts. The system included 32.0 GB of RAM, running at a speed of 3.2 GHz.

The graphical performance was handled by an NVIDIA GeForce RTX 3080 graphics card. This card, built on the Ampere architecture, features 10 GB of GDDR6X VRAM and 8704 CUDA cores. It operated at a base clock speed of 1.44 GHz, with a boost clock speed of 1.71 GHz, and had a thermal design power of 320 watts.

For interaction within the VR environment, a Logitech G25 steering wheel and pedals were used. These controls were mounted on a Playseat Sensation Pro. Additionally, the steering wheel, seat, and seatbelt used in the setup were sourced from a real world 1986 Honda Civic. This provided the participant with the feel of a usual passenger car, rather than a race car. The cable of the head mounted display was suspended with pullies so as not to restrict the participants' movements. Figure 47 shows the setup.



Figure 47. The VR setup adopted in the driving behavior in smoke experiments.

Software solutions: For this experiment, a new environment was developed in Unity 2021.3.22f1. Objects have been designed in Blender and then imported.

Vehicle Physics Pro Community Edition (VPP) was used for the player car physics as it is a highly customizable package. This Unity asset managed driving and physics logic, including controls for steering, brakes, tire friction, and engine parameters. The participant drove the pickup truck that comes with this package. All vehicle settings were set to the default settings, except of the height of the center of mass (moved from 0.6 m to 0.3 m to make the car more stable) and the gear shifting time (decreased to 0 s to prevent shift shocks). The vehicle is shown in Figure 48 and Figure 50.



Figure 48. Road and the vehicle controlled by the participant. In this figure, the extinction factor K equals to 0.05 m^{-1} .

The position of the virtual camera rig in the simulation was fixed to the driver's seat. Moreover, the spin (rotation along the vertical y-axis) was also fixed, ensuring the participant always looked out the front. However, tilt and roll were not fixed to reduce cybersickness and provide a more realistic experience: This design mimicked the natural compensating movements made by the hips, back, and neck muscles while driving a car.

The road was designed as a Swedish country road, with dimensions, markings and equipment (traffic signs and road poles) per the requirements for road and street design, imposed by the Swedish Traffic Authority (Trafikverket 2022). The road was an undivided single carriageway two-lane road with a width of 7.0 m (3.5 m per lane). The shoulders were 1.5 m wide (0.5 m of continued asphalt and 1.0 m of gravel). The entire open field of view, which includes the road, shoulders, and the adjacent clear grassy areas on either side, totalled about 14.5 meters in width.

When driving in the virtual environment, the road was built progressively adopting procedural generation, which means that the road never ended. In practice, the road consisted of four tiles, each 500 m long in the z-direction. The participant started at the start of the second tile. When they reach the third tile, the first tile disappeared and a fifth tile was generated. For each tile, the shape was defined by a "road sway", as indicated by Figure 49. Each time, a random road sway was chosen between 30 m and 100 m (leading to a turning curvature radius of 417 m to 1389 m). These turns hid the horizon and made it possible to render only 700 m of road, without influencing the driving behavior. To build the road tiles, the Unity package "Dreamteck Splines" was used. The entire world was moved back every 500 m to avoid floating point issues (precision errors that occur when using very large numbers for positions in virtual environments).

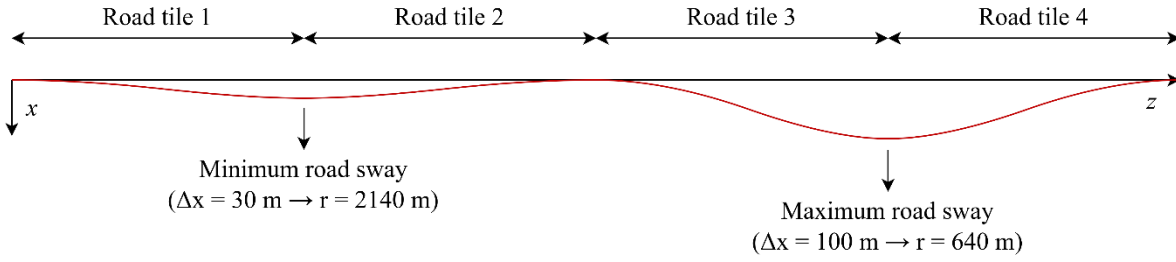


Figure 49. Schematic presentation of the road tiles adopted in the roadway for the VR experiment.

Special attention was paid to building all game object meshes with few polygons and not using high-definition textures when it was not required. The trees, for example, were constructed from three quads, intersecting at a central, vertical axis. The texture of these quads was a cut-out texture, allowing for more complex two-dimensional shapes without a complex mesh. This measure, as well as short rendering distances required by the swaying road, made it possible to run the head-mounted display at a refresh rate of 120 Hz (with a frame loading time of about 5.8 ms, well below the 8.33 ms available at 120 Hz). This high refresh rate was chosen to decrease discomfort and cybersickness among participants.

During the experimental trials, the participant had to drive slowly (as slow as 20% of the speed participants drove in that scenario before other vehicles were inserted. To be able to measure distance headways at these speeds, the participant could not overtake. Rather than telling participants directly how to behave, we choose to take some measures that would discourage them from overtaking:

1. The road was marked with a double solid line, indicating overtaking was not allowed.
2. Traffic signs indicating that overtaking is not allowed were repeated every 2 km.
3. Rather than one leading vehicle, a convoy of six leading vehicles was simulated, which was meant to convince the participant that they were part of a long traffic congestion, and that overtaking is futile.
4. Oncoming traffic passes randomly, about every two to five minutes, which was meant to increase the participant's risk perception of collisions during overtaking.

Moreover, every 2 km, a speed limit sign indicated the speed limit of 80 km/h. Participants were not explicitly instructed to follow the traffic rules. They only received the instruction “Please drive as you would in real life”.

To simulate the smoke, the built-in Unity Fog was used, similar to the two experiments in Canada. However, some efforts were taken to counter the shortcomings of this smoke (see Section 3.4.2):

1. The color of the smoke was derived from the assumed color of sunlight (RGB: 240, 185, 120). Smoke typically absorbs the light of different wavelengths differently; therefore, the smoke color was derived assuming the normalized mass-specific absorption of 1, 1.30 and 1.60 for the color channels red, green and blue (Wahlqvist and Rubini 2023b), leading to the smoke color RGB: 207, 152, 94.
2. Due to the smoke above the road, less sunlight reached the player. The sunlight was dimmed manually by multiplying the light intensity with the factor e^{-10K} . This meant that the direct sunlight was dimmed by a smoke layer equivalent to a homogenous smoke layer with a thickness of 10 m. Forty percent (40%) of this light was assumed not to be absorbed, but scattered, and was therefore added as ambient light. The exact ratio between absorption and

scattering of real smoke depends on the composition: pure water vapour scatters light almost perfectly, while very sooty fuels produce almost perfectly absorbing smoke.

3. The color of the smoke was used as the color of the direct sunlight and the ambient light. The same color was used for the skybox, which lost its contrast with increasing smoke levels (from cloud texture to plain smoke color).
4. Shadows were reduced artistically with increasing smoke levels, diffusing the light.
5. Adjustments were made to the standard shader (written in Microsoft's High-Level Shader Language (HLSL) and Unity's ShaderLab syntax) to prevent smoke from arising within the participant's vehicle.
6. Unity's fog employs the depth texture to assess the distance between the pixels and the camera and then interpolates between the pixel and smoke color. However, these distances are measured only in the camera's direction and are therefore inaccurate at the periphery of the image, especially for head-mounted displays with a large field of view, such as the HTC Vive Pro 2. To solve this issue, the rendering pipeline of Unity (written in Cg, a modified version of the High-Level Shader Language HLSL) was adjusted to calculate the depths in the horizontal direction (along the x and z-plane).

Figure 50 shows the simulated smoke from the participant's perspective.

During pilot tests, participants mentioned that the silence in the car was slightly uncomfortable, and that, in real life, they would tune in on the radio to receive more information concerning the wildfires. Therefore, a radio fragment from the Swedish radio broadcaster Sveriges Radio was playing on the background. The fragment dates from Friday, July 20 2018, 10:00 am and reports on the ongoing wildfires and evacuations all over Sweden. It did not provide any instructions. However, it does mention to look out for fleeing deer and other forest animals. At the start of the test trial, the radio fragment started playing from a randomly selected point within its duration. For the experimental trials, it was programmed so that it seemed like the broadcast had continued while the participant was taking a break.



Figure 50. The participant's view on the road for the five different smoke levels ($K = 0.003, 0.05, 0.10, 0.15$ and 0.20 m^{-1})

Experimental procedure: The participants went through eight phases between arriving at the experiment and leaving. Figure 51 illustrates the procedure. The entire procedure took about one hour for one participant.

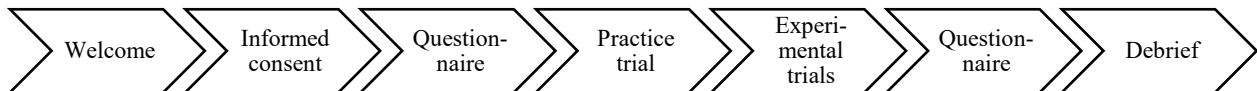


Figure 51. Illustration of the experimental procedure in eight phases.

Welcome: Upon arrival, participants were greeted and thanked for their interest in participating. A researcher gave an overview of the experiment. With this initial step, a comfortable and welcoming environment was established, helping to put participants at ease.

Informed consent: Next, participants were provided with detailed information about the experiment. This included explaining potential risks and benefits as well as giving the opportunity to ask questions about the study protocol. Participants then signed an informed consent form,

indicating their voluntary participation and understanding of their rights. After signing the consent form, participants received a voucher.

Questionnaire: Participants then completed a short pre-experiment questionnaire. This questionnaire was designed to collect baseline data on the symptoms of cybersickness. The sickness score of the experiment was then calculated from the changes in symptoms during the experiment. Just as in Canada, the Virtual Reality Sickness Questionnaire (VRSQ) was used (Kim et al. 2018).

Practice trial: After filling out the questionnaire, the participant was invited to sit down into the driving simulator. The car seat was adjusted (both the distance to the wheel and the angle of the back support) to the comfort of the participant and the seatbelt was fastened. The participant was introduced to the pedals, the steering wheel and the head-mounted display (HMD). The researcher ensured that the VR headset was properly fitted, adjusting the fasteners and lens distances to match the participant's interpupillary distance. This customization is important for ensuring optimal visual clarity and comfort, enhancing the overall VR experience. Then, the participant was asked to drive on an infinite road and to become familiar with the controls. They were instructed to drive as they would in real life.

“It is important that you remember that this is not a video game, but a driving simulator. Please drive as you would in real life.”

During this practice trial, six cars were driving ahead on the road, driving at 60 km/h. No smoke was present in the practice trial. One speaker of the HMD was left open to enable the researcher and participant to communicate with each other. The participant was asked to continue until they felt comfortable with the controls.

Experimental trials: The participant was provided with the scenario description, read by the researcher.

“During a severe summer drought, Sweden has been hit by several large forest fires. Although firefighters are working day and night to extinguish the fires, many are still spreading. Some of them pose an immediate threat to life safety as they are spreading towards places where people live. The Swedish authorities have therefore decided that mandatory evacuations are necessary. You are currently close to a forest fire and have been ordered to evacuate to a safe place. You just need to follow the road to get there.”

Next, the participants went through five trials. All trials had an identical structure, but the smoke level differed in each scenario, with Unity smoke densities (equivalent to the extinction coefficient) varying between $K = 0.003, 0.05, 0.10, 0.15$ and 0.20 m^{-1} . These five trials can be ordered in 120 different ways (permutations). These permutations were randomized in a way that each participant went through the trials in a unique randomized order.

During every trial, the participants went through twelve stages (illustrated in Figure 52):

1. **Idle.** The participant started in the idling vehicle on an empty road. This phase lasted until the participant had driven five meters.
2. **To 100.** During this stage, the participant had time to speed up to their desired free-flow speed. This phase lasted until the participant drove at least one hundred meters and at least $(125-250 K)$ seconds passed, with K the extinction coefficient in m^{-1} .
3. **Go 100.** The third stage took exactly half a minute during which the participants' desired free-flow speed was measured.
4. **To 80.** Next, a convoy of six passenger cars (leading vehicles) was inserted in the simulation, out of sight for the participant. The initial distance was greatest for the scenario without smoke (660 m) and shortest for the densest smoke (34 m). The leading vehicles drove at a speed equal to 80% of the free-flow speed, measured at stage 3. The duration of this stage was set so that the participant had twenty seconds to establish a stable headway after catching up with the leading vehicle, assuming they maintained the speed measured in the previous phase.
5. **Go 80.** Once the stable headway was established, the fifth stage started. Like the third stage, this stage took exactly half a minute during which the participants' distance headway was measured.
6. **To 60.** Next, the leading vehicles slowly slowed down at a deceleration of 0.1 m/s, until they reached a speed that equals 60% of the participants' free-flow speed. Afterwards, this stage took twenty more seconds to allow the participants to stabilize their distance headway.
7. **Go 60.** This stage took exactly half a minute during which the participants' distance headway was measured.
8. **To 40.** The leading vehicles slowed down at the same rate as before until 40% of the participant's free-flow speed. This stage continued for twenty more seconds to allow the distance headway to stabilize.
9. **Go 40.** This stage took exactly half a minute during which the participants' distance headway was measured.
10. **To 20.** The leading vehicles slowed down to 20% of the participants' free-flow speed. This stage continued for twenty more seconds to allow the distance headway to stabilize.
11. **Go 20.** This stage took exactly half a minute during which the participants' distance headway was measured.
12. **Finish.** A message appeared on the screen that the scenario has ended: "Thank you. You can now take off the headset."

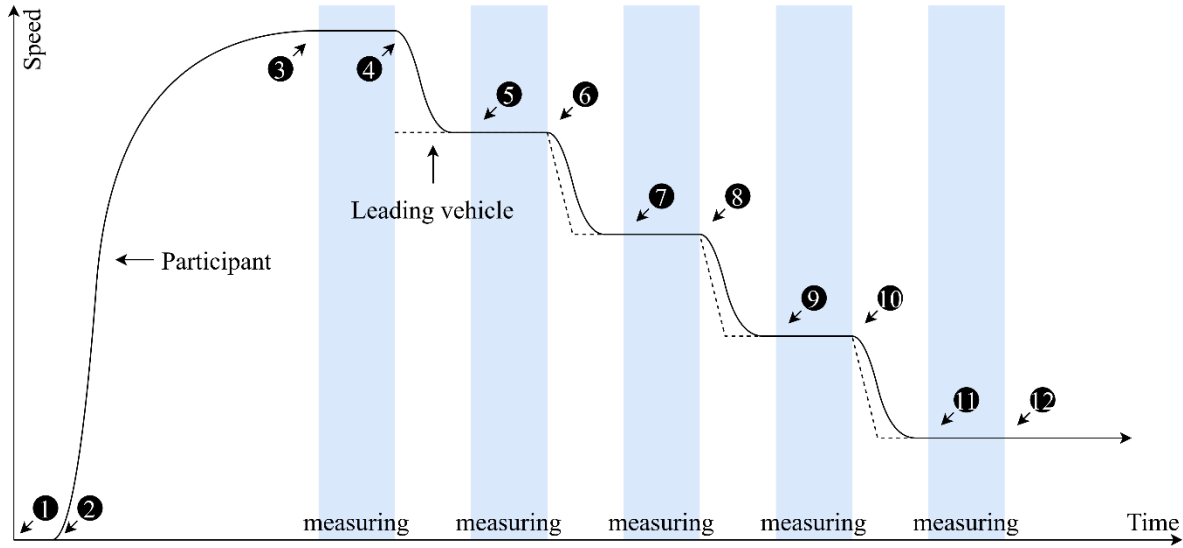


Figure 52. Schematic representation of the vehicle speeds during a trial.

The duration of one trial depended on the smoke density (in dense smoke, the leading vehicles were introduced closer to the participants) and the free-flow speed (at high speeds, it took the leading vehicles longer to slow down). Eventually, the average trial duration (from the start of the second stage till the end of the eleventh stage) took about seven minutes. Between the trials, the researcher checked up on the participants' possible symptoms of cybersickness. They were invited to take short breaks between the scenarios and were offered a glass of water.

Questionnaire: After finishing the experimental trials, participants completed a post-experiment questionnaire. Firstly, they filled out questions identical to those in the pre-experiment questionnaire: the Virtual Reality Sickness Questionnaire (Kim et al. 2018). Next, they were asked to reflect on their experience and driving behavior. Lastly, the questionnaire gathered demographic information. The entire questionnaire and the results were made publicly available in an open-access repository (Rohaert 2024).

Debrief: The procedure concluded with a debriefing session. During this final step, the experimenter explained the purpose and expected outcomes of the experiment to the participants. Participants were also given the opportunity to ask questions and provide feedback on their experience, ensuring they left the study with a clear understanding of its aims and their role in it. Lastly, they were thanked for participating and guided out of the lab.

Data analysis and model calibration: Macroscopic traffic models describe traffic dynamics of uninterrupted roads by three aggregate variables: the traffic density k (veh/km/lane), the vehicle speed v (km/h) and the traffic flow q (veh/h/lane). The speed density relationship (or equivalent; the flow density relationship) is an essential part of macroscopic models and are sometimes referred to as 'macroscopic models' themselves. They quantify how much the traffic slows down, depending on the congestion. Many relationships exist. Here, the model by Daganzo (1994) (see Equation 7) was used, as it is a popular model that fits well to evacuation data (Rohaert et al. 2023d, b). The model consists of two regimes: a free-flow regime, in which drivers can drive their

desired (free-flow) speed, and a congested regime, in which drivers follow slower cars ahead at a safe distance.

$$v = \min \left(v_f, v_f \frac{\frac{1}{k} - \frac{1}{k_j}}{\frac{1}{k_c} - \frac{1}{k_j}} \right) = \min \left(v_f, v_f \frac{h - h_j}{h_c - h_j} \right) \quad [\text{Equation 7}]$$

where v is the vehicle speed, k the traffic density and h the distance headway, which is the inverse of the traffic density. The subscript f denotes free-flow conditions, c denotes critical conditions (when the flow is at peak capacity) and j denotes entirely jammed traffic (total congestion). Figure 53 presents the model graphically.

Microscopic traffic models simulate the behavior of individual vehicles on the road, focusing on the detailed interactions between them rather than using aggregate measures like speed and density. Instead of relying on a speed-density relationship, microscopic models use car-following models to obtain the speed of vehicles, depending on the headway. When assuming steady-state conditions, these car-following models become equivalent to speed-density relationships. In other words: speed-density relationships are not imposed but emerge from the rules individual vehicles use to follow leading vehicles. The car-following model (Krauss 1998a) used in Simulation of Urban Mobility better known as SUMO (Alvarez Lopez et al. 2018), is equivalent to the model by Daganzo (1994) when steady-state conditions are met (see Equation 8).

$$v = \min \left(v_f, v_f \frac{h - h_j}{h_c - h_j} \right) = \min \left(v_f, \frac{h - h_j}{\tau} \right) \rightarrow \tau = \frac{h_c - h_j}{v_f} \quad [\text{Equation 8}]$$

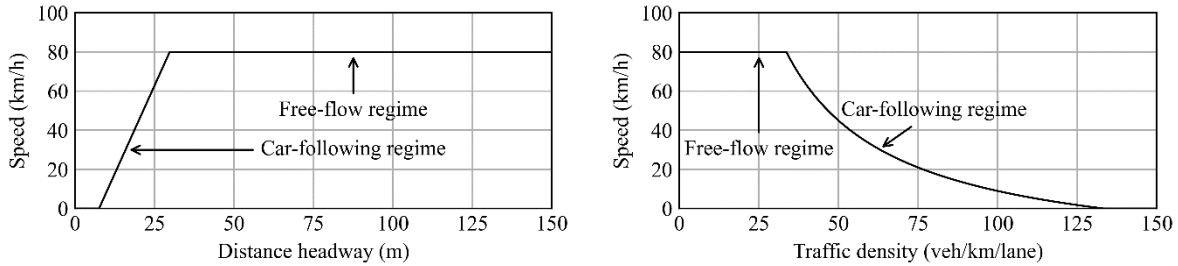


Figure 53. The speed-density relationship by Daganzo (1994). The specific curve follows from the default parameters of a passenger car in SUMO (Alvarez Lopez et al. 2018) ($h_j = 7.5$ m and $\tau = 1$ s; so $h_c = 29.7$ m, $k_c = 33.6$ veh/km/lane and $k_j = 133$ veh/km/lane when $v_f = 80$ km/h).

To investigate how the speed-density relationship is affected by the smoke level, five data points were measured for each participant, at each smoke level: the free-flow speed of the participant and the distance headway at four different speeds (80%, 60%, 40% and 20% of the free-flow speed of the participant). The free-flow speeds occurred at a zero density and therefore have an infinite headway. Consequently, the free-flow regime results from the average free-flow speed and the car-following regime results from a linear fit to the headway-velocity data.

The relationship between speed, headway and extinction have been fitted by means of mixed effects models because the data points were dependent (multiple datapoints for each participant).

The optimal parameters of the models were found by employing the Hastings-Metropolis algorithm (Comets et al. 2017), as implemented in the R package SAEMIX. In SAEMIX, the algorithm optimizes the likelihood function of the nonlinear mixed-effects model.

3.6.2. Results and discussion

In total, 37 participants took part in the experiment. One participant experienced technical issues (loss of video signal due to poorly connected wires). Two participants experienced cybersickness and chose to terminate the experiment after two trials. Four participants had issues controlling the driving simulator; they unintentionally collided with the other vehicles and/or left the roadway. It is the researchers' interpretation that this was due to the high velocity (up to 150 km/h) they were driving at, issues finding the pedals and – in one case – insufficient driving experience. All data presented below excluded these seven participants: only 30 participants were considered in the analysis. On average, participants were immersed in the virtual environment for 34 minutes and 48 seconds. This duration does not include the practice trial.

Data availability: The deidentified data gathered during this experiment is made publicly available on an open-access repository (Rohaert 2024).

Sample demographics: The bar charts of Figure 54 show the demographics of the 30 participants. Of all participants, 53% identified as a man and 47% as a woman. On average, participants were 34 years old and obtained their driving license 15 years ago. Five participants reported not being used to driving in Sweden: they were most used to driving in Belgium (2x), the Netherlands, Hungary and the United States.

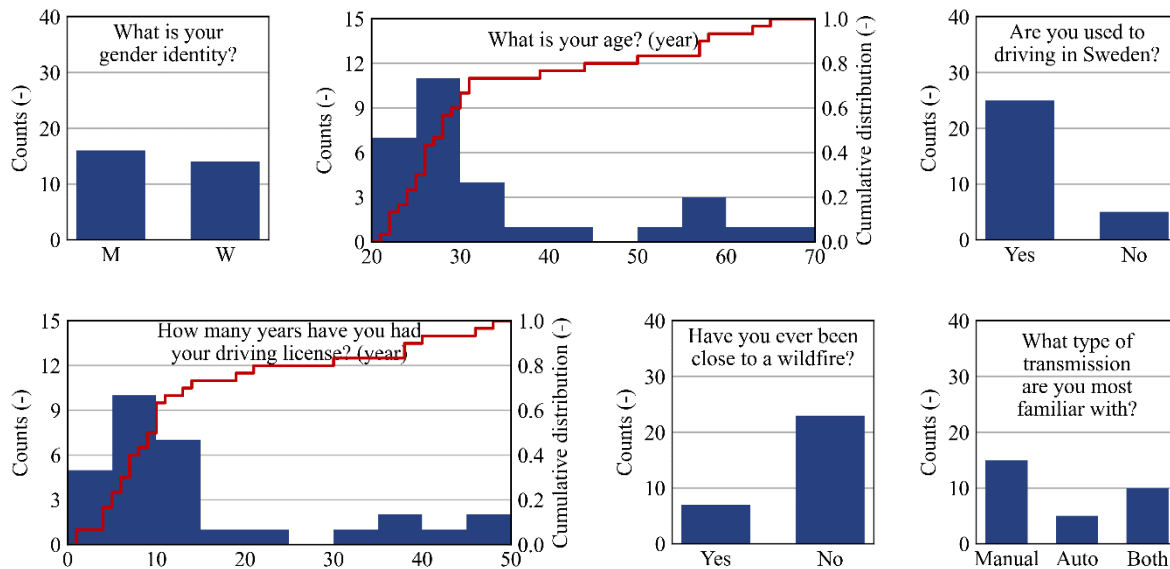


Figure 54. Demographics of the participant sample. The histograms “What is your age?” and “How many years have you had your driving license?” also provide the empirical cumulative distribution (red).

Participants were also asked how prudently/aggressively they drive by comparing their speed and overtaking with other drivers. As shown in Figure 55, participants reported to maintain similar speeds as others and overtake as often as others.

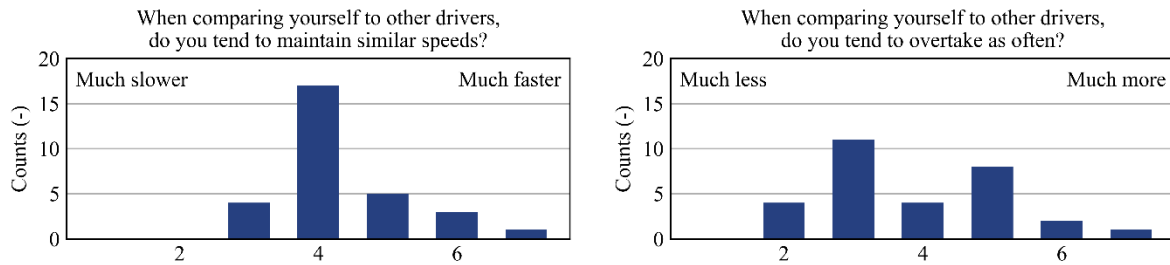


Figure 55. Self-reported driving behavior.

Figure 56 shows how frequently participants drive and game. Most participants (70%) indicated driving regularly – a few days a month or more often. Almost half of all participants (47%) play video games a few days a month or more often, while only one participant (3%) uses virtual reality a few days a month.

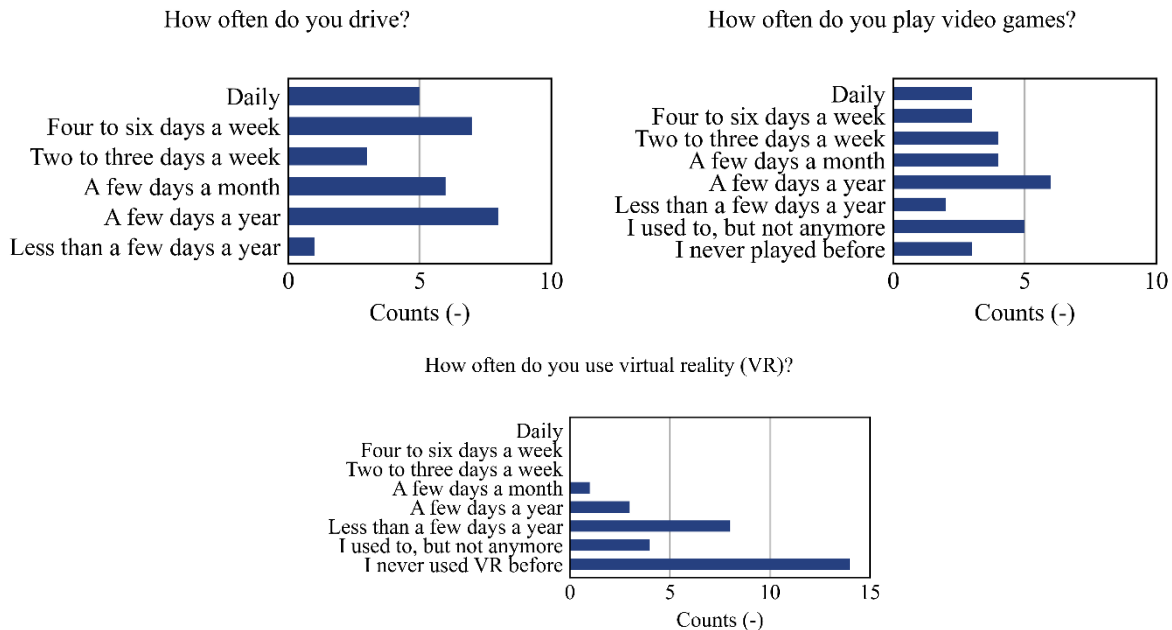


Figure 56. Frequency at which participants drive, play video games, and use VR.

Cyber sickness: Figure 57 presents the cybersickness score of the experiment, calculated in the same way as for the study in Canada (see Section 3.5). The average VRSQ score increase is 11.6% (13.3% for oculomotor and 9.8% for disorientation), which is considerably higher than in the study in Canada (5%). This increase can be partly explained by how long participants were immersed in the environment. In Sweden, immersion took 34 minutes and 48 seconds (with a standard deviation of 18 seconds). In Canada, immersion took about 13 minutes and 30 seconds for participants who completed all trials.

Despite the increased cybersickness score, it should be noted that only two participants out of 37 (5.4%) terminated the experiment due to sickness. In Canada, this was nine out of 51 participants (17.7%).

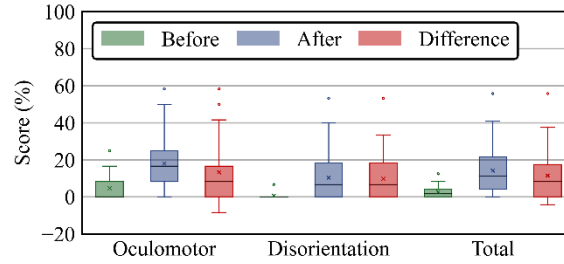


Figure 57. Cybersickness score of the experiment

Free-flow speed: The participants' free-flow speeds were measured during Stage 3 of each trial (see Section 3.6.2). The results are presented in absolute and relative values (in relation to the participants' free-flow speed during the trial without smoke) in Figure 58. The means and sample standard deviations are presented in Table 10.

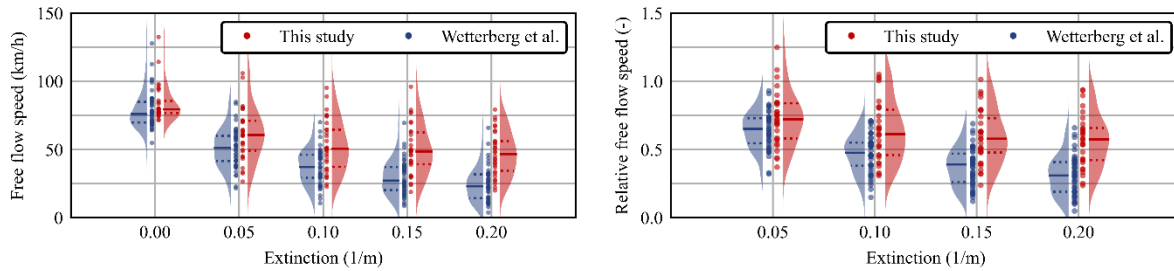


Figure 58. Participants' free-flow speeds in the function of the smoke density (light extinction). The graph on the left shows absolute speeds, while the graph on the right shows relative speeds. The data in blue is obtained by Wetterberg et al. (2021b), the data in red is obtained in this study.

Table 10. The means and sample standards deviation on the free-flow speed

Extinction coefficient (m ⁻¹)	Mean free-flow speed (km/h)	Standard deviation on the free-flow speed (km/h)
0.003	84.0	13.2
0.050	61.1	18.8
0.100	52.8	19.1
0.150	49.8	18.7
0.200	47.0	16.2

From Figure 58 and Table 10, it is clear that the extinction coefficient has a noticeable effect on the free-flow speed, suggesting a monotonic decrease in speed with visibility. The statistical relevance can be shown by a repeated-measures ANOVA using least squares regression ($p = 3.32E^{-25} < 0.05 \rightarrow$ statistical significance). No evidence was found that the normality or the sphericity assumptions of the ANOVA test were violated (Shapiro-Wilk test: $p = 0.191 > 0.05$, Mauchly's Test: $p = 0.172 > 0.05$).

Figure 58 also allows comparing the results of the present study with the study by Wetterberg et al (2021b). Both studies show a similar trend: participants drive slower when smoke causes lower visibility. However, in the study performed by Wetterberg et al., speeds reduce further than in this

study. Note that in that study, the speed limit equaled 70 km/h (while this study had a limit of 80 km/h). Three different monotone functions were fit to the relative free-flow speed: a linear function, a power function and an exponential reciprocal function (see Table 11). Since the data points are not independent, with each participant being measured five times, a stochastic approximation expectation-maximization (SAEM) algorithm was employed to estimate the parameters in a mixed-effects model. More specifically, the Hastings-Metropolis algorithm was used, as implemented in R (Comets et al. 2017).

Table 11. Relationships of the free-flow speed \bar{v}_f (-) and the extinction coefficient K (m^{-1}) fit to the data. All functions are chosen so that the relative speed is 1 for K equal to $0 m^{-1}$. The negative two times the log-likelihood (-2LL), the Akaike Information Criterion (AIC) and the Bayesian Information Criterion (BIC) are computed by importance sampling. Lower values indicate a better model.

Function	Parameter	Value	Covariance		-2LL	AIC	BIC
Linear $\bar{v}_f = 1 - c_1 K$	c_1	$2.664 E^{-0}$	$4.498 E^{-2}$		-87.6	-81.6	-77.4
Power $\bar{v}_f = 1 - c_1 K^{c_2}$	c_1	$1.051 E^{-0}$	$1.647 E^{-2}$	$4.398 E^{-3}$	-154.6	-144.6	-137.6
	c_2	$4.950 E^{-1}$	$4.398 E^{-3}$	$2.093 E^{-3}$			
Exp. reciprocal $\bar{v}_f = 1 - c_1 e^{-c_2/K}$	c_1	$4.967 E^{-1}$	$2.011 E^{-3}$	$9.136 E^{-5}$	-185.1	-175.1	-168.1
	c_2	$2.910 E^{-2}$	$9.136 E^{-5}$	$2.492 E^{-5}$			

After optimizing the parameters, the exponential reciprocal function has the lowest mean error on the prediction and fits best to the data. The function has been presented graphically in Figure 59.

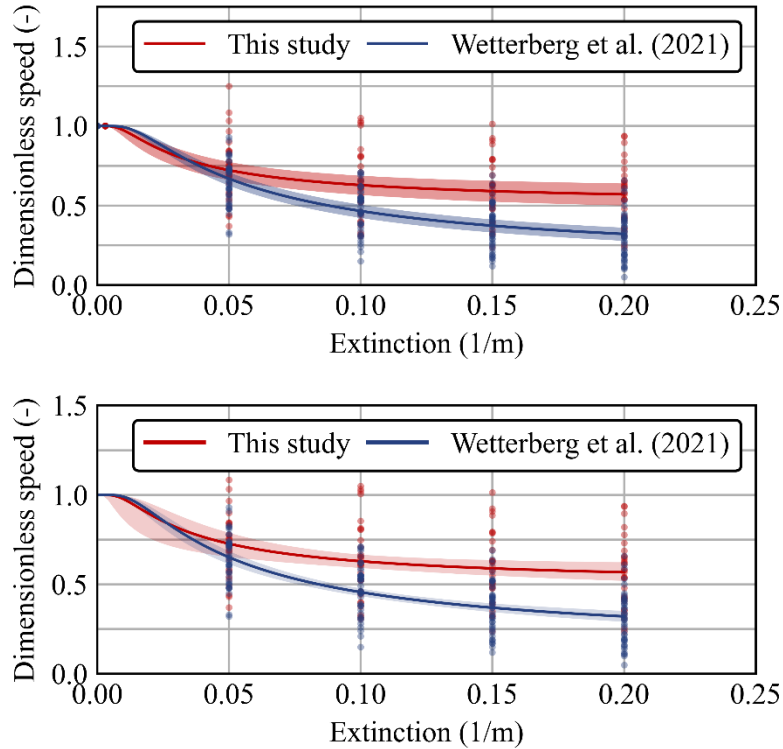


Figure 59. The relative free-flow speed as an exponential reciprocal function of the extinction coefficient. The bands represent the 95% confidence interval of the data fit and are obtained from a Monte-Carlo simulation that employs the covariance, reported in Table 11.

For this study, the best fit exponential reciprocal regression is given by Equation 9.

$$\bar{v}_f = 1 - 0.4967 e^{-0.02910/K} \quad [\text{Equation 9}]$$

Equation 10 is the best fit to the data obtained by Wetterberg et al. (2021b).

$$\bar{v}_f = 1 - 0.8619 e^{-0.04786/K} \quad [\text{Equation 10}]$$

Overtaking: On the road of the virtual environment, overtaking was not allowed (indicated by the double solid lines and the traffic signs). However, overtaking did occur ten times: six participants (20%) overtook once, and one participant (3%) overtook in four out of five trials. Six out of ten times participants who overtook did so in the trial without smoke ($K = 0.003$). This might indicate that participants are less comfortable overtaking when the visibility is poor and the risk of accidents increases. Six out of ten times, overtaking happened after Phase 9 of the trial: in these cases, participants waited to overtake until the convoy of the leading vehicle was reducing or had reduced its speed to 20% of the participants' free-flow speed. This might indicate that participants did not feel comfortable evacuating at such a slow speed.

Similar behavior has been observed anecdotally during real wildfire evacuations: evacuees would drive on the left side of the road or outside the road marking to overtake queues during the 2016 Fort McMurray evacuation, despite road regulations (Carton et al. 2024). However, it is unclear whether the participants in this virtual study had a similar motivation as the evacuees, or simply experienced boredom, frustration or curiosity to explore the boundaries of the simulation.

Distance headway: The distance headway was measured at four different speeds during each trial, which means that there could be 600 data points (four speed levels x five smoke levels x 15 participants). However, no headway could be measured when participants overtook the leading vehicles. Table 12 presents the data point counts per speed and smoke level.

Table 12. Data point count of headways at different speeds and different smoke levels

		Fraction of free-flow speed				Total
		80	60	40	20	
Extinction coefficient (m ⁻¹)	0.003	30	30	28	24	112
	0.05	30	30	30	30	120
	0.10	30	29	29	29	117
	0.15	29	29	29	29	116
	0.20	30	30	30	28	118
Total		149	148	146	140	583

For every headway measurement, the corresponding driving speed was recorded. Figure 60 illustrates this relationship through scatterplots, with each smoke level indicated in another color.

Next, a linear curve was fitted to the headway speed data. This linear curve is the car-following regime of the model by Daganzo (1994), and the emergent steady-state relationship between headway and speed of the car-following model by Krauss (1998b). The optimized parameters are

presented in Table 13, and the curves are visualized in Figure 60. It is reasonable to assume that drivers will leave the same gap between their vehicles when traffic is entirely jammed, regardless of the smoke level. Therefore, the parameters of all five linear fits were optimized simultaneously with separate slopes (τ), but one jam headway (h_j). The car-following regime was joined with the free-flow regime, discussed earlier, to establish the entire model (Figure 60).

Table 13. Relationships of the headway h (m) and the speed v (m/s) fit to the data. The negative two times the log-likelihood (-2LL), the Akaike Information Criterion (AIC) and the Bayesian Information Criterion (BIC) are computed by importance sampling. Lower values indicate a better model. The values for the slope τ are expressed in seconds. If the speed is expressed in km/h rather than m/s, the value should be divided by 3.6.

Function	Parameter	Value	Standard error	-2LL	AIC	BIC
Five linear curves $h = h_0 + \tau_K v$	h_0	8.756 E ⁻⁰	1.826 E ⁻⁰	4269	4295	4313
	$\tau_{K=0.003 \text{ m}^{-1}}$	2.487 E ⁻⁰	1.924 E ⁻¹			
	$\tau_{K=0.050 \text{ m}^{-1}}$	2.898 E ⁻⁰	2.683 E ⁻¹			
	$\tau_{K=0.100 \text{ m}^{-1}}$	2.355 E ⁻⁰	1.530 E ⁻¹			
	$\tau_{K=0.150 \text{ m}^{-1}}$	2.042 E ⁻⁰	1.235 E ⁻¹			
	$\tau_{K=0.200 \text{ m}^{-1}}$	2.314 E ⁻⁰	1.288 E ⁻¹			
One linear curve $h = h_0 + \tau v$	h_0	8.805 E ⁻⁰	1.615 E ⁻⁰	4389	4399	4406
	τ	2.481 E ⁻⁰	1.926 E ⁻¹			

* a minimum headway h_0 of 8.8 m corresponds to a jam density k_j of 114 veh/km/lane

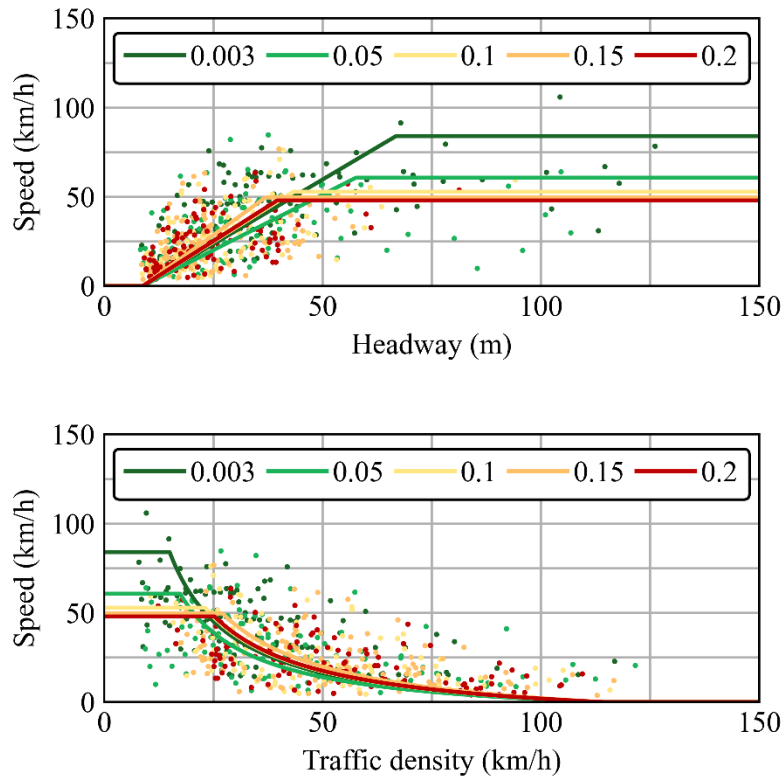


Figure 60. Steady-state relationship of the car-following model by Krauss (1998b), equivalent to the speed density relationship by Daganzo (1994) fitted to the experimental data, assuming a single jam headway (jam density). The legend indicates the smoke level by the extinction coefficient (m^{-1}).

When alone on the road, participants of this study drove slower when the visibility was worse (the extinction coefficient was higher). It is easy to assume that the participants tried to mitigate the increased risk of losing control of the vehicle by slowing down. This means evacuation times might be longer when smoke obscures visibility on the road.

However, Figure 60 reveals that, when other vehicles are inserted into the virtual environment, the participants prefer to keep a shorter distance from the vehicles in front of them when the smoke is denser. An explanation for this behavior might be that participants like to use the leading vehicles as a guide to position themselves on the road. This hypothesis is supported by the responses to the questionnaire (see below). This means that when the traffic is dense (and drivers are following the vehicles in front of them), the evacuation times might be shorter when smoke obscures visibility of the road. Note, however, that this is not a monotone trend. Figure 61 visualizes the prediction of the different slopes τ . Flatter slopes (lower values) translate to shorter headways.

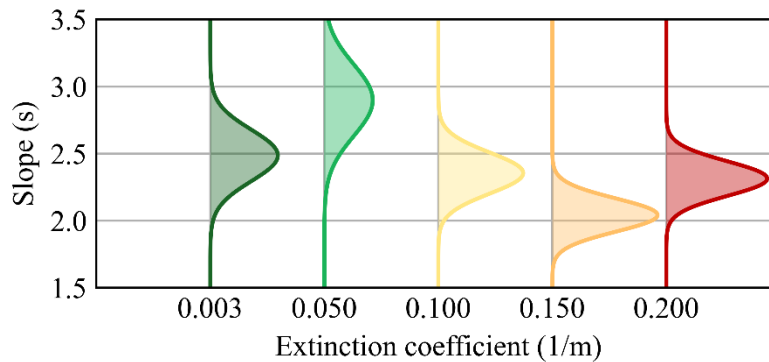


Figure 61. Distribution of the estimated slope parameter τ from the curve fit for the five extinction coefficients (1/m). The distributions represent the certainty of the best fit for all participants, considering the sample size and variation in the driving behavior of the 30 participants.

The figure illustrates that the slope (and therefore the car-following behavior) does not vary monotonously with the extinction coefficient. The overlapping distributions indicate a central trend: The car-following behavior does not depend on the extinction coefficient. For this reason, we propose a conservative model for evacuation time simulations, which does not consider the possible “efficiency gains” in the car-following regime (Figure 62). Instead, the car-following regime of the model is not affected by the smoke level. The vehicle speeds in the free-flow regime decrease according to the exponential reciprocal function (Figure 59).

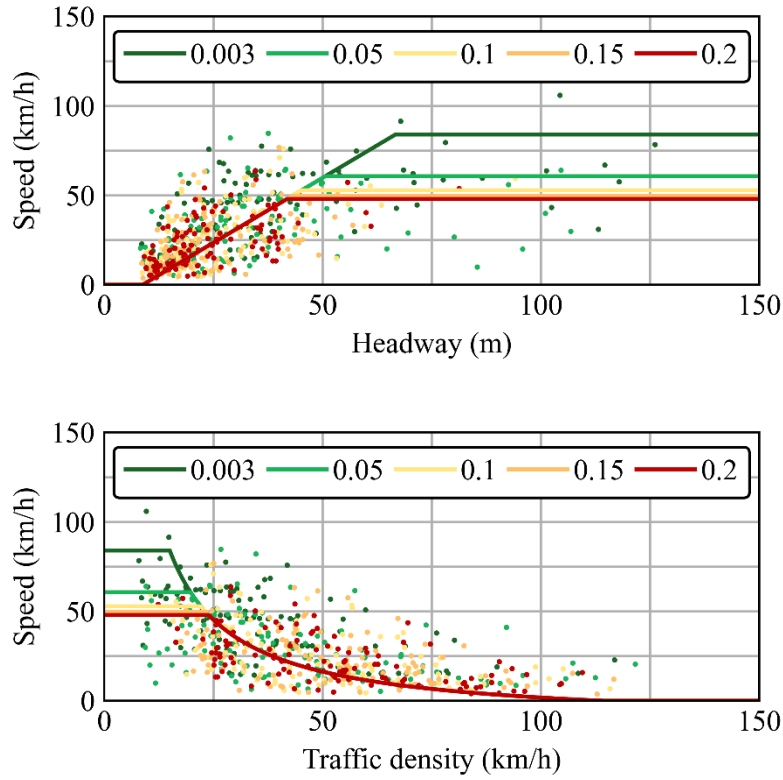


Figure 62. Proposed speed headway and speed density curves for evacuation time simulations. The legend indicates the smoke level by the extinction coefficient (expressed in m^{-1}).

To formulate this model mathematically, it is sufficient to introduce one speed reduction coefficient r into the model by Daganzo (1994) used for macroscopic modelling, as illustrated in Equation 11. Similarly, this reduction coefficient can also be introduced at the desired speed in the car-following by Krauss (1998b).

$$v = \min \left(r v_f, v_f \frac{\frac{1}{k} - \frac{1}{k_j}}{\frac{1}{k_c} - \frac{1}{k_j}} \right) = \min \left(r v_f, v_f \frac{h - h_j}{h_c - h_j} \right) \quad [\text{Equation 11}]$$

With

$$r = 1 - 0.4967 e^{-0.02910/K} \quad [\text{Equation 12}]$$

Moreover, the mathematical formulation of the model can also be easily explained by simple behavioral rules: Drivers wish to drive a certain speed, the free-flow speed v_f . However, they will adjust this speed to the amount of traffic on the road, so to maintain a safe headway. Moreover, they might decrease their speed because of the reduced visibility. These two effects do not interact in this model: Their reduced speed is either a consequence of the smoke or the traffic. For example, when traffic already forces the drivers to slow down significantly, the drivers are not affected by low or medium-dense smoke.

Participants' reflections on the driving experience: After using the driving simulator, participants completed a second questionnaire, which included questions about their cybersickness symptoms

(the VRSQ), their reflection on the driving experience and demographic information. This section focuses on the participants' reflections.

Figure 63 shows the responses to three questions related to the participants' risk perception. Twenty out of 30 participants (66%) did consider the possibility of being involved in a traffic accident (answered with 5, 6 or 7). The fact that such a high percentage of participants were aware of the risk suggests that the driving simulator supplies an immersive environment that prompts participants to reflect on real-world driving risks. Despite the high awareness of traffic accident risk, the perception of the urgency of evacuation and the threat of a wildfire was relatively low among participants. Most participants did not perceive the evacuation as urgent (only eight participants or 27% answered with 5, 6 or 7) nor did they perceive the wildfire as a threat (only 11 participants or 37% answered with 5, 6 or 7).

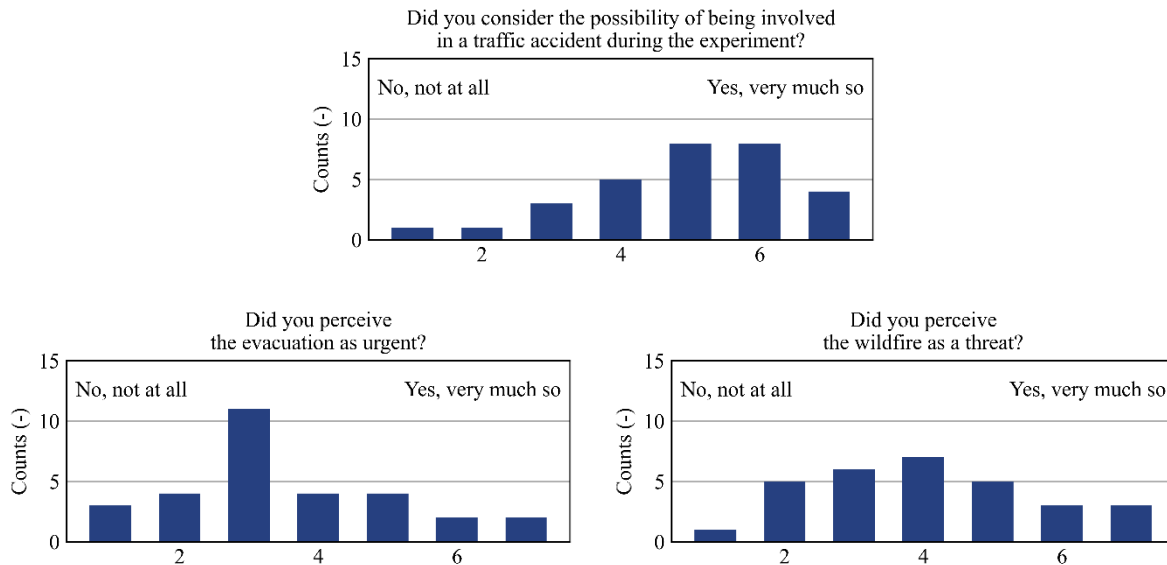


Figure 63. Participants responses to three questions related to risk perception.

This might be due to the static nature of the wildfire cues: a radio report and the constant extinction coefficient. Multiple participants did report orally, after the experiment, that they expected to be surrounded by flames. Three participants wrote about this in the open questions:

"If I had seen the fire, I would have been more inclined to drive faster." (translated)
"If I had seen animals running or the fire, I might have driven differently." (translated)
"I drove as I would in real life. Only thing that would affect my driving is if I had a better idea of the immediate risk of fire in my vicinity."

Figure 64 shows the responses to two questions related to the realism of the simulator. Out of all participants, 20 (67%) reported that both the vehicle physics and the graphics were realistic (answered 5, 6 or 7).

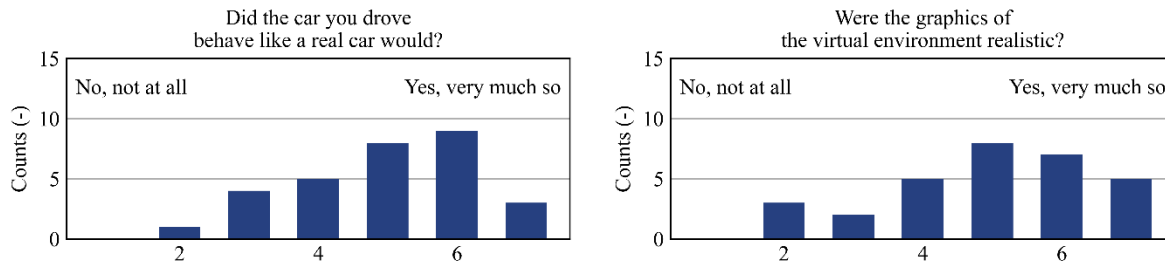


Figure 64. Participants responses to two questions related to the realism of the simulator.

Participants were also asked to reflect on how they drove. On the question “Did you change your driving speed, knowing you were evacuating? Why (not)?” Eight participants (27%) said they did so. Five participants explained they drove faster, due to the urgency. One participant explained that they drove slower as emergency services were occupied, and the consequences of an accident would be high during an evacuation:

“If I got in an accident the risks would be much higher and there would be no emergency assistance to help, or it would be taking away emergency resources from the fire”

Participants were also asked about their distance headway: “When following the car in front of you, did you change the distance between you and the car depending on how far you could see? Why (not)?”. Six participants (20%) reported they kept a larger distance. Two of them mentioned the risk of causing a multiple-vehicle collision when being hit from behind by another car (since they drove slowly in the thick smoke, one specified). Eleven participants (37%) did report that they drove closer. Nine explained they wanted to keep the vehicle in sight and two elaborated, explaining that the leading vehicle helped them position themselves on the road. This reported behavior aligns with the observations from the fitted models (see above). However, a smaller portion of participants did the opposite (20%); they prioritized safety by increasing their following distance.

One could question the ecological validity of the behavior observed in VR. To gain insights into behavioral realism, participants were asked if they would behave differently in real life (“Would you behave differently in real life? If so: What would you have done differently?”). Five participants mentioned they would drive faster, five participants said they might overtake more. Four participants thought they would drive slower. Eight participants thought they would have more stress or anxiety. However, most participants reported that the vehicle that they drove behaved realistically and found the graphics in the virtual environment realistic. During the experiment, a researcher observed several participants trying to use the vehicle’s turn signals, horn and mirrors. Some participants also seemed frustrated with the slow queue. This suggests that participants felt like they were “there” in the virtual environment.

During and after the experiment, some participants questioned out loud if they would even choose to drive in scenarios with poor visibility. It needs to be emphasized that the experiment does not investigate this decision-making process, as participants were instructed to evacuate and follow the road. Although the current model will improve to estimate speeds and headways accurately in poor visibility conditions, it does not answer the question if evacuees would still evacuate by car.

3.6.3 Conclusion

The VR driving study at Lund University provided insights into driving behavior under reduced visibility due to smoke. The study found that participants adjusted their driving speed and headway in response to different levels of smoke density. Specifically:

Driving speed: Participants drove significantly slower as smoke density increased, aligning with the hypothesis that poor visibility leads to reduced speeds. This finding is critical for understanding evacuation times during wildfires, suggesting that dense smoke can significantly slow down the evacuation process.

Distance headway: Contrary to the hypothesis, participants maintained slightly shorter distance headways in denser smoke conditions ($K > 0.100 \text{ m}^{-1}$). However, the trend is not monotonous and the confidence intervals of the slopes on the headway speed graphs overlap (see Figure 61). Therefore, the car-following regime is assumed to not be affected by the smoke.

Proposed model: The study proposes a model for evacuation time simulations that integrates a speed reduction coefficient into the existing Daganzo (1994) speed-density relationship, adjusting for the impact of reduced visibility due to smoke. The proposed speed reduction coefficient r is defined in Equation 12.

The model distinguishes between free-flow and car-following regimes. The free-flow regime speeds decrease according to the speed reduction coefficient, while the headway between vehicles in car-following conditions remains unaffected by the smoke. This approach focuses on the reduction in free-flow speeds due to poor visibility and can be integrated into both macroscopic and microscopic traffic simulation frameworks to better predict evacuation dynamics under varying smoke conditions.

Participant feedback: Participants confirmed they use the leading vehicle as a visual guide when visibility conditions are low. Participants recognized the risk of traffic accidents, the perceived urgency of evacuation and threat from the wildfire was relatively low. This indicates that the virtual environment does not fully replicate the urgency of dire evacuation scenarios.

Cybersickness: The study reported a moderate increase in cybersickness compared to previous studies, attributed to the longer duration of immersion. However, the dropout rate due to cybersickness was lower, indicating a generally well-tolerated VR environment.

3.7 Summary

Driving in a VR simulator differs from driving in the real world. For example, an accident or a collision in the real world can lead to serious injuries. However, this physical consequence does not exist in VR. Users are aware of this, which could lead to differences in behavior between both environments. For example, in the current study, participants were aware that the driving scenario was artificial and that they were physically safe in a laboratory, which could have led them to drive faster in poor visibility than they would if they encountered a similar situation in the real world. Future work could compare driving in VR versus in the real world in low/high visibility conditions (e.g., headway during daytime versus nighttime).

Previous studies have shown that users tend to underestimate distances in VR (Creem-Regehr et al. 2005; Renner et al. 2013), also referred to as distance compression (Buck et al. 2021). Studies have also indicated that users can overestimate distances in VR in some situations (e.g., (Peillard et al. 2019; Choudhary et al. 2021)). Buck et al. (2021) found that distance compression occurred in the Vive Pro headset, which was also used in the current study. Pallamin and Bossard (2016) used a three-monitor driving simulator for accident prevention training. The results showed that participants may violate the safety distance between their vehicle and the vehicle in front of them during driving in VR. Participants also reported having difficulty judging distances in the virtual environment. These studies suggest that distance compression can affect headway. It is possible that participants in the current study drove closer or further away from the lead vehicle than they would in the real world as it was more difficult for them to estimate the distance between the vehicle that they were driving and the lead vehicle. This effect needs to be considered when designing driving studies using VR and when interpreting the results of such studies.

Although VR has limitations, it was determined to be an acceptable tool for the study's purpose since the aim was to assess relative (not absolute) differences between experimental conditions that would be dangerous to study in the real world. In addition, it was possible to obtain a simple relationship considering visibility conditions, traffic density and free flow speed that could be implemented in macroscopic and microscopic traffic evacuation models. This is the first time such a relationship is based on data. Conducting a driving study in VR has practical, ethical, and financial benefits over conducting a similar study in the real world. For instance, studying headway in poor visibility conditions in the real world would require additional resources (a large outdoor space, two vehicles, an experienced lead driver, etc.), and the research team would need to plan around weather conditions. VR also allows experimental control and repeatability of conditions, which can be challenging in the real world as it is not possible to directly manipulate certain variables, such as weather conditions.

4. WUI-NITY enhancements: integration of the microscopic traffic model SUMO

This part of the work focused on integrating a microscopic traffic model within the WUI-NITY platform. The chosen model has been Simulation of Urban Mobility (SUMO) as it is an open source, microscopic and continuous multi-modal traffic simulation package which is originally designed to handle large road networks (Behrisch et al. 2011; Lopez et al. 2018a). The software is mainly developed by the Institute of Transportation Systems at the German Aerospace Centre and its source code is made available for any interested party. Being a microscopic model, it is able to represent each individual vehicle on the road network explicitly, as well as model its route and interaction with other vehicles and the network. By default, SUMO is a deterministic model, but it is possible to introduce variability in inputs/outputs through its implementation of a random-number generator. This can be used to implement randomness in vehicle characteristics, flows, driving dynamics, etc. The readers are referred to the technical documentation⁹ of the model for further information on its modelling assumptions, capabilities and limitations.

SUMO is a microscopic model making use of a car-following model (Song et al. 2014), meaning that vehicle speeds are determined by the traffic density. By default, SUMO adopts the Krauß model (Krauß 1998). This model selects the maximum speed (also called safe velocity (Krajzewicz et al. 2002)) that allows a vehicle to stop at any time without any collision with the following vehicle (Lopez et al. 2018b). SUMO inputs include route files to define travel demand and the details of the vehicles on the road network as well as a network topology file (used to define the configuration of the road network). SUMO can generate outputs related to the information on the trajectories of each vehicle on the road network as well as departure times, arrival times at destinations, speeds, trip duration, route length, etc.

The choice of SUMO as a microscopic model to be implemented in WUI-NITY has been associated with its in-built ability to operate with other applications at run-time. The SUMO developers generally recommend interacting with a running simulation through a Traffic Control Interface which is a networked interaction with SUMO acting as a server. The reason for this choice is that it provides flexibility for doing cross-platform, cross-language interaction as any data exchange is done through a network protocol. This relates to a set of established rules concerning the format to send and receive data between SUMO and other platforms. However, one major drawback of this approach is the communication overhead in terms of computational time due to the protocol and the socket communication. A network socket refers here to the software structure within a network node of a computer network used as endpoint for sending and receiving data. As the goal of WUI-NITY is to simulate large scale evacuations, the computational performance of any included modules is of great concern. For this reason, it was decided to not use a Traffic Control Interface. Alternatively, the choice was to use Libsumo¹⁰, a direct C++ library with the following properties:

- C++ interface based on static functions and a few simple wrapper classes (a class that encapsulates types, so that those types can be used to create object instances and methods

⁹ <https://sumo.dlr.de/docs/index.html>

¹⁰ <https://sumo.dlr.de/docs/Libsumo.html>

in another class that needs those types) for results which can be linked directly to the client code

- Function signatures similar to a Traffic Control interface
- Pre-built language bindings for Java and Python (using SWIG, a software development tool that connects programs written in C and C++ with a variety of high-level programming languages)
- Support for other programming languages

As the WUI-NITY core is written in C#, SWIG bindings had to be defined and compiled in order to make the C++ interface available in C#. This means adding directives to the SUMO source code and compile from source. The produced output is in two parts:

- Libsumocs.dll, the actual SUMO library with exposed PInvoke (Platform Invocation Services, a feature of Common Language Infrastructure implementations) methods
- Wrapper classes for all exposed parameters in libsumocs.dll as well as classes needed to marshal data sent between the managed (C#) and unmanaged codes (C++)

The SUMO code also had to be modified slightly to allow more exposed parameters to be sent through Libsumo, as runtime editing of the road network is desired in WUI-NITY (while the SUMO developers mainly target Libsumo as a control for vehicles). One such parameter was all edges (roads) connected to a specific node (intersection) in the road network. This data was needed to close down roads in case the fire reaches nodes in the network.

In WUI-NITY a new traffic module was created in order to make use of libtraci.dll and the C# SWIG bindings. The way that it works is straightforward:

- At the beginning of the simulation, a traffic module is created, in this case the SUMO module. A general framework for new modules has been created through abstract classes the any new module will inherit from.
- The pedestrian module in WUI-NITY creates new vehicles to be inserted into the SUMO simulation. The actual insertion creates after all modules have been updated (as they arrive at the end of the time step). During this process, WUI-NITY tries to find any cached routes that the new vehicle can use, otherwise a new one is requested through SUMO.
- WUI-NITY calls the Step function to synchronize SUMO with WUI-NITY time wise. After the step is completed, WUI-NITY asks for the position of all vehicles in order to render their position.
- If the fire front reaches any goals or network nodes, WUI-NITY modifies the pathfinding travel time of the edges (roads) making it less desirable to travel along those edges, then a request to SUMO is sent to re-calculate all routes for every vehicle. This process can be quite expensive with many vehicles in the system. The reason for modifying the travel time rather than completely disallowing a vehicle type to travel along the edge is to avoid stuck vehicles which makes SUMO abort abruptly.

A test case scenario was performed to verify the correct implementation of SUMO within WUI-NITY. This included 13,451 people and 5,777 vehicles, based on a previous scenario conducted with the macroscopic traffic modelling within WUI-NITY (Gwynne et al. 2023). The scenarios were run and results were visualized to ensure that 1) congestion appeared in expected locations

(e.g., intersections, see Figure 65), 2) dynamic re-routing worked as expected in of the event part of the road network was blocked by a wildfire (see Figure 66).

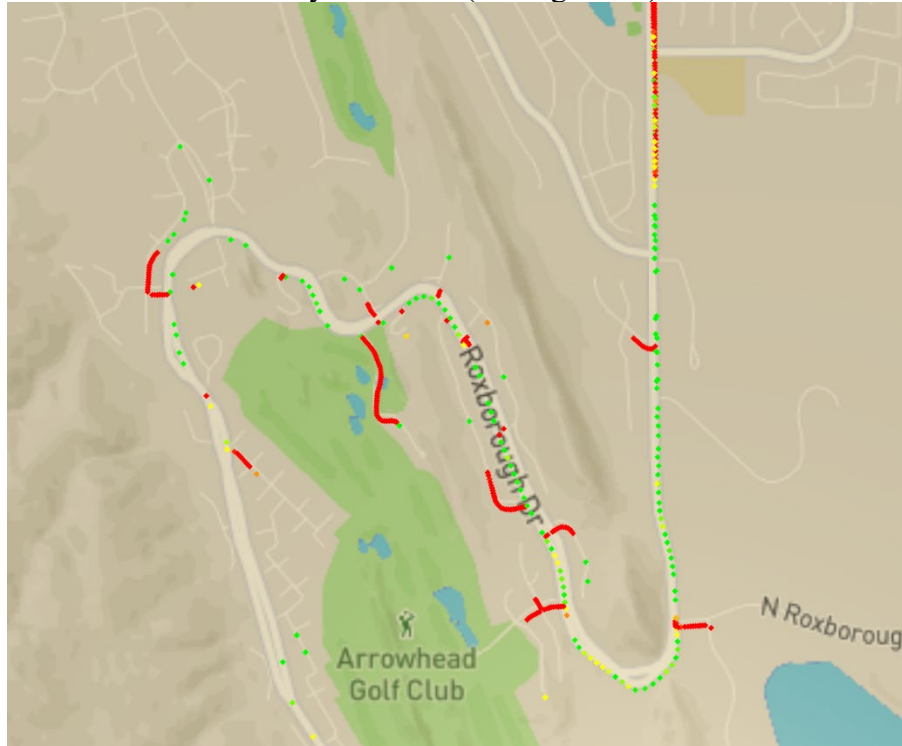


Figure 65. Screenshot from WUI-NITY in which vehicles subjected to congestion are marked in red. Those mostly correspond to intersections between smaller roads accessing the larger road of the community being considered.

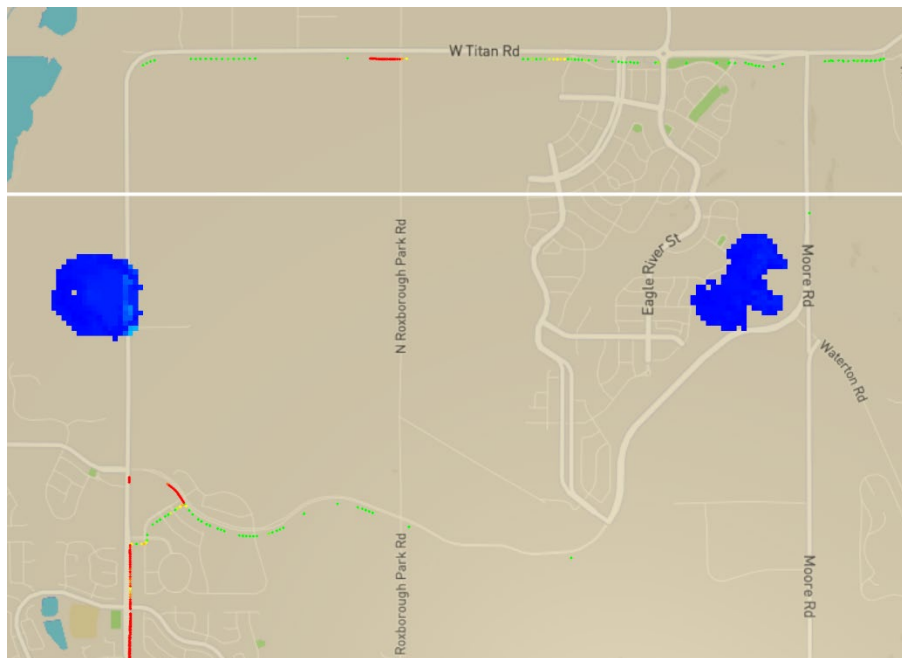


Figure 66. Screenshot from WUI-NITY in dynamic rerouting occurs due to a portion of the road network not being available due to wildfire spread.

Given the implementation of SUMO, WUI-NITY can now be used in two alternative modes related to traffic simulations, namely microscopic and macroscopic mode. The user has the opportunity to select one of the two modes prior to running their simulations. The availability of a microscopic traffic modelling layer introduces the opportunity to represent traffic evacuation at a more refined level of granularity. This allows the representation of heterogeneous features in the vehicles being considered in the traffic (e.g. vehicles with variations in size, free flow speed, etc. as well as varying driver behaviors). Macroscopic models generally need several simplifications for the representation of aggregated variables, e.g. assuming homogeneity in traffic flow, seen more as continuous fluid than the result of movement and driving behavior of individual vehicles. In contrast, microscopic models allow a more detailed representation of movement at the level of individual vehicle trajectory, meaning that the microscopic interactions and variables could be represented. A microscopic modelling approach therefore allows WUI-NITY producing the previously existing aggregated outputs, although with higher accuracy (e.g. injected/exiting/current vehicles in the simulation, average vehicle speed, minimum vehicle speed, vehicles that reached the evacuation goal, chosen routes). In addition, the SUMO implementation would give the opportunity to users to obtain much more refined outputs given the availability of outputs related to individual vehicle trajectories and the use of a car-following sub-model. Key new outputs can include speed and acceleration profiles, frequency and location of lane changes, along with travel times and chosen routes for individual vehicles.

5. Enhancing the k-PERIL model into a probabilistic trigger buffer model

The concept of stochastic trigger boundaries was introduced earlier to accommodate for a wide range of wildfire spread and evacuation scenarios that may occur in a single community (Kalogeropoulos et al. 2023). As discussed in a previous WUI-NITY report (Ronchi et al. 2023), stochastic trigger boundaries (see Figure 67) define a range of perimeters around a community that, once a fire breaches a specific line, will provide sufficient time to evacuate in a specific proportion of wildfire spread scenarios simulated.

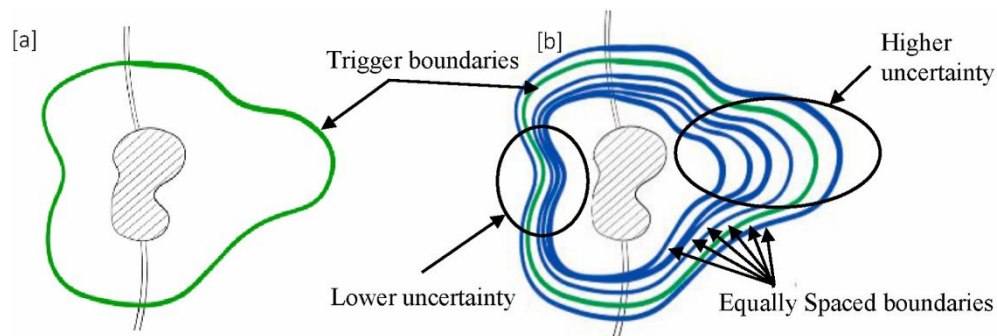


Figure 67. Left: Trigger boundaries for a single wildfire and evacuation scenario (Kalogeropoulos et al. 2023). Right: stochastic trigger boundaries that provide a range of certainties from a range of wildfire spread scenarios.

5.1 – Standardization of inputs/outputs for use in WUI-NITY

Several wildfire spread and evacuation model outputs are required as inputs to operate k-PERIL. This is indicated in the formalized framework for k-PERIL integration depicted in Figure 68. The community WUIRSET time is required from an evacuation model. The rate and direction of spread raster data is required from the wildfire spread model. However, each of these inputs can be varied stochastically, depending on the stochastic variation of input variables to the wildfire and evacuation models. For example, weather data (wind, temperature, and humidity) can be inputted as statistically distributed variables to the wildfire spread model to produce a set of multiple wildfire spread scenarios.

As WUI-NITY introduces the functionality to visualize wildfire spread data from a range of available wildfire models (e.g. FARSITE (Finney 1998)), it is key that k-PERIL can function based on inputs from those wildfire models. The analysis conducted with the Roxborough case study (Kalogeropoulos et al. 2023) required a modified version of FARSITE that could run multiple consecutive simulations whilst varying select input parameters. For the integration of k-PERIL into WUI-NITY, k-PERIL was modified to allow either iterative runs until a predefined convergence criterion is satisfied or to allow multiple simulations to be inputted in bulk. In the current version of k-PERIL, convergence is achieved (by default) when, for 20 consecutive iterations, a simulation does not change the stochastic trigger boundary by more than 0.3%.

The inputs and outputs of k-PERIL have been standardized to allow for robust integration into WUI-NITY using a range of wildfire and evacuation inputs (e.g. standardized landscape orientation to resolve variation in landscape input file types between wildfire spread modelling

tools). Data can also now be saved and passed in the program instead of saving and reading text files.

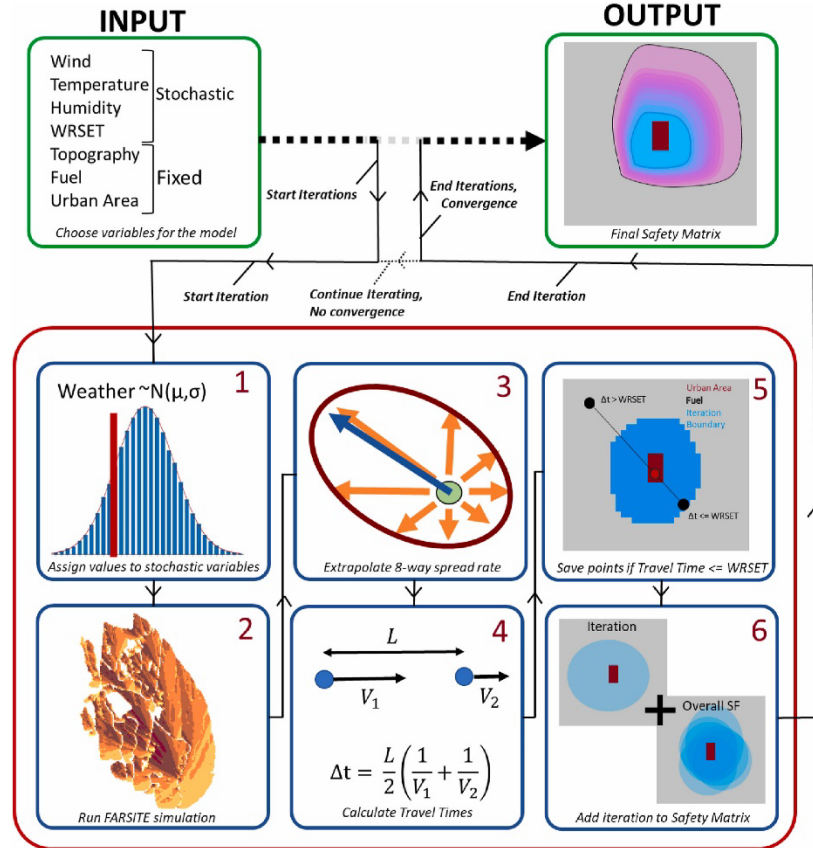


Figure 68. Integration flow diagram of k-PERIL integration into WUI-NITY (Kalogeropoulos et al. 2023).

5.2 – Development and refinement

As shown in Figure 67, k-PERIL was applied to the Roxborough Park community case study (Gwynne et al. 2023) to produce probabilistic trigger boundaries and show the model's ability to find and quantify areas of elevated uncertainty of evacuation. This follows previous efforts in developing individual trigger boundaries for Roxborough Park based on single wildfire and evacuation scenarios using PERIL (Mitchell et al. 2023).

Inputted evacuation scenarios included WUIRSET of 120 min, in line with an evacuation drill and WUI-NITY evacuation model estimations (Gwynne et al. 2023), and the second has an increased WUIRSET to 360 min, which can be attributed to an evacuation called at night, or to roadworks bottlenecking the evacuation. Wildfire spread data was inputted from FARSITE (FLAMMAP (Finney 2006)) simulations, taking key weather parameters (wind magnitude, humidity, and temperatures) as stochastically varied inputs. A total of 1000 FARSITE simulations were inputted into k-PERIL to ensure that there was a sufficient distribution of scenarios to approximate a converged output from k-PERIL. At the time this analysis was conducted, the convergence criterion had not yet been implemented.

The stochastic trigger boundaries shown in Figure 69 provide a useful output to WUI-NITY users. Trigger boundary regions that are comparatively thin with a steep color gradient indicate that input-dependent variation in wildfire spread behavior in this region is minimal. Comparatively, broader trigger boundary regions with a slower color gradient (circled in green in Figure 69) indicate that wildfire behavior varies significantly between each scenario, indicating a reduced reliability in predicting the behavior of wildfires approaching the community from these regions. To further visualize this measure of uncertainty, the concept of uncertainty rosettes is introduced, which show the areas where incoming wildfires cause a larger variation to the boundary location because of higher sensitivity to changes in fuel, wind or evacuation.

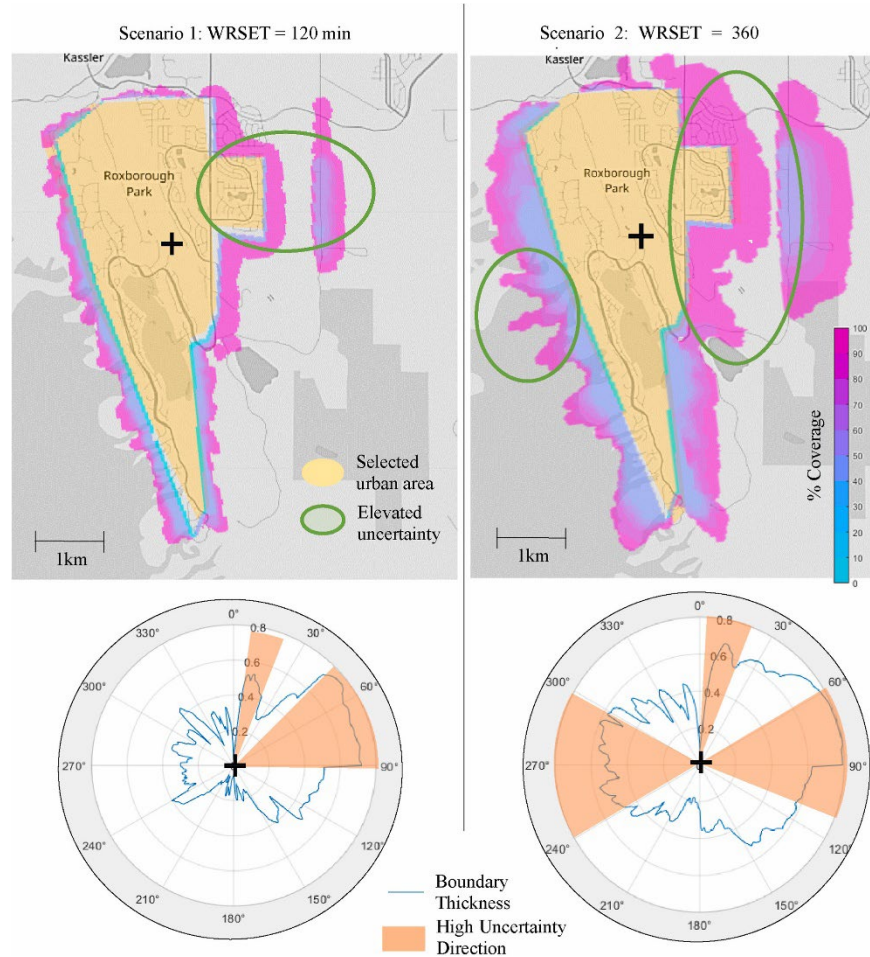


Figure 69. Stochastic trigger boundaries generated by k-PERIL for the Roxborough Park community under two evacuation scenarios. Danger rosettes (bottom) indicate in orange regions surrounding the community that are susceptible to significant uncertainty in wildfire spread.

Based on probabilistic trigger boundaries, the concept of dire evacuations has been defined and explored in a journal paper currently under peer review (Kalogeropoulos et al. 2024). Dire evacuations are those in which – due to a mismatch in the WUIASET and WUIRSET timescales – there is a high probability of entrapment and increased risk of loss of life to evacuees. By using probabilistic trigger boundaries generated by k-PERIL, a distribution of WUIASETs and WUIRSETs can be used to quantify the probability of a dire evacuation, providing a valuable evacuation planning tool and future output of WUI-NITY. To study this concept, the Mati

community was used as a case study, using wildfire spread data calibrated to the 2018 Mati wildfire burn scar, and evacuation times from previously modelled evacuation scenarios (Sinolakis et al. 2018). This work is available in a journal publication (Kalogeropoulos et al. 2024).

5.3 – Integration and implementation into WUI-NITY

One key development in this project is the integration of the stochastic version of k-PERIL into the WUI-NITY engine, taking inputs internally from WUI-NITY (or from external models given user specification), and outputting stochastic trigger boundaries as a valuable user visualization tool.

To support this, k-PERIL was packaged into a DLL format that can be easily implemented and updated in WUI-NITY with very few code changes. This means that as WUI-NITY and k-PERIL are dynamically updated (e.g., future implementation of the dire evacuation index) and improved, k-PERIL will be re-integrated throughout the extended WUI-NITY development period. The language used to code k-PERIL is C# due to its computational speed and its direct integration ability to Unity and by extension WUI-NITY, should the need arise in the future to couple the two at the source-code level.

In collaboration with Lund University who led the integration step of the project, a number of changes were made to the k-PERIL code, compared to the latest reported version. One critical change is that the required wind speed input to k-PERIL has been changed from the mid-flame windspeed to the 10m windspeed. While one is required to calculate the propagation of the fire from a point source, the other is readily available when accessing weather station data. The 10-m windspeed is converted to mid-flame windspeed by multiplying the mid-flame windspeed by 1.15, in accordance with the BEHAVE model (Andrews 1986).

A number of other technical changes to k-PERIL were also implemented, including a thorough cleanup of the code and accompanying files to reduce complexity and improve ease of WUI-NITY integration. The outputs of some functions were updated to reflect more accurately what their name implies. Future key updates include the important addition of a function to specify the points denoted as built-up areas using shapefiles, geographical vector shapes, or coordinate dimensions based on any projection system. Optimization regarding memory use is also planned to help with the memory requirements of k-PERIL and summative requirements of WUI-NITY, improving its usability.

6. User guide and demonstration documentation

As outlined in the previous sections, there have been a number of developments in the WUI-NITY model functionality – both expanding the scope of the model’s functionality and refining it. Inevitably, this means that previous descriptions of the model’s use have now become outdated – both in terms of the technical guidance to make use of the model and the work-flow guidance in how to apply the model to a particular problem.

The user guide presented in Appendix 1 provides a comprehensive overview of the WUI-NITY model and its application in wildfire evacuation analysis. It covers various aspects of data preparation and user inputs, including map preparation, population definition, fire and smoke simulation, traffic network and routing, and evacuation settings. It also details the guided workflow interface, demonstrating how to apply WUI-NITY to build a simulation case in a step-by-step, ordered sequence of actions. The guide includes figures illustrating the process of using WUI-NITY, such as data flow diagrams, map editing modes, and simulation outputs. Where reference is made to externally developed models (e.g. SUMO), the user is directed to the guidance provided and developed by third parties – rather than to reproduce existing content. This approach also reduces the chances of produced outdated guidance for third-party tools. Overall, the guide serves as a resource for users interested in utilizing the WUI-NITY model for wildfire evacuation analysis.

The user guide reflects recent developments and focuses on the use of the model as is reported in this document. It is apparent that the development of WUI-NITY is ongoing with new capabilities being frequently added and existing functionalities being updated. These changes will therefore appear in subsequent versions of the user guide.

Appendix 1: WUI-NITY user guide

WUI-NITY user guide

Table of Contents

Appendix 1: WUI-NITY user guide	126
A1. Introduction – why you might use this model	133
About this guide.....	135
Download and install WUI-NITY	136
System requirements for WUI-NITY	136
A2. Data preparation and user inputs.....	137
Map preparation.....	137
Population Definition.....	140
Fire and smoke simulation.....	142
Landscape file (.lcp)	143
Fuel models file (.fuel)	160
Initial fuel moisture file (.fmc)	160
Weather file (.wtr).....	161
Wind file (.wnd).....	162
Ignition points file (.ign).....	163
Graphical fire input file (.gfi)	164
Traffic network and routing.....	165
Road network and route collection	165
Transportation options	165
Evacuation settings	168
Evacuation group file (.eg)	168
Response Curve file (.rsp)	169
Evacuation goal file (.ed).....	169
Other evacuation settings.....	170
Summary	172
A3. Guided workflow interface	174
The workflow design paradigm.....	174
WUI-NITY Graphical User Interface.....	175
The workflow GUI.....	176
WUI-NITY Project File (.wui)	177
The workflow menu.....	177
The Output Window	189
Simulation outputs	190
A4. Demonstration case	192
Data preparation.....	192
The process of applying WUI-NITY to build the simulation case.....	193
Prepare population, map and traffic network data.....	193

Configure location and size of the region.....	194
Configure population data	195
Configure evacuation goals	197
Configure response curves and evacuation groups.....	199
Configure evacuation settings.....	202
Configure routing data	203
Configure traffic settings	204
Prepare landscape file, fuel models file and other supporting files.....	204
Specify fire characteristics files and edit fire model settings	205
Execute Simulations	205
Simulation settings and outputs	206
Evacuation objective and assumptions	206
Configure evacuation and traffic settings	206
Simulation outputs	207
A5. Summary	211
User guide references	213
Report references	215

List of Figures

Figure 1. The conceptual modelling framework of WUI-NITY.....	134
Figure 2. Data flow within WUI-NITY.	135
Figure 3. Determine the location and size of the region for evacuation analysis.	138
Figure 4. Select required fields to create the download link for the population density data sets.	140
Figure 5. LANDFIRE (LF) data access tool to view and download landscape files.	145
Figure 6. Register a user account at USGS website.....	146
Figure 7. Open Earth Explorer and select the area of interest.	147
Figure 8. Select data set for downloading.....	148
Figure 9. Verify Data Set selection and download.	149
Figure 10. Select download option.	150
Figure 11. The High Resolution Layer Tree Cover Density product offered at Copernicus (UK is selected).	151
Figure 12. Download the European fuel map from EFFIS.	152
Figure 13. Set EPSG:3857 - WGS 84 as the default CRS in QGIS.....	153
Figure 14. Add elevation, fuel map and canopy cover layers into QGIS.	153
Figure 15. Use Raster Analysis tools to calculate the aspect and slope layers respectively.....	154
Figure 16. Create a new Shapefile layer.	154
Figure 17. Set the geometry type and CRS of the new Shapefile layer and save it as a .shp file in the project folder.....	155
Figure 18. Draw a polygon around a rough approximation of the target area (i.e., Marsden Moor).....	155
Figure 19. Open the Processing Toolbox(left) and select ‘Clip raster by extent’ under Raster Extraction in the Processing Toolbox (right).....	156
Figure 20. Specify ‘elevation’ as the input layer and set the clipping extent to that of the recently created Shapefile.	156
Figure 21. A temporary ‘clipped extent’ layer has been created.	156
Figure 22. Right click each layer and select ‘Save As’.....	157
Figure 23. Save the layers as .tif files with the extent of the clipped layer and in the same resolution....	157
Figure 24. The first standardised ‘clipped’ layer has been created.....	158
Figure 25. Standardised elevation, aspect, slope, canopy cover, and fuel map layers in GeoTIFF format.	158
Figure 26. Select ‘Create Landscape File...’ under the ‘Landscape’ menu in FlamMap 6.	158
Figure 27. Select each of the clipped .tif files created in QGIS, and click ‘Save As’.....	159
Figure 28. An example of smoke/speed settings within a .wui file.	166
Figure 29. An example of the opticalDensity.odr file.....	166
Figure 30. The default roads type file defines the properties of road type motorway.	167
Figure 31. An example of an evacuation group file.....	169
Figure 32. An example of a response curve file.....	169
Figure 33. Legacy WUI-NITY GUI and two GUI switch buttons. (When the legacy GUI is running, the workflow GUI is docked on the right. The GUI switch buttons are highlighted in yellow.).....	175
Figure 34. Workflow WUI-NITY GUI and eight function blocks.	176
Figure 35. Section 1 of the workflow menu.....	178
Figure 36. Section 2 of the workflow menu.....	178
Figure 37. The data flow of generating local population data from the global GPW data sets.	179
Figure 38. Section 3 of the workflow menu.....	180
Figure 39. An example project with three evacuation groups, four goals, and two response curves.	181
Figure 40. Section 4 of the workflow menu.....	181
Figure 41. Section 5 of the workflow menu.....	182

Figure 42. Map editing mode for editing spatial arrangement of evacuation groups (Group 1 is selected).	182
Figure 43. Section 6 of the workflow menu.....	183
Figure 44. The data flow of generating local route collection data from OSM data.....	185
Figure 45. Section 7 of the workflow menu.....	185
Figure 46. Section 8 of the workflow menu.....	186
Figure 47. Section 9 of the workflow menu.....	186
Figure 48. Section 10 of the workflow menu.....	187
Figure 49. Section 11 of the workflow menu.....	188
Figure 50. (a) The output window and (b) the display option buttons.....	189
Figure 51. Display of (a) households, evacuating traffic and (b) traffic density on map view windows.	190
Figure 52. Display of (a) fire spread and (b) smoke (as optical density).....	190
Figure 53. Create a new project.	193
Figure 54. Configure the location and size of the modelled region at Marsden Moor.	194
Figure 55. Specify the global GPW files folder.....	195
Figure 56. Specify and load the local GPW file generated in the previous step.....	196
Figure 57. Specify and load the .pop file generated in the previous step.....	196
Figure 58. (a) The local GPW population density on map and (b) the population distribution derived for the selected region at Marsden Moor showing the distribution of 16,017 people.	196
Figure 59. Three evacuation destinations and traffic routes around Marsden and Slaithwaite population centres.	197
Figure 60. Create a new goal file.	198
Figure 61. Enter the required information that defines an evacuation goal.	198
Figure 62. Add a goal file.	198
Figure 63. Create a new response curve file.	200
Figure 64. Enter the required information that defines a response curve.	200
Figure 65. Add a response curve file.	200
Figure 66. Create a new evacuation group file.	201
Figure 67. Enter the required information that defines an evacuation group.....	201
Figure 68. Add an evacuation group file.....	201
Figure 69. Edit spatial arrangement of the evacuation groups.....	202
Figure 70. Evacuation settings used in the demonstration case.	202
Figure 71. Specify the downloaded OSM data for the West Yorkshire region.	203
Figure 72. Specify the router database.....	203
Figure 73. Specify the route collection file.....	204
Figure 74. Traffic settings.....	204
Figure 75. Fire and smoke simulation support files.....	205
Figure 76. Specify all fire characteristics files required for fire and smoke simulation.	205
Figure 77. Evacuation parameters (left) and Traffic simulation parameters (right).	207
Figure 78. The graphical output of the Marsden Moor test case in WUI-NITY (optical density: off).....	207
Figure 79. The graphical output of the Marsden Moor test case in WUI-NITY (optical density: on).	208
Figure 80. The number of individuals who have not yet started evacuation.	209
Figure 81. Overall evacuation performance (Route Choice: EvacGroup).	210
Figure 82. Overall evacuation performance (Route Choice: Random).....	210
Figure 83. Overall evacuation performance comparison.	210

List of Tables

Table 1. Data preparation and user input for map.....	139
Table 2. Data preparation and user input for population definition.....	141
Table 3. Input files for fire and smoke simulation.....	143
Table 4. Additional fire spread model settings.	143
Table 5. The FBFM13 fuel models file.....	160
Table 6. An example of a fuel moisture file with the first three fuels defined in .fuel file.....	161
Table 7. An example of a .wtr file which defines two weather streams on two successive dates.	162
Table 8. An example of a .wnd file with two successive wind conditions in time (1 st format).	163
Table 9. An example of a .wnd file with three successive wind conditions in time (2 nd format).	163
Table 10. An example of a .ign file with two ignition points starting at two different times.	163
Table 11. Inputs to the traffic simulation.	167
Table 12. The entries of the evacuation group file and explanation.	168
Table 13. The entries of the response curve file and explanation.	169
Table 14. The entries of evacuation goal file and explanation.	170
Table 15. Summary of WUI-NITY inputs*.....	172
Table 16: Description of user-accessible evacuation settings.....	183
Table 17. Contact information.	212

Disclaimer

The under-development tool called WUI-NITY combines pedestrian and traffic evacuation simulation in combination with wildfire spread simulation. It uses Unity as a base for adding simulation tools.

To function, you will need the following items:

- OSM data for region of interest from <https://www.geofabrik.de/> (or any other source);
- Mapbox access token (<https://www.mapbox.com/>) (suggested but not needed);
- Population density from <https://sedac.ciesin.columbia.edu/data/collection/gpw-v4>; and
- Landscape (LCP) file for the area of interest for fire spread simulations.

WUI-NITY is licensed under the GNU General Public License v3.0, including third party source code that have their own licenses attached.

Important notice and disclaimers before downloading the WUI-NITY Modelling Platform Tool: By accessing, downloading, and using the WUI-NITY Modelling Platform Tool, you expressly agree to the following notices and disclaimers, as well as the End User License Agreement found [here](#).

The tool simulates fire behavior and human and traffic movement during a wildfire evacuation at the wildland-urban interface (WUI) and represents a way to enhance situational awareness of Authorities Having Jurisdiction (“AHJs”) as they plan and train for a potential WUI fire scenario. This tool and any related suggestions around evacuation are not designed to replace or substitute an AHJ’s decision about evacuation during a wildfire.

Use of this tool is at the user’s own risk; it is provided AS IS and AS AVAILABLE without guarantee or warranty of any kind, express or implied (including the warranties of merchantability and fitness for a particular purpose) and without representation or warranty regarding its accuracy, completeness, usefulness, timeliness, reliability or appropriateness. The creators assume no responsibility or liability in connection with the information or opinions contained in or expressed by this tool, its use or output.

A1. Introduction – why you might use this model

Wildfires are unplanned and uncontrolled fires that burn vegetation in wildland areas. As climate change has contributed to more frequent and intense fire seasons in recent years, wildfires have become a significant challenge in many regions of the world. Where wildfires pose a significant threat to populations near the wildland-urban interface (WUI), evacuation often becomes an inevitable choice for threatened communities.

Wildfires are commonly formed of meteorological, physical, environmental and social elements, which interact in a complex way that determines the likelihood of a wildfire, its propagation, intensity, duration, extent and the scale of damage it may cause. Combined with human factors and decision-making, the interaction of these elements also affects the safety of those communities threatened by wildfires. Given the threat posed by the escalating safety issue and the need for mitigation strategies, it becomes critical to understand fire behavior and its complex interaction with the affected population to establish the threat posed.

The capacity of community members to reach a place of safety in response to a WUI fire incident is influenced by several social, physical, and environmental factors. These include the likely fire scenarios to which the community is exposed, the developmental densities (i.e., distance between households that might affect movement of fire between houses), the layout and capacity of the road network, the surrounding geographical terrain, and the community's demographics, social systems, and capacity to cope with a fire incident. This might be characterized by considering two timelines to assess whether a community response to a wildfire enables a safe evacuation of the community [1]:

- **WUI Available Safe Evacuation Time (WUIASET)** — The time available to evacuate from a WUI site (Ronchi et al., 2019). WUIASET starts at the first detection of the incoming fire and ends when a wildfire reaches the urban area.
- **WUI Required Safe Escape Time (WUIRSET)** — The time required to evacuate the community from a WUI site. This starts when the evacuation order is given and ends when the last member of the community is successfully evacuated to a safe point of egress. WUIRSET takes into account preparation to start evacuating (pre-evacuation time), and foot and vehicle evacuation to a safe point of assembly.

In addition, the interplay between these event timelines related to the fire and evacuation process may be complex and requires a better understanding of the various interactions between the elements present and the underlying dynamics produced (see Figure 1) – the evolution of the fire and the evacuation are not entirely independent and the speeds at which they evolve will affect the severity of the scenario. In general, there are three core components with evolving conditions during a wildfire event involving evacuation:

1. Fire development and spread;
2. Household and pedestrian evacuation decision-making, and movement to transport systems; and
3. Transport/traffic movement to safety.

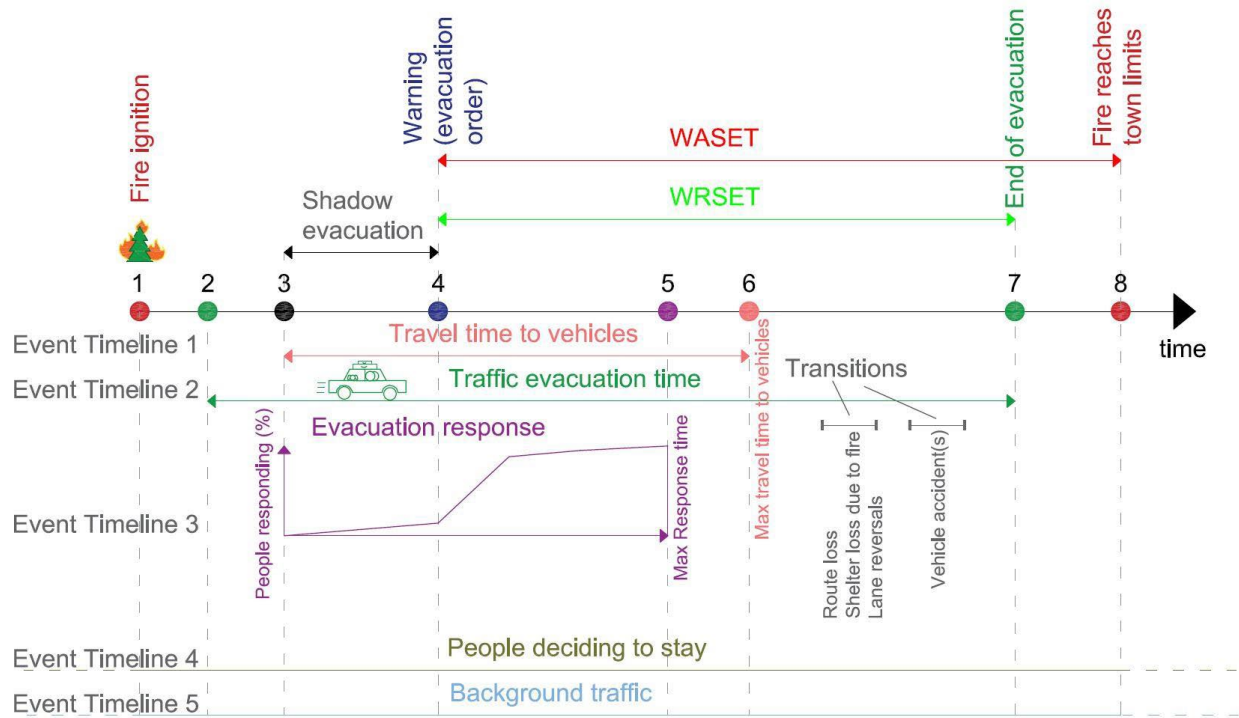


Figure 1. The conceptual modelling framework of WUI-NITY (Ronchi et al. 2020).

To investigate evacuations in response to wildfire emergencies and facilitate the planning and management of evacuation, a modelling platform called WUI-NITY has been developed through a collaborative effort between multiple institutes and organizations¹¹[1-4]. WUI-NITY is a computer modelling tool that allows the integrated simulation of:

- Wildfire development;
- Resident decision-making (how people respond to an evacuation order), and
- Evacuation movement for communities threatened by wildfires [5-14].

WUI-NITY is designed to represent these three core components during a wildfire event, including the potential interaction among them. Each of these components corresponds to a dedicated modelling layer, requiring specific data inputs and producing outputs for other layers (see Figure 2).

To configure and run an evacuation simulation using WUI-NITY, users are required to prepare various data inputs for each modelling layer and understand the data flow between them. Although the model can reflect all three components, it is also possible to run the pedestrian and traffic elements alone – effectively focusing on the evacuation in isolation.¹²

¹¹ An international cross-disciplinary research consortium including Lund University (Sweden), Movement Strategies (UK), Imperial College London (UK), National Research Council Canada (Canada), Royal Melbourne Institute of Technology (Australia) and Fire Protection Research Foundation (USA).

¹² Fire does not automatically block the availability of a route. However, the spread of fire to a refuge (i.e., evacuation goal) does automatically close it for use and require route recalculation. The user is also able to manually reflect such a blockage through an input file called goal blocking event file (under development).

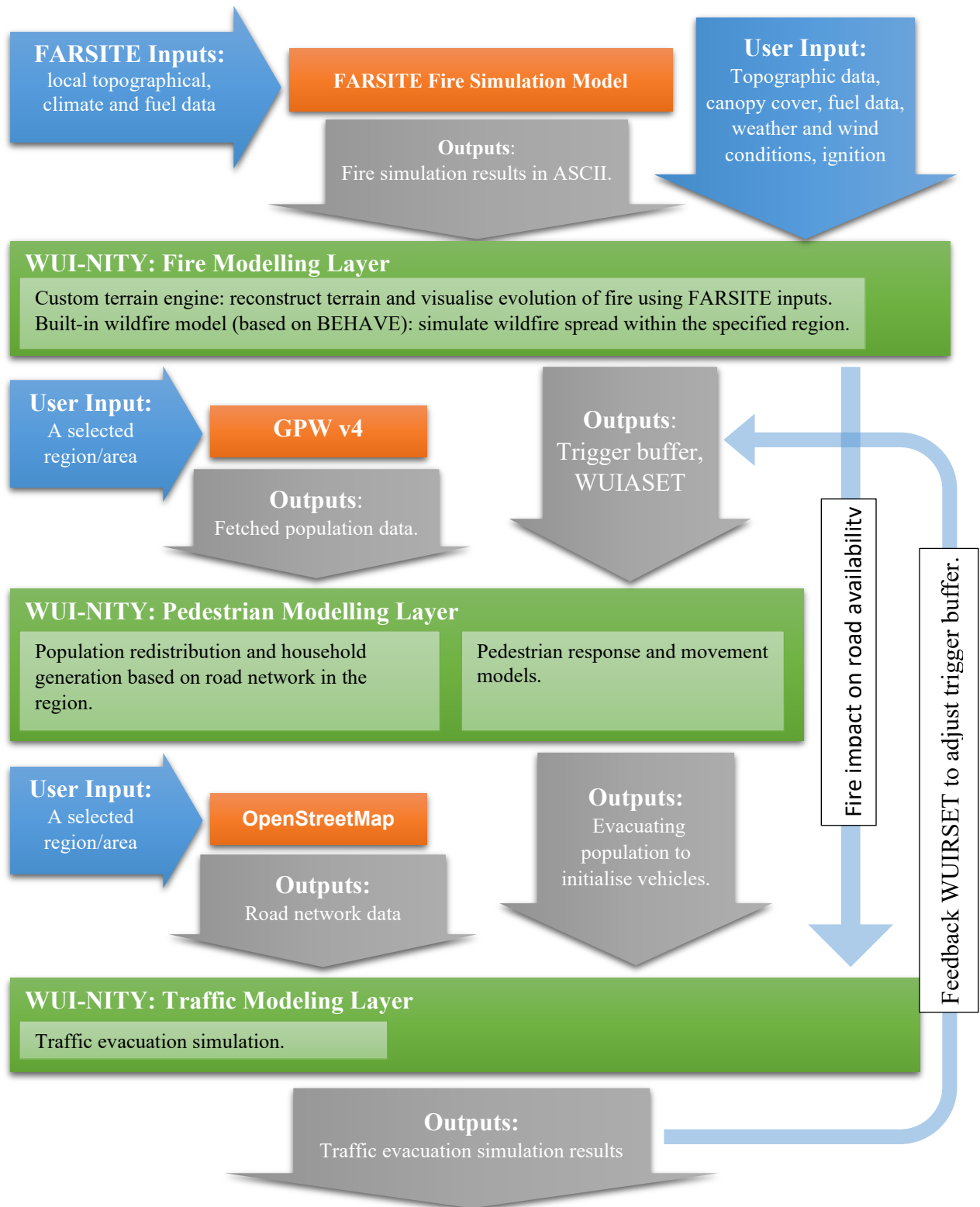


Figure 2. Data flow within WUI-NITY.

(blue boxes: user input; grey boxes: model outputs; orange boxes: data sources; green boxes: modelling layers).

About this guide

This user guide has been developed to facilitate the use of WUI-NITY. Its contents are organized as follows:

1. **Data preparation process** (Section 0)
 - Understand the essential data required for constructing a simulation model.
 - Learn how to source raw data and process it as input for WUI-NITY.
2. **Generalized workflow** (Section 3)
 - Explain the workflow built within WUI-NITY, which guides users through formulating project inputs, configuring settings and running simulations.
 - The workflow embeds a logic within the model that aids in tool configuration and ensures that key questions are addressed during scenario development.
3. **Test case demonstration** (Section 0)
 - Explore a practical example.
 - Learn how to prepare input data and construct a simulation model using the workflow.

In this guide, we summarize user actions using blue text boxes at the end of the subsections. Where we want users to pay attention to the potential limitations and key assumptions of the model, we use gold text boxes (see examples below).

User Actions:

Model Limitations:

It is apparent that the development of WUI-NITY is ongoing with new capabilities being frequently added. As such, this guide reflects the current stable version of WUI-NITY that has been most rigorously tested and applied, and which incorporates key longstanding features. New capabilities (such as the integration of the microscopic traffic model SUMO¹³ and the trigger buffer model k-PERIL [8]) will therefore appear in subsequent versions of this guidance.

Download and install WUI-NITY

WUI-NITY is available on several different platforms:

- Windows 10, 11 (Intel/AMD 64-bit architecture);
- macOS (Intel 64-bit Architecture, Apple silicon architecture).

A portable zip file is available for each platform and can be downloaded from:

<https://www.nfpa.org/education-and-research/research/fire-protection-research-foundation/projects-and-reports/wuinity-a-platform-for-the-simulation-of-wildlandurban-interface-fire-evacuation>

Upon downloading, users can extract the package and run WUI-NITY directly without the need for installation on their computer. A pre-built example case (example.zip) is included in the package, allowing users to practice, and become familiar with the program.

System requirements for WUI-NITY

Any relatively new computer (e.g., less than four years old with moderate specs: four core processors, integrated HD Graphics, 8GB memory, and 10GB free storage space) should be able to run WUI-NITY. For smoother running of the simulation, a dedicated graphics card and 16 GB of memory are recommended. To enhance user experience when working with maps in WUI-NITY, a Full High Definition (1920x1080) monitor or a monitor with higher resolution is recommended for better viewing and operation. WUI-NITY relies on an Internet connection to access the online Mapbox resource (as detailed in Section 2.1). Therefore, users should ensure that their computer remains connected to the internet while using WUI-NITY. If the user is operating within a protected network, add a firewall exception for the program.

¹³ Simulation of Urban MObility (Eclipse SUMO or simply SUMO) is an open source, portable, microscopic, and continuous multi-modal traffic simulation package designed to handle large networks. See <https://eclipse.dev/sumo/>.

A2. Data preparation and user inputs

WUI-NITY requires users to provide a variety of inputs¹⁴ for configuring a model and conducting simulations. While not all inputs are mandatory (for instance, fire modelling is optional), a thorough grasp of the data inputs and associated user actions is essential for navigating the WUI-NITY user interface effectively and confidently configuring the tool. This section outlines the five key input categories:

1. **Map preparation:** preparing geographical data and layout for the modelled region;
2. **Population definition:** specifying population distribution and characteristics within the area;
3. **Fire and smoke simulation:** specifying fire behavior and smoke propagation modelling;
4. **Traffic network and routing:** addressing road networks and transportation options;
5. **Evacuation settings:** configuring parameters related to evacuation planning and execution.

Understanding these input categories ensures a successful workflow within the WUI-NITY platform, which is introduced in the next section.

Map preparation

WUI-NITY uses Mapbox¹⁵, a third-party map application, to render the map as the foundation layer for displaying various components, including evacuation traffic and evacuation goals, etc. To access Mapbox services via Application Programming Interfaces (APIs), an API access token is required¹⁶. An API access token is a string that associates a Mapbox user account with their requests to Mapbox API resources. A token has been already included in the WUI-NITY release package. However, if the user wishes to use their own token, they can create one by registering an account at Mapbox's website at <https://account.mapbox.com/>.

The first step to **building a wildfire evacuation simulation project** involves specifying the location and size of the region. Typically, this region is represented as a rectangle. Users can use mapping platforms such as Google Maps or Bing Maps to examine the target area for evacuation analysis. The goal is to identify the area to be modelled within WUI-NITY, with consideration of the following criteria:

- The region should encompass the entire area where evacuees are initially located and traffic network relevant for evacuation analysis. Depending on the scale of evacuation planning, this could be a local community, a town or even a city.
- Additionally, the region should cover the roads leading out of the populated area to a point where the evacuation is considered to be over. These road segments define the city exit(s) within the region.
- Opt for the minimum region size that fulfils your analysis needs. In general, smaller regions may lead to faster simulations due to reduced road network complexity and less people to be evacuated, while larger regions encompass more people and routes, resulting in slower simulations.

¹⁴ User inputs and settings are recorded in a WUI-NITY project file. Please refer to Section 0 for more information.

¹⁵ <https://www.mapbox.com/>

¹⁶ For more information about Mapbox access token, see: <https://docs.mapbox.com/help/getting-started/access-tokens/>.

To configure the wildfire evacuation simulation project in WUI-NITY, users need to provide the following inputs:

- Latitude and longitude GPS coordinates of the **lower left corner** of the identified region in decimal degrees (right-click on the map to obtain these coordinates);
- The length of the rectangular region in the X and Y directions measured in meters.

Figure 3 showcases a modelling example using a WUI community [3, 10, 12]. The blue box drawn on the map outlines a 10-km-by-10-km region that encompasses the entire community for evacuation analysis. Right-clicking on the location situated at the lower left corner of the blue box (indicated by the yellow circle) yields the corresponding UTM coordinates shown in the first line of the popup menu.

It is important to note that these location and size inputs are also used in other modules of WUI-NITY, such as defining population distribution and routing. Therefore, if any of these inputs are changed, the subsequent procedures need to be repeated.

Finally, the map zoom level is used to render the map in WUI-NITY. The relevant data input details for map preparation are summarized in Table 1.

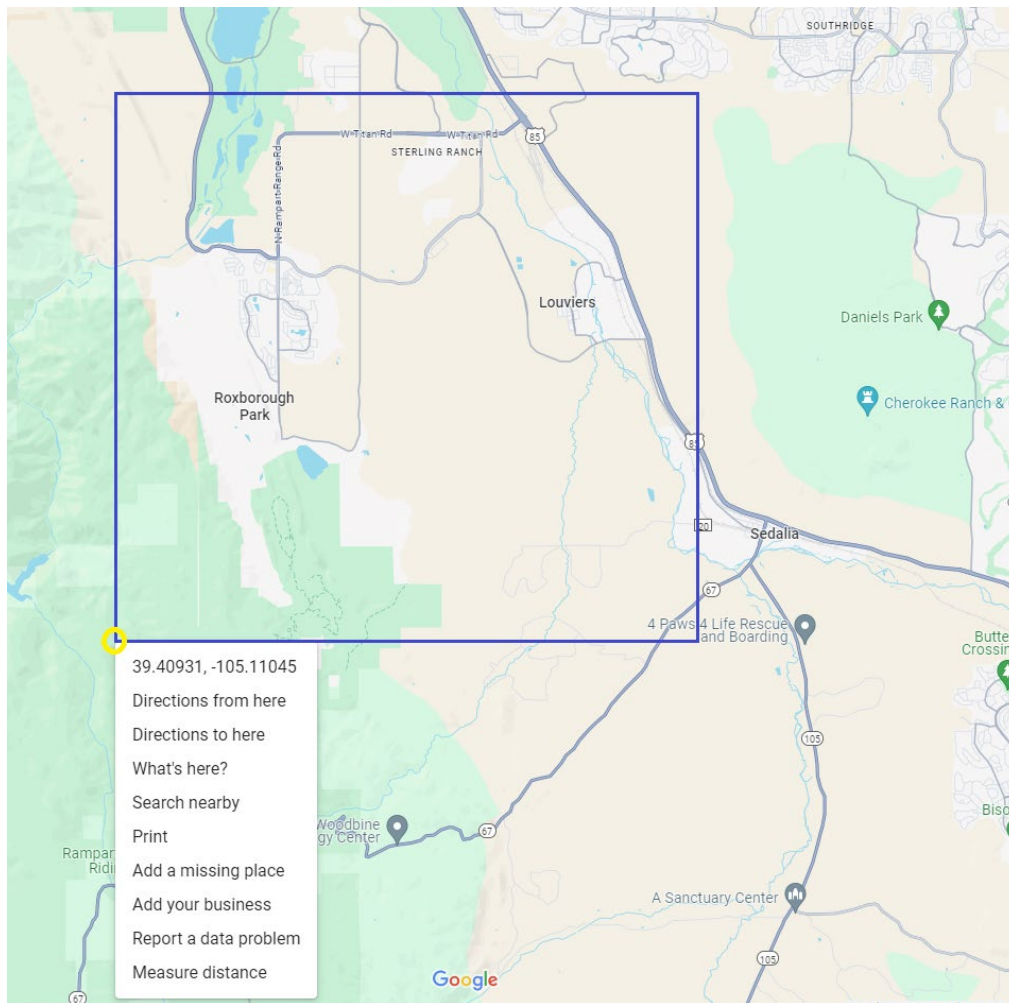


Figure 3. Determine the location and size of the region for evacuation analysis (from a demonstration case study).

Table 1. Data preparation and user input for map.

Input [Unit]	Format	Default value	Explanation/Source
Map LL latitude [degree]	Decimal	-	The latitude of the lower left corner of the map covering the area for modelling.
Map LL longitude [degree]	Decimal	-	The longitude of the lower left corner of the map.
Map size x [m]	Decimal	10,000	The width of the map (in horizontal X direction).
Map size y [m]	Decimal	10,000	The height of the map (in vertical Y direction).
Map zoom level	Decimal	13	The best-fit scale of satellite image to show the map within the GUI window ¹⁷ .
Mapbox API access token	String	-	Create an API access token [Optional].

Section 0 user actions:

- Identify the area for evacuation analysis (a square or a rectangle). Users should select a region size that aligns with their specific evacuation analysis requirements and get the coordinates of the bottom left corner and the vertical and horizontal length of the area.
- Use the values as an input to WUI-NITY to define the modelled region. **Note that if**

Section 0 model limitations:

- Mapbox is used to render the map as the foundation layer only. It does not have any impact on fire and evacuation simulations.
- Some small differences may appear between the road network shown in the Mapbox layer and the traffic network modelled based on the OpenStreetMap data.
- The maximum size of a region has not undergone rigorous testing. In general, smaller regions may lead to faster simulations due to reduced road network complexity and less people to be evacuated, while larger regions encompass more people and routes, resulting in slower simulations. Thus, users should opt for the minimum region size that fulfils their analysis needs.

¹⁷ Subject to the size of the map area and the resolution of the screen, the best-fit scale may vary.

Population Definition

WUI-NITY utilizes the Gridded Population of the World (GPW) collection¹⁸ as the foundation for creating and configuring population data in evacuation simulations. The GPW data sets model the distribution of the global human population on a continuous raster surface with an output resolution of 30 arc-seconds (about 1 km at the equator). Users should register an account at NASA's Earthdata Login¹⁹ and download the population density data sets (v4.11) of the GPW collection from:

<https://sedac.ciesin.columbia.edu/data/set/gpw-v4-population-density-rev11>

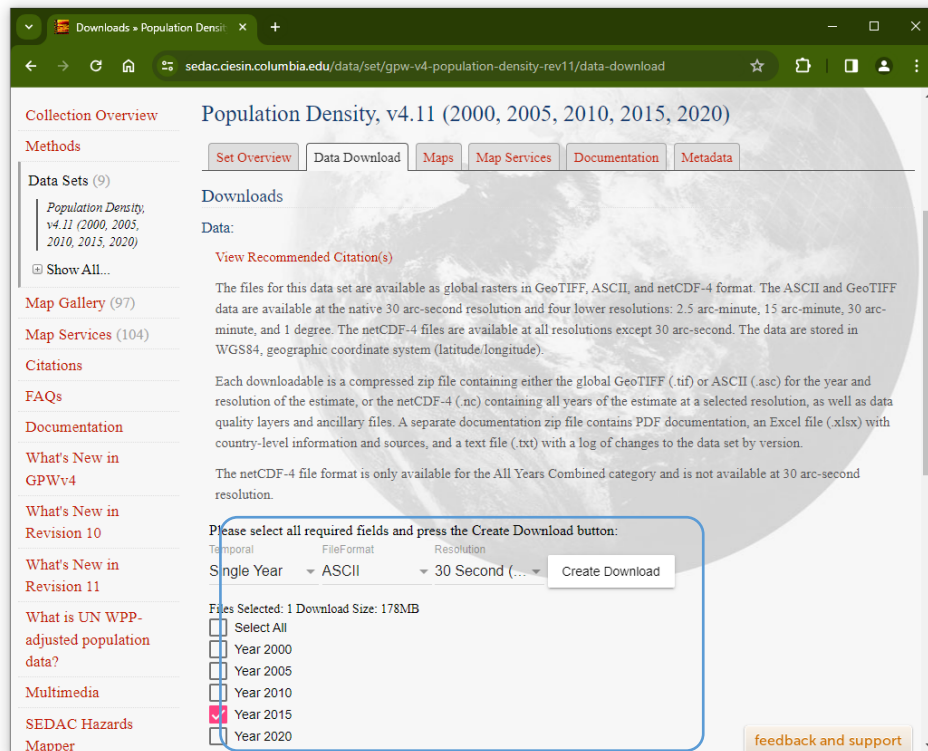


Figure 4. Select required fields to create the download link for the population density data sets.
(URL: <https://sedac.ciesin.columbia.edu/data/set/gpw-v4-population-density-rev11/data-download>)

The criteria for generating the download link include the following (see Figure 4):

- **Signal Year** for temporal;
- **ASCII** for file format;
- **30 Second (approx. 1km)** for resolution; and
- A year.

Among the five available years, the data sets for 2015 and 2020 have undergone testing in WUI-NITY and are therefore recommended for use.

The downloaded GPW data sets, which are packed into a zip file, need to be extracted to a folder²⁰. This folder, containing the extracted data, serves as an input for WUI-NITY. WUI-NITY processes the data sets to generate localized population data for use in the simulation run. This process includes three steps:

¹⁸ <https://sedac.ciesin.columbia.edu/data/collection/gpw-v4>

¹⁹ <https://urs.earthdata.nasa.gov/home>

²⁰ It can be any place in a local drive with at least 6-8GB free space.

- First, a subset of the GPW data covering the area of interest (i.e., the region specified in Section 0) is extracted from the global GPW data sets.
- Second, the population density data is interpolated based on the chosen evacuation cell size (as described in Section 0). This ensures that population counts are appropriately distributed across the area.
- And, finally, the population distribution is adjusted according to the local road network configuration, assuming that people live within a certain distance (influenced by evacuation cell size, see Section 0) of the roads.

This is made to simulate a more realistic space usage by the population by exploiting the information available from the road network and dead ends (i.e., assuming that each household has access to the road network). Households are then randomly generated in space following the population distribution, in which a population between 1-5 people is assigned by default to each household. The relevant data input details for population definition are summarized in Table 2. Note that these three steps do not require additional user intervention or inputs.

Table 2. Data preparation and user input for population definition.

Input [Unit]	Format	Default value	Explanation/Source
The population density data sets from the GPW collection	Path	-	The path in which the downloaded population density data sets are saved.
Evacuation cell size [m]	Decimal	200	The size of the cells used to populate the area (see Section 0).

Users also have the flexibility of adjusting population size and distribution according to their specific requirements. Here are the available customization options:

1. **Customize population size:** Users can rescale the population size to a customized value. This adjustment is done proportionally based on the existing population density distribution. When users enter a new total number of people, WUI-NITY will recalculate the number of people in each population cell using this number and the density distribution.
2. **Customize cell distribution:** For finer control, users can interactively add or remove population cells directly on the map. WUI-NITY then relocates the people affected by the change of the cells.

The population related files and settings are stored in the “population” section of the WUI-NITY project file (see Section 0).

Section 0 user actions:

- Supply the downloaded Gridded Population of the World (GPW) data sets to WUI-NITY to generate the population distribution within the modelled region.
- Customize population size or adjust population distribution (optional).

Section 0 model limitations:

- By default, population distributions are estimated based on coarse data.

Fire and smoke simulation

This section relates to the simulation of fire and smoke. It should be noted that this simulation is not essential for the simulation of the community evacuation. Therefore, if users want to focus on community evacuation analysis only (i.e. without explicitly modelling a fire scenario), they can safely skip this section.

WUI-NITY is capable of importing fire simulation results from FARSITE²¹ (see [3] for more information). FARSITE is a fire growth simulation model that automatically computes wildfire growth and behavior over long time periods under heterogeneous conditions of terrain, fuels and weather. In addition, WUI-NITY has implemented a built-in wildfire model based on BEHAVE, a wildfire modelling tool (see [2] for more information). This tool considers fuel and moisture conditions to obtain a set of key outputs, including surface and crown fire rate of fire spread and intensity, ignition probability, fire size, spotting distance and tree mortality. **In this guide, we focus on introducing the required input and settings of the built-in wildfire model, unless stated otherwise.**

The fire and smoke²² simulation module within WUI-NITY estimates the spread of the fire and smoke effluent. It relies on seven different files to provide supporting data that influences this spread. These files include:

1. **Landscape file (.lcp):** Contains information about the landscape for fire simulation (see Section 0).
2. **Fuel models file (.fuel):** Specifies fuel models used in the simulation (see Section 0).
3. **Initial fuel moisture file (.fmc):** Provides data on initial fuel moisture content (see Section 0).
4. **Weather file (.wtr):** Includes weather data relevant to the simulation (see Section 0).
5. **Wind file (.wnd):** Contains wind-related information (see Section 0).
6. **Ignition points file (.ign):** Specifies ignition points for fire initiation (see Section 0).
7. **Graphical fire input file (.gfi):** Used for saving graphical user input related to fire behavior (see Section 0).

For definitions and specifications of these files, please refer to Table 3.

The creation and preparation of these seven file types are explained in Sections 0 - 0 respectively with examples. Apart from the landscape file and the graphical fire input file, all the others are ASCII text files. Users can manually create and edit these files following the required format and the examples provided in the corresponding sections. If users are unsure about the values to use in preparing these files, they may choose the values given in the examples as a starting point in their model. The tasks required for the use of these files within WUI-NITY are described in Section 0.

²¹ <https://www.firelab.org/project/farsite>

²² Currently a simple smoke spread module is implemented within WUI-NITY, and the simulation results are indicative at this stage. WUI-NITY can represent speed reduction due to reduced visibility conditions. This impact is measured as optical density, either a single static value or a dynamic variable over time, specified by users and has a global influence on driving behaviour (see Section 0).

Table 3. Input Files for Fire and Smoke Simulation

File type*	Format	Postfix	File preparation and specification
lcpFile	text	.lcp	A landscape file contains information about the landscape for the fire simulation. It includes a combination of elevation, slope, aspect, canopy cover and fuel raster layers prepared by users, following the guidance provided in this section. Note that landscape files are available for locations in the US (e.g. https://landfire.gov/getdata.php). If the target location is outside the United States, various data sets need to be individually located, downloaded, modified, and combined using a GIS program to produce the required landscape file (see Section 0).
fuelModelsFile	text	.fuel	A fuel models file specifies fuel models used in the simulation. It includes typical fuel types found in a specific geographic location and their combustion properties. A default LANDFIRE's (LF) 13 Anderson Fire Behavior Fuel Models (FBFM13) is included in WUI-NITY for use.
initialFuelMoistureFile	text	.fmc	User definable level of moisture of each type of fuel.
weatherFile	text	.wtr	User definable weather conditions including precipitation, temperature, and humidity.
windFile	text	.wnd	User definable wind speed and direction as a function of time.
ignitionPointsFile	text	.ign	User definable location and time of ignition point.
graphicalFireInputFile	binary	.gfi	User definable (in WUI-NITY) WUI area, initial ignition, random ignition, and trigger buffer mapped on the fire mesh.

* The naming conventions of file type in this table is defined and used in WUI-NITY project file (.wui). See Section 0.

Additionally, users can adjust several other settings related to the fire spread model, including wind multiplier, random or initial fire ignition. These are listed in Table 4. There is also an optional input which tells WUI-NITY where to find the FARSITE input data if the user wishes to use FARSITE simulation results instead of the built-in fire simulation model. These support files and fire related settings are stored in the “Fire” section of the WUI-NITY project file (see Section 0).

Table 4. Additional Fire Spread Model Settings

Input	Format	Default value	Explanation/source
windMultiplier	Decimal	1	This is a model test parameter, which is used in the fire spread model as a multiplier of the wind speed spline.
useRandomIgnitionMap	Boolean	False	This Boolean controls whether to use random ignition points within a region drawn by users on the map through graphical fire input (see Section 0).
randomIgnitionPoints	Integer	0	The number of random ignition points within the region from graphical fire input.
useInitialIgnitionMap	Boolean	False	This Boolean controls whether to use the ignition points drawn by users on the map through graphical fire input (see Section 0).
FarsiteData*	path	-	The main folder containing FARSITE input data.

* This is an optional input which specifies the folder that contains the FARSITE input data.

Landscape file (.lcp)

The fire simulation model requires a landscape file (.lcp) to simulate the spread of fire and smoke. A landscape file represents the regional topography and is a combination of topographic (elevation, slope, aspect), canopy cover and fuel raster layers. The raster layers are stored in a file format where an image represents a matrix of cells holding information on the physical conditions mentioned. If the target location is within the United States (including Hawaii and Alaska), users can download and use the landscape files readily available at the LANDFIRE database²³, which contains a complete fuel-mapping of the country (see Figure 5). However, if the target location is outside the United States, the raster layers need to be individually located, downloaded, modified, and combined using a GIS program. For instance, the raster layers can be sourced from the following list of resources (not exhaustive):

- **Topographic data** (elevation, slope, aspect): Earth Explorer²⁴, Earth Engine²⁵, Google Earth Pro²⁶;
- **Canopy cover** (contains information regarding how thick and dense the forest is, as well as the crown base height): European Forest Fire Information System (EFFIS)²⁷;
- **Fuel data** (contains information regarding types of trees etc. that is present in the area): European Forest Fire Information System (EFFIS), the Wildfire Fuel Generator (WFG) application²⁸.

In general, the elevation data can be freely downloaded from the three sources provided. The slope and aspect layers can be calculated from the elevation layer using GIS if they are not already included in the downloaded topographical data from these sources. The canopy cover and fuel data may be difficult to obtain in many countries as it requires extensive manual surveying [15, 16]. Users can consult with the local survey authority if such data is not publicly available.

In the following subsections 0-0, we illustrate how to source the necessary data from public resources (i.e., Earth Explorer and EFFIS) to build a landscape file for a location in the UK. The approach is generally applicable to other locations within Europe. For any other locations, users may look for equivalent sources of data and follow the same principles to prepare a landscape file. For instance, the National Bushfire Intelligence Capability (NBIC) is developing a new approach to the mapping and measuring of fuels across Australia²⁹. A fuel type grid developed by NSW Rural Fire Service is used in the development and implementation of the Australian Fire Danger Rating System Research Prototype (AFDRSRP) as a climatology study [17, 18]. However, as of the time of writing, these resources have not been explored further to see if the data provided is compatible with the requirement of WUI-NITY.

²³ <https://landfire.gov/getdata.php>

²⁴ <https://earthexplorer.usgs.gov>

²⁵ <https://earthengine.google.com>

²⁶ https://www.google.com/intl/en_uk/earth/about/versions/#earth-pro

²⁷ <https://effis.jrc.ec.europa.eu/applications/data-and-services>

²⁸ <https://forsite.ca/wildfire-fuels-mapping/>

²⁹ <https://research.csiro.au/nbic/contemporary-fuels-information/>

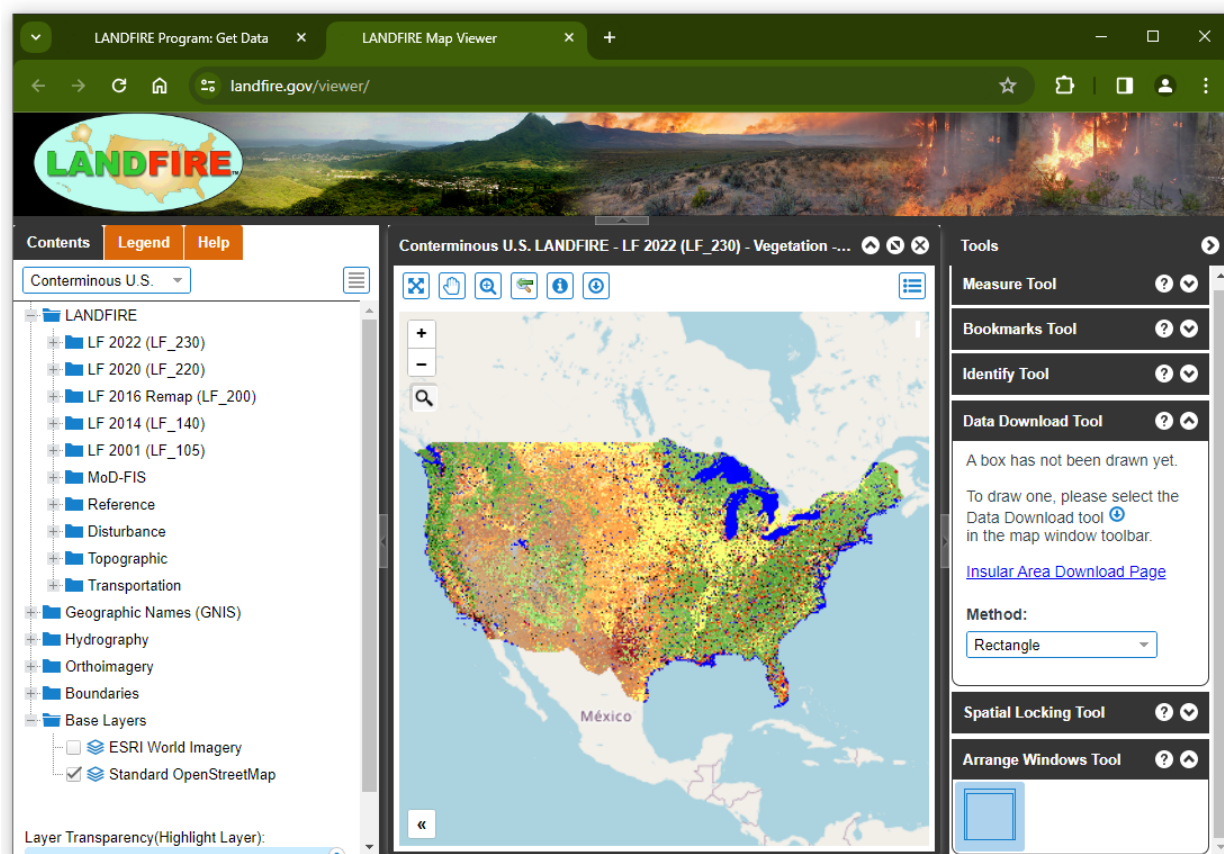


Figure 5. LANDFIRE (LF) data access tool to view and download landscape files.

Topographic data (elevation, slope, aspect layers)

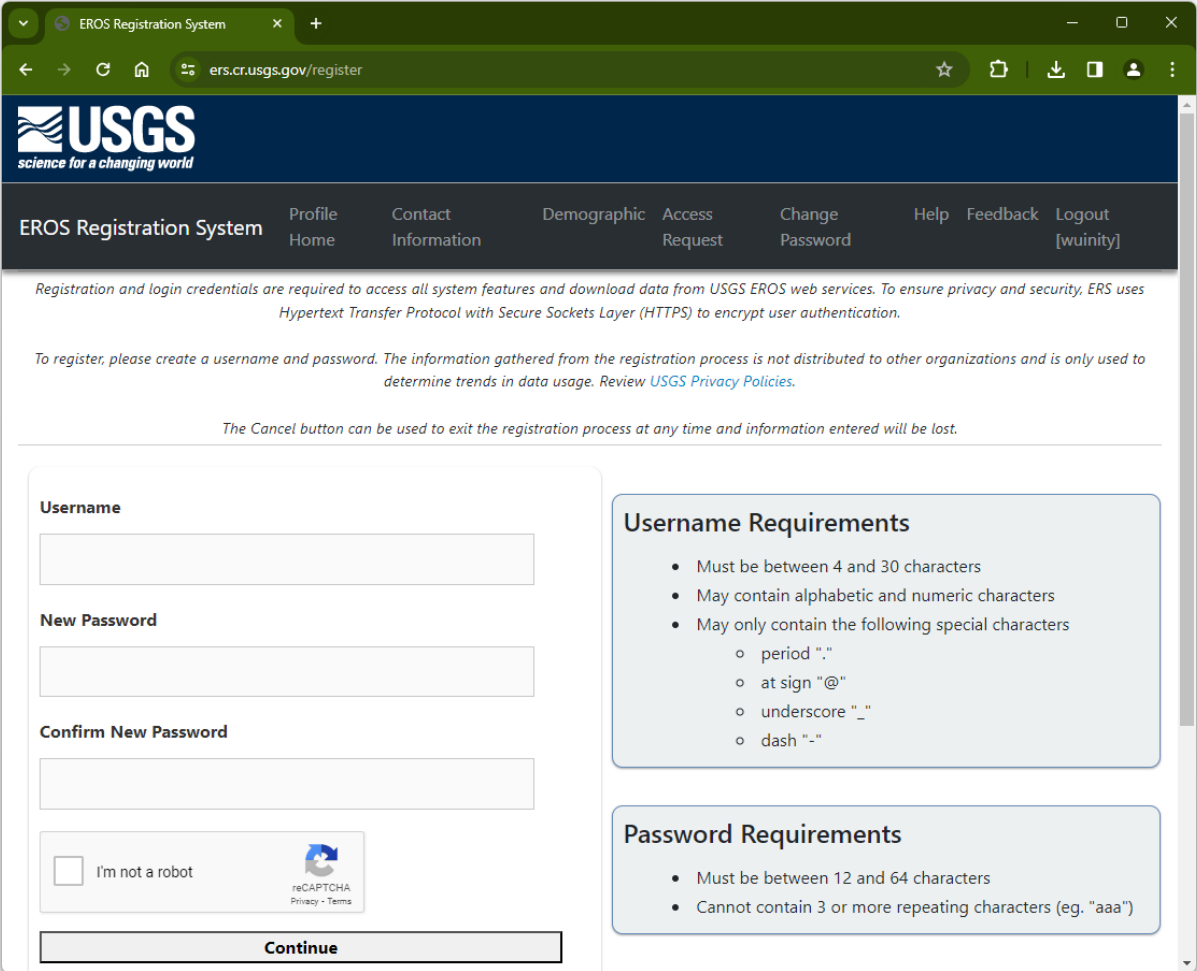
While topographic data is available from a variety of resources (such as Earth Explorer, Earth Engine), the process to obtain the necessary data for creating the .lcp file is not straightforward. A detailed description of an example performed by Lund University of the work needed can be found here³⁰. The topographic data used in this guide for the test case described in Section 0 was obtained from Earth Explorer using the approach described below.

Earth Explorer is a valuable resource jointly provided by NASA and the United States Geological Survey (USGS). It grants registered users access to a wealth of geospatial data sets, satellite imagery, elevation data, data of land coverage, and map products. By using specific coordinates or the interactive map, users can outline a desired area and download selected data specific for the area of interest. We illustrate how to use Earth Explorer to retrieve the topographical data required for creating a landscape file in the following four steps.

³⁰ <https://lup.lub.lu.se/luur/download?func=downloadFile&recordId=9104264&fileId=9104265>

Step 1: Register a user account.

Users should open the link <https://ers.cr.usgs.gov/register> in a browser and register a user account (see Figure 6). Note a valid email address is required to confirm registration.



The screenshot shows a web browser window with the URL ers.cr.usgs.gov/register. The page features the USGS logo and a navigation bar with links: EROS Registration System, Profile Home, Contact Information, Demographic, Access Request, Change Password, Help, Feedback, and Logout [wuinity].

Below the navigation bar, there is a disclaimer: "Registration and login credentials are required to access all system features and download data from USGS EROS web services. To ensure privacy and security, ERS uses Hypertext Transfer Protocol with Secure Sockets Layer (HTTPS) to encrypt user authentication." and another note: "To register, please create a username and password. The information gathered from the registration process is not distributed to other organizations and is only used to determine trends in data usage. Review [USGS Privacy Policies](#)." A final note states: "The Cancel button can be used to exit the registration process at any time and information entered will be lost."

The registration form includes the following fields and sections:

- Username**: A text input field.
- New Password**: A text input field.
- Confirm New Password**: A text input field.
- reCAPTCHA**: A checkbox labeled "I'm not a robot" and a reCAPTCHA logo with links for "Privacy" and "Terms".
- Continue**: A button at the bottom of the form.
- Username Requirements**: A list of requirements:
 - Must be between 4 and 30 characters
 - May contain alphabetic and numeric characters
 - May only contain the following special characters:
 - period "."
 - at sign "@"
 - underscore "_"
 - dash "-"
- Password Requirements**: A list of requirements:
 - Must be between 12 and 64 characters
 - Cannot contain 3 or more repeating characters (eg. "aaa")

Figure 6. Register a user account at USGS website. (URL: <https://earthexplorer.usgs.gov/>)

Step 2: Open Earth Explorer and select the area of interest.

- **Login to Earth Explorer** with username and password at <https://earthexplorer.usgs.gov/>;
- In the map view window, drag the map to display the country where the area of interest is located;
- Set the **Search Criteria** as shown in Figure 7 (ignore the coordinates for now, as they will be automatically generated in the next step);
- Click the **Use Map** button at the bottom left corner of the window. Zoom out the map slightly;
- A rectangular area highlighted in red along with four pairs of coordinates will appear on the map view. Drag the four blue coordinate marks on the map to narrow down the highlighted area to the size that is large enough to cover the entire area intended for modelling in WUI-NITY.

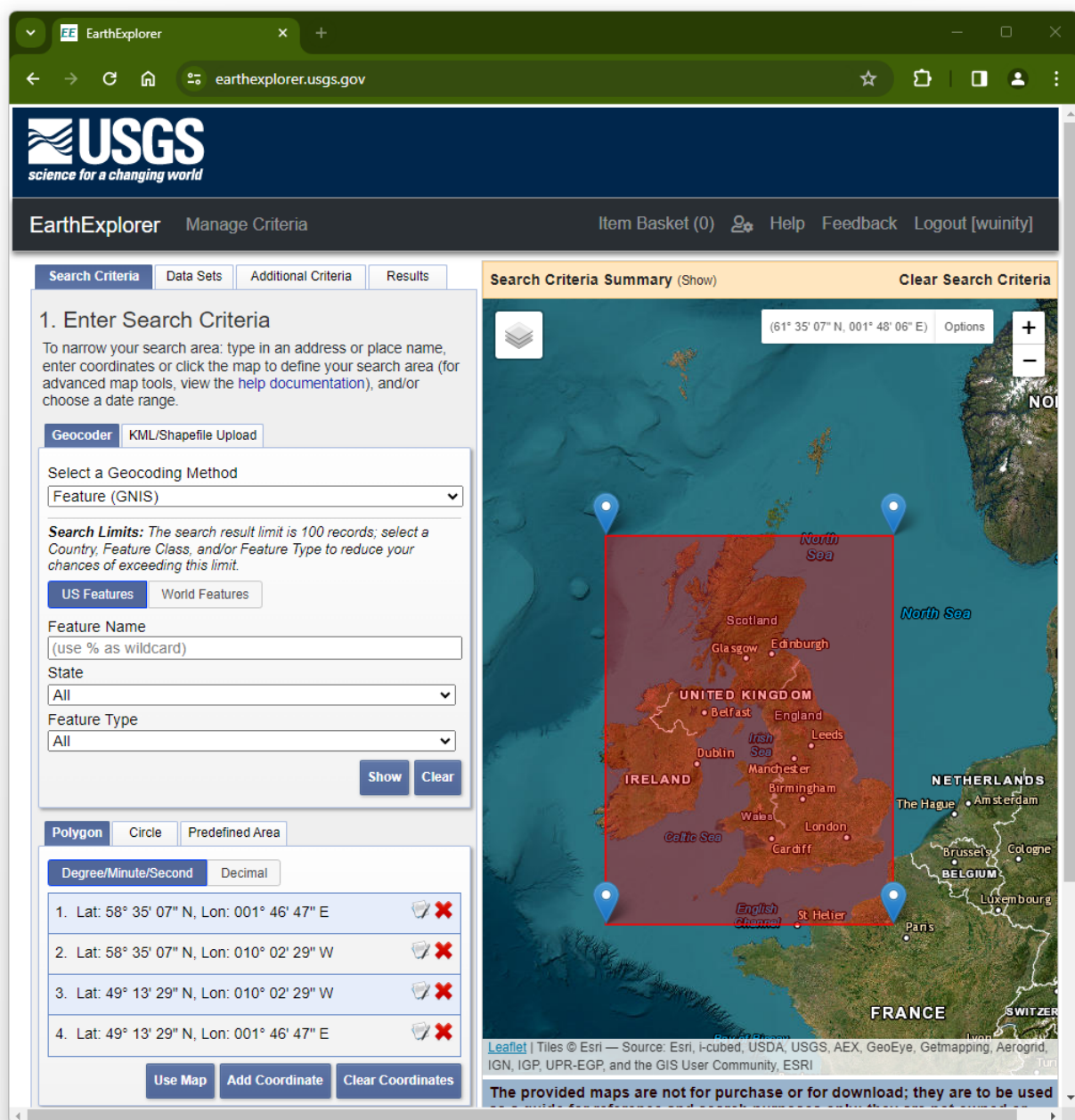


Figure 7. Open Earth Explorer and select the area of interest. (URL: <https://earthexplorer.usgs.gov/>)

Step 3: Select data set for downloading.

- Click the second tab of Earth Explorer, labelled “**Data Sets**” (see Figure 8),
- Navigate the data set list by expanding **Digital Elevation** -> **SRTM** and tick the option **SRTM 1 Arc-Second Global**,
- Click the **Results** button at the bottom.

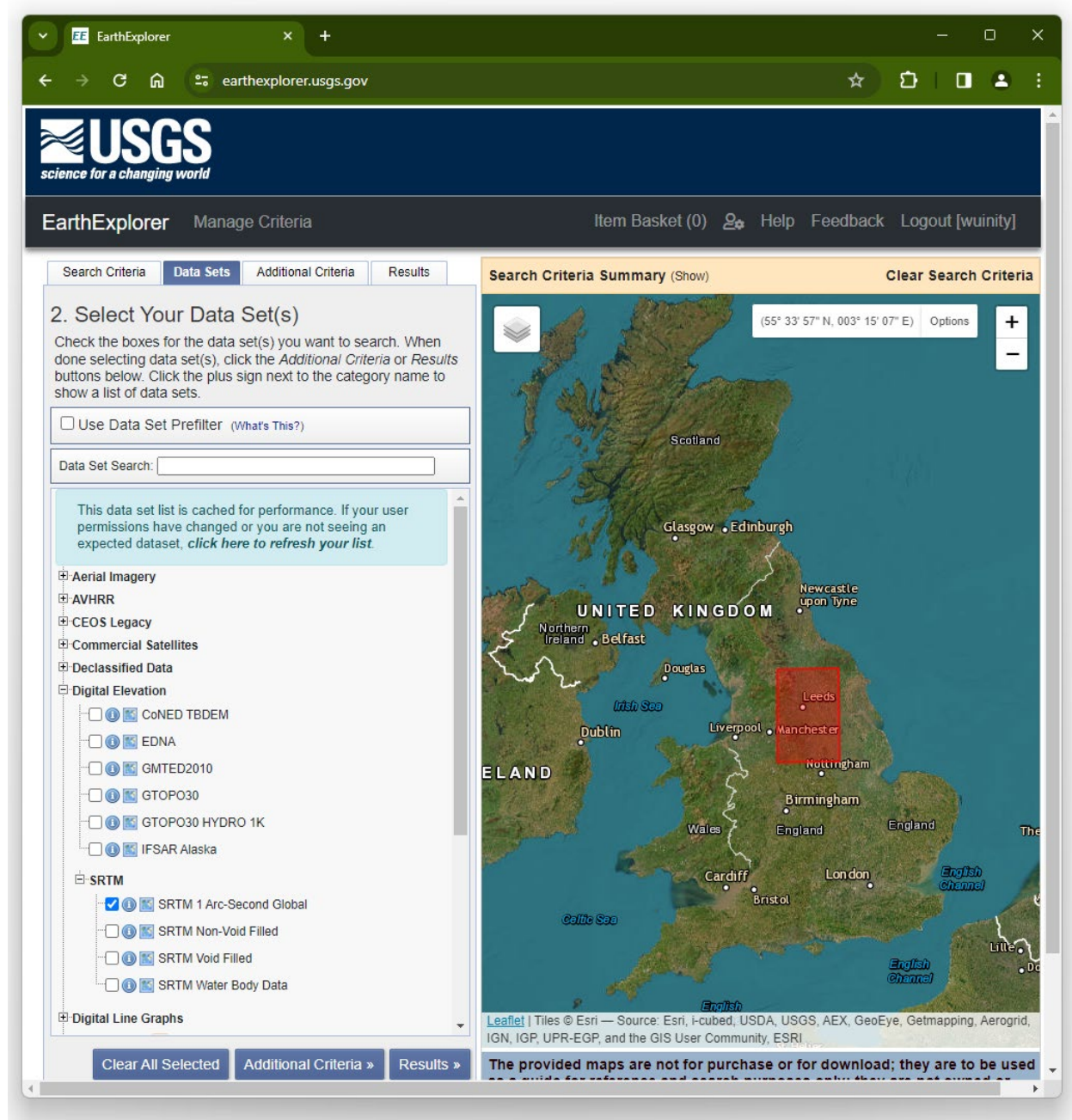


Figure 8. Select data set for downloading. (URL: <https://earthexplorer.usgs.gov/>)

Step 4: Verify data set selection and download.

After clicking the **Results** button in Step 3, Earth Explorer will open the fourth tab, labelled “**Results**”, and show several data sets in the Search Results list (see Figure 9). Each of these data sets overlaps with the selected area in red at some point. To pinpoint the data set that accurately covers the intended modelling area in WUI-NITY, users should click the “**Show Footprint**” icon under each data set to examine them individually. The footprint of the selected data set will appear as a light blue layer on the map view.

Once the appropriate data set is identified, click the fourth **Download Option** icon associated with the data set. A popup window will appear (see Figure 10). Users should select the third option “**GeoTIFF 1 Arc-second**” and download the data set, which contains the elevation data specific to the area of interest.

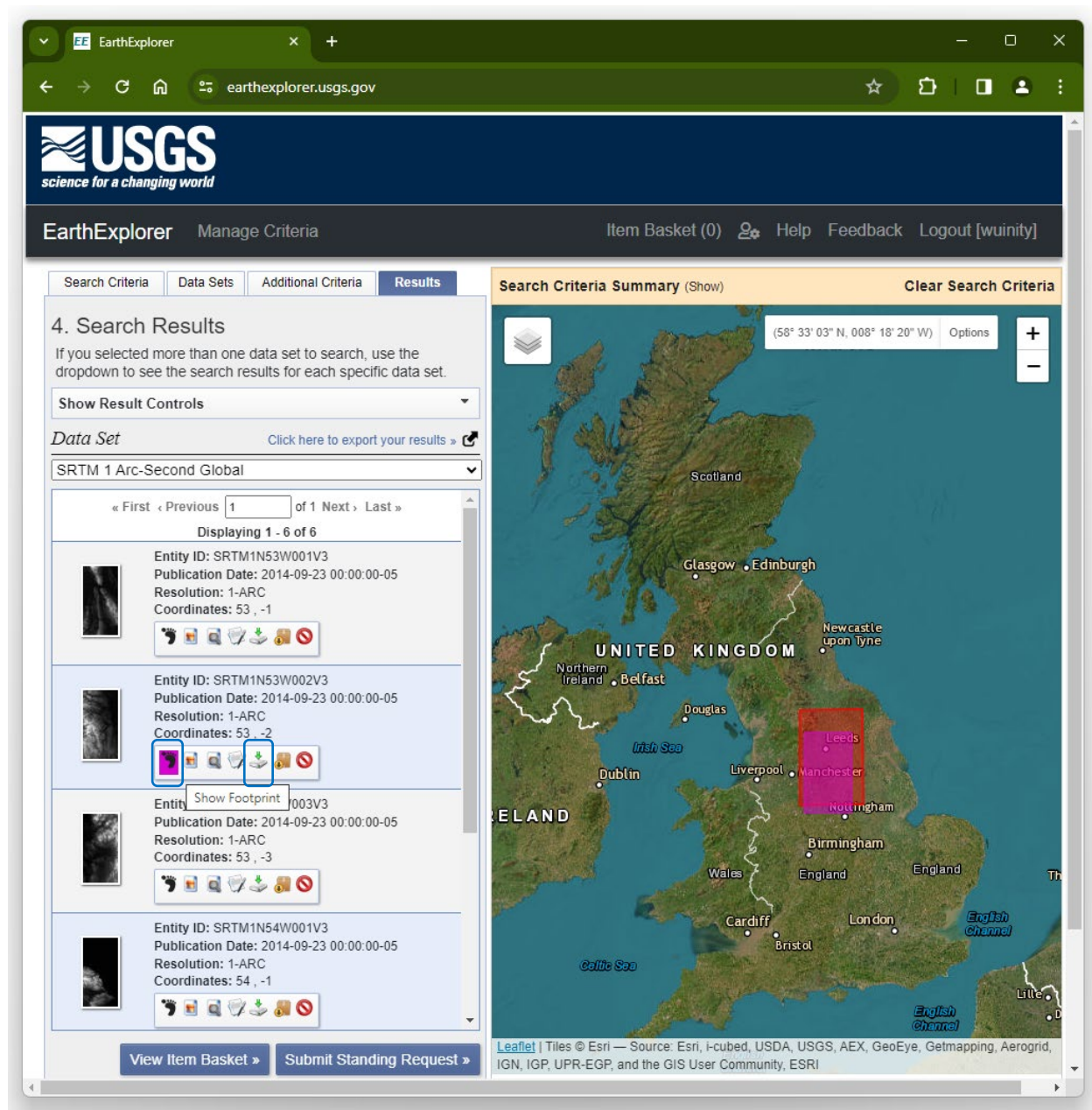


Figure 9. Verify data set selection and download. (URL: <https://earthexplorer.usgs.gov/>)

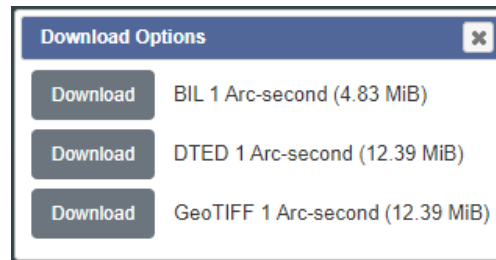


Figure 10. Select download option.

It should be noted that Earth Explorer may not always contain the topographical data for an area of interest. Users are recommended to read the previous work done at Lund University (see the link³⁰ on page 145) for alternative approaches to preparing the required topographic data.

Canopy cover layer

The canopy cover layer contains information regarding how thick and dense the forest is, as well as the crown base height. For locations within Europe, this information can be obtained from the European Forest Fire Information System (EFFIS) via a service called Copernicus. Resources for Australia are presented in Section 0. The data is called the High Resolution Layer Tree Cover Density, which is available from the Earth observation component of the European Union's Space Programme at:

<https://land.copernicus.eu/en/products/high-resolution-layer-tree-cover-density>

The datasets cover the EEA38 countries and the United Kingdom and provide at the pan-European level in the spatial resolution of 10 m and 100 m the level of tree cover density in a range from 0% to 100% for a selected reference year.

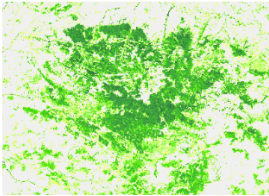
To build a landscape file for a location in the UK, navigate to the dataset category '**Tree Cover Density 2018 (raster 10 m and 100 m), Europe, 3-yearly**', and then select '**United Kingdom**' as Area of interest (see Figure 11). Note that an EU Login account is required for downloading. Users can create such an account at:

<https://ecas.ec.europa.eu/cas/eim/external/register.cgi>

Tree Cover Density 2018 (raster 10 m and 100 m), Europe, 3-yearly


General Info


Download



View in the data viewer

Services

WMS 

REST API 

Download by area

Use this option if you would like to download the dataset for area(s) of interest.

Go to download by area


Download full dataset


You can download the full dataset as pre-packaged data collections. You can also download the full dataset, using the CLMS download API. Click [here](#) to learn more about the CLMS download API.

Download pre-packaged data collections

Pre-packaged Tree Cover Density 2018 datasets can be downloaded as 10 m raster files in 100 x 100 km tiles for each EEA38 country and the United Kingdom, as well as a full mosaic for EEA38 countries and the United Kingdom. The 100 m aggregated raster file is provided as a full mosaic for EEA38 countries and the United Kingdom.

Search in the pre-packaged data collection

1 selected file(s) - Clear selection 
Select all

 File	Area of interest	Version	Resolution	Type	Format	Size
<input type="checkbox"/> TCD_2018_010m_de_03035_v020	Germany	v020	10 m	Raster	Geotiff	1 GB
<input type="checkbox"/> TCD_2018_010m_dk_03035_v020	Denmark	v020	10 m	Raster	Geotiff	103 MB
<input type="checkbox"/> TCD_2018_010m_ee_03035_v020	Estonia	v020	10 m	Raster	Geotiff	241 MB
<input type="checkbox"/> TCD_2018_010m_es_03035_v020	Spain	v020	10 m	Raster	Geotiff	2 GB
<input type="checkbox"/> TCD_2018_010m_fi_03035_v020	Finland	v020	10 m	Raster	Geotiff	2 GB
<input type="checkbox"/> TCD_2018_010m_fr_03035_v020	France	v020	10 m	Raster	Geotiff	2 GB
<input checked="" type="checkbox"/> TCD_2018_010m_gb_03035_v020	United Kingdom	v020	10 m	Raster	Geotiff	348 MB
<input type="checkbox"/> TCD_2018_010m_gr_03035_v020	Greece	v020	10 m	Raster	Geotiff	1 GB
<input type="checkbox"/> TCD_2018_010m_hr_03035_v020	Croatia	v020	10 m	Raster	Geotiff	1 GB
<input type="checkbox"/> TCD_2018_010m_hu_03035_v020	Hungary	v020	10 m	Raster	Geotiff	409 MB

< 1 2 3 4 5 >

Add to cartShow cart

Figure 11. The High Resolution Layer Tree Cover Density product offered at Copernicus (UK is selected). (URL: <https://land.copernicus.eu/en/products/high-resolution-layer-tree-cover-density/tree-cover-density-2018>)

Fuel map layer

Fuel map specifies the location and types of the vegetation (e.g., tree types, bushes, lakes, fields etc.) in an area. The fuel data depicts the different types of fuel (i.e., burnable vegetation types) with different colors. Each color is associated with a number, which is also used to link with a fuel type defined in the .fuel file (see Section 0), which defines the attributes of the specific fuel type.

For a location within Europe, the fuel map (a single GeoTIFF³¹ file with the resolution of 50 x 50 m) can be obtained from EFFIS via Copernicus at (see Figure 12):

<https://effis.jrc.ec.europa.eu/applications/data-and-services>

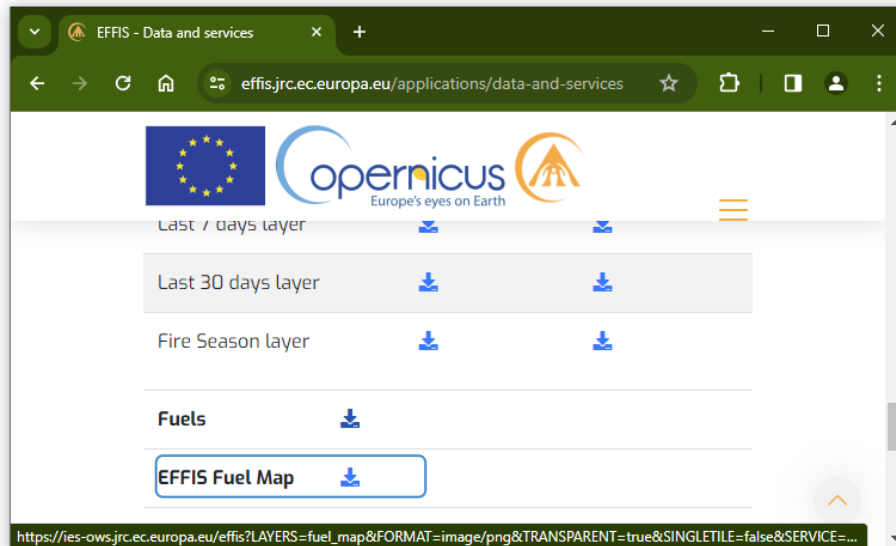


Figure 12. Download the European fuel map from EFFIS. (URL: <https://effis.jrc.ec.europa.eu/applications/data-and-services>)

Combine the raster layers to generate a landscape file

When the topographic (elevation, slope, aspect), canopy cover and fuel raster layers are ready, they need to be set to the same resolution, dimension and coordinate reference system (CRS) to produce the final landscape file. This can be done in either QGIS³² (a free GIS tool) or ArcGIS³³ (a commercial GIS tool).

In QGIS (version 3.28.5 LTR), for example, it takes the following preparation steps:

- **Set default CRS:** Set the CRS of any base map used to **EPSG:3857 - WGS 84/Pseudo-Mercator**³⁴ from the main menu 'Project -> Properties ...-> CRS'. See Figure 13.

³¹ GeoTIFF is based on the TIFF format and is used as an interchange format for georeferenced raster imagery.

³² <https://qgis.org/en/site/>

³³ <https://www.arcgis.com/index.html>

³⁴ EPSG:3857 - WGS 84 is a projected coordinate system used for rendering maps in Google Maps, OpenStreetMap. It is valid everywhere in the world between 85.06°S and 85.06°N. However, as EPSG:3857 covers such a large distance there may be small errors associated with distance estimate.

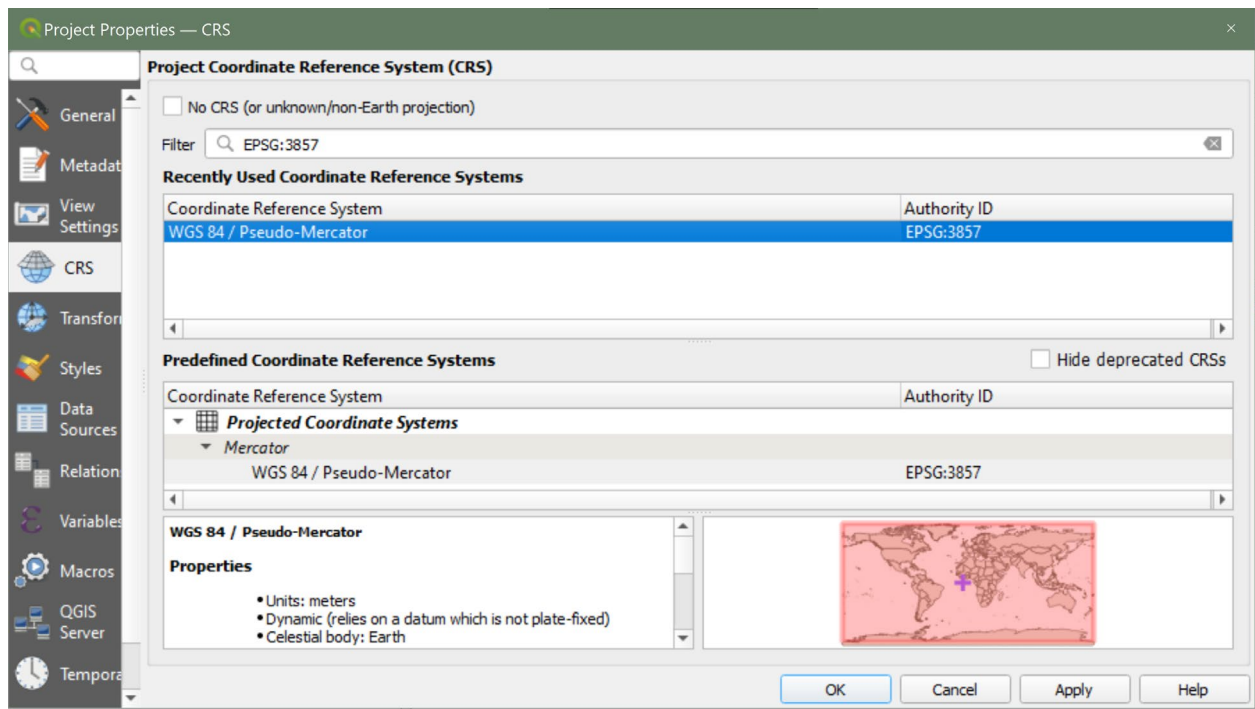


Figure 13. Set EPSG:3857 - WGS 84 as the default CRS in QGIS.

- **Load raster layers:** Add the elevation, fuel map and canopy cover layers into QGIS from the main menu 'Layer -> Add Layer -> Add Raster Layer', as shown in Figure 14.

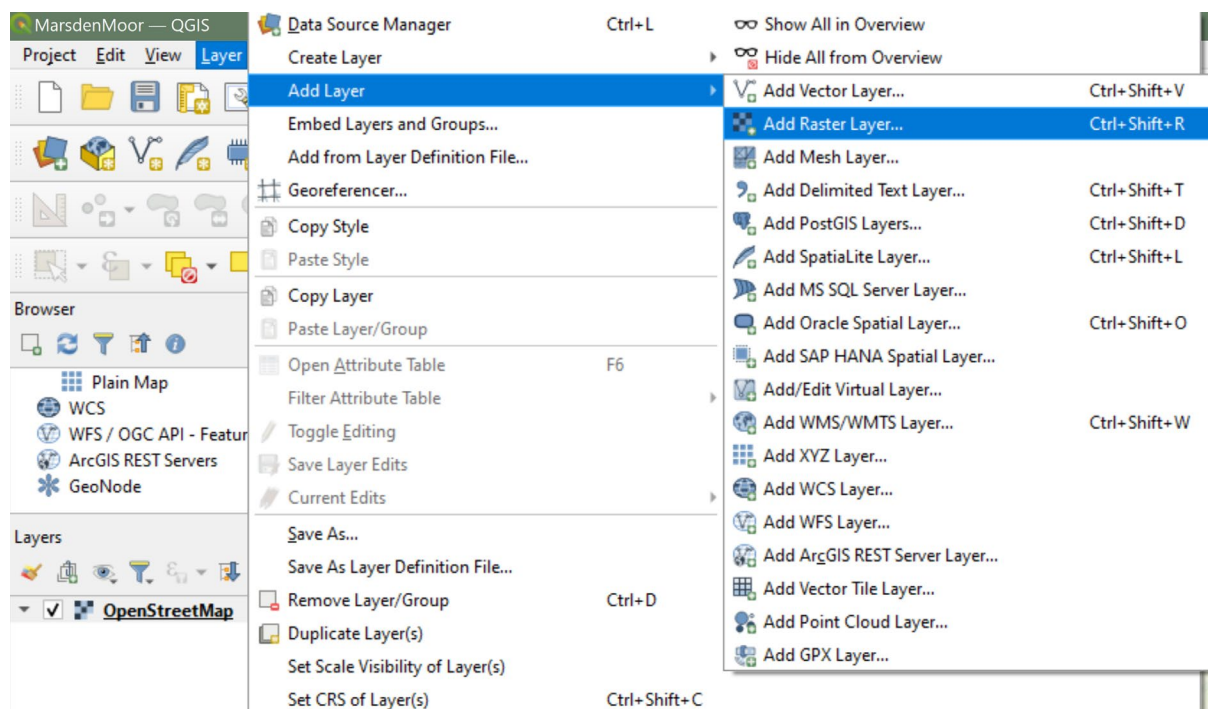


Figure 14. Add elevation, fuel map and canopy cover layers into QGIS.

- **Create aspect and slope layers:** QGIS can calculate the aspect and slope layers based on the elevation layer. This can be done using the tools accessed from the main menu 'Raster -> Analysis-> Aspect/Slope...', using the existing elevation layer as an input (see Figure 15).

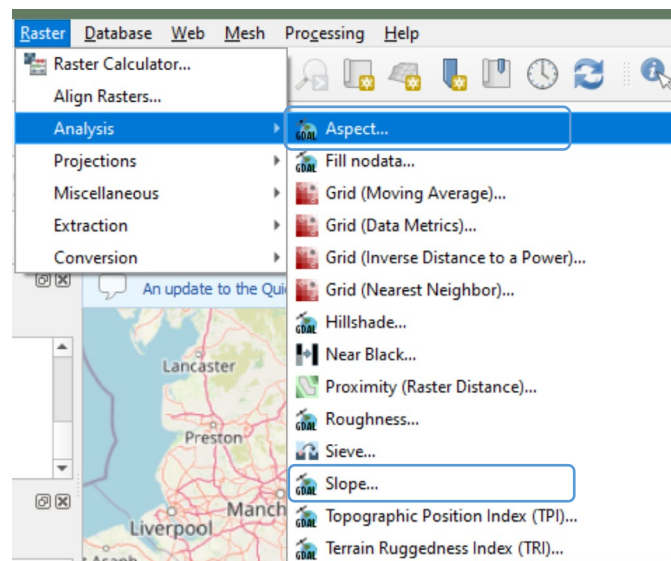


Figure 15. Use Raster Analysis tools to calculate the aspect and slope layers respectively.

- **Create a new shapefile layer:** Create a shapefile around the target area using 'Layer -> Create Layer -> New Shapefile Layer...' (see Figure 16) and set its Geometry Type to be 'Polygon' and CRS to be EPSG:3857 (see Figure 17).

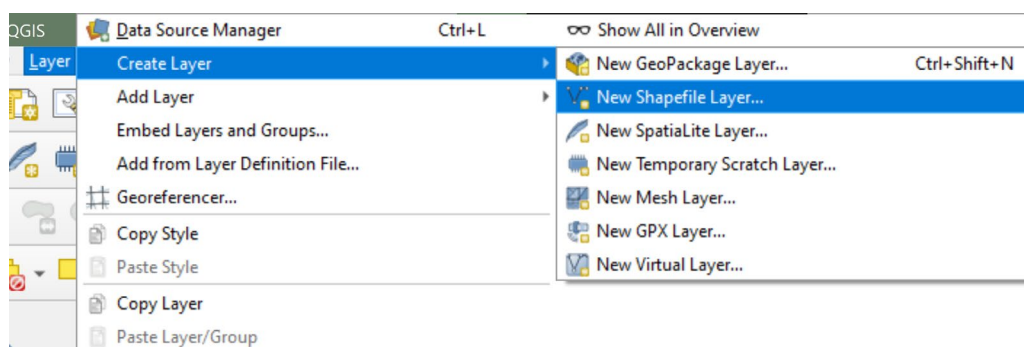


Figure 16. Create a new Shapefile layer.

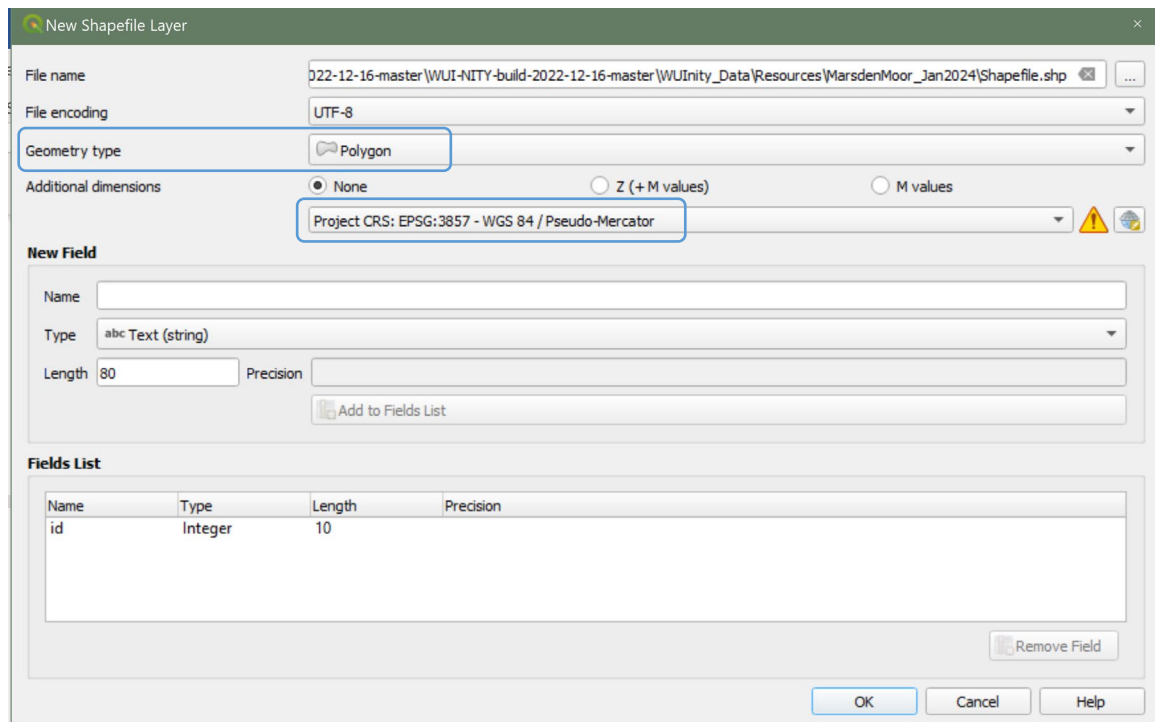


Figure 17. Set the geometry type and CRS of the new Shapefile layer and save it as a .shp file in the project folder.

- **Draw a polygon to cover the target area:** Select the newly created Shapefile layer, turn on 'Editing' and draw a polygon around a rough approximation of the target area (see Figure 18). Here we use Marsden Moor, situated in West Yorkshire of the United Kingdom as the test location (see also Section 0).

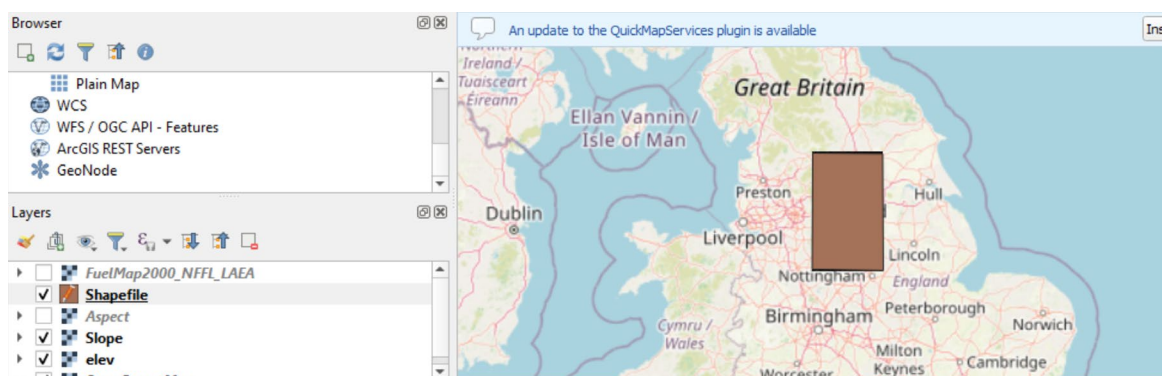


Figure 18. Draw a polygon around a rough approximation of the target area (i.e., Marsden Moor).

- **Clip raster by extent:** Use the Geoprocessing Tools -> Clip functionality to clip the elevation file to the shapefile extents to create a Clipped Extent layer. This is accessed via the Processing Toolbox (see Figure 19). Specify Elevation as the input layer and set the clipping extent to that of the recently created Shapefile (see Figure 20). This creates a new clipped extents layer, which forms the basis for further transformations to be done on other layers (see Figure 21).

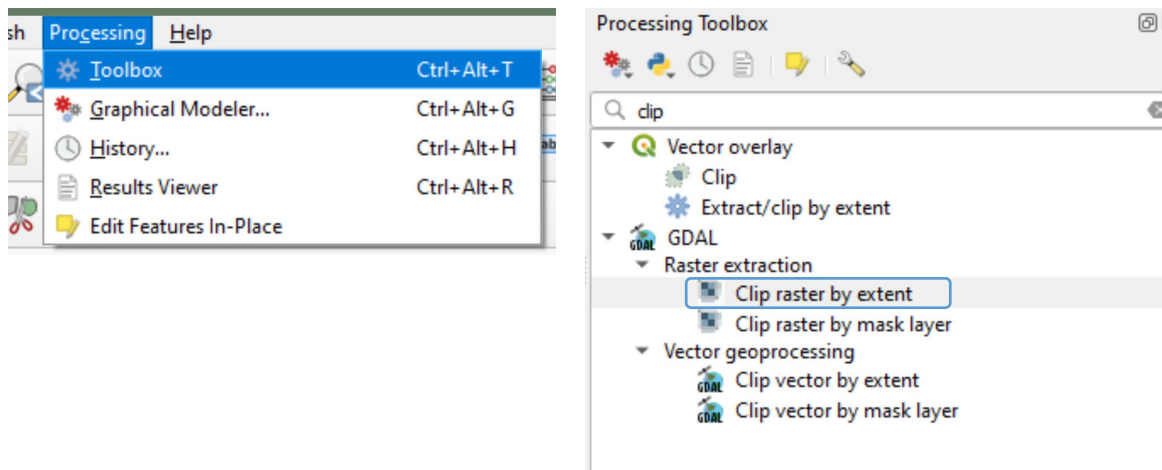


Figure 19. Open the Processing Toolbox(left) and select Clip Raster by Extent under Raster Extraction in the Processing Toolbox (right).

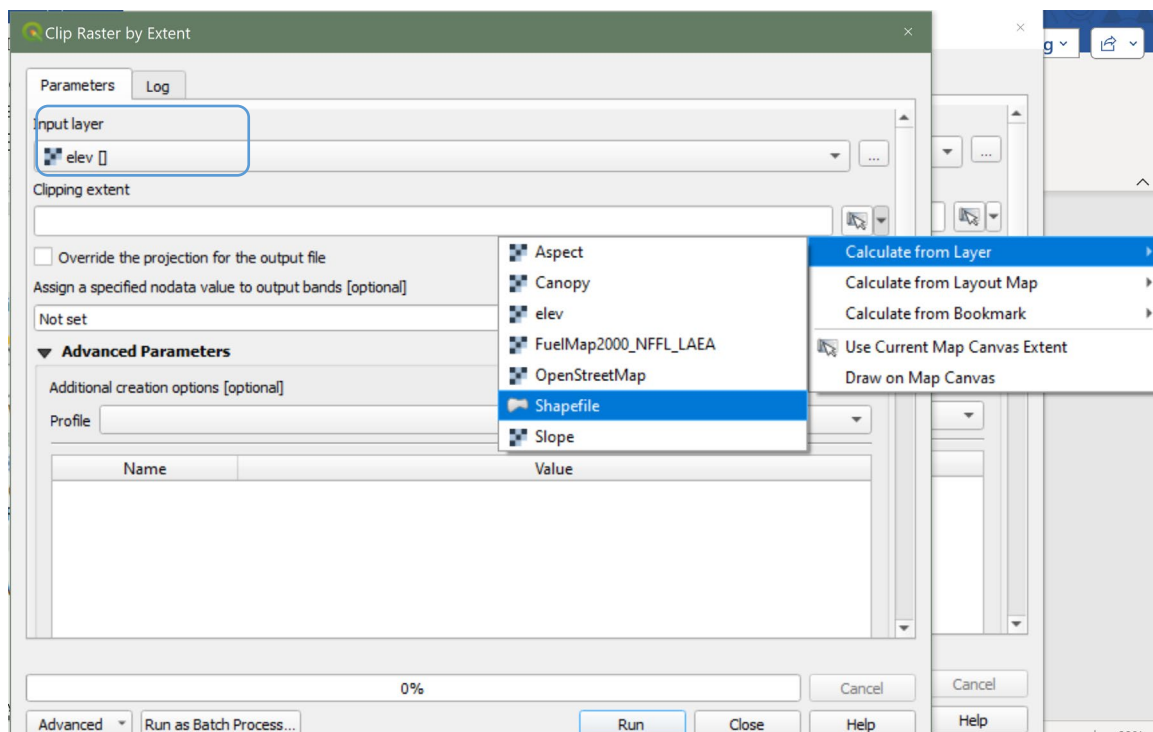


Figure 20. Specify Elevation as the input layer and set the clipping extent to that of the recently created Shapefile.

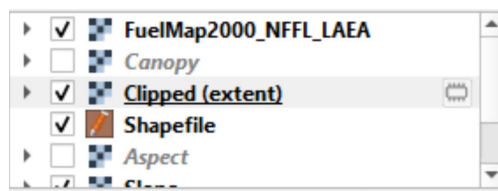


Figure 21. A temporary Clipped extent layer has been created.

- **Standardize and generate .tif output file for raster layer:** Standardize properties for every layer (elevation, slope, aspect, canopy and fuel map) and export them as clipped .tif files.
 - Right click each layer in the Layers window, and then click Export -> Save As (see Figure 22).

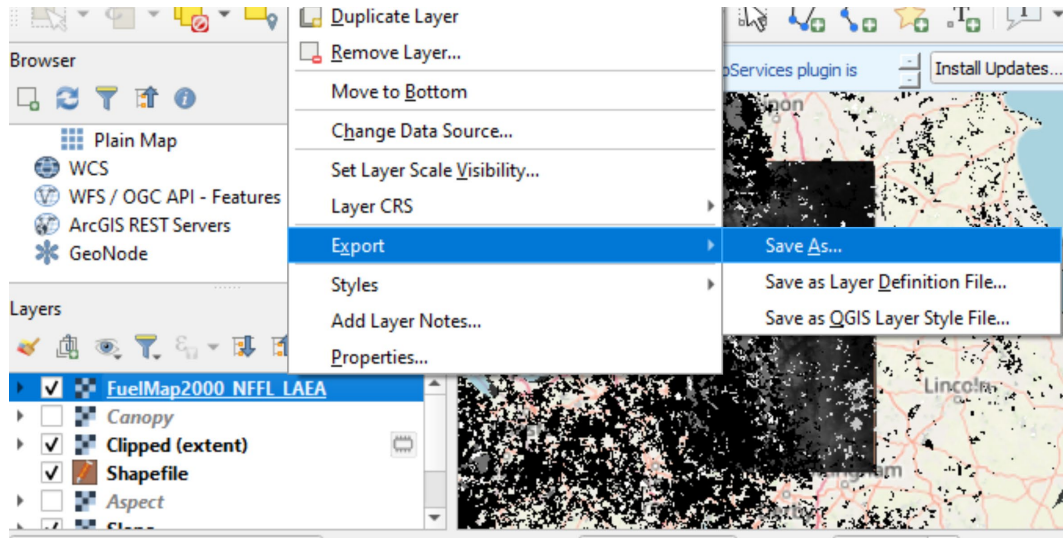


Figure 22. Right click each layer and select 'Save As'.

- Create a clipped version of elevation, slope, aspect, canopy cover and fuel map. Set the projection to EPSG:3857, change resolution (any resolution is fine, but it is important that all layers have the same resolution) and clip it to the Clipped extent layer (see Figure 23). A standardized clipped is created (see Figure 24).

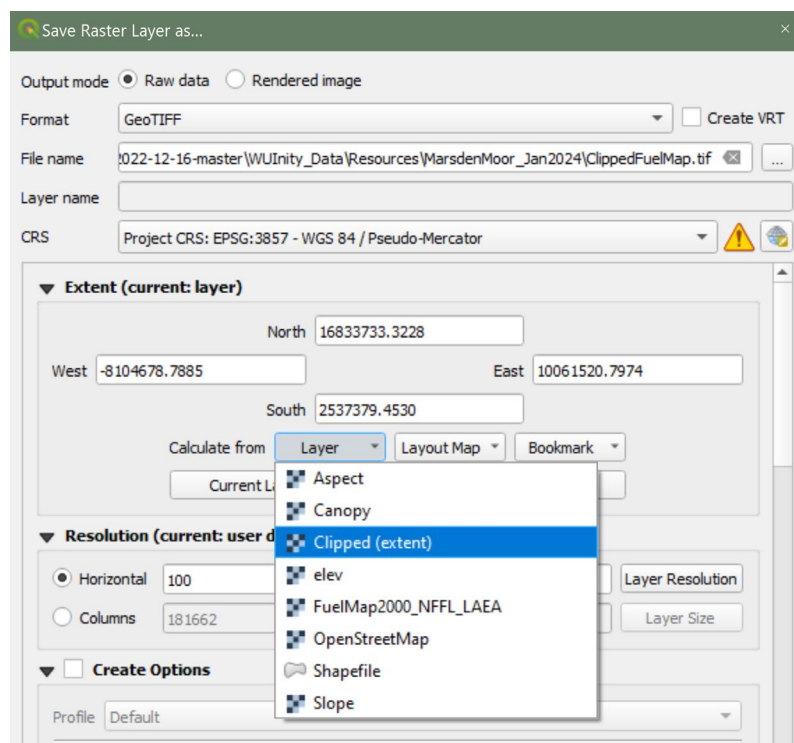


Figure 23. Save the layers as .tif files with the extent of the clipped layer and in the same resolution.

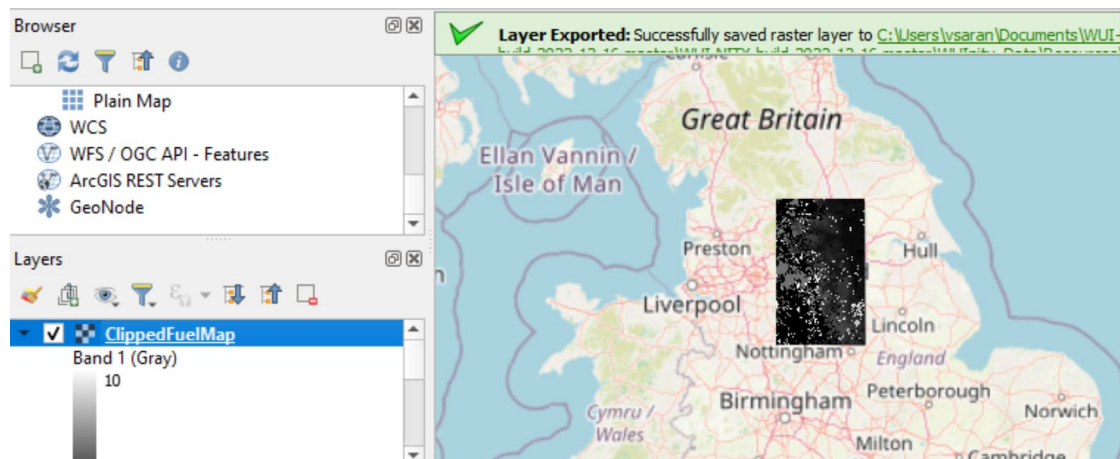


Figure 24. The first standardised 'clipped' layer has been created.

- Repeat this process until you have five standardised and 'clipped' raster layers (see Figure 25).



Figure 25. Standardized elevation, aspect, slope, canopy cover and fuel map layers in GeoTIFF format

Finally, the standardized raster layers need to be combined using either one of two specialist programs to generate the landscape file: FlamMap or ArcFuels. FlamMap is a free windows-based fire analysis desktop application. It can be downloaded from:

<https://www.firelab.org/project/flammap>

ArcFuels is distributed as an ESRI ArcGIS Add-In file, which adds a toolbar to ArcGIS. Users can download ArcFuels from:

<https://www.firelab.org/sites/default/files/images/downloads/ArcFuels-help/Content/01Download&Setup/cDownload.htm>

Assuming the user has either FlamMap or ArcFuels/ArcGIS installed in their computer, along with the .tif files generated in QGIS from previous steps.

- If using FlamMap:
 - Click on 'Landscape -> Create Landscape file...' (see Figure 26),
 - Specify the five raster layers prepared in QGIS under 'Required Themes' (see Figure 27),
 - Finally, click the 'Save As...' button to save an .lcp in the WUI-NITY project folder.

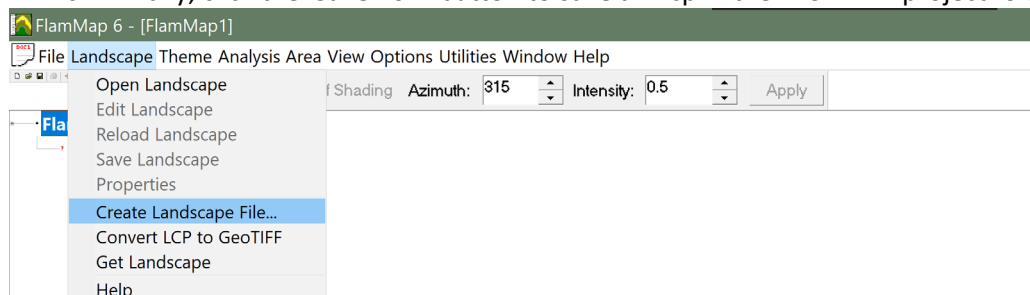


Figure 26. Select 'Create Landscape File...' under the 'Landscape' menu in FlamMap 6.

Landscape File Generation

Source Landscape File: Clear Fields Save As... Help

Projection File:

General

Latitude: 45 Grid Distance Units: Meters
 Rows: 1872 Lower Left X: -222669.9037 CellSize: 99.99102335
 Columns: 1114 Lower Left Y: 6982982.5979

Required Themes

	Source	Use LCP	Source Units	Constants
Elevation:	C:\Users\vsar...\ClippedElevation.tif	<input type="checkbox"/>	Meters	Constant: 0
Slope:	C:\Users\vsar...\ClippedSlope.tif	<input type="checkbox"/>	Degrees	Constant: 0
Aspect:	C:\Users\vsar...\ClippedAspect.tif	<input type="checkbox"/>	Degrees	Constant: 0
Fuel Model:	C:\Users\vsar...\ClippedFuelMap.tif	<input type="checkbox"/>	Class	Constant: 1
Canopy Cover:	C:\Users\vsar...\ClippedCanopy.tif	<input type="checkbox"/>	Percent	Constant: 50

Crown Fuels

Include Crown Fuels: ☐

Stand Height:	NA	<input type="checkbox"/>	Meters	Constant: 15
Canopy Base Height:	NA	<input type="checkbox"/>	Meters	Constant: 1
Canopy Bulk Density:	NA	<input type="checkbox"/>	kg/m3	Constant: 0.2

Description:

Figure 27. Select each of the clipped .tif files created in QGIS, and click 'Save As'.

- If using ArcFuels (as an ESRI ArcGIS Add-In):
 - In ArcMap, click on the ArcFuels10 toolbar: Build LCP -> Build LCP using Raster Data.
 - Add the needed raster images under Raster Data.
 - Click on: Output.
 - Use coordinates or another layer to define the LCP image boundaries.
 - Click on: Build LCP.
 - Save the .lcp file generated in the WUI-NITY project folder.

The fire simulation module in WUI-NITY requires specific inputs, including a landscape file (see Section 0). This section outlines how to obtain or generate such a file based on the location. For a location in the United States, the file can be downloaded directly. For a location in Europe, users can gather relevant data as indicated, and follow the instructions provided in this section to compile the necessary data into a landscape file. For a location that falls outside the United States and Europe, users need to seek equivalent data sources and apply the same principles used for the European locations to prepare a landscape file specific to their area of interest.

Section 0 user actions:

- If users intend to simulate fire growth in WUI-NITY, obtain or generate a landscape file for the area of interest, following the instructions in this section.

Section 0 model limitations:

- For a location outside the United States and Europe, how to get the necessary information for creating a landscape file for fire simulation has not been fully

Fuel models file (.fuel)

The fuel models file (.fuel) serves as a repository for typical fuel types and their combustion properties specific to a geographic location. The fuel models file has 17 entries in each line which define one type of fuel, following the order of combustion properties provided in the first line (header). Users can provide their own data if they have information that can describe the type of fuels present in their area of interest. If detailed data is unavailable, users can use the 13 Anderson Fire Behavior Fuel Models (FBFM13)³⁵ (Anderson 1981)³⁶ included with WUINITY (see Table 5). The FBFM13 model represents distributions of fuel loading across surface fuel components (live and dead), size classes and fuel types. The fuel models include the most common fire-carrying fuel type (grass, brush, timber litter or slash), loading and surface area-to-volume ratio by size class and component, fuel bed depth, and moisture of extinction.

Table 5. The FBFM13 fuel models file.

```
fuelModelNumber, code, name, fuelBedDepth, moistureOfExtinctionDead, heatOfCombustionDead,
heatOfCombustionLive, fuelLoadOneHour, fuelLoadTenHour, fuelLoadHundredHour,
fuelLoadliveHerbaceous, fuelLoadliveWoody, savrOneHour, savrLiveHerbaceous, savrLiveWoody, isDynamic,
isReserved
1, "FM1", "Short grass [1]", 1.0, 0.12, 8000, 8000, 0.034, 0, 0, 0, 3500, 1500, 1500, false, true
2, "FM2", "Timber grass and understory [2]", 1.0, 0.15, 8000, 8000, 0.092, 0.046, 0.023, 0, 3000, 1500,
1500, false, true
3, "FM3", "Tall grass [3]", 2.5, 0.25, 8000, 8000, 0.138, 0, 0, 0, 1500, 1500, 1500, false, true
4, "FM4", "Chaparral [4]", 6.0, 0.2, 8000, 8000, 0.230, 0.184, 0.092, 0, 0.230, 2000, 1500, 1500, false, true
5, "FM5", "Brush [5]", 2.0, 0.20, 8000, 8000, 0.046, 0.023, 0, 0, 0.092, 2000, 1500, 1500, false, true
6, "FM6", "Dormant brush, hardwood slash [6]", 2.5, 0.25, 8000, 8000, 0.069, 0.115, 0.092, 0, 0, 1750, 1500,
1500, false, true
7, "FM7", "Southern rough [7]", 2.5, 0.40, 8000, 8000, 0.052, 0.086, 0.069, 0, 0.017, 1750, 1500, 1500, false,
true
8, "FM8", "Short needle litter [8]", 0.2, 0.3, 8000, 8000, 0.069, 0.046, 0.115, 0, 0, 2000, 1500, 1500, false, true
9, "FM9", "Long needle or hardwood litter [9]", 0.2, 0.25, 8000, 8000, 0.134, 0.019, 0.007, 0, 0, 2500, 1500,
1500, false, true
10, "FM10", "Timber litter & understory [10]", 1.0, 0.25, 8000, 8000, 0.138, 0.092, 0.230, 0, 0.092, 2000, 1500,
1500, false, true
11, "FM11", "Light logging slash [11]", 1.0, 0.15, 8000, 8000, 0.069, 0.207, 0.253, 0, 0, 1500, 1500, 1500, false,
true
12, "FM12", "Medium logging slash [12]", 2.3, 0.20, 8000, 8000, 0.184, 0.644, 0.759, 0, 0, 1500, 1500, 1500,
false, true
13, "FM13", "Heavy logging slash [13]", 3.0, 0.25, 8000, 8000, 0.322, 1.058, 1.288, 0, 0, 1500, 1500, 1500,
false, true
```

Initial fuel moisture file (.fmc)

Fuel Moisture Content (FMC)³⁷ is a measure that quantifies the water content within a fuel, such as vegetation, available to a fire. It is the single most important factor determining how much of the fuel is available to burn, and how much fuel might be consumed during a wildfire. FMC affects ignition, combustion, the amount of available fuel, fire severity and spread, and smoke generation and composition. Therefore, it is one of the primary variables used in many

³⁵ <https://www.landfire.gov/fbfm13.php>

³⁶ Anderson, H. E. (1981). Aids to determining fuel models for estimating fire behavior (Vol. 122). US Department of Agriculture,

³⁷ <https://nwfirescience.org/sites/default/files/publications/FuelMoistureContent.pdf>

wildfire behavior prediction models and fire danger indices, including the built-in fire simulation module in WUI-NITY.

In WUI-NITY, the initial fuel moisture file (.fmc)³⁸ defines the level of moisture for each fuel type listed in the fuel models file (defined in Section 0), separating into dead fuel moisture content and live fuel moisture content. Dead fuels consist of a variety of categories, including down and dead woody fuels (such as fallen branches, logs, and twigs) with various diameter, dead grasses and forbs, and surface litter such as fallen leaves and needles. Dead fuel moistures are classed by time lag, which is a measure of the rate at which a given dead fuel gains or loses moisture. The time lag categories defined in .fmc file include:

- **1Hour**, 1-hour time lag fuels: These are fuels with a diameter of less than 1/4 inch.
- **10Hour**, 10-hour time lag fuels: These fuels have a diameter ranging from 1/4 to 1 inch.
- **100Hour**, 100-hour time lag fuels: These fuels exhibit diameters between 1 to 3 inches.

Live fuel moistures are separated into **LiveH** (live herbaceous) and **LiveW** (live woody) fuel moisture, and are expressed as a percentage of the dry weight of that specific fuel. The formula for calculating live FMC is:

$$\text{Weight of Water} / \text{Oven-dry Weight of Fuel} \times 100\%$$

For reference, an example of the .fmc file is given in Table 6. Note that for each fuel type defined in the .fuel file, there must be a corresponding line of initial fuel moistures specified in this file.

Table 6. An example of a fuel moisture file with the first three fuels defined in .fuel file.

```
FuelMod, 1Hour, 10Hour, 100Hour, LiveH, LiveW
1, 6.0, 7.0, 8.0, 60.0, 90.0
2, 6.0, 7.0, 8.0, 60.0, 90.0
3, 6.0, 7.0, 8.0, 60.0, 90.0
4, ... (other fuel type and their initial fuel moistures)
```

Weather file (.wtr)

The Weather file (.wtr)³⁹ serves as an input for weather conditions in the simulation model for fire and smoke spread in WUI-NITY. The file contains daily observations on temperature and humidity as well as precipitation that depict a temporal weather stream. The fire model fits the temperature and humidity data to a sine curve form for interpolation of these parameters throughout the day cycle. Using the weather data and the initial fuel moistures, the model provides dynamic inputs of weather and fuel moistures over the simulation time. Note that the weather stream represents a great oversimplification of actual variation in weather. However, this format is an attempt to reduce the user provision of weather information required for a simulation to a practical level.

The Weather file has ten entries in each line which define the weather conditions on a given day, following the order given in the first line (for reference, an example of the weather file is given in Table 7). The ten inputs of a temporal weather stream are explained as follows:

³⁸ See also: https://www.fire.org/downloads/farsite/WebHelp/referenceguide/pop_ups/pu_initial_fuel_moistures.htm

³⁹ See also: https://www.fire.org/downloads/farsite/WebHelp/referenceguide/pop_ups/pu_weather_file.htm

- **Month** and **Day** define the date of the weather stream.
- **Precip** (i.e., **precipitation**) is the daily rain amount specified in hundredths of millimeters (integer).
- **Hour1/Hour2** correspond to the hours at which the **minimum/maximum** temperatures were recorded (0-24).
- **Temp1/Temp2** correspond to the **minimum/maximum** temperatures in Celsius degrees (integer).
- **Humid1/Humid2** correspond to the **maximum/minimum** humidities in percent, 0 to 99 (integer).
- **Elevation**, aka altitude, is the distance in meters above sea level (integer), which is used to calculate the adiabatic adjustment to the local temperature and humidity. NOTE: These units do not have to be the same as the landscape elevation theme.

Table 7. An example of a .wtr file which defines two weather streams on two successive dates.

```
Month, Day, Precip, Hour1, Hour2, Temp1, Temp2, Humid1, Humid2, Elevation
7, 15, 0, 4, 16, 13, 33, 10, 10, 1803
7, 16, 25, 4, 16, 10, 30, 18, 15, 1803
```

Wind file (.wnd)

Wind conditions play a crucial role in a wildfire and, therefore, must be considered in fire and smoke spread simulations too. In reality, winds usually vary in space and time. However, the fire model assumes winds to be constant in space for a given wind stream but variable in time, i.e., topographic effects on winds are not considered. Again, this simplification is an attempt to limit to a practical level to provide the amount of wind information required for a simulation.

In WUI-NITY, wind information is defined as wind streams in a wind file (.wnd)⁴⁰. The wind file can be in one of two acceptable formats which differ in temporal resolution. The first format consists of four entries in each line, which define the wind speed (km/h) and wind direction (in degrees) for a predominant wind condition starting from a given time measured in seconds from the start of the simulation. The four entries follow the order of entries shown in the first line of the file (see Seconds is a given time measured in seconds from the start of the simulation, which specifies the moment when the wind condition starts (integer).

- **Month, Day, Hour** define the starting time of the wind condition in calendar units. Note **Hour** is specified as 0-2400, to the nearest minute (integer).
- **Speed** is the 10-m wind speed in kilometers per hour (integer).
- **Direction** is specified in degrees, clockwise from south (0-360) (integer).
- **CloudCover** is specified as a percentage, 0 to 100 (integer).

Table 8).

In the second format, the wind condition is defined with time measured in calendar units, so that each line has six entries in the order of Month, Day, Hour, Speed (km/h), Direction (in degrees), and CloudCover (see Table 9). Note that 0° refers to the South and 180° refers to the North for wind direction. CloudCover (i.e., cloud cover) refers to the fraction of the sky obscured by clouds on average when observed from a particular location. The value of CloudCover is ranging from 0 (i.e., indicating clear skies with no visible clouds, allowing 100%

⁴⁰ See also: https://www.fire.org/downloads/farsite/WebHelp/referenceguide/pop_ups/pu_wind_file.htm

of solar radiation to pass through) to 100 (i.e., complete cloud cover, preventing any solar radiation from passing through). The wind condition defined in each line lasts until the simulation clock reaches the time defined in the next line for a change in wind condition. Wind conditions do not have to be on a regular interval. Users can, for example, enter wind conditions every 10 minutes during the afternoon, and only every 2 hours at night in the same .wnd file.

For reference, examples of both formats are given in Seconds is a given time measured in seconds from the start of the simulation, which specifies the moment when the wind condition starts (integer).

- **Month, Day, Hour** define the starting time of the wind condition in calendar units. Note **Hour** is specified as 0-2400, to the nearest minute (integer).
- **Speed** is the 10-m wind speed in kilometers per hour (integer).
- **Direction** is specified in degrees, clockwise from south (0-360) (integer).
- **CloudCover** is specified as a percentage, 0 to 100 (integer).

Table 8 and Table 9 respectively. The inputs used to define a temporal wind condition are explained as follows:

- **Seconds** is a given time measured in seconds from the start of the simulation, which specifies the moment when the wind condition starts (integer).
- **Month, Day, Hour** define the starting time of the wind condition in calendar units. Note **Hour** is specified as 0-2400, to the nearest minute (integer).
- **Speed** is the 10-m wind speed in kilometers per hour (integer).
- **Direction** is specified in degrees, clockwise from south (0-360) (integer).
- **CloudCover** is specified as a percentage, 0 to 100 (integer).

Table 8. An example of a .wnd file with two successive wind conditions in time (1st format).

```
Seconds, Speed, Direction, CloudCover
0, 10, 0, 0
3600, 2, 180, 0
-----
```

Table 9. An example of a .wnd file with three successive wind conditions in time (2nd format).

```
Month, Day, Hour, Speed, Direction, CloudCover
8, 10, 0, 1, 54, 0
8, 10, 100, 2, 67, 0
8, 10, 200, 2, 102, 0
```

Ignition points file (.ign)

The ignition points file (.ign) contains information about the location and timing of ignition during a wildfire. It has three entries in each line which define one ignition point, following the order given in the first line, i.e., latitude, longitude, IgnitionTime (measured in seconds from the start of the simulation). For reference, an example of the ignition points file is given in **Error! Not a valid bookmark self-reference..**

Table 10. An example of a .ign file with two ignition points starting at two different times.

```
Latitude, Longitude, IgnitionTime
39.479633, -105.037355, 0.0
39.450355, -105.040773, 3600.0
```

Graphical fire input file (.gfi)

Apart from the inputs in text format, WUI-NITY allows users to interactively add four types of inputs on the map (i.e., via the WUI-NITY GUI). These are the indices of the **WUI area**, **random ignition area**, **initial ignition** and **trigger buffer**, within the fire mesh (defined according to the LCP file). These inputs are stored in binary format in a graphical fire input file (.gfi). For a new project, WUI-NITY will initialize the indices with null value. The .gfi file can only be viewed and edited within WUI-NITY.

The indices of the **WUI area** and **trigger buffer** are implemented as part of a toolkit called PERIL (**p**opulation **e**vacuation **t**rigger **a**lgorithm) for generating spatial evacuation triggers in the WUI area through the coupling evacuation and wildfire models. The evacuation triggers define a point or perimeter in advance of a community. When a wildfire reaches the designated locations, it signals the need for a safe evacuation order to be issued. This concept has been previously implemented in tools used for informing prompt evacuation from wildfires and other natural disasters such as hurricanes. For more information about PERIL, please refer to [8]. The full integration of PERIL with WUI-NITY will be completed in the future release. Therefore, these two graphical inputs have no effect on simulations at this stage.

The graphical inputs of **random ignition area** and **initial ignition** define two ways of simulating fire ignition, in addition to using coordinates in an ignition points file (.ign) described in Section 0. The graphical input of random ignition area defines a region within which a certain number of ignition points are randomly assigned as the starting point of the fires⁴¹. The graphical input of initial ignition directly labels the ignition points on map. Users have the option to choose any one of the ways in simulations.

Section 0 user actions:

- Follow the instructions provided in this section to prepare the required input files for fire and smoke simulation (optional).

⁴¹ This function is currently under development.

Traffic network and routing

Road network and route collection

WUI-NITY uses OpenStreetMap (OSM) data extracts to model evacuation via the road network. The OSM data can be extracted for a specific area of interest and can be sourced from: <https://download.geofabrik.de/index.html>.

The website hosts OSM data at various scales, ranging from continents and countries down to administrative regions (such as counties or provinces). To minimize the file size when downloading OSM data, users should follow the **Sub Region** links on the webpage, starting from the continent level and navigating to the smallest sub region that covers the area of interest. Finally, use the link to the .osm.pbf file⁴² on the last page to download the appropriate OSM data extract file.

The downloaded OSM data file undergoes three processing steps in WUI-NITY to build the traffic simulation model.

- Firstly, the OSM data file is filtered based on the range of the modelled region defined in Section 0.
- Secondly, a routing network database (.routerdb) for traffic pathfinding within the area of interest is calculated from the filtered OSM data file.
- And finally, the O/D (origin-destination) matrices are calculated from the router database and stored in a route collection file (.rc). This represents the set of routes that might be traversed during an evacuation and are extracted directly from the road network.

How the routes are used is determined by the transportation options selected by the user, which are described in Section 0 and, similarly, some of the evacuation settings, which are described in Section 0. Note that these three steps do not require additional user intervention or inputs.

How the routes are used is determined by the transportation options selected by the user, which are described in Section 0 and, similarly, some of the evacuation settings, which are described in Section 0. Note that these three steps do not require additional user intervention or inputs.

Transportation options

The road network and route allocation define the available routes that can be used for evacuation. The transportation settings described in this section affect the evacuation traffic in simulations. At the current stage of development, all these are global variables which affect the entire simulated region. Detailed descriptions of these options are as follows.

1. Route choice:

Route choice in traffic refers to the evacuee's decision on which route to take to reach a destination. The decision making can be based on if the route is faster or shorter (i.e., calculated as being closer to the individual's starting position) but can also be affected by other conditions (such as route familiarity or route blockages due to fire or smoke). There are four route choices that are modelled in WUI-NITY: *fastest*, *closest*, *random* and *EvacGroup*. These choices are explained as follows:

⁴² PBF format is OpenStreetMap (OSM) native Protocol Binary Format (PBF), a vector format that provides total native access to every detail of OSM data using OSM's recommended format.

- **Fastest:** Evacuees will choose a route towards a *non-blocked* evacuation goal, which requires the shortest driving time. It is important to note that this decision does not consider potential delays due to congestions. If many people choose a limited set of routes while other viable alternatives remain underused, this option may not yield the shortest overall evacuation time.
- **Closest:** Evacuees will choose a route towards a non-blocked evacuation goal, which has the shortest driving distance.
- **Random:** Evacuees will first choose a random evacuation goal from the goals available and then the first route identified that connects this goal. If the chosen goal is blocked, evacuees will switch to the fastest route towards a non-blocked evacuation goal, i.e., the *fastest* option.
- **EvacGroup:** This choice simulates user defined groups with an assigned probability to go towards a given destination – i.e. the user is able to prescribe the routes used by identified groups and associated destinations (see Sections 0 and 0). In this case, evacuees will choose an evacuation goal from their group settings and the first route identified connecting this goal. Again, if such a goal is blocked, evacuees will switch to the *fastest* option towards a non-blocked evacuation goal.

If no route can be chosen, an error message will be displayed.

2. Vehicle speed at maximum road capacity:

This is a user-defined vehicle speed at maximum road capacity to avoid a complete stall of vehicle movement.

3. Minimum and maximum background traffic density (vehicles/km/lane):

The background traffic represents vehicles present on a road which are not actively evacuating. This type of traffic affects the vehicle density modifier which reduces the free flow speed for all vehicles since the road becomes more occupied and slower driving behavior is adapted to the new traffic circumstances. These are global variables that are assumed across the whole modelled area.

4. Whether speed is affected by smoke:

Here, users can simulate whether the smoke impacts on driving speeds during the evacuation. At this stage of development, this feature allows for the reduction of driving speeds based on a global visibility variable – namely, optical density (expressed in units of 1/m) – which users can set. This optical density can be a fixed value or vary over time. Figure 28 illustrates the relevant settings within a .wui file. The first field serves as a switch to enable or disable the smoke impact simulation on speeds. The second field defines the time/optical density relationship file (.odr), specifying how optical density varies as a function of time (see Figure 29). If this field is left blank, WUI-NITY will default to the optical density value specified in the third field in simulation.

```
"visibilityAffectsSpeed": true,
"opticalDensityFile": "opticalDensity.odr",
"opticalDensity": 0.05,
```

Figure 28. An example of smoke/speed settings within a .wui file.

```
time, optical density [1/m]
0.0, 0.0
1200.0, 0.05
```

Figure 29. An example of the opticalDensity.odr file.

5. Road types:

This is a road type file which defines the properties associated with each type of road found in the OSM data. The properties include speed limit (km/h), number of lanes, max capacity (i.e., the number of vehicles per km per lane), and whether the traffic is allowed to be reversed. A default roads type file (defaults.roads), which define 26 types of roads (e.g., see the definition of ‘motorway’ in the file in Figure 30), is provided with WUI-NITY. WUI-NITY tries to match the road section defined in OSM data with these predefined road types to determine the speed limit, number of lanes, max capacity etc. Users can edit this file to meet the road conditions within the modelled region if the actual use of the roads differs from the default properties.

```
"name": "motorway",  
"speedLimit": 120.0,  
"lanes": 2,  
"maxCapacity": 75.0,  
"canBeReversed": true
```

Figure 30. The default roads type file defines the properties of road type motorway.

The inputs for traffic simulation are summarized in Table 11.

Table 11. Inputs to the Traffic Simulation.

Input [Unit]	Format	Default value*	Explanation/Source
OSM data extract	.osm.pbf file	-	The regional OSM data file for a specific sub region that covers the modelled area. The OSM data file will be filtered and then processed to generate a router database and O/D matrices.
Route choice	Options	EvacGroup	Evacuee's decision on which route to take to reach a destination (i.e., evacuation goal).
Vehicle speed at maximum road capacity [km/h]	Decimal	1	User definable vehicle speed at maximum road capacity.
Minimum and maximum background traffic density [vehicles/km/lane]	Decimal	0; 0	User definable background traffic represents vehicles present on a road which are not actively evacuating.
Whether speed is affected by smoke	Boolean	No	Select whether smoke impacts driving speeds during the evacuation.
Optical density as the global visibility variable	Decimal	0.05	The smoke density measured as optical density, which impacts driving speeds.
Road types	.roads file	default.roads	A default roads type file is included in WUI-NITY, which defines 26 types of roads and their properties.

* These default values are used in model development but may not represent recommended values. Users should adjust these values according to their modelling requirements and assumptions.

Section 0 user actions:

- Given the identified area for evacuation analysis, find and download the appropriate sub-regional OpenStreetMap data file.
- Supply the downloaded OSM data file to WUI-NITY to generate a series of files that are required for traffic modelling within the modelled region.
- Select the appropriate transportation options and review the definition of road types.

Evacuation settings

WUI-NITY provides the capability to divide the modelled region into multiple zones, known as evacuation groups, and assign distinct evacuation responses and evacuation goals to people located in different zones. These zones might represent designated areas as part of a procedure (e.g., evacuation zones or emergency management zones) or reflect known differences in the underlying community. This function can therefore be used to define and test different evacuation plans in which the order of evacuation of these zones can be manipulated to develop an efficient plan to evacuate all people or an adaptive plan in response to different threats (e.g., fires approaching from different directions towards the area). **The definition of zones, evacuation goals and responses form the core elements for developing and testing evacuation plans.**

WUI-NITY uses three files to characterize the evacuation response of specific resident evacuation groups: evacuation group files (.eg), response curves files (.rsp) and evacuation goal files (.ed). The group definition is shown below – outlining the response profile and the movement goals for different groups.

Evacuation group file (.eg)

The evacuation group file defines a collection of individuals or households within a specific sub-division of the region. Each group is associated with a series of response curves and evacuation destinations (see Table 12). For each response curve and destination, a probability is assigned, indicating the likelihood that the agents in the group will adopt the depicted response curves and evacuation destinations. The evacuation group file is an ASCII text file, which can be edited using a standard text editor or within WUI-NITY GUI. Additionally, the spatial arrangement of evacuation groups is interactively defined on the map through the GUI, as introduced in Section 0.

Table 12. The entries of the evacuation group file and explanation.

Entry name	Format	Explanation
Name	String	The identification name given to an evacuation group.
Response curves	Array of string	A list of response curves defined as an array of response curve files storing the details of these curves.
Response curve probabilities	Array of decimals	The accumulative probabilities associated with the response curves.
Destinations	Array of string	A list of evacuation goals defined as an array of goal files storing the details of these goals.
Destination probabilities	Array of decimals	The accumulative probabilities associated with the evacuation goals.
Color	RGB values	The color selected to draw the distribution of the evacuation group as a collection of population cells on map.

Figure 31 shows an example group labelled as “Group_1”. All individuals within this group adhere to a response curve denoted as “Observed_average”, and the probabilities of them choosing “Goal_E”, “Goal_R” and “Goal_F” in evacuation are 10%, 20% and 70%, respectively.

```

Name: "Group_1"
Response curves: "Observed_average"
Response curve probabilities: 1.0
Destinations: "Goal_E", "Goal_R", "Goal_F"
Destination probabilities: 0.1, 0.3, 1.0
Color: 1.0, 1.0, 0.0

```

Figure 31. An example of an evacuation group file.

Response Curve file (.rsp)

The response curve represents the time starting when the individual/household becomes aware of the fire event until they start purposive evacuation movement (or travel). Individuals can become aware of the fire in different ways, including seeing or smelling smoke from the wildfire, witnessing neighborhood activity, and/or receiving messages, including an evacuation order, from official or unofficial sources via various communication channels (e.g., mobile phones). People can start evacuating before evacuation warnings/orders are issued, delay their evacuation, or not evacuate at all.

In WUI-NITY, the response curve file defines a cumulative probability from 0 to 1.0 as a function of time. The file has two entries which are explained in Table 13. The response curve file is an ASCII text file, which can be edited in a standard text editor (see Figure 32 for an example).

Table 13. The entries of the response curve file and explanation.

Entry name	Format	Explanation
Time	Decimal	The time measured in seconds from the beginning of the simulation.
Cumulative probability	Decimal	A cumulative response probability from 0 to 1.0.

```

Time, Cumulative probability
0, 0
900, 0.79
1800, 0.91
3600, 1.0

```

Figure 32. An example of a response curve file.

Evacuation goal file (.ed)

The evacuation goal file defines the target point for individuals to evacuate and its associated attributes. Each goal file specifies a particular evacuation goal. Currently, WUI-NITY models two types of goals defined as follows.

- **Refuge** represents planned shelters (a place of safety for evacuees) situated far from the wildfire threat. Typically, refuges have limited car and people capacity. If a refuge reaches its maximum capacity, it will appear blocked in WUI-NITY. Individuals who are still evacuating toward a full refuge will need to be redirected to other available evacuation goals.
- **Exit** refers to a location on a freeway or motorway that lies relatively distant from the threatened area. Unlike refuges, which serve as planned shelters, exits have a different purpose - they are used to model individuals who are heading toward their own chosen

destinations (apart from a refuge), which can be specific addresses, homes, or other safe locations. Evacuees drive along the related route, guided by their personal preferences. Since these individual destinations cannot be explicitly represented in the simulation, we designate a location on the route as an “exit”. This exit point signifies the path leading to potential destinations beyond the immediate threatened area. Unlike refuges, exits do not have car or people capacity limits. Evacuees can continue their journey beyond the exit points without restriction. However, the journeys beyond the exit points are not simulated nor represented in WUI-NITY.

The evacuation goal file has nine entries which are explained in Table 14.

Table 14. The entries of evacuation goal file and explanation.

Entry name	Format	Explanation
Name	String	The identification name given to an evacuation goal.
Latitude	Decimal degree	The latitude of the evacuation goal.
Longitude	Decimal degree	The longitude of the evacuation goal.
Goal type	Options	The type of the target point for individuals to evacuate.
Max flow	Decimal	The max flow through the evacuation goal.
Car capacity	Number	The capacity of the goal in accommodating cars if it is a refuge area.
People capacity	Number	The capacity of the goal in accommodating people if it is a refuge area.
Initially blocked	Boolean	Whether the goal is available for use in the evacuation.
Color	RGB values	The color selected to draw the evacuation destination on map.

Other evacuation settings

In addition to the evacuation group/zone settings, there are several other user-definable inputs that affect the evacuation simulation settings. These include the distribution of the population and vehicles across the space, and the speed and timing of evacuee movement. These are explained below and their default values, if any, are given in Table 16 in Section 0 which illustrates the corresponding settings in the UI.

1. Cell size:

This defines the resolution of the population distribution within the region for generating the households for evacuation.

2. Allow more than one car per house:

Each household is assumed to evacuate using one car by default, but users can configure a probability distribution of vehicles leaving the household if there are more than one person per household. This will affect the number of vehicles on the road.

3. Max vehicles per household and the associated probability:

If more than one car per house is allowed, this user input sets the maximum number of vehicles a household can have access to and use in an evacuation, since it is possible for household members to evacuate (or engage in travel activities) separately and/or evacuate at the same time in multiple vehicles. The assumptions of the number of vehicles available at each household could be tested with a probability to take additional vehicles.

4. Min.-Max. persons per household:

This user input specifies the range of the number of persons assigned to a household. A small number of persons per household is likely to increase the number of households generated, hence more vehicles in evacuation.

5. Min.-Max. walking speed:

This user input sets the range of pedestrian walking speed when they walk from their starting location to a traffic node to evacuate the area. This speed setting will affect how fast the vehicle may enter the road network.

6. Walking speed and distance modifier:

This is defined as a multiplier of pedestrian walking speed or distance for verification tests. It is a test parameter in the pedestrian model mostly used by developers in verification tests. It may also be used in sensitivity tests of pedestrian walking speed and distance.

7. Evacuation order time (time after fire):

The period of time between the fire ignition time and the moment when an evacuation order is given. This user input allows the simulated fire to grow a certain amount of time before the evacuation commences.

Section 0 user actions:

- Conduct evacuation management and planning analysis for the modelling area, considering the population distribution, the layout and capacity of the road network, the potential response delays, and the available emergency management resources etc.
- Based on the results of the analysis, define evacuation goal(s), response curve(s) and evacuation group(s) and other evacuation settings.
- Format the collected information and prepare it as input to WUI-NITY following the format specified in this section.

Summary

summarizes the input requirements for WUI-NITY simulation, categorized as follows:

- **Mandatory inputs:** These are essential to simulations and must be provided.
- **Optional inputs:** These are not strictly required but are subject to modelling requirements.

These inputs can be prepared or sourced by the following means:

- **User-definable inputs:** Users have the flexibility to define inputs according to the required format, and examples are provided. These inputs allow customization to suit specific modelling conditions.
- **Default sources:** These inputs can be directly loaded from system default. However, users should check these inputs to ensure that these default inputs align with their specific requirements.
- **Third-party resources:** These inputs can be sourced from specified third-party resources. It is important to note that additional data processing is always necessary when using user-downloaded data from these external sources.
- **Generated by WUI-NITY:** These inputs are dynamically generated by WUI-NITY, leveraging data obtained from third-party resources. We will delve deeper into these inputs in subsequent sections.

Table 15 summarizes the input requirements for WUI-NITY simulation, categorized as follows:

- **Mandatory inputs:** These are essential to simulations and must be provided.
- **Optional inputs:** These are not strictly required but are subject to modelling requirements.

These inputs can be prepared or sourced by the following means:

- **User-definable inputs:** Users have the flexibility to define inputs according to the required format, and examples are provided. These inputs allow customization to suit specific modelling conditions.
- **Default sources:** These inputs can be directly loaded from system default. However, users should check these inputs to ensure that these default inputs align with their specific requirements.
- **Third-party resources:** These inputs can be sourced from specified third-party resources. It is important to note that additional data processing is always necessary when using user-downloaded data from these external sources.
- **Generated by WUI-NITY:** These inputs are dynamically generated by WUI-NITY, leveraging data obtained from third-party resources. We will delve deeper into these inputs in subsequent sections.

Table 15. Summary of WUI-NITY inputs*.

Section	Input	Type	Has Default?	Source of input
0 Map preparation	Map Lower Left latitude, longitude	Mandatory	No	User definable
	Map size x, y	Mandatory	No	User definable
	Mapbox API access token	Optional	Yes (built-in)	3 rd party source of data.
0 Population Definition	The population density data sets from the GPW collection	Mandatory	No	User downloaded from 3 rd party source of data.
	Local GPW file (.gpw)	Mandatory	No	Generated by WUI-NITY
	Local population file (.pop)	Mandatory	No	Generated by WUI-NITY
0 Fire and smoke simulation**	Landscape file (.lcp)	Optional	No	User downloaded or created using data from 3 rd party source of data.
	Fuel models file (.fuel)	Optional	Yes	default.fuel

	Initial fuel moisture file (.fmc)	Optional	No	User definable
	Weather file (.wtr)	Optional	No	User definable
	Wind file (.wnd)	Optional	No	User definable
	Ignition points file (.ign)	Optional	No	User definable
	Graphical fire input file (.gfi)	Optional	Yes (an empty file)	User definable
	Farsite data	Optional	No	User provided results generated from 3rd party simulation software.
0 Traffic network and routing	OSM data extract	Mandatory	No	User downloaded from 3 rd party source of data.
	Router database (.routerdb)	Mandatory	No	Generated by WUI-NITY
	Route collection file (.rc)	Mandatory	No	Generated by WUI-NITY
	Road types file (.roads)	Mandatory	Yes	default.roads
0 Evacuation settings	Evacuation group file (.eg)	Mandatory	No	User definable
	Response curve file (.rsp)	Mandatory	No	User definable
	Evacuation goal file (.ed)	Mandatory	No	User definable

* User definable settings are excluded in this table.

** Either the seven input files or Farsite data within this section become mandatory if fire and smoke simulation is required.

A3. Guided workflow interface

WUI-NITY is built on the Unity3D game engine and allows for the representation and visualization of wildfire spread, pedestrian response, and traffic movement during wildfire evacuation scenarios – a platform for the simulation of wildland-urban interface fire evacuation. At the first stage of developing the platform, there are three main goals: identifying the required data sets, selecting the component models based on performance criteria, and implementing fire, pedestrian and traffic modelling layers into a single modelling environment. To enhance the useability of WUI-NITY and develop it into a more practical engineering tool, a generalized workflow has been developed to guide users to formulate the inputs (as described in Section 0), configure and run a simulation. **This section introduces this workflow-based graphical user interface (GUI).**

The workflow design paradigm

WUI-NITY is a comprehensive platform for simulating the combination of terrain definition, vegetation (as “fuels”), atmospheric factors, growth and spread of fire and smoke, people movement and traffic movement through road network. The required input data needs to be gathered from various sources. The disparate nature of these data sources can make the data preparation and processing complicated. For instance, data may be in different formats for different countries. This complex process requires a long and complex workflow. While the core UI for WUI-NITY does support the required functionality for data definitions for technical expert and highly experienced users, it is also desirable to have a user interface layer which could guide users through the model definition and simulation processes – to make the software more “accessible” – although still requiring expertise in the underlying subject matter.

To guide users through the process of creating a complex simulation model, a “workflow navigator” based on the “Vertical Navigation” design paradigm⁴³ is adopted to develop a second WUI-NITY GUI. The intention is to enable a collapsible hierarchy of interface, which reflects the start-to-end workflow and guide users through different sections. Each significant step or phase of model development is a collapsible branch, with each item in the “tree” providing both the option for users to track their progress and take decisions and configure the model accordingly. Each item can either serve directly as a data entry point or to launch a data definition or functional unit for simulation, such that the user may track their progress entirely from start to finish while executing the start-to-end workflow. In addition, a “help” text panel is also added which is updated whenever the user hovers the mouse across a UI workflow element.

⁴³ A vertical navigation, also known as a vertical sidebar or vertical navbar, is a navigation menu that stretches along the side of a page or window. It presents all the links or components that guide users to different pages of a website or sections of an app. Typically, vertical navigation has a clear tree structure or group layout, allowing for fast navigation to desired areas and easy movement between different pages/sections within the website or app.

WUI-NITY Graphical User Interface

WUI-NITY has two built-in GUIs, a legacy core GUI (see Figure 33) and a new workflow GUI (Figure 34). The new GUI will be shown at the start, and the user can switch between them while running WUI-NITY using the GUI switch buttons. Both have similar functions and operate on the same set of runtime data (with slight differences in data dependency), so either of them can be used to configure and run a simulation. However, it is recommended to use one GUI at a time to work on a project to avoid triggering expected conflicts in data dependency. **This document focuses on the introduction of the workflow GUI** – given that it aids the user’s understanding of the configuration process and is also more consistent with the logic applied in other engineering tools.

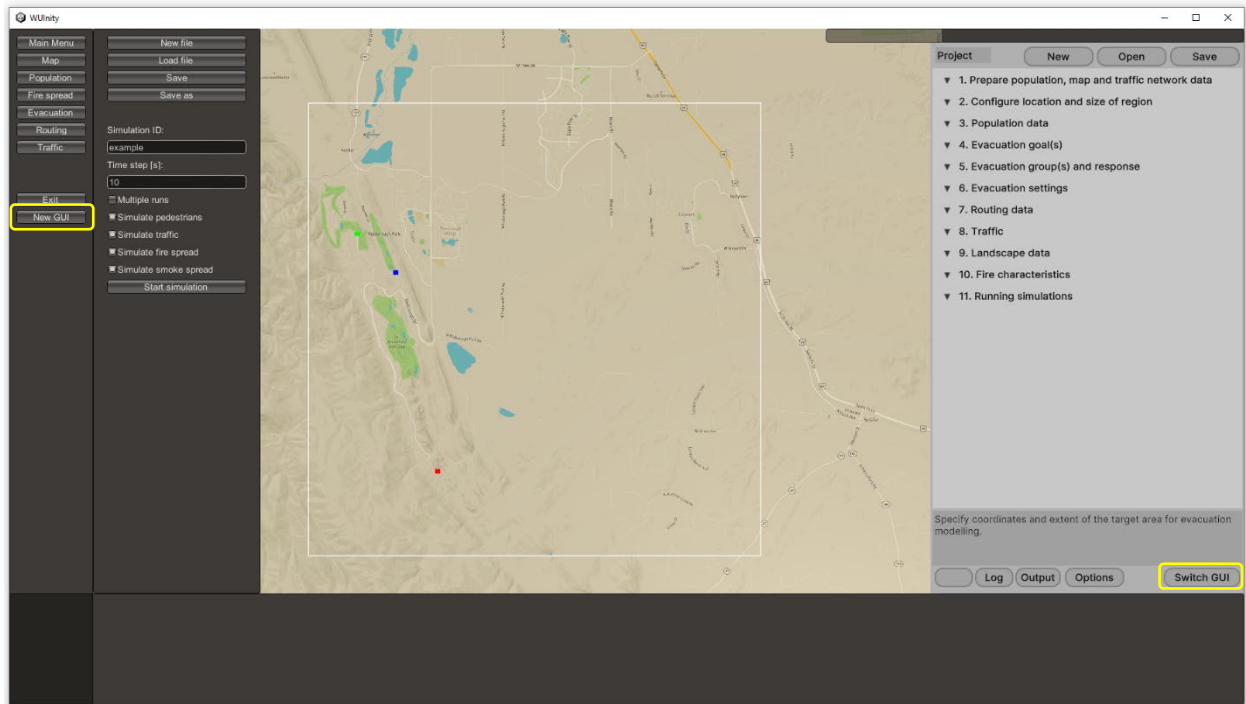


*Figure 33. Legacy WUI-NITY GUI and two GUI switch buttons.
(When the legacy GUI is running, the workflow GUI is docked on the right. The GUI switch buttons are highlighted in yellow.)*

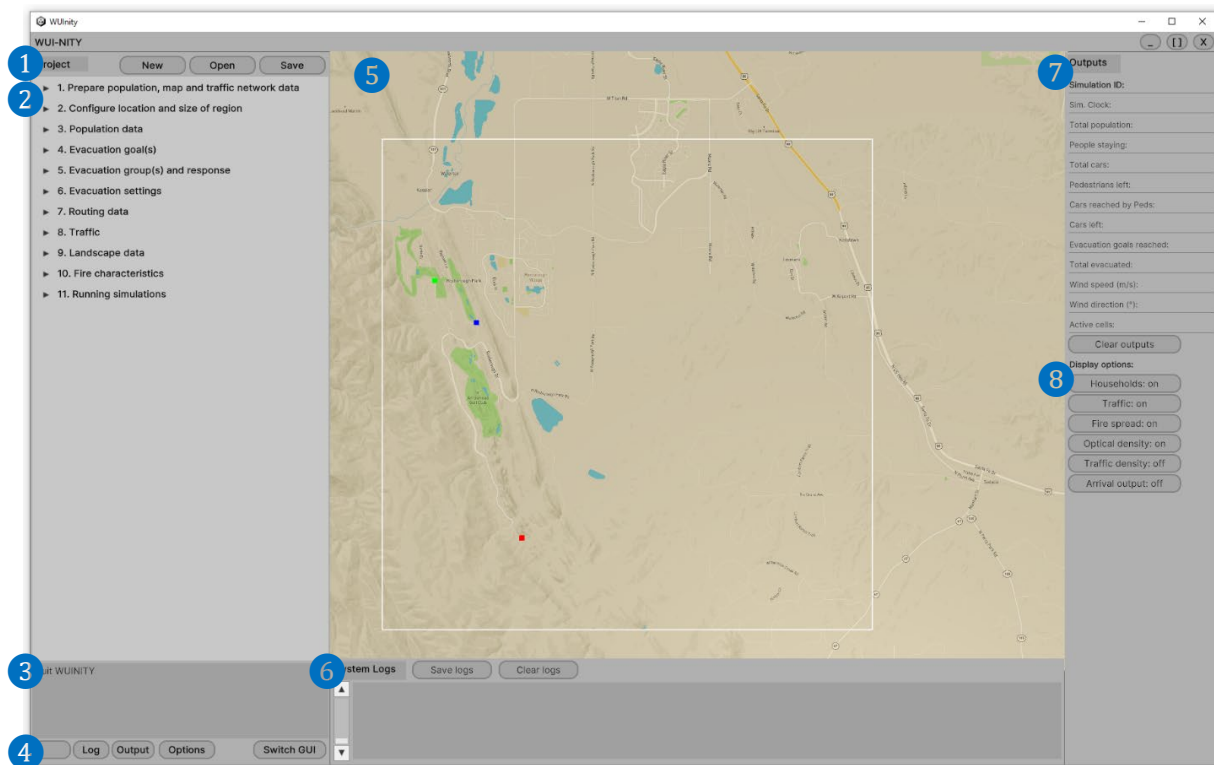


Figure 34. Workflow WUI-NITY GUI and eight function blocks.
(The numbers in the figure correspond to the eight function blocks described in Section 0, explaining different parts of the GUI.)

The workflow GUI

The workflow GUI can be divided into three sections from left to right, with eight function blocks (see Figure 34). Detailed descriptions of these functions are as follows.

1. Project buttons

Three project buttons, **New**, **Open** and **Save**, are used to create a new project, open an existing project, and save an opened project respectively. This functionality is consistent with comparable software tools.

2. Workflow menu

The collapsible hierarchy workflow menu consists of 11 function sections to guide the user to build a complete simulation model, including the functions to prepare the necessary data inputs, configure the model and run a simulation. These are described in detail in Section 0.

3. Help text window

Help text will be displayed in this window when the mouse cursor is hovering above any item of the workflow menu.

4. Operation buttons

There are five operation buttons. The first one will expand or collapse the workflow menu. The **Log** and **Output** buttons will toggle the display of the system logs window and the output window, respectively. The **Options** button is a reserved button for further development. And finally, the **Switch GUI** button turns off the workflow GUI and activates the legacy GUI.

5. Map window

This window displays the map and the simulated evacuation traffic flows, fire and smoke.

6. System logs window

This window displays WUI-NITY system logs, including the results of operations, running warnings, and errors if any.

7. Output window

This window displays various simulation outputs.

8. Display control buttons

These control buttons toggle on and off the display of the simulated features in the map window, including households, traffic, fire spread, optical density (as a function of smoke density), traffic density and arrival output window⁴⁴.

WUI-NITY Project File (.wui)

WUI-NITY manages a wildfire evacuation model along with various associated data inputs and settings, treating them as a cohesive project. A WUI-NITY project consists of a project file (with the extension .wui) and other related data input files introduced in Section 0. When a new project is created, WUI-NITY generates a .wui file with either blank or default settings. Subsequently, users are guided through the workflow menu to provide the necessary data sets and input various parameters, ultimately constructing a complete simulation model. The .wui file will be updated by WUI-NITY during this process. Note that the .wui file is stored in JSON format⁴⁵, allowing manual editing and verification using a text editor – provided the user is familiar with the expected input format⁴⁶. Occasionally, manual editing may be necessary because currently not all WUI-NITY settings in the .wui files have been implemented in the GUI. However, caution is advised, as an incorrect input or change could potentially cause unexpected errors and even crash WUI-NITY.

The workflow menu

The workflow menu consists of 11 function sections that guide the user through the process of building a complete simulation model (i.e., a WUI-NITY project) from scratch. These sections help the user prepare the necessary data inputs, configure the model, and run a simulation.

Prepare population, map and traffic network data

WUI-NITY requires an internet connection to access the online Mapbox resource (as detailed in Section 0). Given that ongoing access to this resource is required, it is necessary to add a firewall exception for WUI-NITY if the user is operating within a protected network. The first checkbox in this section serves as a reminder for taking this action (see Figure 35). Other than being a reminder, checking this box has no other function.

This section of the workflow menu guides users to external websites for downloading both population density data (as described in Section 0) and OpenStreetMap data (as described in Section 0). For example, ticking the checkbox under the label **“1.1 Fetch GPWv4 population density data”** will open a web browser with the corresponding website link. Ticking the next checkbox below (“Download GPW Population Density v4 data-set”) will open a file folder where users should save the downloaded data sets⁴⁷.

⁴⁴ The display of arrival output is under development at this stage.

⁴⁵ <https://en.wikipedia.org/wiki/JSON>

⁴⁶ Manual editing of the .wui file may be useful for experienced users to quickly change the project settings for testing purpose.

⁴⁷ The data sets need to be extracted from the downloaded zip file.

The step labelled “**1.2 Fetch Mapbox API access token**” is optional. WUI-NITY already includes a built-in token, so there is no need to fetch an additional access token (see Section 0). This step is included in this section to emphasize that Mapbox is an integral part of the model’s input.

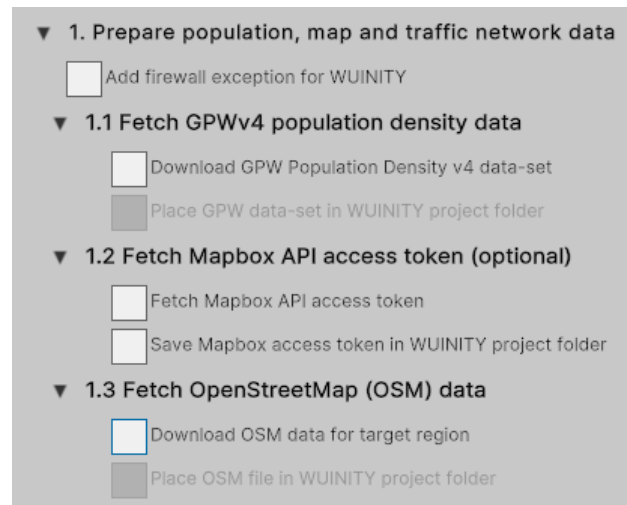


Figure 35. Section 1 of the workflow menu.

User actions (Menu Section 1):

- Follow the links in the opened web browser to download the population density data and the OpenStreetMap data.
- Save the downloaded data sets in the file folder indicated by WUI-NITY.

Configure Location and Size of Region

This menu section includes three input fields, which take the user inputs described in Section 0 to define the region for evacuation modelling. Once the map information is entered, users can click the **Update Map** button to load the map in the map window.

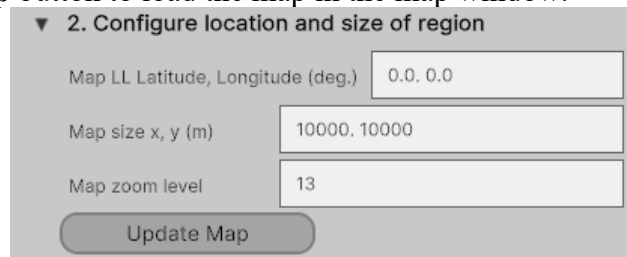


Figure 36. Section 2 of the workflow menu.

User actions (Menu Section 2):

- Enter the map information prepared in Section 0 in the three input fields and load the map.

Population Data

This menu section guides users through a three-step process for constructing the population data needed for evacuation. The steps are as follows:

Step 1: Specify global GPW data folder and generate local GPW data:

In the first step, users are prompted to indicate the folder where they have stored the downloaded global population density datasets (as outlined in Section 0). Next, users should click the **Build local GPW data** button. This action generates a .gpw file - a representation of local population density distribution within the specified area of interest.

Step 2: Specify local GPW file:

In the second step, users specify the filename for the local population density distribution. They can choose to use the file generated in the previous step. If a valid .gpw file exists, WUI-NITY will create a local population file (.pop) that represents the number of people distributed across a grid of population cells. The **Show/hide GPW data** button allows users to visually check the population density (GPW data) on the map.

Step 3: Specify local POP file:

The last step involves specifying the filename for the local population file. Users can opt to use the file generated in Step 2. The **Show/hide POP data** button allows users to visually check the population distribution (POP data) on the map.

Figure 37 illustrates the data flow during this process. If users wish to work with alternative versions of .gpw or .pop files, they can specify the desired filename in the second or third step. Remember to choose filenames that reflect the purpose and content of each file (if the user would like to test multiple population settings), ensuring clarity and ease of management during the evacuation modelling process.

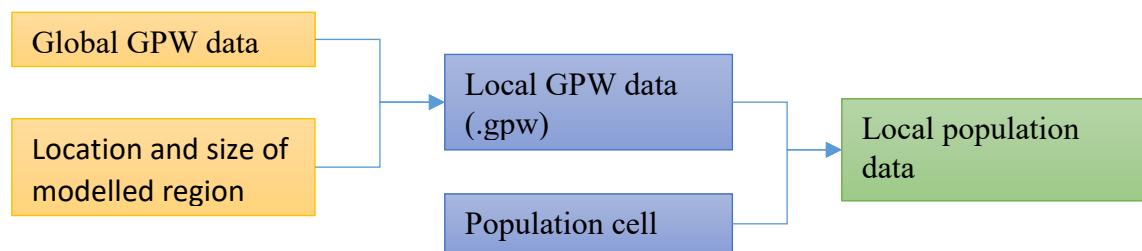


Figure 37. The data flow of generating local population data from the global GPW data sets.

In this section, WUI-NITY constructs a .gpw file and subsequently generates a .pop file from the global GPW data sets. This process requires no additional user intervention - users simply need to follow the three steps described to complete the task. Although it is technically feasible to combine these three steps into a single operation, we intentionally implement them as separate steps. By allowing users to manually specify the file generated in the previous step for use in the current one, we aim to provide transparency and facilitate a deeper understanding of the population data that relates to the evacuation demand.

In addition, there are two buttons that allow users to adjust the population distribution generated. The first button, **Correct for route access**, is used to proportionally redistribute the people located in population cells that do not have road access to other places⁴⁸. This step will also be performed by WUI-NITY automatically before running a simulation. This function is included here to allow users to visually check the redistribution of the population according to route access. The second button, **Rescale population to**, allows users to increase or reduce the population size to the number supplied by the user.

Finally, the text output box at the bottom of this section shows the population information in the area.

⁴⁸ This operation requires the traffic network and routing data built in Section 0.

▼ 3. Population data

☐ Set global GPW files folder Build local GPW data Step 1

GPW folder: not set

☐ Populate from local GPW file Show/hide GPW data Step 2

GPW file: not set

☐ Populate from POP file Show/hide POP data Step 3

POP file: not set

Correct for route access

Rescale population to:

GPW total population:

Total population (adjusted):

Total active cells:

Figure 38. Section 3 of the workflow menu.

User actions (Menu Section 3):

- Specify the folder containing the downloaded global GPW data in WUI-NITY to generate local population data following the three-step process.
- Customize population size or adjust population distribution (optional).

Evacuation goal(s)

WUI-NITY allows the division of the modelled region into multiple zones (also referred to as **evacuation groups**). This can be used, for example, to explore how to optimally assign residents (at the zone level) to an evacuation route. Within each of these zones, different **evacuation goals** and **responses** can be assigned to individuals. The definition of zones, evacuation goals, and responses constitutes the fundamental elements for creating and testing evacuation plans. In addition, the temporal factor can be added to the plans by manipulating the order of evacuation for these zones. These plans can be tailored to evacuate all people effectively or adaptively in response to various threats (such as fires approaching from different directions) enhancing community safety during emergencies.

In the example project depicted in Figure 39, there are three evacuation groups (located across different areas), four evacuation goals (different evacuation objectives) and two different response curves (initial delay distributions). When it comes to selecting an evacuation destination, **Group A** is divided into two subgroups: 80% of the population will choose **Goal A**, while the remaining 20% will go to **Goal B**. People in **Group B** will equally use all four goals as their evacuation destination. **Group C** is also divided into two subgroups: both subgroups will equally go to **Goal B** and **Goal D**. It should be noted that if an assigned goal is blocked (either through manual setting, or the goal was compromised due to fire or reached full capacity), people would switch to the quickest route to an unblocked goal.

In terms of responding to the call for evacuation, **Group A** is again divided into two subgroups: half of the population will follow **Response Curve A**, while the other half will follow **Response Curve B**. **Group B** is divided into two subgroups: 60% of the population will follow **Response Curve A**, and the remaining 40% will follow **Response Curve B**. Finally, all people in **Group C** will follow **Response Curve B**.

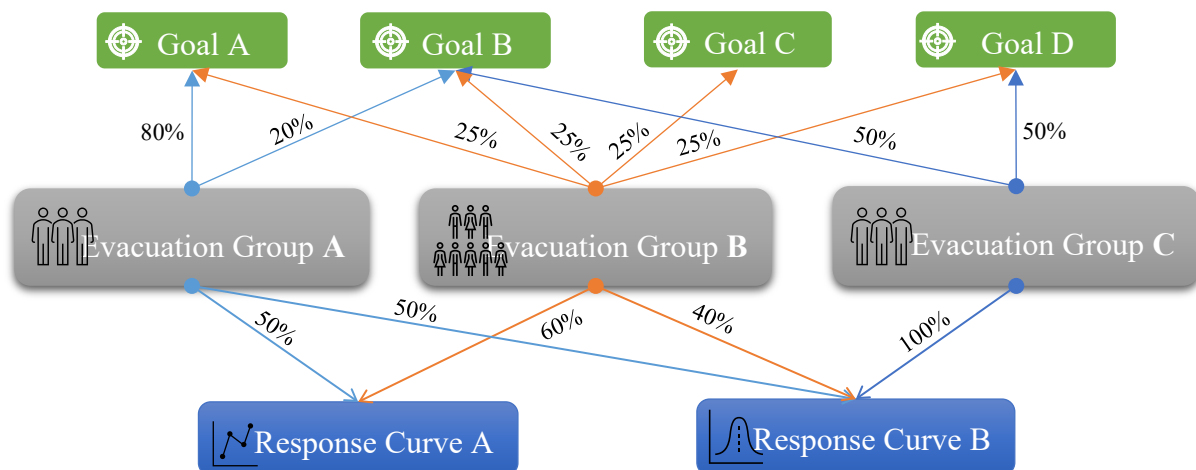


Figure 39. An example project with three evacuation groups, four goals, and two response curves.

This menu section allows the user to define and manage evacuation goals, which are a prerequisite for defining evacuation groups. Users can create new goals with null values, add pre-defined goals to the list, remove goals from the list, and edit any goal in the list using the four buttons shown in Figure 40.

When editing a goal file, please refer to Section 0 for the format. Currently, the properties of a goal are only editable through a text editor. Therefore, once a change is made and saved, the goal file needs to be reloaded into WUI-NITY to incorporate the change (remove and then add the goal again or reload the project).

Figure 40. Section 4 of the workflow menu.

User actions (Menu Section 4):

- Define and manage the evacuation goal list.

Evacuation group(s) and response(s)

This menu section allows users to manage both the **evacuation group** and **response curve** file lists (see Figure 41). User actions include creating new files with null values, adding existing files to the list, removing files from the list, and editing any selected file in the list (in a system default text editor). Note that the response curve is also a prerequisite for defining an evacuation group. Therefore, it needs to be defined before being added to an evacuation group. The evacuation group file defines the association of the group with evacuation goal(s) and response

curve(s). For the format of evacuation group file and response curve file, please refer to Section 0 and 0, respectively.

Users can click the **View/Edit evacuation** buttons to open a text editor to edit the current response curve and group files. Similar to goal files, any changes made to evacuation group and response curve files need to be reloaded into WUI-NITY to incorporate the changes (remove and then add the corresponding file again or reload the project).

The spatial arrangement of evacuation groups can be interactively edited on the map by clicking the **Edit evacuation group on map** button to turn on the map editing mode (see Figure 41). The map will display regions divided into different colours, each representing a different evacuation group (see Figure 42). To add a population cell into an evacuation group or change the group for a cell, first select the corresponding evacuation group from the dropdown list, and then click on the cell on the map. The colour of the cell will change to the colour defined for the selected group. Once the editing is completed, click on the **Stop editing** button to turn off the map editing mode.

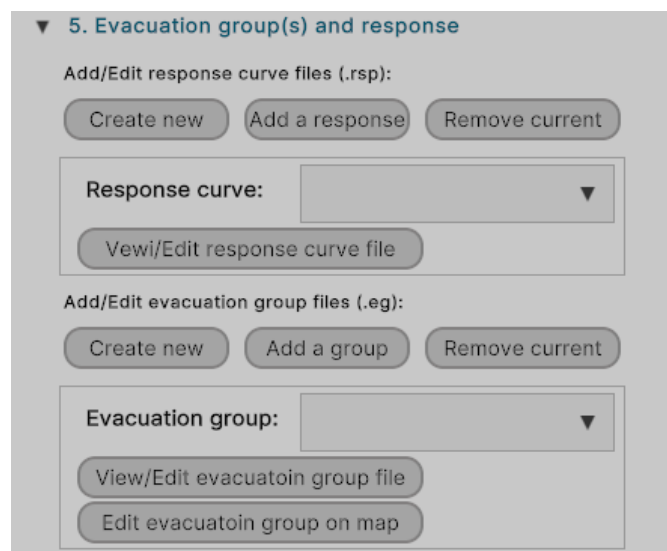


Figure 41. Section 5 of the workflow menu.

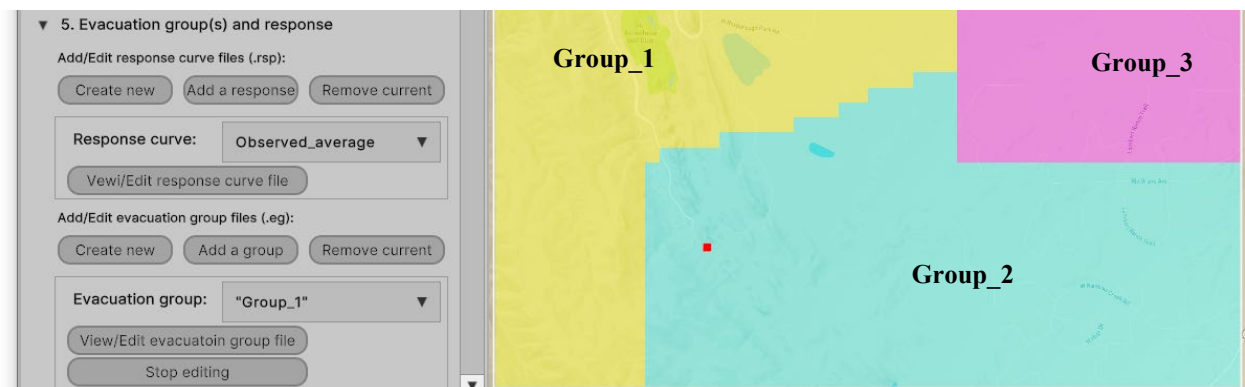


Figure 42. Map editing mode for editing spatial arrangement of evacuation groups (Group 1 is selected).

User actions (Menu Section 5):

- Define and manage the lists of evacuation groups and response curves.
- Define and edit the spatial arrangement of evacuation groups according to the evacuation zone division.

Evacuation settings

There are several evacuation settings in this menu section which need user input. Please refer to Section 0 for how the user can manipulate these settings and what the impact on performance might be. Table 16 provides the default values or range of these settings.

Figure 43. Section 6 of the workflow menu.

Table 16: Description of user-accessible evacuation settings.

Input name [unit]	Format	Default value*	Explanation/Source
Evacuation cell size [m]	Decimal	200**	This defines the resolution of the population distribution within the region for generating the households for evacuation.
Allow more than one car per house	Boolean	True	One vehicle per household by default. Might be used to represent different socio-economic conditions.
Max cars	Number	2	The maximum number of vehicles a household has access to and uses in an evacuation varies. If more than one car per house is checked, then the maximum is set to 2 by default.
Probability for max cars	Decimal	0.3 (i.e., 30%)	The likelihood that the maximum number of cars can be assigned to a household, rather than the default single vehicle per household.
Min.-Max. persons per household	Number	1-5	The range of the number of persons assigned to a household.
Min.-Max. walking speed [m/s]	Decimal	0.7-1.0	The range of walking speed of individual evacuees [19]. Used to calculate the movement time between the residence and the vehicle.
Walking speed and distance modifier	Decimal	1.0	This is a model test parameter used by developers for testing the pedestrian model. It is defined as a multiplier of pedestrian walking speed and distance in the verification test. It should be left as the default value or used for testing the sensitivity of walking speed and distance in modelling.
Evacuation order time (time after fire in seconds)	Decimal	0	The period of time between the fire ignition time and the moment when an evacuation order is given.

* These default values are used in model development but may not represent recommended values. Users should adjust these values (e.g., range of walking speed) according to their modelling requirements and assumptions.

** This defines a square cell of 200m x 200m

User actions (Menu Section 6):

- Provide inputs to the evacuation settings in this menu section.

Routing data

This menu section guides users through a three-step process to build the necessary routing data needed for evacuation from OpenStreetMap data (see Figure 45). The steps are as follows:

Step 1: Specify OSM data file to build router database:

This initial step identifies all available routes from the OSM data for the modelled region. First, users should tick the checkbox labelled '**Set OSM data file**' and specify the downloaded OSM data file (as outlined in Section 0). Next, users should click the '**Filter OSM data**' button to generate a filtered OSM data file, which represents the local traffic network within the specified area of interest. Finally, users should click the '**Build router database**' button to create a routing network database (.routerdb) for traffic pathfinding within the area of interest. This process takes a few minutes⁴⁹ subject to the size of the OSM data file, the complexity of the road network layout, and the computational power.

Step 2: Specify router database to build route collection:

In the second step, users need to specify the filename for the routing network database to build the OD matrix employed by the evacuees as the basis for route choice. They can choose to use the file generated in the previous step. After a valid .routerdb file is loaded, the user should click the '**Build route collection**' button to create a route collection file (.rc) that represents the origin-destination (O/D) matrices built upon the traffic network. The matrices include all possible routes from any point of the network to the defined evacuation goals.

Step 3: Specify route collection file:

The last step involves specifying the filename for the route collection file. Users can choose to use the file generated in Step 2.

Figure 44 illustrates the data flow during this process. If users wish to work with alternative versions of .routerdb or .rc files, they can specify the desired filename in either the second or third step. Remember to choose filenames that reflect the purpose and content of each file, ensuring clarity and ease of management during the evacuation modelling process.

In this section, WUI-NITY constructs a .routerdb file and subsequently generates a .rc file from the OSM data file specified. This process requires no additional user intervention - users simply need to follow the three steps described to complete the task. Although it is technically feasible to combine these three steps into a single operation, we intentionally maintain them as separate steps. By allowing users to manually specify the file generated in the previous step for use in the current one, we aim to provide transparency and facilitate a deeper understanding of the underlying data governing evacuation movements.

⁴⁹ It may take a considerable amount of time if the computer is less powerful. Users should leave WUI-NITY to finish the task.

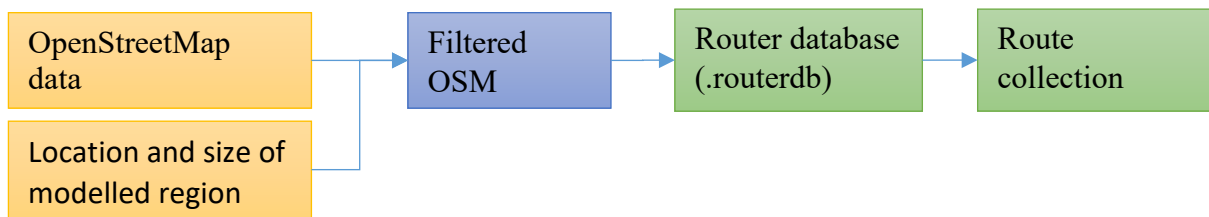


Figure 44. The data flow of generating local route collection data from OSM data.

Figure 45. Section 7 of the workflow menu.

User actions (Menu Section 7):

- Specify the download OSM data file to generate local route collection following the three-step process.

Traffic

The traffic network and routing information are built in the previous section, which serve as the foundation for modelling evacuation traffic. This menu section allows users to provide the inputs that affect the speed and route choice of the vehicles in evacuation. These inputs include selecting the route choice within the modelled evacuation scenario, specifying vehicle speed at maximum route capacity, setting the range of the background traffic density, and deciding whether to model the impact of smoke on vehicle speed. Additionally, users can view and edit road types to align with the conditions in the modelled area. For detailed information about these traffic options and default values, please refer to Section 0 and Table 11.

8. Traffic

Route choice: null

Specify vehicle speed at max. capacity: 5.0

Min background traffic density (vehicles/km/lane): 0

Max background traffic density (vehicles/km/lane): 0

☐ Speed is affected by smoke?

Road type: null

Speed limit (km/h):

Number of lanes:

Max. capacity:

Can be reversed?:

View/Edit road type file

Figure 46. Section 8 of the workflow menu.

User actions (Menu Section 8):

- Provide inputs to traffic settings and check road types.

Landscape data

This menu provides guidance (a list of actions) for users to prepare the landscape file and several other supporting files for the fire simulation using third-party programs and external sources of data. It acts as a reminder to ensure that the user completes these key steps. For detailed information about the actions of preparing the files, please refer to Section 0.

9. Landscape data

Target region: Within the USA

☐ Use LANDFIRE to create and download .lcp file

☐ Download slope, aspect and elevation data

☐ Download a fuel data map from EFFIS or other source

☐ Download canopy cover data from EFFIS (or other) source

☐ Compile landscape file with QGIS or ArcGIS:

► QGIS landscape definition

► ArcGIS landscape definition

► Create fire characteristics files

Figure 47. Section 9 of the workflow menu.

User actions (Menu Section 9):

- Follow the guidance in this section and refer to Section 0 to prepare the landscape file and other supporting files for the fire simulation.

Fire Characteristics

If users intend to include fire and smoke simulation in the WUI-NITY project, they need to prepare a range of files to provide supporting data. For detailed instructions on how to prepare

these files, please refer to Section 0 and Section 0. This menu allows users to specify the files that have been prepared and open the corresponding file in a text editor to edit and verify the contents of the file. Note that the fire and smoke simulation will not run if any of the required files are not present.

▼ 10. Fire characteristics

☐ Load landscape file (.lcp) Toggle LCP display

LCP file: not set

☐ Load fuel models file (.fuel) View fuel model

Fuel model file: not set

☐ Load fuel moisture file (.fmc) View fuel moisture

Fuel moisture file: not set

☐ Load weather file (.wtr) View weather file

Weather file: not set

☐ Load wind file (.wnd) View wind file

Wind file: not set

☐ Load ignition points file (.ign) View ignition points file

Ignition points file: not set

☐ Load graphical fire input file (.gfi)

Graphical fire input file: not set

☐ Edit WUI (fire model) area

☐ Edit (fire) trigger buffer

☐ Use random ignition

☐ Use initial ignition

Figure 48. Section 10 of the workflow menu.

User actions (Menu Section 10):

- Prepare and specify the required files for fire and smoke simulation.
- Edit fire model settings including:
 - Edit WUI (fire model) area and (fire) trigger buffer (this function is under development),

Running simulations

The last menu section allows users to specify simulation-related parameters and select options for running the simulation. These parameters include simulation ID, simulation time step and maximum simulation time measured in seconds. The simulation ID is a user-specified string that is used to differentiate the simulation and the associated output files. The simulation time step defines the minimum interval to update the status of the simulated agents during a simulation run. Finally, the maximum simulation time defines the terminal time to force stopping a simulation.

The simulation options include simulating **pedestrian movements**, **traffic flow**, **fire spread**, and **smoke spread**, corresponding to the four switches within WUI-NITY to control the

activation of the three simulation layers (as depicted in Figure 2). The aim is to allow developers or users to execute individual simulation modules to facilitate debugging or diagnosis of simulations. These options are explained as follows:

- **Pedestrian movements:**
This is the main switch, which controls the activation of the Pedestrian Modelling Layer. When activated, the module generates households based on population distribution, road network and related settings within the region. It then simulates pedestrian responses and movements towards their vehicles. If deactivated, the Traffic Modelling Layer will remain inactive, as it will not receive any input.
- **Traffic flow:**
This switch controls the activation of the Traffic Modelling Layer. When activated, the module will simulate the evacuation flows of vehicles in the traffic network, based on the evacuation settings. If deactivated, the simulation will end when all pedestrians reach their vehicles.
- **Fire spread and smoke spread:**
These two switches control the activation of fire and smoke simulation in the Fire Modelling Layer. The aim is to allow users to execute fire and smoke simulation independently, facilitating the setup of the fire and smoke simulations. If deactivated, users can perform evacuation simulation without the added complexity of fire and smoke simulations.

Users also have the option to run multiple simulations concurrently. When this box is ticked, an input box will appear, allowing the user to specify the number of simulation runs. It is important to note that these multiple simulations will be executed in a batch model, **without visual outputs on the map view window**, except for the standard simulation result files in the output folder.

Finally, within this section, two buttons are provided at the bottom of this section: one to execute and stop a simulation, and the other to pause and resume the ongoing simulation. When a simulation is running, users should avoid making any changes to the project settings.

Figure 49. Section 11 of the workflow menu.

User actions (Menu Section 11):

- Provide inputs to simulation parameters and selection simulation options.
- Execute the simulation.

The Output Window

WUI-NITY produces a range of simulation outputs. The output window only lists a few main simulation results as shown in Figure 50(a). In addition, there are six buttons under the output list, which toggle the display of the simulated features superimposed on the map view window (see Figure 50(b)). These features are explained as follows.

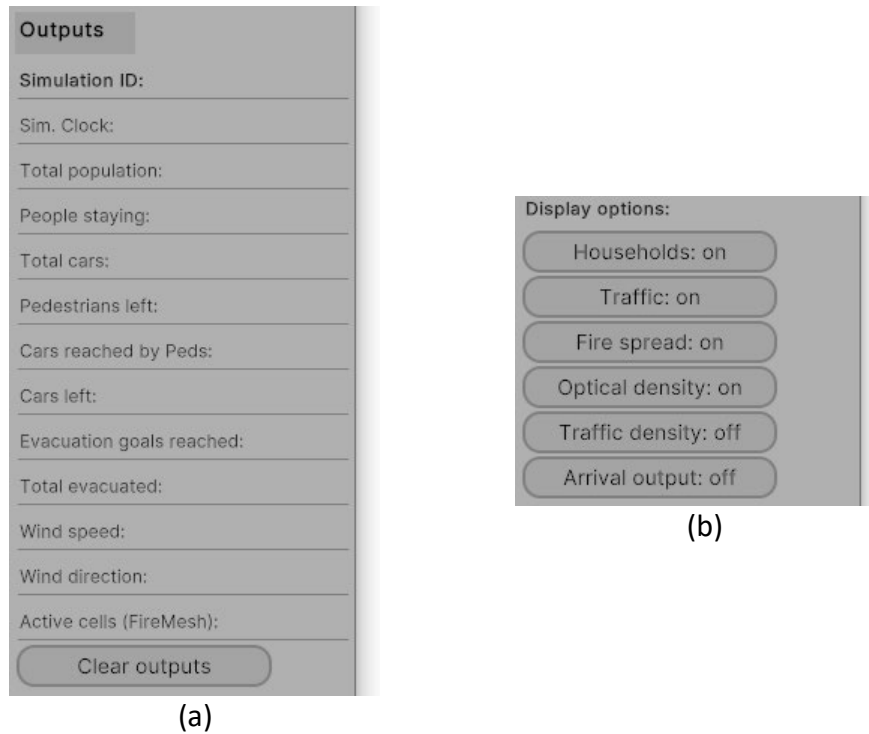


Figure 50. (a) The output window and (b) the display option buttons.

- Households:**
 In WUI-NITY, households are depicted as small pentagons (as shown in Figure 51a). The pentagons appear in blue if the residents within the households have not responded to evacuation orders during the simulations. Conversely, they appear green if the residents start to evacuate. Additionally, there are also a number of grey pentagons on the map, which signify the connection points between households and the road network. The evacuees firstly drive from their houses to the connection points before they can drive on the road network to evacuate.
- Traffic:**
 Evacuating vehicles on the road are depicted as small diamonds. These vehicles appear in green if they are moving at free speed, or red if they are slowing down due to congestion (as shown in Figure 51a).
- Traffic density:**
 In addition to depicting evacuating vehicles as diamonds, WUI-NITY provides an estimate of traffic density displayed as a layer of 100x100m cells on top of the map. Notably, red cells indicate high traffic density road segments, while blue cells denote low traffic density road segments (as shown in Figure 51b). Note that the density is calculated for all traffic within the cells regardless of direction.
- Fire spread and optical density:**
 Fire spread and smoke spread (expressed as optical density) predicted by the wildfire simulation module (refer to Section 0) can be visualized as additional layers superimposed on the map (as depicted in Figure 52). The optical density layer uses a

blue color background to represent areas with zero optical density, i.e., no smoke. Conversely, warmer colors (yellow, red) indicate areas with high optical density. Note that the smoke simulation results are indicative at this stage.

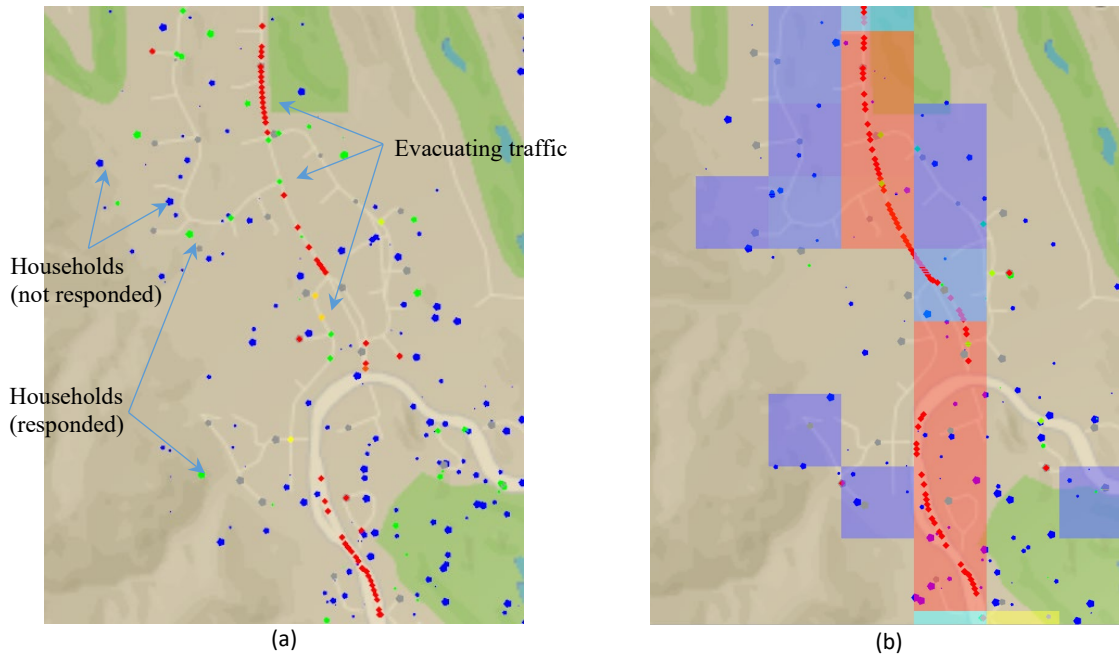


Figure 51. Display of (a) households, evacuating traffic and (b) traffic density on map view windows.

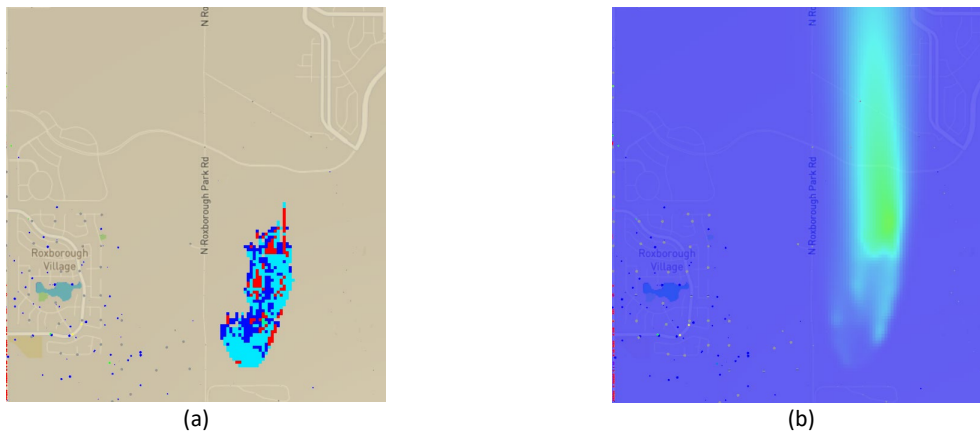


Figure 52. Display of (a) fire spread and (b) smoke (as optical density).

Simulation outputs

The WUI-NITY simulation generates a set of output files. Specifically, it creates an ‘output’ folder containing two CSV files: one for ‘pedestrian output’ and another for ‘traffic output’. Additionally, the simulation produces a series of snapshot images in PNG format, illustrating the dynamic changes in traffic density across the map. The outputs contained in each .csv file are summarized below.

1. Pedestrian output per time:

- **Time (s):** The simulation time measured in seconds as an increment of a fixed time step.

- **Households left:** The total number of households from which people have not yet started evacuation and are still located in the affected area.
- **People Left:** The total number of individuals who have not yet started evacuation and are still located in the affected areas.
- **Households started moving:** The number of households from which people have initiated evacuation during the interval period.
- **People started moving:** The number of people who have begun evacuation during the interval period.
- **Households reached car:** The number of households whose residents have reached their cars during the interval period.
- **People reached car:** The number of individuals who have reached their cars during the interval period.
- **Total cars activated:** The total number of cars that have started evacuation in the simulation.
- **Average walking distance:** The average walking distance of evacuees in meters during the evacuation.

2. Traffic output per time:

- **Time (s):** The simulation time measured in seconds as an increment of a fixed time step.
- **Injected cars:** The number of cars that have started evacuation during the interval period.
- **Exiting cars:** The number of cars that reached their destination within the specified time interval.
- **Current cars in system:** The total number of evacuating cars currently in the simulated traffic network system for evacuation.
- **Exiting people:** The number of drivers/passengers who reached their destination during the specified time interval.
- **Average Vehicle Speed (km/h):** The average speed of evacuating cars observed during the specified time interval.
- **Minimum vehicle speed (km/h):** The minimum speed of evacuating cars observed during the specified time interval.
- **Number of individuals that have reached each evacuation goal:** The number of people who have successfully reached each evacuation goal.

A4. Demonstration case

To demonstrate the process of constructing a project and conducting fire and evacuation simulations in WUI-NITY, a simulation case was set up from scratch (see also [1]). The chosen test location was Marsden Moor, situated in West Yorkshire, United Kingdom. Marsden Moor has encountered several wildfire incidents in recent years, drawing attention from news outlets, including the BBC in April 2021⁵⁰. The UK National Trust even maintains a dedicated “appeal page” to raise awareness about the wildfire risk during dry summers with low rainfall⁵¹. Given its history of wildfires, Marsden Moor serves as a compelling case study. Notably, this location provides an opportunity to explore the manual creation process of landscape (.lcp) files, distinct from the readily available .lcp files provided by LANDFIRE, as Marsden Moor lies outside the United States.

It is important to note that the objective of this exercise was not to undertake a rigorous scientific investigation of this region. Instead, our focus was on selecting a representative WUI area – one distinct from the United States, where a previous WUI-NITY case study was conducted in Roxborough Park [3, 10, 12]. By choosing Marsden Moor, we aimed to explore the usability and application process of WUI-NITY in a different geographical context, leveraging the workflow embedded in the graphical user interface (GUI). The subsequent steps closely aligned with the outlined workflow in Section 3, demonstrating how WUI-NITY can be effectively applied.

Data preparation

To build the Marsden Moor case, the following data sets and input files were sourced or created:

- **Population modelling:**
 - We chose the [Population Density, v4.11 \(2015\)](#) data set from the [Global Population of the World \(GPW\), v4](#) (refer to Section 2.2).
- **Traffic network modelling:**
 - Marsden Moor is an extensive moorland area situated in the South Pennines, between the conurbations of West Yorkshire and Greater Manchester in the north of England. To model the traffic network within this region, we chose OpenStreetMap (OSM) extracts data specifically for [the West Yorkshire region](#) that encompasses Marsden Moor.
- **Fire and smoke modelling:**

In the context of Marsden Moor, we illustrated the process of preparing essential data for configuring a fire and smoke simulation. The following datasets were either sourced or created:

 - Raster layers for Landscape file creation:
 - Elevation layer (refer to Section 0)
 - Slope (calculated from elevation)
 - Aspect (calculated from elevation)
 - Canopy cover layer (refer to Section 0)
 - Fuel map layer (refer to Section 0)

⁵⁰ <https://www.bbc.com/news/uk-england-leeds-56884655>

⁵¹ <https://www.nationaltrust.org.uk/support-us/appeals/marsden-moor-fires-appeal>

- Creation of Landscape file using QGIS (refer to Section 0)
- Fuel models file (sing the default FBFM13, as described in Section 0)
- Fuel moisture content file (based on postulated values, detailed in Section 0)
- Weather file (using postulated values, outlined in Section 0)
- Wind file (employing postulated values, as specified in Section 0)
- Ignition point file (using postulated values, as referenced in Section 0)

In the next section, we detailed the steps to set up the wildfire and evacuation simulation in the Marsden Moor region.

The process of applying WUI-NITY to build the simulation case

The Marsden Moor case was built in 11 steps, as detailed in Sections 0 through 0, adhering to the workflow outlined in Section 0. Each step underwent thorough verification within the GUI and was successfully completed. The simulation was executed in the last step to produce the results that were analyzed and reported in Section 0. All resources referenced in this section are publicly available and free to use. The process to create the Marsden Moor case is now described.

After launching WUI-NITY⁵², click the **New** button to create an empty new project, as shown in Figure 53. If the user is returning to an existing project they have worked on previously, click the **Open** button to open that project.

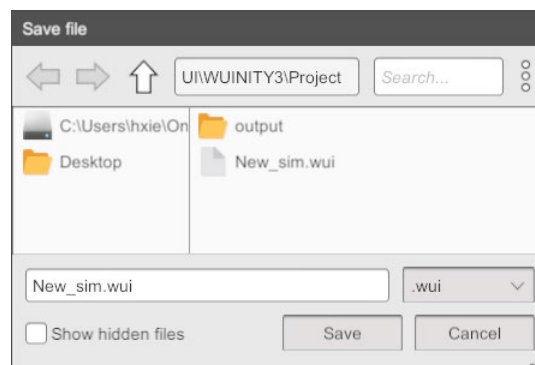




Figure 53. Create a new project.

Prepare population, map and traffic network data

This step sources the essential data to build the population and traffic network through downloading the global GPW data sets and obtaining OpenStreetMap (OSM) data for the West Yorkshire region.

- First, select and download the global GPW data sets, and organize them within the WUI-NITY case folder (see Section 0):
 - Open the [Global Population of the World \(GPW\), v4](#) page via the link built in WUI-NITY,
 - Download the [Population Density, v4.11 \(2015\)](#) data set:
 -  gpw-v4-population-density-rev11_2015_30_sec_asc.zip
 - Extract all files in the downloaded zip file.
 - Place all extracted files in WUI-NITY project folder as indicated.

⁵² See also Section 0 for the project buttons.

- Next, fetch OpenStreetMap (OSM) data specifically for the West Yorkshire region (see Section 0):
 - Open the OpenStreetMap Data Extracts webpage at [Geofabrik](#),
 - Navigate the Sub Region links from Europe, United Kingdom, England, to [West Yorkshire](#),
 - Download the OSM data for West Yorkshire: [west-yorkshire-latest.osm.pbf](#)
 -  west-yorkshire-latest.osm.pbf
Type: PBF File
 - Place the downloaded OSM data file in WUI-NITY project folder as indicated.

Refer to Section 0 for user actions.

Configure location and size of the region

This step guides the configuration of the location and size of the modelled region at Marsden Moor. It involves specifying UTM coordinates for latitude and longitude, determining the map dimensions, and selecting an appropriate map zoom level for the target area.

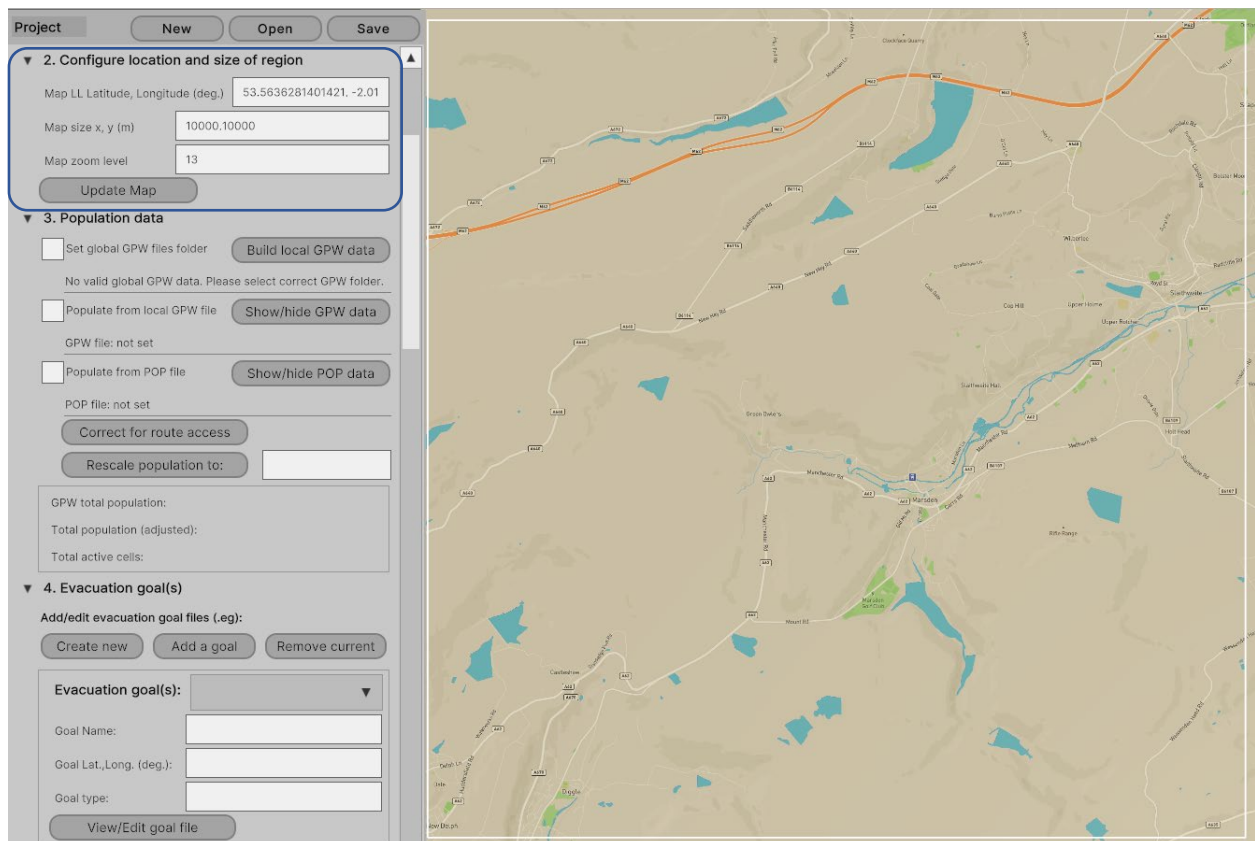


Figure 54. Configure the location and size of the modelled region at Marsden Moor.

For the demonstration case, we have chosen an arbitrary point on Google Maps to serve as the lower left corner of a 10x10 km region that approximately covers Marsden Moor. Users should refer to Section 0 for guidance on how to identify the location and size of their modelled region.

- **Specify the map latitude and longitude using UTM coordinates:** These coordinates were obtained by right-clicking on the selected point (i.e., the lower left corner of the

modelling region) on Google Maps⁵³. Specifically, the latitude and longitude obtained are (53.563628, -2.0196466).

- **Specify map size:** Opt for the default dimensions: 10,000 meters by 10,000 meters.
- **Specify map zoom level:** The default zoom level of 13 was chosen to provide an appropriate view of the target area. It determines the magnification level for the map area being viewed. It might be adjusted according to user preference.
- Finally, click the **Update Map** button to load the map (see Figure 54).

Refer to Section 0 for user actions.

Configure population data

This step guides the configuration of population data, including specifying the folder for global GPW data, creating a local GPW file, and generating a .pop file. Additionally, it highlights the option to graphically edit custom populations or adjust population size if needed.

- Specify the folder where the global GPW data downloaded in Step 1 (see Section 0) was saved and create local GPW data by clicking the **Build local GPW data** button (see Figure 55).
- Specify the local GPW file created in the previous step. Note that a .pop file will be automatically generated and saved in the same folder (see Figure 56).
- Specify the .pop file generated in the previous step (see Figure 57). This file, which contains local population distribution obtained by interpolating the local GPW data, will be used to generate households for evaluation.
- Users can inspect the local GPW population density (New_sim.gpw) and local population distribution (New_sim.pop) on the map by clicking the **Show/hide GPW/POP data** buttons (see Figure 58). Note that the local GPW population density is shown in the same resolution as the original data set, approximately 1km x 1km cells, while the local population distribution uses the population cell size specified by users (see Section 0).
- If necessary, there is an option to graphically edit custom populations directly from the map or rescale the population size.

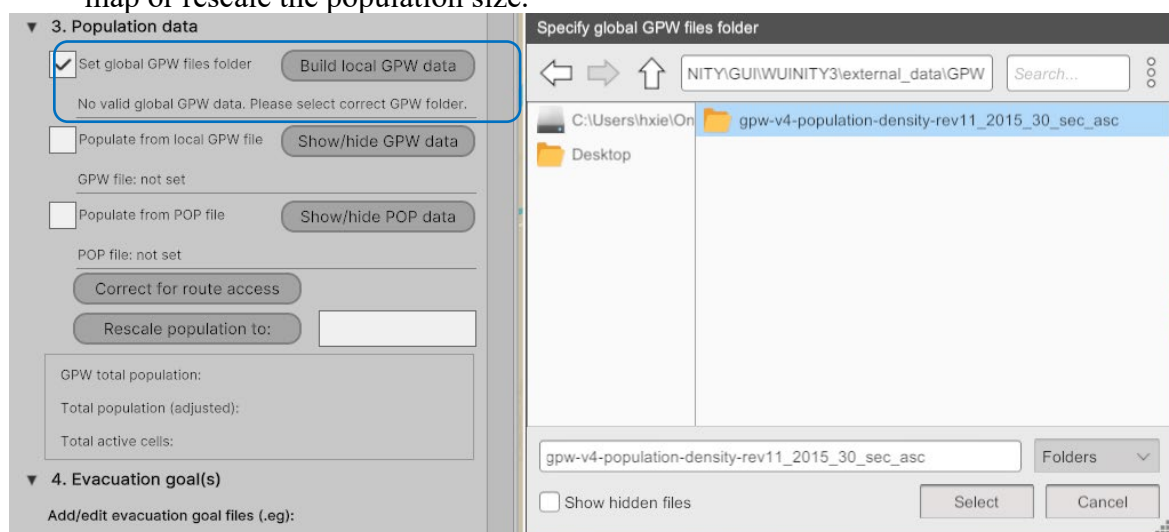


Figure 55. Specify the global GPW files folder.

⁵³ Equivalent functionality is available in other map platforms.

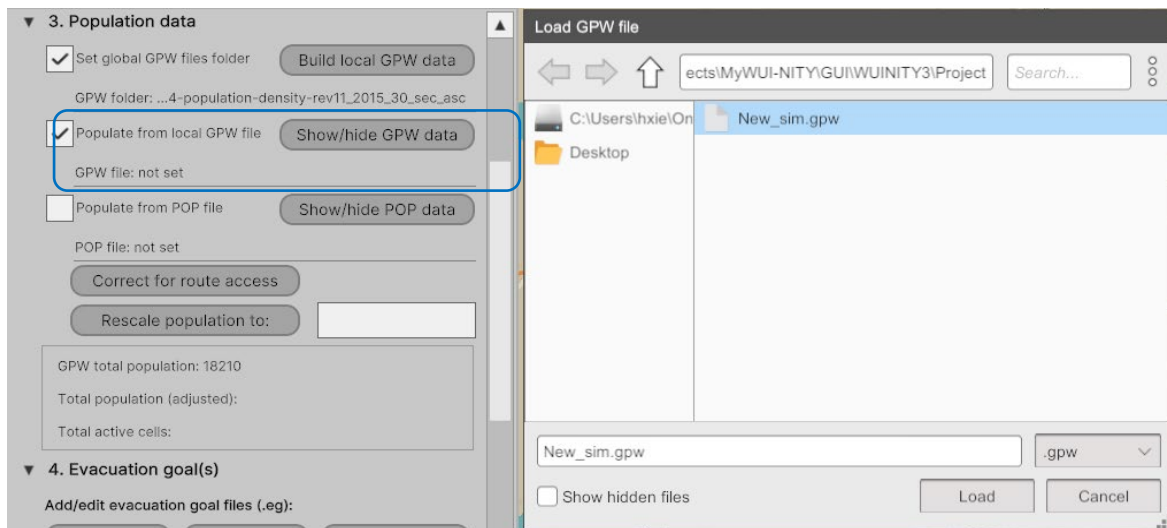


Figure 56. Specify and load the local GPW file generated in the previous step.

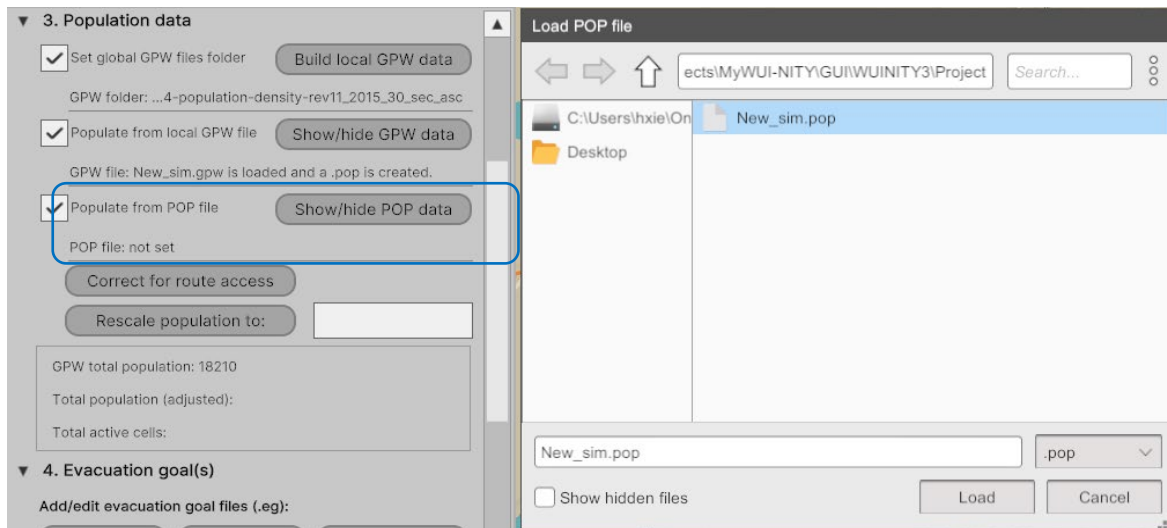


Figure 57. Specify and load the .pop file generated in the previous step.

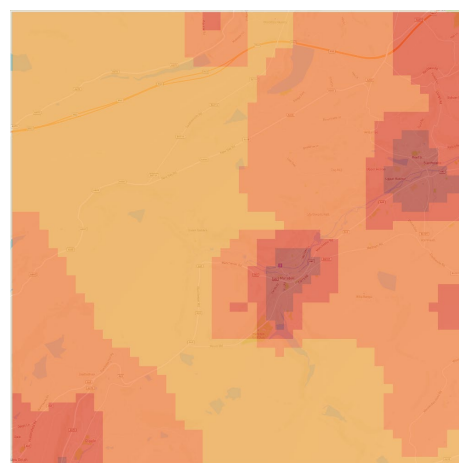
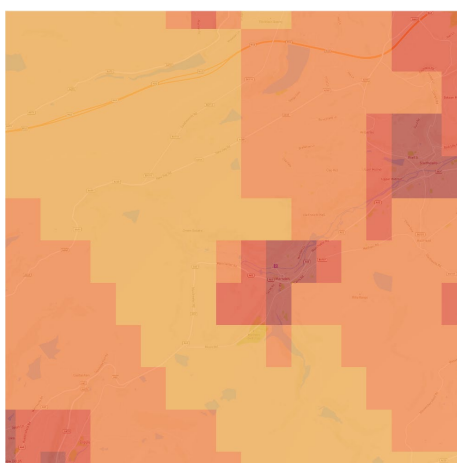


Figure 58. (a) The local GPW population density on map and (b) the population distribution derived for the selected region at Marsden Moor showing the distribution of 16,017 people.

Refer to Section 0 for user actions.

Configure evacuation goals

This step guides the definition and management of evacuation goals. WUI-NITY allows two types of evacuation destinations, **refuge** and **exit** (see Section 0). Users need to analyze the evacuation plan for the region to identify the number and location of shelters and exit points (on motorways). Users also need to further consider how individuals/households in the region may choose to use these evacuation destinations as part of the plan. Once the number and location of the evacuation destinations are confirmed, users need to obtain the UTM coordinates using a map platform (e.g., Google Maps).

In the context of Marsden Moor, we arbitrarily defined three exit points — namely, Goal_E, Goal_F, and Goal_R — located along three roads leading out of the town for demonstration purpose. These exit points serve as designated evacuation destinations as illustrated in Figure 59. The subsequent section outlines the process for integrating these evacuation goals into WUI-NITY.



Figure 59. Three evacuation destinations and traffic routes around Marsden and Slaithwaite population centers.

- **Prepare goal information:** Analyze the evacuation plan for the region to identify the number, location, and type of goals and get their UTM coordinates. For any refuges, estimate their capacities for accommodating cars and people. Repeat the following two steps to add all goals.
- **Create a new goal:**
 - Click the **Create new** button and enter a filename for the goal (which can be the same name given to the goal), as shown in Figure 60.
 - After clicking the **Save** button, a text editor will automatically open, allowing the user to enter information about the goal, as shown in Figure 61.

- Refer to Table 14 in Section 0 for the expected entry format and provide the information as required.
- **Add a goal:** Once the user has defined the new goal and saved the goal file, it can be added to WUI-NITY.
 - Click the **Add a goal** button, specify the new goal file to be added, and click the **Load** button, as shown in Figure 62.
 - The primary information of the newly added goal will be displayed in the text boxes below. Additionally, the goal will also appear as a small square in the color specified on the map view window, as shown in Figure 59.
- **Modify a goal:** To modify a goal, the user should firstly select the desired goal from the dropdown list, and then click the View/Edit goal file button. A text editor will be automatically open, displaying the information of the selected goal and allowing the user to make changes.

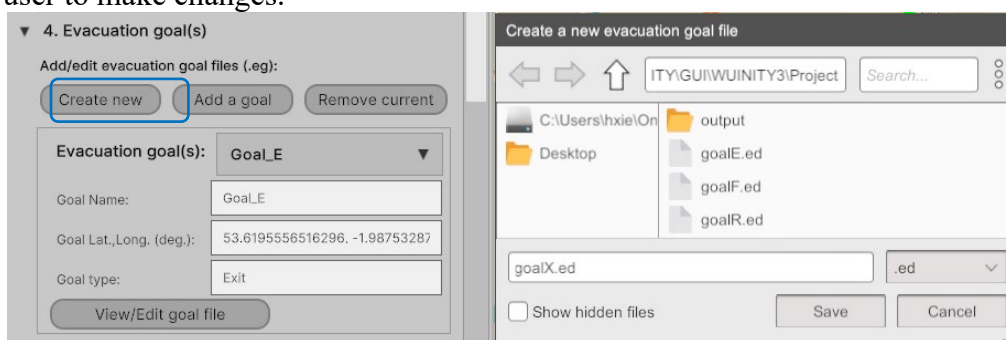


Figure 60. Create a new goal file.

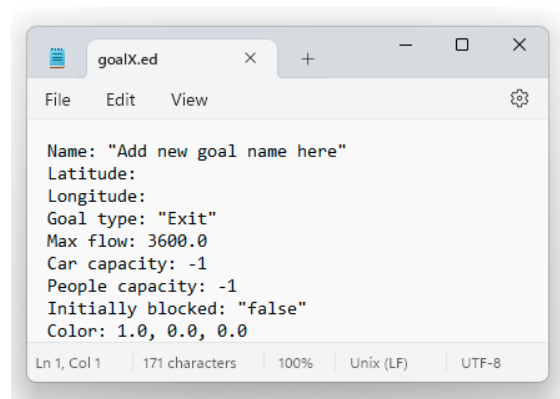


Figure 61. Enter the required information that defines an evacuation goal.

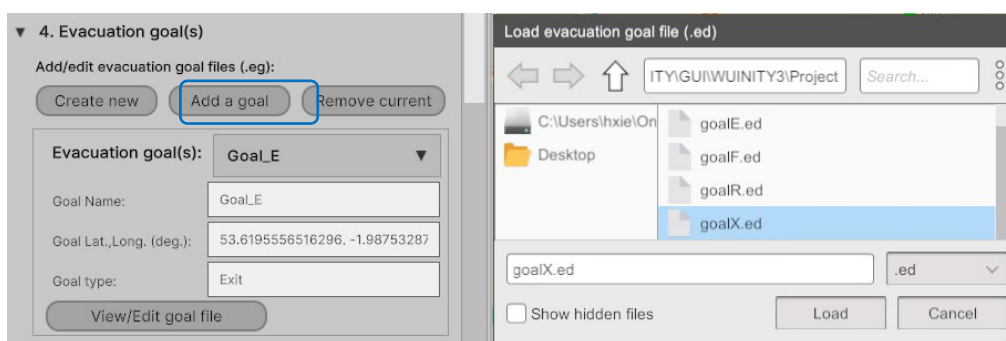


Figure 62. Add a goal file.

Refer to Section 0 for user actions.

Configure response curves and evacuation groups

This step guides users to define how individuals/households become aware of the fire event and start purposive evacuation movement and how they choose evacuation destinations defined in previous step (see also 0). The user needs to prepare the necessary information through analyzing the evacuation plan for the region, the likely evacuation scenario as well as literature. The following influencing facts need to be considered:

- **The threat:** When a fire is detected, the direction and speed of fire spread, and its distance to the community combine to determine the fire risk, i.e., the level of threat posed to the community. The threat also affects the range of the area to be evacuated, the available time for evacuation and the available routes.
- **The evacuation demand:** The demographics, size, and distribution of the population within the community form the demand for evacuation. This demand is also affected by the layout and distribution of the community properties, including the residential streets within the community as well as the demographic and socioeconomic makeup of a community.
- **The routes for evacuation:** In most WUI communities, evacuation will need to be facilitated by the road network. That is, the evacuating population will need to leave the threatened area via either familiar routes or designated evacuation routes through the road network to a place of safety. Thus, the layout and capacity of the road network, given their availability and use, will influence capacity and therefore the required evacuation time assuming demand is at a manageable level.
- **The resources required for the evacuation:** The resources required include fire intervention and traffic control, fire prevention and traffic control, the availability of vehicles for evacuation, and the notification system in place to convey the instructions to the residents (assuming that this affects the time to initiate evacuation along with preparatory activities).
- **The evacuation goal:** The availability of safe locations to accommodate the evacuees and their tools for transportation, or the routes to remote safe areas.

The information can be visualized in the form shown in Figure 39.

In the case of Marsden Moor, we arbitrarily define two response curves and three evacuation groups for demonstration purposes. The process to add the information into WUI-NITY is now explained.

- **Create a new response curve:**
 - Click the **Create new** button and enter a filename for the response curve file, as shown in Figure 63.
 - After clicking the **Save** button, a text editor will automatically open, allowing the user to enter information to define a new response curve, as shown in Figure 64.
 - Refer to Section 0 for the expected entry format and provide the information as required.
- **Add a response curve:** Once the user has defined the new response curve and saved the corresponding file, it can be added into WUI-NITY.
 - Click the **Add a response** button, specify the new response curve file to be added, and click the **Load** button, as shown in Figure 65.

- **Add other response curve(s):** Repeat the above two steps to add all response curves.
- **Modify a response curve:** To modify a **response curve**, the user should firstly select the desired response curve from the dropdown list, and then click the **View/Edit response curve file** button. A text editor will be automatically open, displaying the information of the selected response curve and allowing the user to make changes.

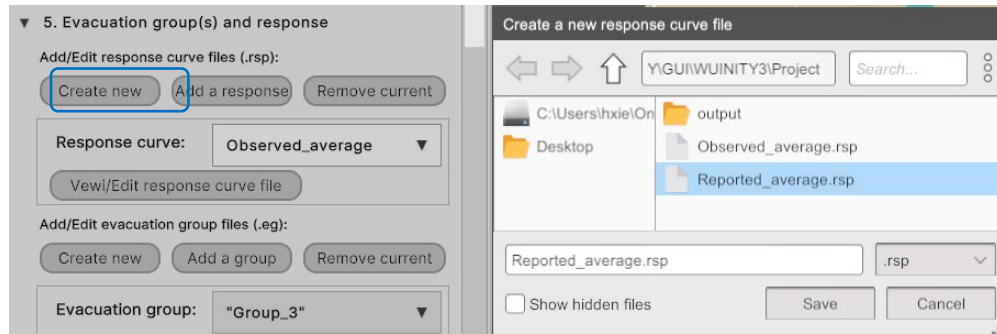


Figure 63. Create a new response curve file.

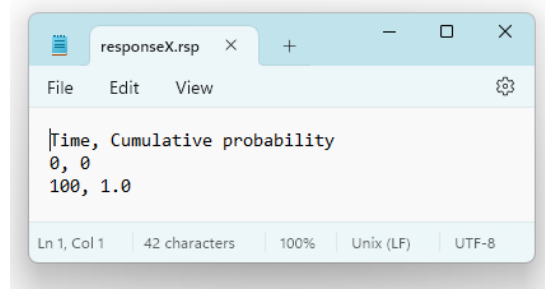


Figure 64. Enter the required information that defines a response curve.

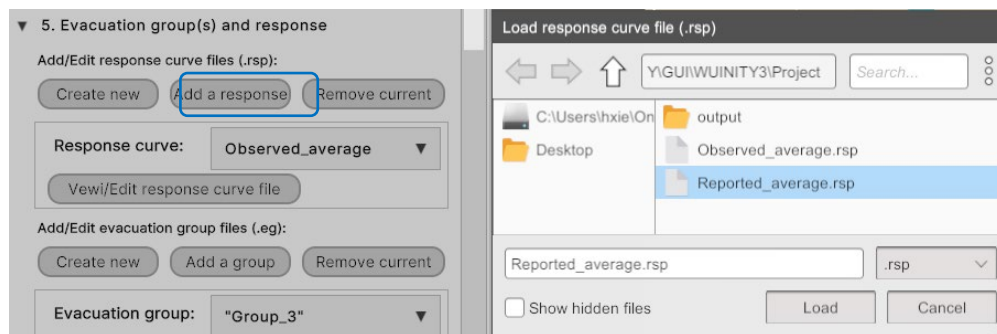


Figure 65. Add a response curve file.

- **Create a new evacuation group:**
 - Click the **Create new** button and enter a filename for the evacuation group file, as shown in Figure 66.
 - After clicking the **Save** button, a text editor will automatically open, allowing the user to enter information to define a new evacuation group, as shown in Figure 67.
 - Refer to Section 0 for the expected entry format and provide the information as required.
- **Add an evacuation group:** Once the user has defined the new evacuation group and saved the corresponding file, it can be added into WUI-NITY.

- Click the **Add a group** button, specify the new evacuation group file to be added, and click the **Load** button, as shown in Figure 68.
- **Add other evacuation group(s):** Repeat the above two steps to add all evacuation groups.
- **Modify an evacuation group:** To modify an evacuation group, the user should firstly select the desired evacuation group from the dropdown list, and then click the **View/Edit evacuation group file** button. A text editor will be automatically open, displaying the information of the selected evacuation group and allowing the user to make changes.

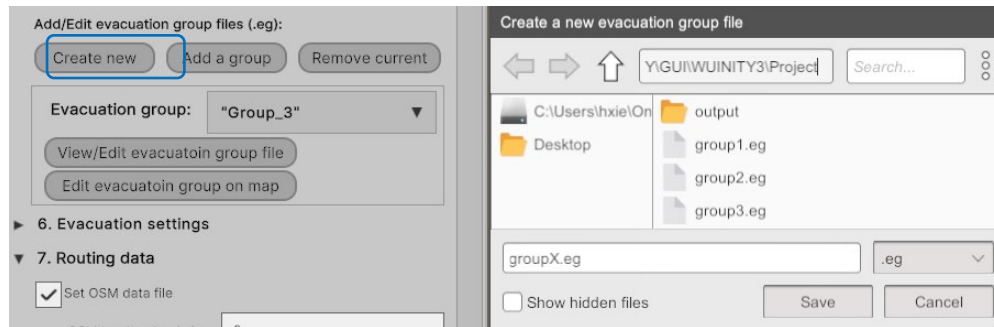


Figure 66. Create a new evacuation group file.

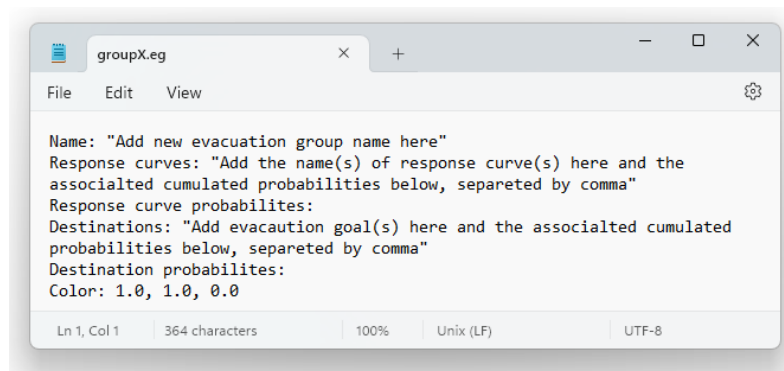


Figure 67. Enter the required information that defines an evacuation group.

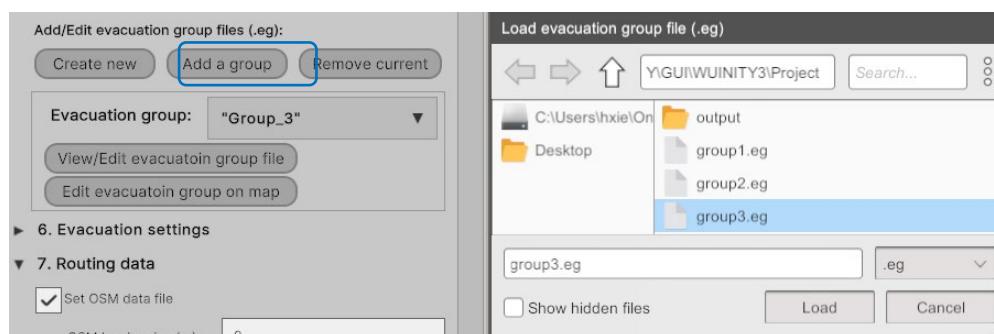


Figure 68. Add an evacuation group file.

Once all evacuation groups have been added. The user can click the **Edit evacuation group on map** button to edit the spatial arrangement of evacuation groups.

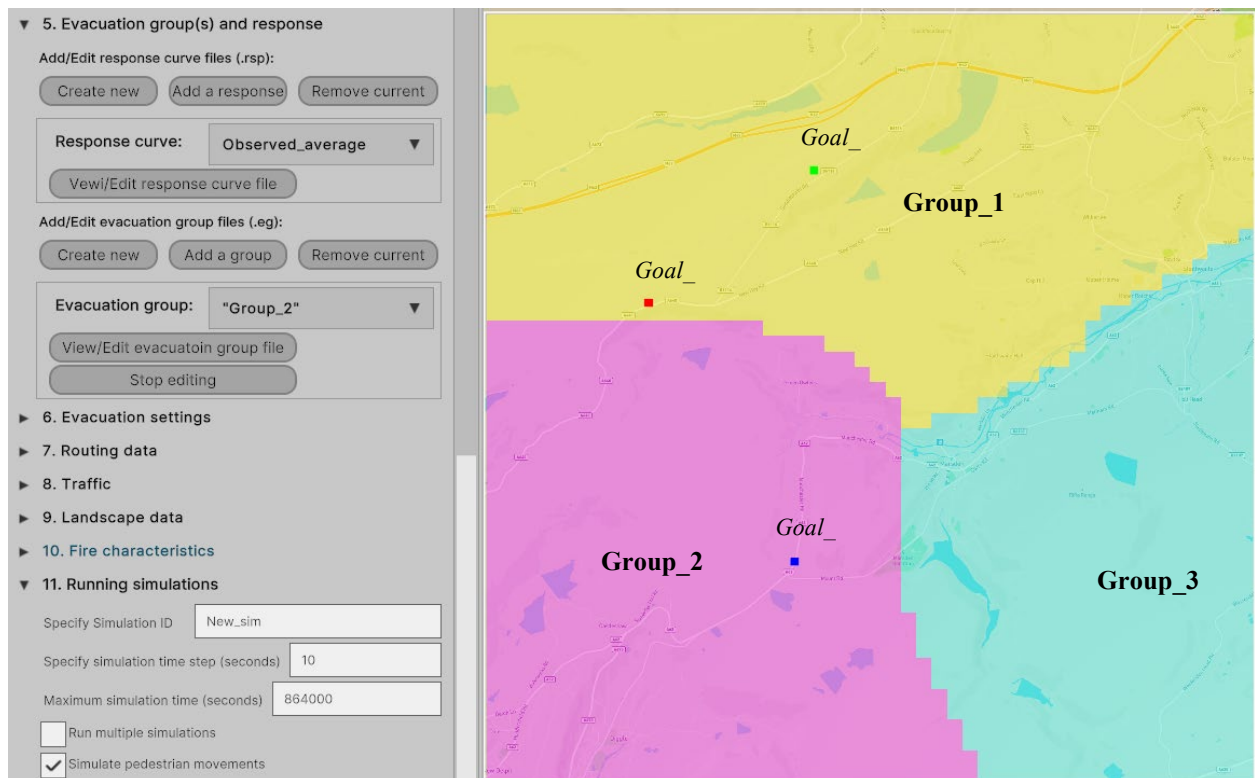


Figure 69. Edit spatial arrangement of the evacuation groups.

Refer to Section 0 for user actions.

Configure evacuation settings

This step requires users to specify several evacuation parameters to be used in simulation. These settings have been explained in detail in Section 0. For the demonstration case, we simply adopt the system default values, as shown in Figure 70.

▼ 6. Evacuation settings

Specify cell size (m)

☒ Allow more than one car/house

Specify Max cars

Specify Probability for max cars

Specify Min persons per household

Specify Max persons per household

Specify Min walking speed (m/s)

Specify Max walking speed (m/s)

Specify Walking speed modifier

Specify Walking distance modifier

Specify Evacuation order time [time after fire]

Figure 70. Evacuation settings used in the demonstration case.

Refer to Section 0 for user actions.

Configure routing data

This menu section guides users through a three-step process to build the necessary routing data from the OSM data downloaded in Step 1 (see Section 0) for the demonstration case.

- **Specify OSM data file to build router database:**
 - Tick the box **Set OSM data file** and specify the folder where the downloaded OSM data for the West Yorkshire region was saved, as shown in Figure 71.
 - Click the **Filter OSM data** button to generate a filtered OSM data file, i.e., the local traffic network within the modelled area.
 - Click the **Build router database** button to create a routing network database (.routerdb) for traffic pathfinding.
- **Specify router database to build route collection:**
 - Tick the box **Load router database** and specify the router database generated in the previous step (i.e., New_sim.routerdb), as shown in Figure 72.
 - Click the **Build router database** button to create a route collection file (.rc), i.e., the origin-destination (O/D) matrices built upon the local traffic network.
- **Specify route collection file:**
 - Tick the box **Load router database** and specify the route collection file generated in the previous step (i.e., New_sim.rc), as shown in Figure 73. This file will facilitate route calculations and navigation within the modelled area.

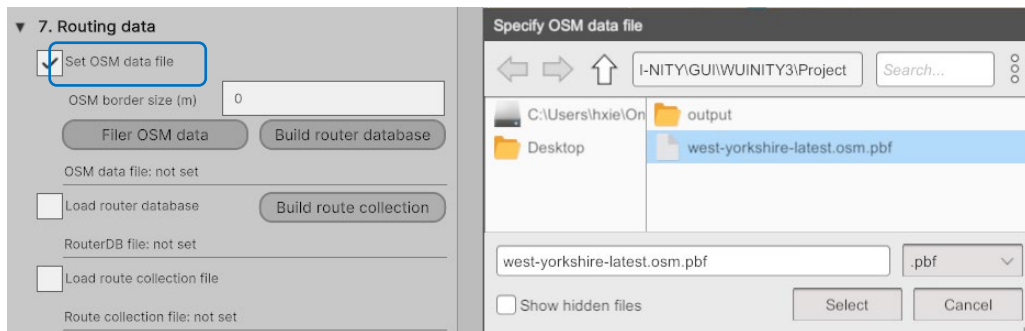


Figure 71. Specify the downloaded OSM data for the West Yorkshire region.

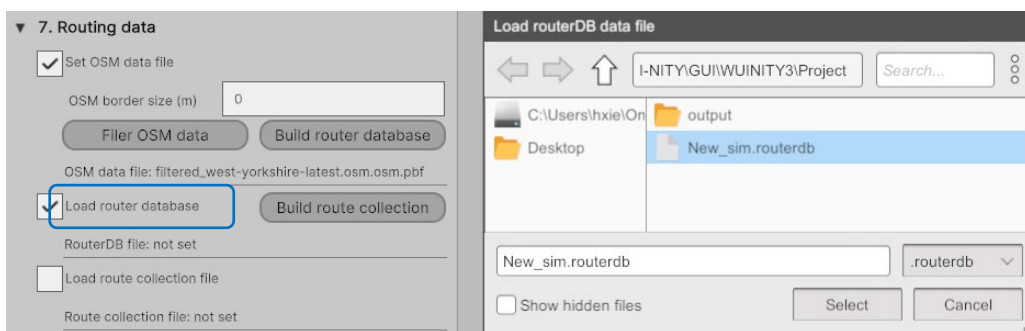


Figure 72. Specify the router database.

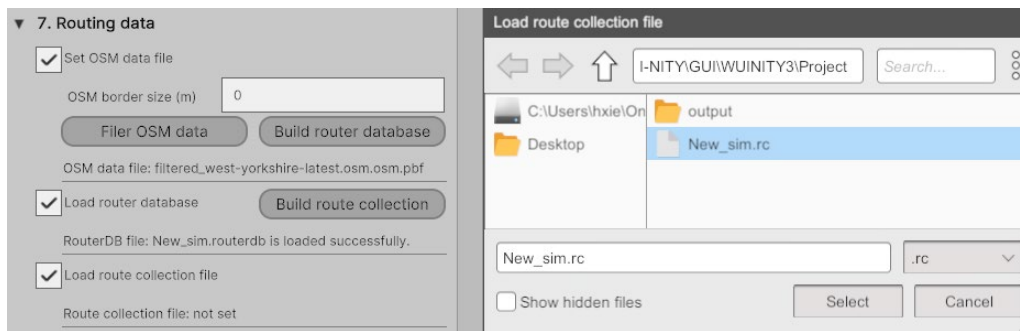


Figure 73. Specify the route collection file.

Refer to Section 0 for user actions.

Configure traffic settings

This step requires users to specify several traffic parameters to be used in the simulation. These settings have been explained in detail in Section 0 and Section 0. For this demonstration case, we simply adopt the system default values, as shown in Figure 74.

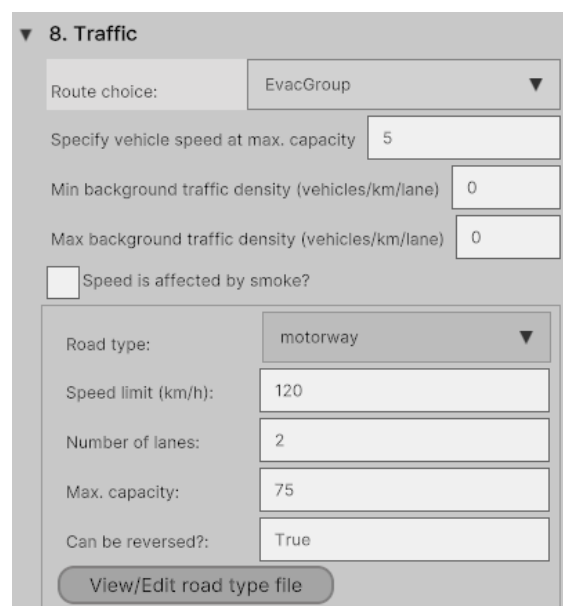


Figure 74. Traffic settings.

Refer to Section 0 for user actions.

Prepare landscape file, fuel models file and other supporting files

This menu section lists the steps to prepare the landscape file and several other supporting files for the fire and smoke simulation. The purpose of this list is to serve as a reminder, ensuring that users complete each required action to prepare the files. In the context of this demonization case, we use all the supporting fire generated by following the procedures outlined in Section 0 (see Figure 75).





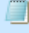

 MarsdenMoor.lcp	13/12/2022 10:37	LCP File	3,858 KB
 default.fmc	12/10/2022 09:44	FMC File	1 KB
 default.fuel	16/12/2022 13:07	FUEL File	2 KB
 default.ign	23/11/2022 10:58	IGN File	1 KB
 default.wnd	12/10/2022 09:44	WND File	1 KB
 default.wtr	12/10/2022 09:44	WTR File	1 KB

Figure 75. Fire and smoke simulation support files.

Refer to Section 0 for user actions.

Specify fire characteristics files and edit fire model settings

This step requires users to specify and load all the necessary fire characteristics files for fire and smoke simulation. The user should tick each checkbox corresponding to the relevant file prepared in the previous step (as depicted in Figure 76). The user could also click on the buttons next to the checkboxes to view and edit these files.

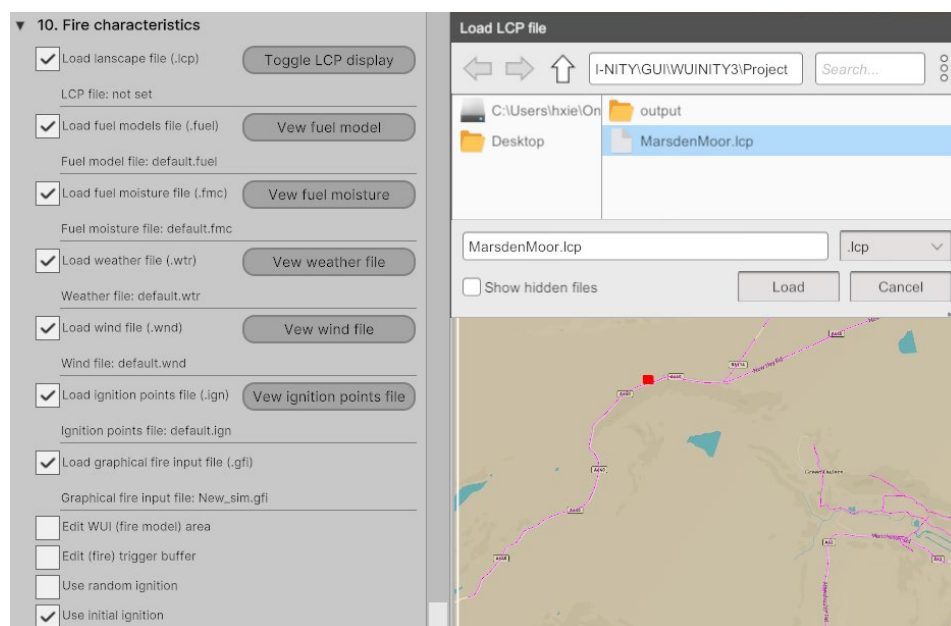


Figure 76. Specify all fire characteristics files required for fire and smoke simulation.

Execute Simulations

This step guides the execution of simulations. It involves specifying simulation parameters, and simulation options, followed by running the simulation. See Section 0 for details.

- **Specify simulation parameters and options:**
 - **Simulation ID:** Choose a unique Simulation ID for your desired simulation.
 - **Simulation time step:** Determine the granularity of simulation by specifying the time step.
 - **Multiple runs:** Decide the number of simulation iterations to run.
 - **Simulate pedestrians:** Select whether to simulate pedestrians in the scenario.
 - **Simulate traffic:** Choose whether to simulate traffic flow.

- **Simulate fire spread:** Indicate whether fire spread simulation should be included.
- **Simulate smoke spread:** Specify whether smoke spread simulation is part of the scenario.
- **Run simulation.**

Refer to Section 0 for user actions.

Simulation settings and outputs

This section summarises the evacuation simulation of Marsden Moor, including the immediate vicinity of the town. The following subsections focus on the assumptions made during the modelling process and provide an overview of the outputs as follows:

1. **Evacuation objective and assumptions** – Define the evacuation goals and relevant assumptions.
2. **Evacuation and traffic settings** – Configure parameters related to evacuation procedures and traffic flow.
3. **Outputs** – Describe the simulation results, including key metrics and visual representations.

Evacuation objective and assumptions

In the simulated area depicted in Figure 59, Marsden and Slaithwaite are the major population centers. Figure 58 provides an estimate of the population density and distribution within this region, derived from the GPW data. Here are the key points related to the simulation:

1. **Evacuation destinations** – Three evacuation destinations have been positioned in an arc outside the towns. It should be noted that these locations were arbitrarily selected along the roads leading out of the town, providing routes toward other regions. Other more appropriate locations may be employed.
2. **Fire ignition point** – The fire ignition point is deliberately located south of Marsden, so that residents would evacuate away from the fire source.
3. **Fire characteristics input** – Due to the absence of real-world fire data specific to this region and the demonstration nature of this case, we opted to use fire characteristics input files similar to those employed in the Roxborough Park case study (Ronchi et al., 2020).
4. **Road network** – Slaithwaite, Marsden, and the evacuation destinations are interconnected by a network of A-roads (A640 and A62) and several B-roads.

Configure evacuation and traffic settings

The following evacuation and traffic parameters were applied to the simulation, as shown in Figure 77.

6. Evacuation settings

Specify cell size (m)

☒ Allow more than one car/house

Specify Max cars

Specify Probability for max cars

Specify Min persons per household

Specify Max persons per household

Specify Min walking speed (m/s)

Specify Max walking speed (m/s)

Specify Walking speed modifier

Specify Walking distance modifier

Specify Evacuation order time [time after fire]

8. Traffic

Route choice:

Specify vehicle speed at max. capacity

Min background traffic density (vehicles/km/lane)

Max background traffic density (vehicles/km/lane)

☐ Speed is affected by smoke?

Road type:

Speed limit (km/h):

Number of lanes:

Max. capacity:

Can be reversed?:

View/Edit road type file

Figure 77. Evacuation parameters (left) and Traffic simulation parameters (right).

Simulation outputs

During the simulation, the status of households, evacuating traffic dynamics and density, and fire and smoke spread are shown on the map view window (see Section 0). A snapshot of the WUI-NITY simulation of the Marsden Moor case is shown in Figure 78 and Figure 79, with optical density being turned on and off.

WUInity

WUI-NITY

Project

New

Open

Save

☒ Load landscape file (.lcp)

☒ Load fuel models file (.fuel)

☒ Load fuel moisture file (.fmc)

☒ Load weather file (.wtr)

☒ Load wind file (.wnd)

☒ Load ignition points file (.lgn)

☒ Load graphical fire input file (.gfi)

Toggle LCP display

View fuel model

View fuel moisture

View weather file

View wind file

View ignition points file

Weather file: default.wtr

Wind file: default.wnd

Ignition points file: default.lgn

Graphical fire input file: MarsdenMoor.gfi

☐ Edit WUI (fire model) area

☐ Edit (fire) trigger buffer

☐ Use random ignition

☐ Use initial ignition

11. Running simulations

Specify Simulation ID: MarsdenMoor

Specify simulation time step (seconds): 10

Maximum simulation time (seconds): 864000

☐ Run multiple simulations

☒ Simulate pedestrian movements

☒ Simulate traffic flow

Hints to help guide you through the workflow

<< Log Output Options

Switch GUI

System Logs

Save logs Clear logs

[16:52:33] WARNING: Simulation started, please wait.

[16:52:33] LOG: Total households: 5771

[16:52:33] LOG: Total cars: 7087

[16:52:33] LOG: Total people who will not evacuate: 0

[16:52:33] LOG: [0s] Adding custom fuel model specifications.

[16:52:34] LOG: [0s] Ignition started in cell 324, 142 which has fuel model number 5

Outputs

Simulation ID: MarsdenMoor

Sim. Clock: 5780 s

dd:hh:mm:ss - 00:01:36:20

Total population: 16017

People staying: 0

Total cars: 7087

Pedestrians left: 313 (2%)

Cars reached by Peds: 6935

Cars left: 6578 (94.9%)

Evacuation goals reached:

Goal_E: 0 by 0 cars

Goal_R: 0 by 0 cars

Goal_F: 0 by 0 cars

Total evacuated: 0

Wind speed: 7.3 m/s

Wind direction: 315.4 °

Active cells (FireMesh): 270

Clear outputs

Display options:

Households: on

Traffic: on

Fire spread: on

Optical density: off

Traffic density: off

Arrival output: off

Figure 78. The graphical output of the Marsden Moor test case in WUI-NITY (optical density: off).

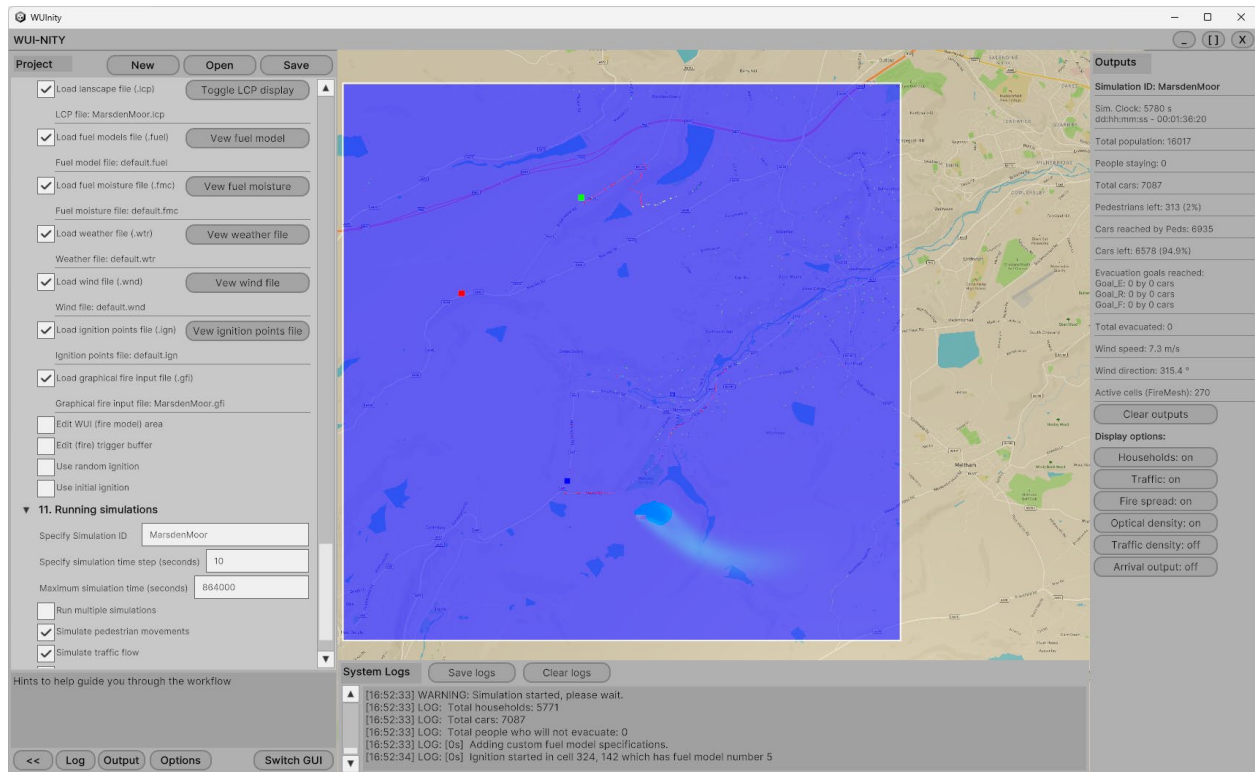


Figure 79. The graphical output of the Marsden Moor test case in WUI-NITY (optical density: on).

For this demonstration, we examined two scenarios: one using the ‘**EvacGroup**’ route choice and the other using ‘**Random**’ route choice, while keeping all other settings constant. The goal was to illustrate the disparities in evacuation outcomes. In the first scenario, we intentionally influenced people’s route choices by biasing their evacuation goals. A significantly larger number of individuals were directed towards Goal_E compared to Goal_R – demonstrating that evacuation groups predominantly followed prescribed evacuation goals. In contrast, the second scenario involved random goal selection, where evacuees equally considered Goal_E, Goal_F and Goal_R. This allowed us to observe evacuation behavior without external influence, although it may not fully represent real-world random choices.

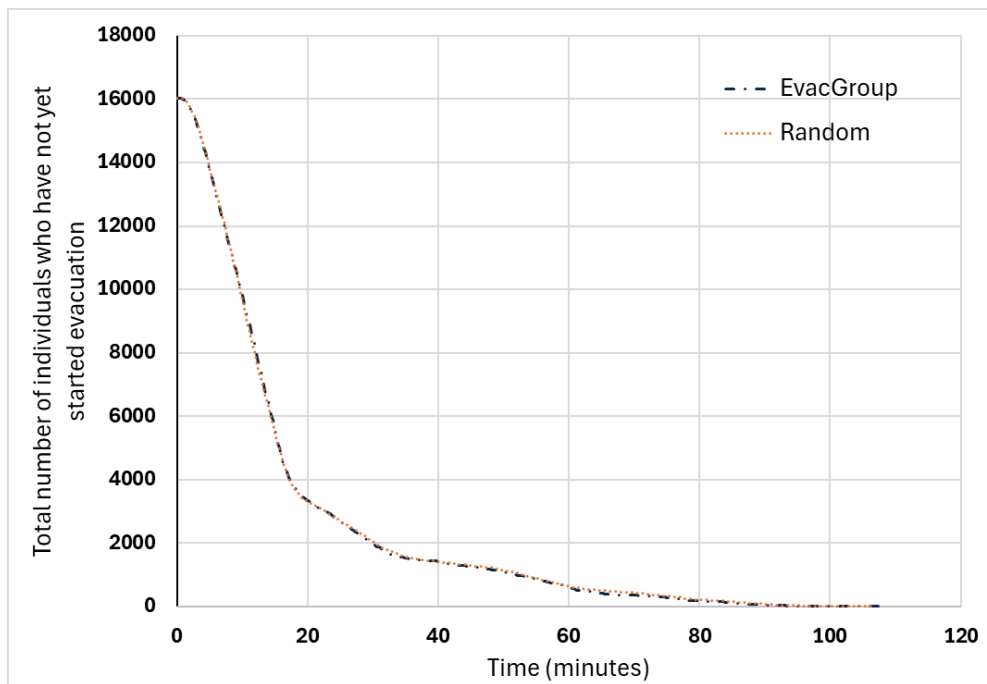
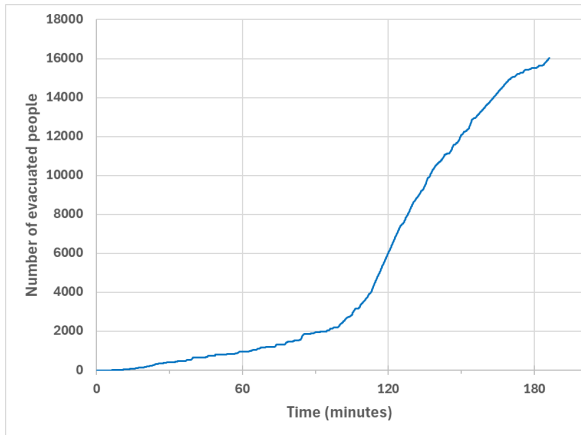


Figure 80. The number of individuals who have not yet started evacuation.

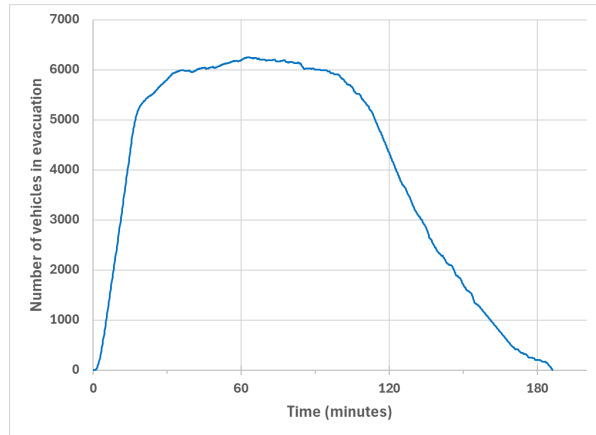
Figure 80 provides insight into the initial progression of evacuation by depicting the number of individuals who have not yet started evacuation, reflecting the impact of the imposed response curves. Since both scenarios involved the same population and response curves, the resulting curves were identical.

However, despite the similarity in the response phrase of the evacuation, the two different route choices employed in the two scenarios resulted in significant deviation in evacuation performance. Figure 81 and Figure 82 show the difference between the two scenarios in the number of people who successfully reached their evacuation goals and the number of vehicles in evacuation. Specifically, Figure 81 depicts individuals who adhered to the prescribed evacuation goals set by their evacuation groups, while Figure 82 represents people who randomly selected evacuation goals. In the first 60 minutes, approximately 3000 people reached their evacuation goals in the second scenario, while the number was around 1000 in the first scenario. By the 120-minute mark, more than 9000 people successfully evacuated in the second scenario, while the number was around 6000 in the first scenario. The evacuation route choice significantly impacted the overall evacuation performance, despite the evacuees having the same evacuation responses. Additionally, Figure 83 illustrates the other evacuation performance indicators for these two scenarios with different route choices.

In this simple demonstration, we illustrated how altering a single evacuation parameter can lead to significant differences in evacuation outcomes. In a comprehensive evacuation analysis where the impact of varying multiple parameters is examined, we expect a more intricate interplay of factors affecting evacuation performance – emphasizing the importance of leveraging WUI-NITY to tackle the complex challenge of large-scale evacuation planning and management in response to wildfire threats.

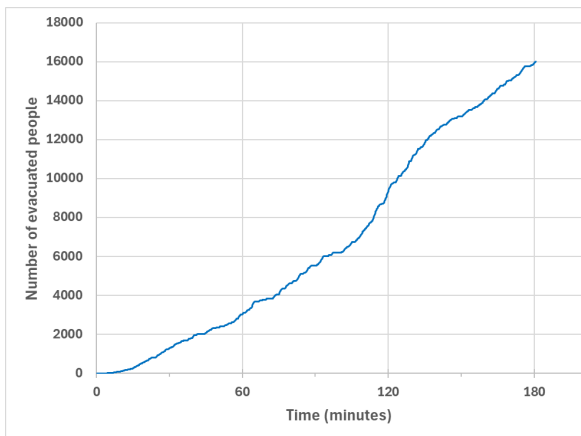


(a) The number of people reached evacuation destinations as a function of time.

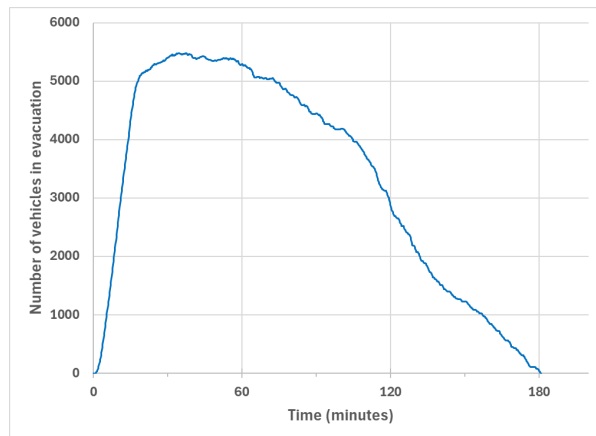


(b) The number of vehicles in evacuation as a function of time.

Figure 81. Overall evacuation performance (route choice: EvacGroup).



(a) The number of people reached evacuation destinations as a function of time.



(b) The number of vehicles in evacuation as a function of time.

Figure 82. Overall evacuation performance (route choice: random).

Outputs
Simulation ID: New_sim
Sim. Clock: 11170 s dd:hh:mm:ss - 00:03:06:10
Total population: 16017
People staying: 0
Total cars: 6876
Pedestrians left: 0 (0%)
Cars reached by Peds: 6876
Cars left: 0 (0%)
Evacuation goals reached: Goal_E: 8335 by 3551 cars Goal_F: 6607 by 2862 cars Goal_R: 1075 by 463 cars
Total evacuated: 16017

(a) Route choice: EvacGroup.

Outputs
Simulation ID: New_sim
Sim. Clock: 10850 s dd:hh:mm:ss - 00:03:00:50
Total population: 16017
People staying: 0
Total cars: 6909
Pedestrians left: 0 (0%)
Cars reached by Peds: 6909
Cars left: 0 (0%)
Evacuation goals reached: Goal_E: 5339 by 2290 cars Goal_F: 5553 by 2375 cars Goal_R: 5125 by 2244 cars
Total evacuated: 16017

(b) Route choice: Random.

Figure 83. Overall evacuation performance comparison.

A5. Summary

WUI-NITY is a computer modelling tool developed to simulate wildfire development, resident decision-making, and evacuation movement for communities threatened by wildfires. It is designed to represent three core components during a wildfire event: fire development and spread, household and pedestrian evacuation decision-making, and transport/traffic movement to an area of safety. WUI-NITY provides a platform for simulating wildland-urban interface fire evacuation scenarios and facilitates the planning and management of evacuations. WUI-NITY serves as a powerful and freely available tool for emergency planners, researchers, and policymakers to make informed decisions during wildfire events. Its versatility and user-friendly interface make it a valuable asset in safeguarding communities from the ravages of natural disasters.

This user guide provides a comprehensive overview of the WUI-NITY model and its application in wildfire evacuation analysis. The document covers various aspects of data preparation and user inputs, including map preparation, population definition, fire and smoke simulation, traffic network and routing, and evacuation settings. It also details the guided workflow interface, demonstrating how to apply WUI-NITY to build a simulation case data model in a step-by-step, ordered sequence of actions. The guide includes figures illustrating the process of using WUI-NITY, such as data flow diagrams, map editing modes, and simulation outputs. Overall, the guide serves as a resource for users interested in using the WUI-NITY model for wildfire evacuation analysis.

It is noted that various external models can be used to support WUI-NITY applications. Where this is the case, we provide guidance on the introduction of the output produced by such models rather than detailed guidance on their application, which is covered in dedicated documentation provided by the developers.

The key components covered in this user guide include:

- **Introduction to the WUI-NITY model and its relevance:** WUI-NITY is designed to address the challenge posed by wildfires, especially in regions where wildfires pose a significant threat to populations near the wildland-urban interface, making evacuation a crucial choice for threatened communities.
- **Data preparation and user inputs:** Before running simulations, thorough data preparation is essential. This section involves gathering necessary population distribution data, geographical data (road network), and fire behavior characteristics data. This document also provides the step-by-step guidance to explain how to transform the source data into accepted inputs for WUI-NITY with defined format.
- **Fire and smoke simulation:** Fire propagation and smoke dispersion are two key influencing factors involved in evacuation. The part explains the current development of the fire and smoke simulation capacity with required fire behavior characteristics.
- **Traffic network settings:** Wildfire evacuation scenarios heavily rely on traffic networks. This section explains the method of simulating evacuation traffic, including assumptions.
- **Evacuation settings:** Users can configure evacuation zones, shelter locations, evacuation procedure and human behavioral attributes, which are used to predict the evacuation performance.
- **Guided workflow interface for applying WUI-NITY:** Finally, the tool offers an intuitive interface that guides users through the entire process to prepare, build and run evacuation simulations.

To illustrate the practical application of WUI-NITY, a demonstration case is presented. In this case, we construct a wildfire evacuation simulation, considering:

- **Data preparation:** Gathering topographic data, population density data, and fire behavior parameters.
- **Evacuation objectives and assumptions:** Defining evacuation destinations, evacuation groups and making informed assumptions about human behavior during emergencies (goals, responses and route choices).
- **Model configuration:** Setting up the simulation with all the required inputs.
- **Simulation outputs:** Producing simulation outputs for performance analysis and guidance for evacuation planning.

It is important to note that all model predictions are estimations, which can be influenced by:

- **Input data quality:** The accuracy and reliability of input data will have a significant impact on model predictions. In general, high-quality data leads to more robust results, while low-quality data may only be suitable for trend analysis or qualitative assessments.
- **Modelling capabilities:** All modelling modules are a simplification of reality. The sophistication of algorithms, modelling assumptions and their ability to capture real-world dynamics affect the outcomes.
- **Assumptions:** Assumptions are often made when data is scarce or uncertain. They may stem from estimates, predictions or incomplete information.
- **Inherited uncertainties:** Some uncertainties stem from external factors, historical data limitations or inherent complexities in the problem domain.

When using WUI-NITY, users should be aware of these limitations and the potential impact of their modelling assumptions. While we have diligently calibrated the modules within WUI-NITY [1-4], users are encouraged to fine-tune the model for their specific cases. Calibration ensures alignment with local conditions and enhances the reliability of predictions.

Finally, we welcome any feedback, issue reports, and requests for new functionality. Contact information can be found in the author lists at the beginning of this document or in Table 17.

Table 17. Contact information.

Area of question/interest	Contacts
The WUI-NITY project	Amanda Kimball (AKimball@nfpa.org) Fire Protection Research Foundation, USA
WUI-NITY software, installation, issue reports	wuinity@gmail.com
WUI-NITY modules, application, development, feedback, and requests for new functionality	Enrico Ronchi (enrico.ronchi@brand.lth.se) Jonathan Wahlqvist (jonathan.wahlqvist@brand.lth.se) Lund University, Sweden
	Steve Gwynne (Steve.Gwynne@ghd.com) Hui Xie (Hui.Xie@ghd.com) Movement Strategies, UK
	Guillermo Rein (g.rein@imperial.ac.uk) Imperial College London, UK
	Erica Kuligowski (erica.kuligowski@rmit.edu.au) Royal Melbourne Institute of Technology, Australia
	Max Kinateder (Max.Kinateder@nrc-cnrc.gc.ca) National Research Council, Canada

User guide references

1. E. Ronchi, J. Wahlqvist, A. Rohaert, E. Kuligowski, N. Janfeshanaraghi, G. Rein, H. Mitchell, N. Kalogeropoulos, S. M. V. Gwynne, H. Xie, P. Thompson, M. Kinatader, H. Mozaffari Maaref, M. Berthiaume, J. Daoust-Séguin, N. Bénichou, A. Kimball (2023). WUI-NITY 3: Multi-method traffic movement data collection for WUI fire evacuation modelling. National Fire Protection Association, Quincy (MA), USA.
2. E. Ronchi, J. Wahlqvist, A. Rohaert, A. Ardinge, S. M. V. Gwynne, G. Rein, H. Mitchell, N. Kalogeropoulos, M. Kinatader, N. Bénichou, E. Kuligowski, A. Westbury, A. Kimball (2021). WUI-NITY 2: the integration, verification, and validation of the wildfire evacuation platform WUI-NITY. National Fire Protection Association, Quincy (MA), USA.
3. E. Ronchi, J. Wahlqvist, S. M. V. Gwynne, M. Kinatader, N. Bénichou, C. Ma, G. Rein, H. Mitchell, A. Kimball (2020). WUI-NITY: a platform for the simulation of wildland-urban interface fire evacuation. National Fire Protection Association, Quincy (MA), USA.
4. E. Ronchi, G. Rein, S. M. V. Gwynne, P. Intini, R. Wadhwani, A. Bergstedt (2017). e-Sanctuary: Open Multi-Physics Framework for Modelling Wildfire Urban Evacuation. Fire Protection Research Foundation, Quincy (USA).
5. N. Kalogeropoulos, H. Mitchell, E. Ronchi, S. Gwynne, G. Rein. Design of stochastic trigger boundaries for rural communities evacuating from a wildfire (2023). *Fire Safety Journal* 140, 103854. Doi: 10.1016/j.firesaf.2023.103854
6. A. Rohaert, N. Janfeshanaraghi, E. Kuligowski, E. Ronchi (2023). The analysis of traffic data of wildfire evacuation: the case study of the 2020 Glass Fire. *Fire Safety Journal* 141, 103909. Doi: 10.1016/j.firesaf.2023.103909
7. E. Ronchi, J. Wahlqvist, A. Rohaert, A. Ardinge, S. M. V. Gwynne, G. Rein, H. Mitchell, N. Kalogeropoulos, M. Kinatader, N. Bénichou, E. Kuligowski, A. Kimball (2023). The verification of wildland-urban interface fire evacuation models. *Natural Hazards* 117, pp. 1493-1519. Doi: 10.1007/s11069-023-05913-2
8. H. Mitchell, G. Rein, S. M. V. Gwynne, E. Ronchi (2023). Integrating wildfire spread and evacuation times to design safe triggers: application to two rural communities using PERIL model. *Safety Science* 157, 105914. Doi: 10.1016/j.ssci.2022.105914
9. A. Rohaert, E. D. Kuligowski, A. Ardinge, J. Wahlqvist, S. M. V. Gwynne, A. Kimball, N. Bénichou, E. Ronchi (2023). Traffic dynamics during the 2019 Kincade wildfire evacuation. *Transportation Research Part D: Transport and Environment* 116, 103610. Doi: 10.1016/j.trd.2023.103610
10. S.M.V. Gwynne, E. Ronchi, J. Wahlqvist, A. Cuesta, J. Gonzalez Villa, E. Kuligowski, A. Kimball, G. Rein, M. Kinatader, Hui Xie (2023). Roxborough Park Community Wildfire Evacuation Drill: Data Collection and Model Benchmarking. *Fire Technology* 59, pp. 879-901. Doi: 10.1007/s10694-023-01371-1
11. E. Kuligowski, E. Ronchi, J. Wahlqvist, S.M.V. Gwynne, M. Kinatader, G. Rein, H. Mitchell, N. Bénichou, A. Kimball (2022). Evacuation Modelling for Bushfire: An introduction to the WUI-NITY simulation platform. *Australian Journal of Emergency Management (AJEM)* 37:4 pp. 40-43.
12. J. Wahlqvist, E. Ronchi, S.M.V. Gwynne, M. Kinatader, G. Rein, H. Mitchell, N. Benichou, C. Ma, A. Kimball, E. Kuligowski (2021) The simulation of wildland-urban interface fire evacuation - the WUI-NITY platform. *Safety Science* 136:105145. Doi: 10.1016/j.ssci.2020.105145
13. E. Ronchi, G. Rein, S. M. V. Gwynne, P. Intini, R. Wadhwani (2019). An open multi-physics framework for modelling wildland-urban interface fire evacuations. *Safety Science* 118, 868-880. Doi: 10.1016/j.ssci.2019.06.009

14. S. M. V. Gwynne, E. Ronchi, N. Benichou, M. Kinatader, E. Kuligowski, I. Gomaa, M. Adelzadeh (2019). Modelling and Mapping Dynamic Vulnerability to Better Assess WUI Evacuation Performance. *Fire and Materials* 43, pp. 644-660. Doi: 10.1002/fam.2708.
15. Nadeau LB, Englefield P (2006). Fine-resolution mapping of wildfire fuel types for Canada: Fuzzy logic modeling for an Alberta pilot area. *Environ Monit Assess.* 2006 Sep;120(1-3):127-52. doi: 10.1007/s10661-005-9053-0. Epub 2006 Jun 13. PMID: 16770507.
16. Price OF, Gordon CE (2016). The potential for LiDAR technology to map fire fuel hazard over large areas of Australian forest. *J Environ Manage.* 2016 Oct 1;181:663-673. doi: 10.1016/j.jenvman.2016.08.042. Epub 2016 Aug 21. PMID: 27558828.
17. Sauvage S et al. (2024) Australian Fire Danger Rating System Research Prototype: a climatology. *International Journal of Wildland Fire* 33, WF23144. doi:10.1071/WF23144
18. Kenny BJ, Matthews S, Sauvage S, Grootemaat S, Hollis JJ, Fox-Hughes P, Runcie J, Holmes A (2024) Australian Fire Danger Rating System: implementing fire behavior calculations to forecast fire danger in a research prototype. *International Journal of Wildland Fire*, In press. doi:10.1071/WF23142
19. Gwynne, S., & Boyce, K. E. (2016). Engineering Data. In M. J. Hurley, D. T. Gottuk, J. R. Hall, K. Harada, E. D. Kuligowski, M. Puchovsky, J. L. Torero, J. M. Watts, & C. J. Wieczorek (Eds.), *SFPE Handbook of Fire Protection Engineering* (pp. 2429–2551). Springer New York. http://link.springer.com/10.1007/978-1-4939-2565-0_64

Report references

- Abel F, Hauff C, Houben G-J, et al (2012) Twitcident: fighting fire with information from social web streams. In: Proceedings of the 21st international conference on world wide web. pp 305–308
- Abirami S, Chitra P, others (2019) Real time twitter based disaster response system for indian scenarios. In: 2019 26th International Conference on High Performance Computing, Data and Analytics Workshop (HiPCW). IEEE, pp 82–86
- Akizuki Y (2024) Evacuation route design based on visibility for reducing evacuation delays. *Fire Safety Journal* 144:104099. <https://doi.org/10.1016/j.firesaf.2024.104099>
- Allen RW, Park GD, Cook ML (2010) Simulator Fidelity and Validity in a Transfer-of-Training Context. *Transportation Research Record* 2185:40–47. <https://doi.org/10.3141/2185-06>
- Almallah M, Hussain Q, Reinolsmann N, Alhajyaseen WKM (2021) Driving simulation sickness and the sense of presence: Correlation and contributing factors. *Transportation Research Part F: Traffic Psychology and Behaviour* 78:180–193. <https://doi.org/10.1016/j.trf.2021.02.005>
- Alvarez Lopez P, Behrisch M, Bieker-Walz L, et al (2018) Microscopic Traffic Simulation using SUMO. In: The 21st IEEE International Conference on Intelligent Transportation Systems. IEEE
- Anderson HE (1981) Aids to determining fuel models for estimating fire behavior. US Department of Agriculture, Forest Service, Intermountain Forest and Range ...
- Andrews PL (1986) BEHAVE: fire behavior prediction and fuel modeling system-BURN subsystem, Part 1
- Arias S, Wahlqvist J, Nilsson D, et al (2021) Pursuing behavioral realism in Virtual Reality for fire evacuation research. *Fire and Materials* 45:462–472. <https://doi.org/10.1002/fam.2922>
- Arthur KW (2000) Effects of field of view on performance with head-mounted displays. The University of North Carolina at Chapel Hill
- Balech S, Benavent C, Calciu M, Monnot J (2021) The covid-19 crisis: an NLP exploration of the french Twitter feed (February-May 2020). In: International Conference on Human-Computer Interaction. Springer, pp 308–321
- Behrisch M, Bieker L, Erdmann J, Krajzewicz D (2011) SUMO—simulation of urban mobility: an overview. In: Proceedings of SIMUL 2011, The Third International Conference on Advances in System Simulation. ThinkMind
- Bianchi Piccinini GF, Rodrigues CM, Leitão M, Simões A (2014) Driver's behavioral adaptation to Adaptive Cruise Control (ACC): The case of speed and time headway. *Journal of Safety Research* 49:77.e1-84. <https://doi.org/10.1016/j.jsr.2014.02.010>
- Biswas RK, Friswell R, Olivier J, et al (2021) A systematic review of definitions of motor vehicle headways in driver behaviour and performance studies. *Transportation Research Part F: Traffic Psychology and Behaviour* 77:38–54. <https://doi.org/10.1016/j.trf.2020.12.011>
- Blissing B, Bruzelius F (2018) Exploring the suitability of virtual reality for driving simulation. In: Driving Simulation Conference 2018. pp 163–166
- Bouchard S, St-Jacques J, Robillard G, Renaud P (2008) Anxiety Increases the Feeling of Presence in Virtual Reality. *Presence: Teleoperators and Virtual Environments* 17:376–391. <https://doi.org/10.1162/pres.17.4.376>
- Brooke J, others (1996) SUS-A quick and dirty usability scale. *Usability evaluation in industry* 189:4–7

- Brooks JO, Goodenough RR, Crisler MC, et al (2010) Simulator sickness during driving simulation studies. *Accident Analysis & Prevention* 42:788–796. <https://doi.org/10.1016/j.aap.2009.04.013>
- Broughton KLM, Switzer F, Scott D (2007) Car following decisions under three visibility conditions and two speeds tested with a driving simulator. *Accident Analysis & Prevention* 39:106–116. <https://doi.org/10.1016/j.aap.2006.06.009>
- Bruck L, Haycock B, Emadi A (2021) A Review of Driving Simulation Technology and Applications. *IEEE Open J Veh Technol* 2:1–16. <https://doi.org/10.1109/OJVT.2020.3036582>
- Bruns A, Liang YE (2012) Tools and methods for capturing Twitter data during natural disasters. *First Monday* 17:1–8
- Buck L, Paris R, Bodenheimer B (2021) Distance Compression in the HTC Vive Pro: A Quick Revisitation of Resolution. *Front Virtual Real* 2:728667. <https://doi.org/10.3389/frvir.2021.728667>
- Cameron MA, Power R, Robinson B, Yin J (2012) Emergency situation awareness from twitter for crisis management. In: *Proceedings of the 21st international conference on world wide web*. pp 695–698
- Carr R, Palmer S, Hagel P (2015) Active learning: The importance of developing a comprehensive measure. *Active learning in higher education* 16:173–186
- Carton H, Gales J, Kennedy EB (2024) Video analysis of human behaviour during wildfire evacuations. *Can J Civ Eng* cjce-2023-0450. <https://doi.org/10.1139/cjce-2023-0450>
- Chang Y, Wang X, Wang J, et al (2024) A survey on evaluation of large language models. *ACM Transactions on Intelligent Systems and Technology* 15:1–45
- Choudhary Z, Gottsacker M, Kim K, et al (2021) Revisiting Distance Perception with Scaled Embodied Cues in Social Virtual Reality. In: *2021 IEEE Virtual Reality and 3D User Interfaces (VR)*. IEEE, Lisboa, Portugal, pp 788–797
- Chowdhary K, Chowdhary K (2020) Natural language processing. *Fundamentals of artificial intelligence* 603–649
- Chowdhury JR, Caragea C, Caragea D (2020) On identifying hashtags in disaster twitter data. In: *Proceedings of the AAAI Conference on Artificial Intelligence*. pp 498–506
- Cipresso P, Giglioli IAC, Raya MA, Riva G (2018) The Past, Present, and Future of Virtual and Augmented Reality Research: A Network and Cluster Analysis of the Literature. *Front Psychol* 9:2086. <https://doi.org/10.3389/fpsyg.2018.02086>
- Cobo A, Parra D, Navón J (2015) Identifying relevant messages in a twitter-based citizen channel for natural disaster situations. In: *Proceedings of the 24th international conference on world wide web*. pp 1189–1194
- Collins BL, Dahir MS, Madrzykowski D (1992) Visibility of exit signs in clear and smoky conditions. *Journal of the Illuminating Engineering Society* 21:69–84
- Comets E, Lavenu A, Lavielle M (2017) Parameter Estimation in Nonlinear Mixed Effect Models Using saemix, an R Implementation of the SAEM Algorithm. *J Stat Soft* 80:. <https://doi.org/10.18637/jss.v080.i03>
- Cova TJ, Sun Y, Zhao X, et al (2024) Destination unknown: Examining wildfire evacuee trips using GPS data. *Journal of Transport Geography* 117:103863. <https://doi.org/10.1016/j.jtrangeo.2024.103863>
- Creem-Regehr SH, Willemsen P, Gooch AA, Thompson WB (2005) The Influence of Restricted Viewing Conditions on Egocentric Distance Perception: Implications for Real and Virtual Indoor Environments. *Perception* 34:191–204. <https://doi.org/10.1068/p5144>

- Cuéllar L, Kubicek D, Hengartner N, Hansson A (2009) Emergency relocation: population response model to disasters. In: Technologies for Homeland Security, 2009. HST'09. IEEE Conference on. IEEE, pp 628–635
- Daganzo CF (1994) The cell transmission model: A dynamic representation of highway traffic consistent with the hydrodynamic theory. *Transportation Research Part B: Methodological* 28:269–287. [https://doi.org/10.1016/0191-2615\(94\)90002-7](https://doi.org/10.1016/0191-2615(94)90002-7)
- Dai E, Shu K, Sun Y, Wang S (2021) Labeled data generation with inexact supervision. In: Proceedings of the 27th ACM SIGKDD Conference on Knowledge Discovery & Data Mining. pp 218–226
- Davis A, Veloso A (2016) Subject-related message filtering in social media through context-enriched language models. In: Transactions on Computational Collective Intelligence XXI: Special Issue on Keyword Search and Big Data. Springer, pp 97–138
- Davis C, Sole C, Khan H, Nilsson D (2023) Investigating movement through smoke in virtual reality. *Fire Safety Journal* 140:103890. <https://doi.org/10.1016/j.firesaf.2023.103890>
- Dhuliawala S, Komeili M, Xu J, et al (2023) Chain-of-verification reduces hallucination in large language models. arXiv preprint arXiv:230911495
- Döhling L, Leser U (2011) Equatornlp: Pattern-based information extraction for disaster response. In: Terra Cognita 2011 Workshop, Foundations, Technologies and Applications of the Geospatial Web. Citeseer, pp 127–138
- Elhokayem L (2022) Visibility in Smoke With Different Extinction Coefficients. Department of Fire Safety Engineering, Lund University, Lund, Sweden
- Farahani A, Pourshojae B, Rasheed K, Arabnia HR (2020) A concise review of transfer learning. In: 2020 international conference on computational science and computational intelligence (CSCI). IEEE, pp 344–351
- Finney MA (1998) FARSITE, Fire Area Simulator–model development and evaluation. US Department of Agriculture, Forest Service, Rocky Mountain Research Station Ogden, UT
- Finney MA (2006) An overview of FlamMap fire modeling capabilities
- Fridolf K, Nilsson D, Frantzich H (2015) Evacuation of a Metro Train in an Underground Rail Transportation System: Flow Rate Capacity of Train Exits, Tunnel Walking Speeds and Exit Choice. *Fire Technology*. <https://doi.org/10.1007/s10694-015-0471-4>
- Fridolf K, Ronchi E, Nilsson D, Frantzich H (2019) The representation of evacuation movement in smoke-filled underground transportation systems. *Tunnelling and Underground Space Technology* 90:28–41
- Fridolf K, Ronchi E, Nilsson D, Frantzich H (2013) Movement speed and exit choice in smoke-filled rail tunnels. *Fire Safety Journal* 59:8–21. <https://doi.org/10.1016/j.firesaf.2013.03.007>
- Fujii K, Sano T, Ohmiya Y (2021) Influence of lit emergency signs and illuminated settings on walking speeds in smoky corridors. *Fire Safety Journal* 120:103026. <https://doi.org/10.1016/j.firesaf.2020.103026>
- Gao K, Tu H, Sun L, et al (2020) Impacts of reduced visibility under hazy weather condition on collision risk and car-following behavior: Implications for traffic control and management. *International Journal of Sustainable Transportation* 14:635–642. <https://doi.org/10.1080/15568318.2019.1597226>
- Gerlach T (2011) Visualisation of the brownout phenomenon, integration and test on a helicopter flight simulator. *Aeronaut j* 115:57–63. <https://doi.org/10.1017/S0001924000005364>
- Goedicke D, Li J, Evers V, Ju W (2018) VR-OOM: Virtual Reality On-rOad driving siMulation. In: Proceedings of the 2018 CHI Conference on Human Factors in Computing Systems. ACM, Montreal QC Canada, pp 1–11

- Goodrick SL, Achtemeier GL, Larkin NK, et al (2013) Modelling smoke transport from wildland fires: a review. *International Journal of Wildland Fire* 22:83. <https://doi.org/10.1071/WF11116>
- Gwynne SMV, Ronchi E, Wahlqvist J, et al (2023) Roxborough Park Community Wildfire Evacuation Drill: Data Collection and Model Benchmarking. *Fire Technol* 59:879–901. <https://doi.org/10.1007/s10694-023-01371-1>
- Hartfiel B, Stark R (2021) Validity of primary driving tasks in head-mounted display-based driving simulators. *Virtual Reality* 25:819–833. <https://doi.org/10.1007/s10055-020-00496-w>
- Hernandez-Suarez A, Sanchez-Perez G, Toscano-Medina K, et al (2019) Using twitter data to monitor natural disaster social dynamics: A recurrent neural network approach with word embeddings and kernel density estimation. *Sensors* 19:1746
- Hodas NO, Ver Steeg G, Harrison J, et al (2015) Disentangling the lexicons of disaster response in twitter. In: *Proceedings of the 24th International Conference on World Wide Web*. pp 1201–1204
- Houston JB, Hawthorne J, Perreault MF, et al (2015) Social media and disasters: a functional framework for social media use in disaster planning, response, and research. *Disasters* 39:1–22
- Imran M, Mitra P, Castillo C (2016) Twitter as a lifeline: Human-annotated twitter corpora for NLP of crisis-related messages. *arXiv preprint arXiv:160505894*
- Innes RJ, Howard ZL, Thorpe A, et al (2021) The effects of increased visual information on cognitive workload in a helicopter simulator. *Human factors* 63:788–803
- Intini P, Colonna P, Olaussen Ryeng E (2019a) Route familiarity in road safety: A literature review and an identification proposal. *Transportation Research Part F: Traffic Psychology and Behaviour* 62:651–671. <https://doi.org/10.1016/j.trf.2018.12.020>
- Intini P, Ronchi E, Gwynne S, Pel A (2019b) Traffic Modeling for Wildland–Urban Interface Fire Evacuation. *Journal of Transportation Engineering, Part A: Systems* 145:04019002
- Intini P, Wahlqvist J, Wetterberg N, Ronchi E (2022) Modelling the impact of wildfire smoke on driving speed. *International Journal of Disaster Risk Reduction* 80:103211. <https://doi.org/10.1016/j.ijdr.2022.103211>
- Ji Z, Lee N, Frieske R, et al (2023) Survey of hallucination in natural language generation. *ACM Computing Surveys* 55:1–38
- Jin T (2008) Visibility and Human Behavior in Fire Smoke. In: *SFPE Handbook of Fire Protection Engineering* (3rd edition), Di Nenno P. National Fire Protection Association, Quincy, MA (USA), pp 2-42-2–53
- Jin T (1978) Visibility through fire smoke. *Journal of Fire and Flammability* 9:135–155
- Jin T, Yamada T (1985) Irritating effects of fire smoke on visibility. *Fire Science and Technology* 5:79–90
- Kalogeropoulos N, Mitchell H, Kuligowski ED, Rein G (2024) Dire evacuations from wildfires and trigger boundaries. Submitted for publication
- Kalogeropoulos N, Mitchell H, Ronchi E, et al (2023) Design of stochastic trigger boundaries for rural communities evacuating from a wildfire. *Fire Safety Journal* 140:103854. <https://doi.org/10.1016/j.firesaf.2023.103854>
- Kang JJ, Ni R, Andersen GJ (2008) Effects of Reduced Visibility from Fog on Car-Following Performance. *Transportation Research Record* 2069:9–15. <https://doi.org/10.3141/2069-02>
- Khanal S, Medasetti US, Mashal M, et al (2022) Virtual and Augmented Reality in the Disaster Management Technology: A Literature Review of the Past 11 years. *Front Virtual Real* 3:843195. <https://doi.org/10.3389/frvir.2022.843195>

- Kim HK, Park J, Choi Y, Choe M (2018) Virtual reality sickness questionnaire (VRSQ): Motion sickness measurement index in a virtual reality environment. *Applied Ergonomics* 69:66–73. <https://doi.org/10.1016/j.apergo.2017.12.016>
- Kim J, Park J, Kim K, Kim M (2021) RnR-SMART: Resilient smart city evacuation plan based on road network reconfiguration in outbreak response. *Sustainable Cities and Society* 75:103386. <https://doi.org/10.1016/j.scs.2021.103386>
- Kinater M, Ronchi E, Nilsson D, et al (2014) Virtual Reality for Fire Evacuation Research. In: 1st Workshop “Complex Events and Information Modelling.” Warsaw, pp 319–327
- Krajzewicz D, Hertkorn G, Rössel C, Wagner P (2002) SUMO (Simulation of Urban MObility)-an open-source traffic simulation. In: Proceedings of the 4th middle East Symposium on Simulation and Modelling (MESM2002). pp 183–187
- Krauss S (1998a) Microscopic modeling of traffic flow: investigation of collision free vehicle dynamics
- Krauss S (1998b) Microscopic modeling of traffic flow: investigation of collision free vehicle dynamics. DLR Forschungszentrum fuer Luft- und Raumfahrt e.V., Koeln (Germany). Hauptabt. Mobilitaet und Systemtechnik, Germany
- Krauß S (1998) Microscopic modeling of traffic flow: Investigation of collision free vehicle dynamics
- Kuligowski E (2020) Evacuation decision-making and behavior in wildfires: Past research, current challenges and a future research agenda. *Fire Safety Journal* 103:129. <https://doi.org/10.1016/j.firesaf.2020.103129>
- Kumar D, Ukkusuri SV (2020) Enhancing demographic coverage of hurricane evacuation behavior modeling using social media. *Journal of Computational Science* 45:101184
- Kumar P, Sharma M (2022) Data, Machine Learning, and Human Domain Experts: None Is Better than Their Collaboration. *International Journal of Human–Computer Interaction* 38:1307–1320. <https://doi.org/10.1080/10447318.2021.2002040>
- Li L, Ma Z, Cao T (2021) Data-driven investigations of using social media to aid evacuations amid Western United States wildfire season. *Fire Safety Journal* 126:103480. <https://doi.org/10.1016/j.firesaf.2021.103480>
- Liberatore MJ, Wagner WP (2021) Virtual, mixed, and augmented reality: a systematic review for immersive systems research. *Virtual Reality* 25:773–799. <https://doi.org/10.1007/s10055-020-00492-0>
- Lindell MK, Prater CS (2007) Critical behavioral assumptions in evacuation time estimate analysis for private vehicles: Examples from hurricane research and planning. *Journal of Urban Planning and Development* 133:18–29
- Llorca C, Farah H (2016) Passing Behavior on Two-Lane Roads in Real and Simulated Environments. *Transportation Research Record* 2556:29–38. <https://doi.org/10.3141/2556-04>
- Lopez PA, Behrisch M, Bieker-Walz L, et al (2018a) Microscopic traffic simulation using sumo. In: 2018 21st international conference on intelligent transportation systems (ITSC). IEEE, pp 2575–2582
- Lopez PA, Behrisch M, Bieker-Walz L, et al (2018b) Microscopic Traffic Simulation using SUMO. In: The 21st IEEE International Conference on Intelligent Transportation Systems. IEEE
- Martín Y, Cutter SL, Li Z (2020) Bridging twitter and survey data for evacuation assessment of Hurricane Matthew and Hurricane Irma. *Natural hazards review* 21:04020003
- Matas NA, Nettelbeck T, Burns NR (2015) Dropout during a driving simulator study: A survival analysis. *Journal of Safety Research* 55:159–169. <https://doi.org/10.1016/j.jsr.2015.08.004>

- McKenna N, Li T, Cheng L, et al (2023) Sources of hallucination by large language models on inference tasks. arXiv preprint arXiv:230514552
- McLennan J, Ryan B, Bearman C, Toh K (2019) Should We Leave Now? Behavioral Factors in Evacuation Under Wildfire Threat. *Fire Technology* 55:487–516. <https://doi.org/10.1007/s10694-018-0753-8>
- Meima N (2021) Augmented Reality to Support Helicopter Pilots Hovering in Brownout Conditions
- Miao J, Zhu W (2022) Precision–recall curve (PRC) classification trees. *Evol Intel* 15:1545–1569. <https://doi.org/10.1007/s12065-021-00565-2>
- Minaee S, Mikolov T, Nikzad N, et al (2024) Large language models: A survey. arXiv preprint arXiv:240206196
- Mitchell H (2019) PERIL: Wildfire Behaviour and Optimum Evacuation of the Population in the Wild-Urban Interface. Imperial College London, London, UK
- Mitchell H, Gwynne S, Ronchi E, et al (2023) Integrating wildfire spread and evacuation times to design safe triggers: Application to two rural communities using PERIL model. *Safety Science* 157:105914. <https://doi.org/10.1016/j.ssci.2022.105914>
- Morshed SA, Ahmed KM, Amine K, Moinuddin KA (2021) Trend Analysis of Large-Scale Twitter Data Based on Witnesses during a Hazardous Event: A Case Study on California Wildfire Evacuation. *World Journal of Engineering and Technology* 09:229–239. <https://doi.org/10.4236/wjet.2021.92016>
- Mueller AS, Trick LM (2012) Driving in fog: The effects of driving experience and visibility on speed compensation and hazard avoidance. *Accident Analysis & Prevention* 48:472–479. <https://doi.org/10.1016/j.aap.2012.03.003>
- Mulholland GW (1995) Smoke production and properties. *SFPE handbook of fire protection engineering* 3:2–258
- Murray-Tuite P, Mahmassani H (2004) Transportation Network Evacuation Planning with Household Activity Interactions. *Transportation Research Record: Journal of the Transportation Research Board* 1894:150–159. <https://doi.org/10.3141/1894-16>
- Murray-Tuite P, Wolshon B (2013) Evacuation transportation modeling: An overview of research, development, and practice. *Transportation Research Part C: Emerging Technologies* 27:25–45. <https://doi.org/10.1016/j.trc.2012.11.005>
- Olteanu A, Castillo C, Diaz F, Vieweg S (2014) Crisislex: A lexicon for collecting and filtering microblogged communications in crises. In: *Proceedings of the international AAAI conference on web and social media*. pp 376–385
- Opdyke A, Javernick-Will A (2014) Building coordination capacity: Post-disaster organizational twitter networks. In: *IEEE global humanitarian technology conference (GHTC 2014)*. IEEE, pp 86–92
- Paes D, Arantes E, Irizarry J (2017) Immersive environment for improving the understanding of architectural 3D models: Comparing user spatial perception between immersive and traditional virtual reality systems. *Automation in Construction* 84:292–303. <https://doi.org/10.1016/j.autcon.2017.09.016>
- Palacios-Alonso D, Barbas-Cubero J, Betancourt-Ortega L, Fernández-Fernández M (2022) Measuring Motion Sickness Through Racing Simulator Based on Virtual Reality. In: Ferrández Vicente JM, Álvarez-Sánchez JR, De La Paz López F, Adeli H (eds) *Artificial Intelligence in Neuroscience: Affective Analysis and Health Applications*. Springer International Publishing, Cham, pp 494–504
- Pallamin N, Bossard C (2016) Presence, Behavioural Realism and Performances in Driving Simulation. *IFAC-PapersOnLine* 49:408–413. <https://doi.org/10.1016/j.ifacol.2016.10.600>

- Peillard E (2020) Toward a Characterization of Perceptual Biases in Mixed Reality: A Study of Factors Inducing Distance Misperception. PhD Thesis, École centrale de Nantes
- Peillard E, Thebaud T, Normand J-M, et al (2019) Virtual Objects Look Farther on the Sides: The Anisotropy of Distance Perception in Virtual Reality. In: 2019 IEEE Conference on Virtual Reality and 3D User Interfaces (VR). IEEE, Osaka, Japan, pp 227–236
- Pel AJ, Bliemer MCJ, Hoogendoorn SP (2012) A review on travel behaviour modelling in dynamic traffic simulation models for evacuations. *Transportation* 39:97–123. <https://doi.org/10.1007/s11116-011-9320-6>
- Pel AJ, Hoogendoorn SP, Bliemer MC (2010) Evacuation modeling including traveler information and compliance behavior. *Procedia Engineering* 3:101–111
- Philips BH, Morton T, others (2015) Making Driving Simulators More Useful for Behavioral Research: Simulator Characteristics Comparison and Model-Based Transformation, Summary Report. United States. Federal Highway Administration. Office of Safety Research and ...
- Priot A, Albery W (2012) Rotary-wing brownout mitigation: technologies and training. North Atlantic Treaty Organisation, RTO-TR-HFM-162
- Renner RS, Velichkovsky BM, Helmert JR (2013) The perception of egocentric distances in virtual environments - A review. *ACM Comput Surv* 46:1–40. <https://doi.org/10.1145/2543581.2543590>
- Risto M, Martens MH (2014) Driver headway choice: A comparison between driving simulator and real-road driving. *Transportation Research Part F: Traffic Psychology and Behaviour* 25:1–9. <https://doi.org/10.1016/j.trf.2014.05.001>
- Risto M, Martens MH (2013) Time and space: The difference between following time headway and distance headway instructions. *Transportation Research Part F: Traffic Psychology and Behaviour* 17:45–51. <https://doi.org/10.1016/j.trf.2012.09.004>
- Rohaert A (2024) Experiment dataset of people driving through simulated wildfire smoke using a driving simulator
- Rohaert A, Janfeshanaraghi N, Kuligowski E, Ronchi E (2023a) The analysis of traffic data of wildfire evacuation: the case study of the 2020 Glass Fire. *Fire Safety Journal* 141:103909. <https://doi.org/10.1016/j.firesaf.2023.103909>
- Rohaert A, Janfeshanaraghi N, Kuligowski E, Ronchi E (2023b) The analysis of traffic data of wildfire evacuation: the case study of the 2020 Glass Fire. *Fire Safety Journal* 141:103909. <https://doi.org/10.1016/j.firesaf.2023.103909>
- Rohaert A, Kuligowski ED, Ardinge A, et al (2023c) Traffic dynamics during the 2019 Kincadee wildfire evacuation. *Transportation Research Part D: Transport and Environment* 116:103610. <https://doi.org/10.1016/j.trd.2023.103610>
- Rohaert A, Kuligowski ED, Ardinge A, et al (2023d) Traffic dynamics during the 2019 Kincadee wildfire evacuation. *Transportation Research Part D: Transport and Environment* 116:103610. <https://doi.org/10.1016/j.trd.2023.103610>
- Ronchi E, Fridolf K, Frantzich H, et al (2018) A tunnel evacuation experiment on movement speed and exit choice in smoke. *Fire Safety Journal* 97:126–136. <https://doi.org/10.1016/j.firesaf.2017.06.002>
- Ronchi E, Nilsson D (2018) Pedestrian Movement in Smoke: Theory, Data and Modelling Approaches. In: Gibelli L, Bellomo N (eds) *Crowd Dynamics*, Volume 1. Springer International Publishing, Cham, pp 37–62
- Ronchi E, Wahlqvist J, Gwynne S, et al (2020) WUI-NITY: a platform for the simulation of wildland-urban interface fire evacuation. Fire Protection Research Foundation, Quincy, MA (USA)

- Ronchi E, Wahlqvist J, Rohaert A, et al (2021) WUI-NITY 2: the integration, verification, and validation of the wildfire evacuation platform WUI-NITY. Fire Protection Research Foundation, Quincy, MA (USA)
- Ronchi E, Wahlqvist J, Rohaert A, et al (2023) WUI-NITY 3: Multi-method traffic movement data collection for WUI fire evacuation modelling. Fire Protection Research Foundation, Quincy, MA (USA)
- Sadri AM, Ukkusuri SV, Gladwin H (2017) The Role of Social Networks and Information Sources on Hurricane Evacuation Decision Making. *Nat Hazards Rev* 18:04017005. [https://doi.org/10.1061/\(ASCE\)NH.1527-6996.0000244](https://doi.org/10.1061/(ASCE)NH.1527-6996.0000244)
- Saffarian M, Happee R, Winter JCFD (2012) Why do drivers maintain short headways in fog? A driving-simulator study evaluating feeling of risk and lateral control during automated and manual car following. *Ergonomics* 55:971–985. <https://doi.org/10.1080/00140139.2012.691993>
- Şahin C, Rokne J, Alhajj R (2019) Emergency detection and evacuation planning using social media. *Social networks and surveillance for society* 149–164
- Seabold S, Perktold J (2010) statsmodels: Econometric and statistical modeling with python. In: 9th Python in Science Conference
- Shetab Boushehri S, Qasim AB, Waibel D, et al (2022) Systematic Comparison of Incomplete-Supervision Approaches for Biomedical Image Classification. In: International Conference on Artificial Neural Networks. Springer, pp 355–365
- Sinolakis C, Kalligeris Ni, Skanavis V, et al (2018) The deadly fire of the 23rd July in Mati: Wildfire and Evacuation Simulation Originally: Η φονική φωτιά της 23ης Ιουλίου στο Μάτι: Προσομοίωση πυρκαγιάς και εκκένωσης)
- Slater M, Sanchez-Vives MV (2016) Enhancing Our Lives with Immersive Virtual Reality. *Front Robot AI* 3:. <https://doi.org/10.3389/frobt.2016.00074>
- Song J, Wu Y, Xu Z, Lin X (2014) Research on car-following model based on SUMO. In: The 7th IEEE/international conference on advanced infocomm technology. IEEE, pp 47–55
- Suh A, Prophet J (2018) The state of immersive technology research: A literature analysis. *Computers in Human Behavior* 86:77–90. <https://doi.org/10.1016/j.chb.2018.04.019>
- Taheri SM, Matsushita K, Sasaki M (2017) Development of a Driving Simulator with Analyzing Driver's Characteristics Based on a Virtual Reality Head Mounted Display. *JTTs* 07:351–366. <https://doi.org/10.4236/jtts.2017.73023>
- Tamakloe R, Hong J, Tak J, Park D (2021) Finding evacuation routes using traffic and network structure information. *Transportation Research Part D: Transport and Environment* 95:102853. <https://doi.org/10.1016/j.trd.2021.102853>
- Törnros J (1998) Driving behaviour in a real and a simulated road tunnel—a validation study. *Accident Analysis & Prevention* 30:497–503. [https://doi.org/10.1016/S0001-4575\(97\)00099-7](https://doi.org/10.1016/S0001-4575(97)00099-7)
- Trafikverket STA (2022) Krav - VGU: Vägars och gators utformning. Trafikverket, Borlänge
- Venkatakrishnan R, Volonte M, Bhargava A, et al (2019) Towards an Immersive Driving Simulator to Study Factors Related to Cybersickness. In: 2019 IEEE Conference on Virtual Reality and 3D User Interfaces (VR). IEEE, Osaka, Japan, pp 1201–1202
- Wahlqvist J, Ronchi E, Gwynne SMV, et al (2021) The simulation of wildland-urban interface fire evacuation: The WUI-NITY platform. *Safety Science* 136:105145. <https://doi.org/10.1016/j.ssci.2020.105145>
- Wahlqvist J, Rubini P (2023a) Real-time visualization of smoke for fire safety engineering applications. *Fire Safety Journal* 140:103878. <https://doi.org/10.1016/j.firesaf.2023.103878>

- Wahlqvist J, Rubini P (2023b) Real-time visualization of smoke for fire safety engineering applications. *Fire Safety Journal* 140:103878. <https://doi.org/10.1016/j.firesaf.2023.103878>
- Wetterberg N, Ronchi E, Wahlqvist J (2021a) Individual Driving Behaviour in Wildfire Smoke. *Fire Technology* 57:1041–1061
- Wetterberg N, Ronchi E, Wahlqvist J (2021b) Individual Driving Behaviour in Wildfire Smoke. *Fire Technol* 57:1041–1061. <https://doi.org/10.1007/s10694-020-01026-5>
- Wong S, Broader J, Shaheen SA (2020) Review of California Wildfire Evacuations from 2017 to 2019. University of California, Institute of Transportation Studies. <https://doi.org/10.7922/G29G5K2R>
- Wu J, Zhou X, Kuligowski ED, et al (2024) Social Media Data Mining of Human Behaviour during Bushfire Evacuation. Submitted for publication
- Wynne RA, Beanland V, Salmon PM (2019) Systematic review of driving simulator validation studies. *Safety Science* 117:138–151. <https://doi.org/10.1016/j.ssci.2019.04.004>
- Xiong J, Hsiang E-L, He Z, et al (2021) Augmented reality and virtual reality displays: emerging technologies and future perspectives. *Light Sci Appl* 10:216. <https://doi.org/10.1038/s41377-021-00658-8>
- Zhan T, Xiong J, Zou J, Wu S-T (2020) Multifocal displays: review and prospect. *PhotonIX* 1:10. <https://doi.org/10.1186/s43074-020-00010-0>
- Zhang C, Fan C, Yao W, et al (2019) Social media for intelligent public information and warning in disasters: An interdisciplinary review. *International Journal of Information Management* 49:190–207
- Zhang Y, Guo Z, Sun Z (2020) Driving Simulator Validity of Driving Behavior in Work Zones. *Journal of Advanced Transportation* 2020:1–10. <https://doi.org/10.1155/2020/4629132>
- Zhou X, Chen L (2022) Migrating social event recommendation over microblogs. *Proceedings of the VLDB Endowment* 15:3213–3225
- Zhu M, Wang X, Wang X (2016) Car-Following Headways in Different Driving Situations: A Naturalistic Driving Study. In: CICTP 2016. American Society of Civil Engineers, Shanghai, China, pp 1419–1428